

THE RELATION BETWEEN CHANNEL INSTABILITY  
AND SEDIMENT TRANSPORT ON LOWER FRASER RIVER

By

DAVID GEORGE McLEAN

B.A.Sc. The University of British Columbia, 1975  
M.A.Sc. The University of British Columbia, 1980

A THESIS SUBMITTED IN PARTIAL FULFILLMENT OF  
THE REQUIREMENTS FOR THE DEGREE OF  
DOCTOR OF PHILOSOPHY

in

THE FACULTY OF GRADUATE STUDIES

Interdisciplinary Hydrology Program

We accept this thesis as conforming  
to the required standard

THE UNIVERSITY OF BRITISH COLUMBIA

February 1990

©David George McLean, 1990

In presenting this thesis in partial fulfilment of the requirements for an advanced degree at the University of British Columbia, I agree that the Library shall make it freely available for reference and study. I further agree that permission for extensive copying of this thesis for scholarly purposes may be granted by the head of my department or by his or her representatives. It is understood that copying or publication of this thesis for financial gain shall not be allowed without my written permission.

Department of Geography

The University of British Columbia  
Vancouver, Canada

Date April 30 1990



## ABSTRACT

This study investigates the relation between channel instability and sediment transport along an 80 km reach of lower Fraser River, British Columbia. The major processes governing instability, bank erosion and sedimentation were investigated by analyzing the patterns of morphologic change along the river over the last century. Morphologic changes were documented using historical maps and air photographs. The method of approach can be considered a "macroscopic" one since the investigation focused primarily on the gross patterns of change that occurred over periods of years to decades. It was found that this interval is the most appropriate time scale for investigating channel instability and sedimentation processes on a large stream such as the Fraser River. This is because the major features governing instability and sedimentation also develop over comparatively long time periods.

Several examples are presented to illustrate how sequences of major channel instability have propagated along the river over periods of 10 to 30 years. These disturbances often initiated new patterns of sedimentation, local erosion and subsequent channel instability further downstream. The most common diagnostic feature associated with these travelling disturbances are relatively large, low amplitude, linguoidal-shaped "gravel sheets" that attach to more stable lateral bars and islands. These bars may cause strong flow impingement against previously stable banks and islands. As a result, rapid scour and erosion may be initiated even during periods of low discharge.

Four different approaches were used to estimate the long term gravel transport rate along the river. These methods included direct measurements using trap samplers (carried out by Water Survey of Canada over a period of 12 years), a sediment budget calculation which related changes in transport through a reach to changes in the volume of sediment stored in the channel determined by surveys, a morphologic approach which used a simple model of sediment transfers through a reach, and finally theoretical bed load formulae. It was found that the sediment budget and the morphological model provided the most reliable and most generally applicable results. This was because the methods rely on observations of sediment movement over periods of years or decades. It was found that on Fraser River, the time scales of the major processes governing gravel bed load transport were also measured in years or decades. As a result, short term measurements such as from bed load trap samplers show only a poor correlation between transport rate and flow variables. Therefore, to estimate long term transport rates with these data, a very large number of observations is required to integrate the transport rates over time.

## TABLE OF CONTENTS

ABSTRACT	ii
LIST OF FIGURES	viii
LIST OF TABLES	xii
ACKNOWLEDGEMENTS	xiv
1.0 PURPOSE AND STUDY OBJECTIVES .....	1
1.1 Introduction .....	1
1.2 Study Objectives .....	4
1.3 Selection of Study Reach .....	5
1.4 Outline of the Report .....	6
2.0 THEORETICAL BASIS OF THE STUDY .....	8
2.1 Sediment Transport in Gravel Bed Rivers .....	8
2.2 Sediment Budgets .....	11
2.3 Relation between Sediment Transfers and Sediment Transport ..	20
3.0 AVAILABLE DATA .....	26
3.1 Morphologic Data .....	26
3.2 Topographic Data .....	27
3.3 Channel and Floodplain Sediments .....	28
3.4 Sediment Transport Measurements .....	29
3.4.1 Suspended Load .....	30
3.4.2 Bed Load .....	34
3.5 Channel Hydraulics .....	34

3.6	Water Temperature .....	35
3.7	Water Surface Profiles .....	35
4.0	BACKGROUND INFORMATION .....	36
4.1	Physical Setting .....	36
4.2	Hydrologic Regime .....	39
4.3	Sediment Yield .....	48
4.3.1	Total Suspended Load Characteristics .....	49
4.4	History of Improvements on Lower Fraser River .....	58
4.4.1	Dyke Construction .....	59
4.4.2	Erosion Control Structures .....	60
4.4.3	Dredging and Gravel Mining .....	63
5.0	CHANNEL MORPHOLOGY .....	66
5.1	Principal Morphological Sub-Division .....	66
5.2	Channel Characteristics & Dimensions .....	69
5.2.1	Water Surface Profiles .....	69
5.2.2	Channel Dimensions and Hydraulics .....	77
5.3	Bed Materials .....	80
5.3.1	Sampling Objectives .....	80
5.3.2	Variability of Sediments Within Bars .....	84
5.3.4	Downstream Changes in Grain Size .....	89
5.4	Bank Materials .....	99

6.0 PATTERNS OF CHANNEL INSTABILITY .....	104
6.1 Introduction .....	104
6.2 Historical Channel Changes .....	104
6.3 Factors Governing Channel Instability .....	118
7.0 SEDIMENT BUDGET OF THE LOWER FRASER RIVER .....	124
7.1 Methods .....	124
7.2 The Data .....	130
7.3 Accuracy of the Computations .....	132
7.4 Assumptions .....	141
7.5 Results .....	145
8.0 SEDIMENT TRANSFERS AND MORPHOLOGIC CHANGE .....	152
8.1 Assumptions .....	152
8.2 Long Term Sediment Transfers Along Fraser River .....	153
8.3 Estimating Bed Load Transport Rates .....	161
8.3.1 Sediment Transfers and Sediment Loads .....	161
8.3.2 Test of Neill's Approach .....	164
9.0 SEDIMENT TRANSPORT MEASUREMENTS .....	173
9.1 The Bed Load .....	173
9.1.1 Measurement Procedures .....	173
9.1.2 Data Adjustment: Sampler Efficiency .....	176
9.1.3 Reliability of the Measurements .....	178

9.1.4	Analysis of Agassiz Bedload Data .....	185
9.1.5	Estimation of Bed Load by Formulae .....	194
9.1.6	Analysis of Mission Bedload Data .....	197
9.2	The Suspended Sand Load .....	199
9.2.1	Analysis of Mission data .....	199
9.2.2	Comparisons with Agassiz and Hope .....	207
10.0	COMPARISON OF BED LOAD ESTIMATES .....	209
10.1	Objectives .....	209
10.2	Assessment of Methods .....	210
10.2.1	Reliability of the Methods .....	210
10.2.2	Appropriateness of the Methods .....	215
11.0	CONCLUSIONS .....	218
12.0	REFERENCES .....	222
	APPENDIX A .....	238

## LIST OF FIGURES

Figure		
1.1	Lower Fraser River Region	2
1.2	Study reach of lower Fraser River between Mission and Hope	3
2.1	Schematic sketch of a river showing the main sediment transfer components	14
2.2	Representation of travel times through a sediment reservoir	19
2.3	Simplified meander sweep process in natural rivers assumed by Neill	22
2.4	Sediment step lengths in a wandering river	25
3.1	Suspended load sampling frequency at Mission	31
3.2	Suspended load sampling frequency at Agassiz	32
4.1	Fraser River drainage basin	37
4.2	Extent of non-alluvial materials along lower Fraser River	40
4.3	Longterm trends in runoff; Fraser River at Hope	43
4.4	Seasonal distribution of runoff; Fraser River at Hope	44
4.5	Flow frequency distribution; Fraser River at Hope	46
4.6	Suspended load durations - Mission and Agassiz	52
4.7	Seasonal distributions of loads at Agassiz and Mission	53
4.8	Fraction of annual load transported by different flow ranges at Agassiz and Mission	55
4.9	Annual flow and sediment transport hydrographs at Agassiz, 1972	56
4.10	Seasonal hysteresis of sediment transport at Agassiz	57
5.1	Confined channel pattern between Yale and Laidlaw	67
5.2	Typical bar and island morphology in wandering reach between Peters Island and Sumas Mountain	68

5.3	Transition from gravel bed to sand bed reach near Sumas Mountain	70
5.4	Water surface profiles from Hope to Mission of 1972 and 1974 floods	71
5.5	Water surface profile in June, 1985 downstream of Agassiz - Rosedale bridge	72
5.6	Water surface profile in June, 1985 at Mission	73
5.7	Thickness of floodplain sediments on islands and banks as a function of vegetation age	75
5.8	Channel cross sections along Fraser River	78
5.9	Channel cross sections at Hope, Agassiz and Mission gauging stations	81
5.10	At a station hydraulic geometry measured at Agassiz and Mission hydrometric stations	82
5.11	Comparison of a sub-surface bar head sample with a composite sample from the entire bar - Fraser River near Sumas Mountain	86
5.12	Comparison of a sub-surface bar head sample with a composite sample of the entire bar near Agassiz - Rosedale bridge	87
5.13	Comparison of three sub-surface samples from a gravel bar near Chilliwack	88
5.14	Location of bed material samples collected in 1983 and 1984	90
5.15	Downstream variation in sub-surface particle size between Hope and Mission	93
5.16	Downstream variation in the gravel content of sub-surface samples between Hope and Mission	95
5.17	Volumetric bed material samples collected from the main channel of the river near Sumas Mountain	97
5.18	Bed material characteristics at Mission hydrometric station	98
5.19	Downstream variations in bank materials between Hope and Mission	100
5.20	Downstream variation in the gravel content of bank samples between Hope and Mission	101
6.1	Channel shift maps of lower Fraser River, 1890 to 1971	105



6.2	Channel changes in the Peters Island to Herrling Island reach	106
6.3	Channel changes in the Herrling Island -Rosedale bridge reach	107
6.4	Channel changes in the Greyell Island - Carey Point reach	108
6.5	Channel changes in the Carey Point - Harrison River reach	109
6.6	Channel changes in the Chilliwack Mountain to Sumas Mountain reach	110
6.7	Comparative surveys of bankline changes near Carey Point	116
6.8	Stability of channel bends in the wandering gravel bed reach	121
7.1	Location of sub-reaches in sediment budget analysis	126
7.2	Flow chart of digital terrain model computing volumetric changes between successive surveys	128
7.3	Comparison tests to evaluate the effect of grid cell spacing on the precision of mean bed levels in a 2 km long, 1 km wide reach	133
7.4	Average gravel transport between Agassiz-Rosedale bridge and Mission over the period 1952 to 1984	149
8.1	Overall pattern of deposition and erosion along lower Fraser River	154
8.2	Distribution of historical bank erosion rate along the wandering reach	155
8.3	Cumulative distribution of basal gravel bank erosion quantities in three time periods	158
8.4	Cumulative distribution of sandy-silty floodplain sediment bank erosion quantities in three time periods	160
8.5	Test reach for estimating gravel sediment transport from meander sweep progression	166
8.6	Historical variations in bank erosion at lower Herrling Island	167
8.7	Historical channel changes at Agassiz gauging cross section	170
8.8	Channel aggradation at mid-channel bar downstream of Agassiz-Rosedale bridge	171
9.1	Sediment sampling vertical at Agassiz hydrometric station	175

9.2	Replicate sampling to measure variations in bed load sample catches at Agassiz and Mission	181
9.3	Precision of n-sample bed load measurements at a single vertical at Agassiz and Mission	183
9.4	Precision of 3 sample per vertical bed load measurements in a hypothetical cross section	187
9.5	Bed load rating curve at Agassiz hydrometric station, 1968-1976	188
9.6	Variation in annual bed load transport at Agassiz, based on rating curve estimates	190
9.7	Fraction of annual bed load transported by various discharge ranges	193
9.8	Range in bed load transport predictions at Agassiz from theoretical formulae using at-a-station hydraulic geometry	196
9.9	Bed load rating curve at Mission, 1968 - 1979	198
9.10	Average particle size characteristics of bed load trapped at Mission	201
9.11	Average particle size distribution of depth integrated suspended sediment samples at Hope, Agassiz, Mission and Port Mann	208

## LIST OF TABLES

### Table

3.1	Lower Fraser River hydrometric station summary	33
4.1	Discharge summary for lower Fraser River	42
4.2	Historical flood occurrences at Hope and Mission	47
4.3	Annual suspended load on lower Fraser River, 1966 to 1983	50
4.4	History of early erosion control work	61
4.5	Extent of bank protection works along Fraser River	62
4.6	Estimates of gravel quantities removed from the Fraser River between Hope and Sumas Mountain as a result of gravel mining operations	65
5.1	Relation between vegetation age and bankfull discharge capacity along lower Fraser River	76
5.2	Mean hydraulic geometry at various reaches of the Fraser River between Hope and Mission	79
5.3	Channel characteristics at Hope, Agassiz and Mission gauging stations	83
5.4	Sub-surface bed material characteristics along Fraser River	91
5.5	Basal gravel layer bank material characteristics along Fraser River	102
7.1	Root mean square errors of spot elevations computed from digital terrain model	135
7.2	Precision classes assigned to each sub-reach in the sediment budget	142
7.3	Assumed composition of bed and bank materials in each sub-reach in the sediment budget	144
7.4	Overall results of sediment budget analysis, 1952 to 1984	146
7.5	Bed and bank changes in each sub-reach of the sediment budget, 1952 to 1984	147
8.1	Summary of bank erosion rates along lower Fraser River	156
8.2	Summary of sediment transfers and bed load transport estimates	163

9.1	Annual bed load transport rate at Mission, 1966 to 1986	200
9.2	Average composition of the suspended load at Mission by month	205
9.3	Annual suspended load at Mission by size fraction	206
10.1	Comparison of estimated gravel loads by different methods	211

## ACKNOWLEDGEMENTS

I would like to thank all members of my committee for their time and efforts involved in bringing this study to completion. In particular I would like to thank Dr. Mike Church for his support, inspiration and guidance throughout the study. I would also like to acknowledge the generous support and technical assistance provided by Mr. Bruno Tassone, P. Eng. and Dr. Terry Day of the Sediment Survey, Environment Canada. Much of this research was funded through Supply and Services Canada Contract 1ST83-00170, administered by Sediment Survey, Ottawa.

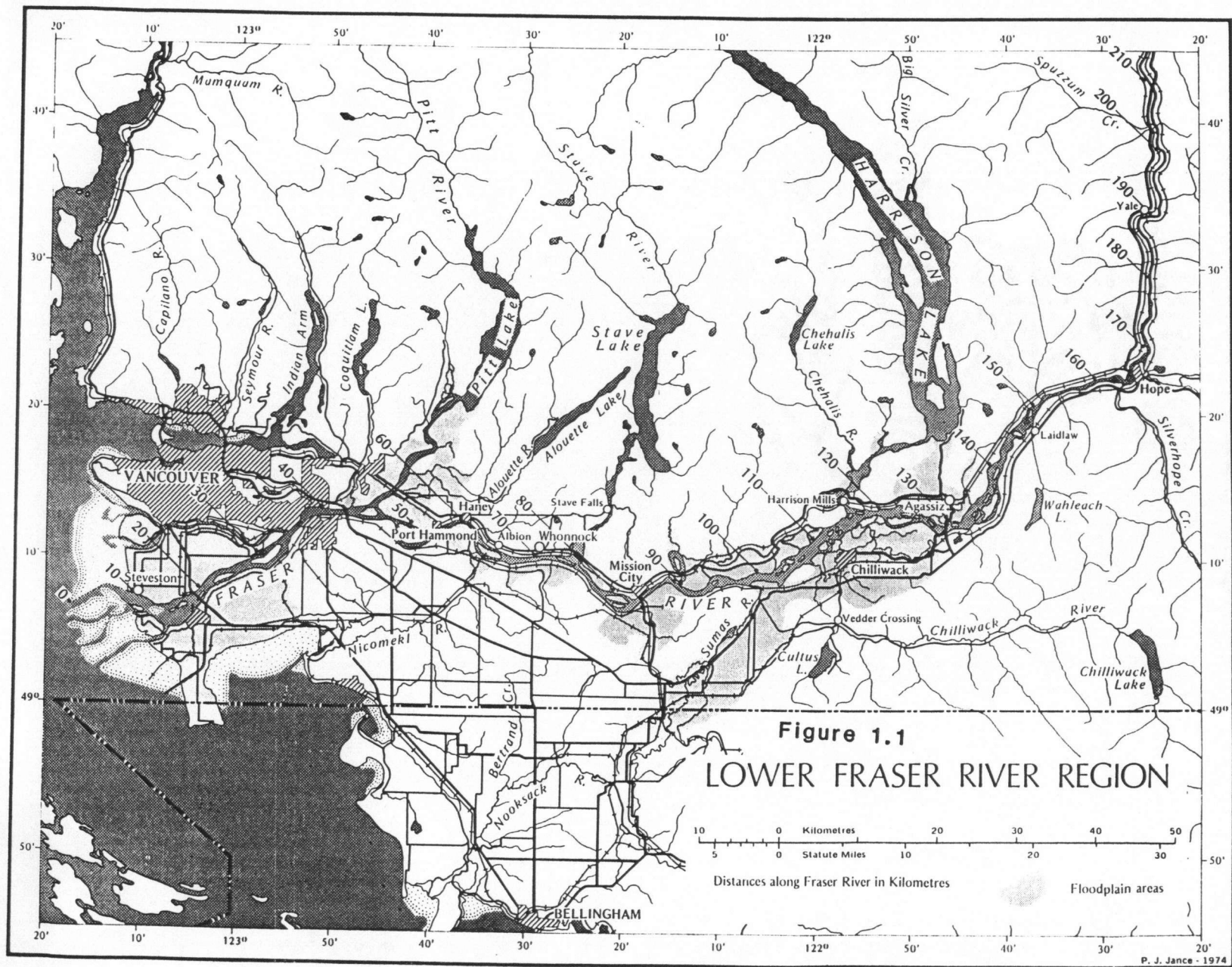
Finally, I would like to thank my wonderful wife, Cathy who provided so much support when I was on the verge of giving up.

## 1.0 PURPOSE AND STUDY OBJECTIVES

### 1.1 Introduction

This study investigates the major processes governing channel instability, sedimentation and channel morphology on the lower Fraser River, British Columbia. The study reach extends approximately 85 km from below the Fraser Canyon near Hope to the commencement of the tidally influenced sand bed portion of the river near Mission (Figure 1.1). In this reach the Fraser River has developed a very characteristic "wandering" channel pattern (Figure 1.2). The term "wandering river" was first used by Neill (1973) to describe a particular stream "type" that flows in several channels which are divided by wooded islands. The channels are subject to irregular channel shifting and erosion of floodplain banks and islands. This produces an ongoing sequence of erosion, downstream transfer of sediment and island/floodplain re-construction along the river. The "wandering" river pattern is one of the most common types found in large mainstem rivers within the mountains and foothills of Western Canada. The pattern differs from more classic "anastomosing" patterns (Smith, 1983) in which the sinuosity is higher, the bed sediments are finer, and the islands and bars are more permanent features.

A number of engineering and river management problems arise on "wandering" rivers. Solving these problems generally requires having to answer questions concerning the future evolution of the river channel.





Laidlaw



Figure 1.2 Study reach of lower Fraser River between Mission and Laidlaw



## 1.2 Study Objectives

The overall objective of this study is to demonstrate the feasibility of assessing the processes governing channel instability and sedimentation on a "wandering" gravel bed river by examining its morphological features and by reviewing its history of past channel behaviour. As a result, observed morphological changes may be used to make inferences about the river's sediment transport processes (Kellerhals, Church and Bray, 1975). Furthermore, this work assesses the relation between channel instability and sediment transport by examining the linkage between the transfers of sediments from floodplain and islands to the channel and subsequent downstream morphologic change. The connection between channel morphology and sediment transport is investigated over time scales of years to decades, which is the appropriate scale for characterizing sediment movement and channel evolution on most large rivers.

The emphasis of this work has been placed on three main topics.

Patterns of Channel Instability: Can patterns of channel instability be identified on "wandering" rivers and are there diagnostic features that can be used to predict where future instability is most likely to occur?

Factors Governing Channel Instability: What are the most important factors that govern the occurrence of channel instability along a "wandering" river and what is

the appropriate time scale for characterizing the channel evolution associated with this instability?

Relation Between Sediment Transport and Transfers: Can observed sediment transfers resulting from bank and island erosion and re-construction be used to estimate the bed load transport along a "wandering" gravel bed river? What is the relation between the sediment transfers which result from morphologic change along the river, and the sediment transport through the reach?

Stemming from this last topic a second objective of the report has been to assess some aspects of the methodology that is presently used in field investigations of sedimentation and sediment transport on gravel bed rivers. This work has focused on the issue of field measurement reliability and assesses the most appropriate operational methods to investigate sediment transport processes on large gravel bed rivers.

### 1.3 Selection of Study Reach

There are two main reasons for choosing the lower Fraser River as the study reach in this investigation. First, the sedimentation issues on Fraser River are important and there are many practical river management problems that require better understanding of sedimentation processes (Kellerhals Engineering Services, 1985).

Second, the available sediment transport and morphologic data that have been collected on the lower Fraser River are very extensive. In fact, it is fair to state that the sediment records on the Fraser River, (collected mainly by Water Survey of Canada) are as complete as on any large river in the world. This has provided an opportunity to test different computational methods and to check estimates by a number of independent techniques. As a result, it has been possible to evaluate the suitability of different methods for assessing sediment transport on large gravel bed rivers.

#### 1.4 Outline of the Report

The theoretical bases for the methods used in this study are outlined in Chapter 2. Chapter 3 summarizes the basic data used in the analysis while Chapter 4 provides additional background data on the physical setting of the test reach. Chapter 5 documents the river's morphology and Chapter 6 describes the patterns of channel instability that have occurred within historic times. This chapter also illustrates some of the most important factors that have governed the river's instability. Chapter 7 presents a detailed, reach by reach sediment budget for the gravel load. This analysis is based on a comparison of hydrographic surveys that were conducted on the river in 1952 and 1984. In Chapter 8 estimates of long term bed load transport are derived from observed morphologic changes along the river. Chapter 9 presents an analysis of sediment transport measurements collected by Water Survey of Canada using conventional sediment sampling techniques over the last 25 years.

The results from the bed load measurements are also compared with predictions from theoretical sediment transport formulae. This work provides an additional, independent means for assessing the results of the morphologic computations and the sediment budget analysis. Finally, Chapter 10 compares the results from the three independent methods of analysis and discusses the limitations, reliability and practical requirements associated with each method. The final study conclusions are presented in Chapter 11.

## 2.0 THEORETICAL BASIS OF THE STUDY

### 2.1 Sediment Transport in Gravel Bed Rivers

Traditionally, most research on gravel bed load transport has utilized a "mechanistic" approach to formulate the important factors or variables that govern sediment entrainment or transport. These approaches have used deterministic methods (Bagnold, 1977), stochastic methods (Einstein, 1950) and analyses based on dimensional analysis (Meyer-Peter & Muller, 1948; Ackers and White, 1973; Parker et al, 1982).

Recent comparisons between field measurements from gravel bed streams and predictions from equations illustrated the limitations of sediment transport equations (Gomez and Church, 1989; White, Milli and Crabbe, 1975). Some of the complicating factors that limit the usefulness of sediment transport theories on gravel-bed rivers are summarized in Church (1985).

One important feature of gravel bed streams is that they usually display "macroscopic" segregation of sediments in the active channel zone. For example, sediments in bar heads and riffles may consist of gravel and cobble sized materials while the sediments in more distal areas and the inner sides of bars may consist almost entirely of sands. Describing this spatial variability in a quantitative fashion presents an enormous field sampling problem (Church, McLean and Wolcott, 1986).

Incorporating this variability into analytical models has not been attempted to-date so that sediment transport has traditionally been represented by means of a one dimensional analysis.

In addition to "macroscopic" variations, it is well known that gravel sediments tend to become segregated into a coarse surface layer and a finer, underlying sub-surface layer. This segregation has been termed "armouring" or "paving" and has been interpreted as one mechanism for maintaining near equal mobility of the sediments composing the channel (Parker and Klingeman, 1982). Until the coarse surface layer is mobilized, the bed load transport rate will not be in equilibrium with the local channel hydraulics. Bed load movement during flows below this threshold has been described as analogous to "wash load" since its rate will depend on its availability and not the local hydraulic conditions (Parker et al, 1982). For example, during relatively low flows a bank may collapse and add a "slug" of poorly sorted, fine gravel sediments to the stream. These materials may move over top of the immobile, relatively coarser surface layer in the channel. However, once this supply is exhausted the transport will return to near zero.

The flow condition necessary for equilibrium transport will depend on the stresses necessary for mobilizing the surface layer. This condition can be described in terms of the Shields relation. In previous studies, a dimensionless Shields parameter of 0.03 has been commonly used to describe the initiation of motion of sediment mixtures. On most gravel-bed streams in western Canada, the Shields parameters

are very close to threshold, even during relatively severe floods (Kellerhals, Neill & Bray, 1972). Over most flow conditions in gravel bed streams, the armoured surface layer probably will not be in motion. Therefore, equilibrium transport will not be achieved under most flow conditions. Studies by Hudson (1981) on the Elbow River in Alberta and Andrews (1983) on the East Fork River have emphasized this point.

There are several other features that are known to affect entrainment from the surface layer and sediment mobility. For example, imbrication and particle clustering can cause "structural strengthening" of the surface sediments and greatly reduce their mobility (Church, 1972; Laronne and Carson, 1976; Brayshaw, 1983). As a result, the hydraulic conditions required to mobilize the bed will often depend on the history of past flow and sediment transport events. Such processes can not easily be characterized in a deterministic fashion and add a stochastic component to the nature of sediment transport. Again, this will cause the sediment transport rate to become dependent on the flow history and not just on the local hydraulic conditions.

Finally, it is generally recognized that bed load transport is linked with erosion and deposition of bar and bank material along the channel. Long term fluctuations in bed load transport may be associated with bar migration and other channel evolution processes. "Wave-like" movement of gravels along a stream has been described by Griffiths and Sutherland (1977) and Meade (1984).

Traditionally, it has been a goal of sediment transport researchers to develop models that rely on sediment transport equations to try to predict the pattern and rate of morphologic changes along a river (Hydrologic Engineering Center, 1977). However, in light of the foregoing considerations it is perhaps more appropriate to study the patterns of past morphologic change along a reach of river and use this information to infer something about the sediment transport regime. Two variations of this "morphologic approach" have been tested in this study. The first approach involves developing an overall sediment budget for a reach of the Fraser River in order to describe the relation between the incoming and outgoing loads and the channel changes occurring within the reach over a period of time. This approach is based simply on the continuity equation and therefore is very general in its application. However, the data requirements for its application are quite large. The second approach that has been tested infers sediment transport rates from observed planimetric changes in a reach. This approach requires accepting a model that relates patterns of sediment movement (deposition and erosion) and sediment transport, (flux at a particular cross section). Since the data requirements for this approach are relatively modest, the method is potentially a very powerful tool.

## 2.2 Sediment Budgets

A sediment budget is simply an accounting procedure that quantifies the sediment inflows and outflows and changes in storage within a specified control volume. The approach was formally presented by Popov (1962) and was used to assess



sedimentation processes along a 450 km reach of the Ob River, U.S.S.R. More recently sediment budgets have been promoted as a useful tool for assessing rates of sediment production in small, mountainous basins (Swanson et al, 1982).

Over any arbitrary time period  $\Delta t$  a sediment budget can be expressed as:

$$Q_o = Q_i + \Delta S / \Delta t \quad \text{where;}$$

$Q_o$  and  $Q_i$  are the sediment output and input respectively;

$\Delta S$  is the net change in storage within the reach, per unit of time  $\Delta t$ .

Since  $Q_i$  for the reach in question is equal to  $Q_o$  for the next reach upstream, the calculations can be extended upstream on a reach by reach basis. Furthermore, if the sediment transport is known at the most distal section in the reach, then the incoming load may be calculated.

Construction of a sediment budget involves several tasks, including:

- definition of the storage reservoirs to be considered;
- identification of the sediment transfer processes or linkages between the various storage reservoirs;
- deciding on the appropriate time scale for conducting the sediment budget;

- comparing successive surveys or other historical data to estimate rates of morphologic change within the study reach;
- applying the continuity equation to solve for the unknown terms in the budget.

For a relatively large lowland gravel bed river there are two primary storage reservoirs to be considered. These are the active channel zone, which consists of sediments contained in gravel bars and the channel bed; and the floodplain (including wooded islands). Figure 2.1 illustrates the most important sediment transfers that occur between these reservoirs. These include bank erosion ( $E_f$ ), which transfers sediment from the floodplain and islands into the active channel zone; and island/floodplain reconstruction ( $D_f$ ) which involves a transfer of sediments from the active channel back into the floodplain. The net volume change in the floodplain reservoir,  $\Delta S_f$  is  $D_f - E_f$ . The corresponding net volume changes in the active channel reservoir,  $\Delta S_c$  are computed as the difference between channel deposition,  $D_c$  and channel scour  $E_c$ . The sediment budget for the active channel reach can be written as:

$$Q_i - Q_o = \Delta S_f / \Delta t + \Delta S_c / \Delta t$$

Therefore, the load into a reach can be computed as:

$$Q_i = Q_o + (\Delta S_f + \Delta S_c) / \Delta t$$

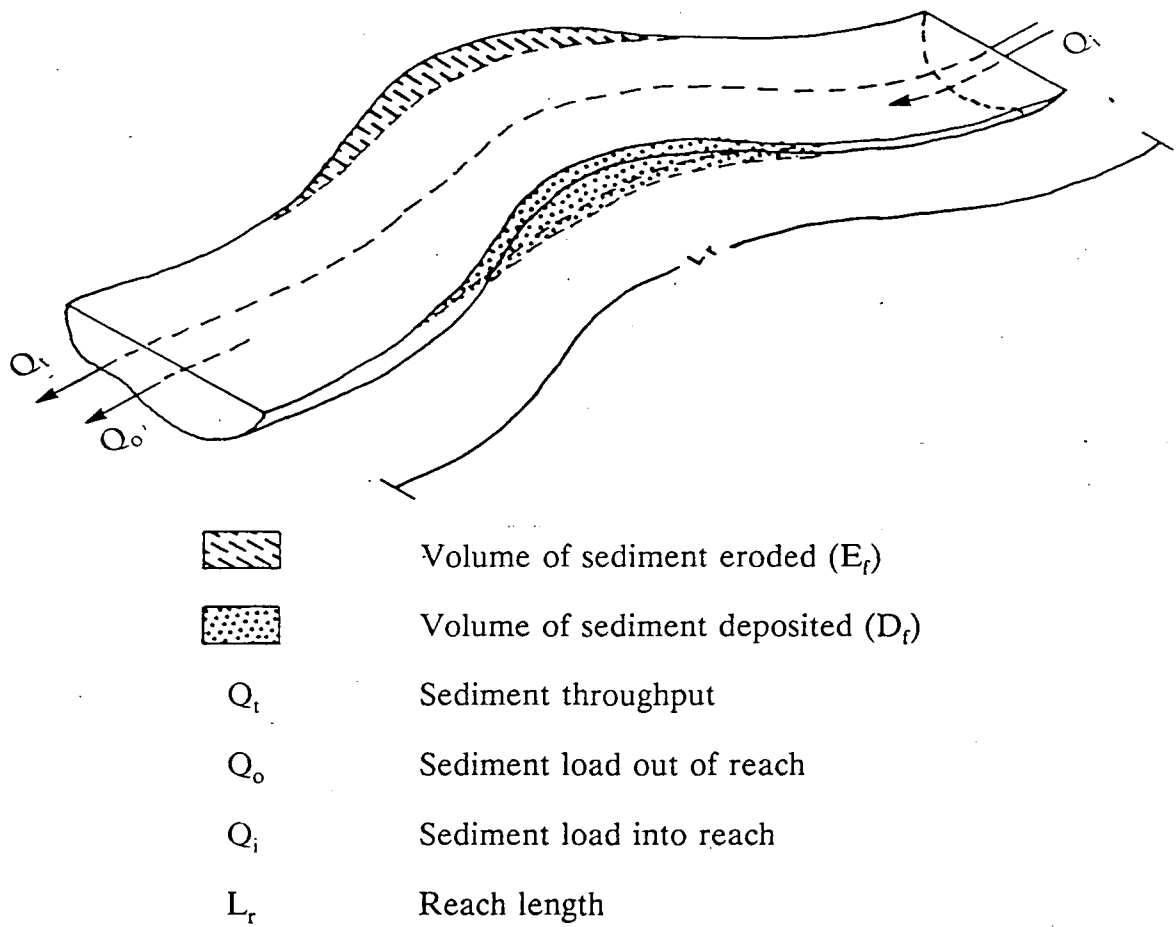


Figure 2.1 Schematic sketch of a river reach showing the main sediment transfer components

If the outgoing load from the reach is known, then direct estimates can be made of the incoming load. The outgoing load may be known from direct measurements. In other cases the downstream boundary condition for the sediment budget can be pre-selected so that the outgoing load is known. For example, the sediment load at the outlet of a lake or reservoir may be negligible.

In such circumstances the calculations can be repeated upstream on successive reaches and estimates of sediment transport can be made along the river without resort to direct measurements.

The sediment "throughput" has been defined (Church et al, 1987) as :

$$Q_t = Q_o - E_f - E_c = Q_i - D_c - D_f$$

This quantity represents the portion of the sediment load that, once entrained, travels all the way through the reach without being redeposited in it.

If the outgoing load is not known then only the net change in transport ( $Q_i - Q_o$ ) may be evaluated. For a river reach that is in equilibrium, so that the net erosion and deposition balance, this quantity must be zero. However, the time scale over which the comparison is made will have a major impact on the results from the sediment budget. If the time scale for channel adjustments is very long then

sequences of apparent deposition or erosion within a reach may persist over periods of years to decades, and be difficult to detect in short-term data.

The relation between time scales and interactions between sediment "reservoirs" has been addressed by Dietrich and Dunne (1978) and Dietrich et al (1982). This work has involved identifying specific reservoirs in a watershed and then investigating the movement of materials through them. The initial volume of sediment in the floodplain ( $V_f$ ) and active channel ( $V_c$ ) reservoirs can be defined from channel surveys. One common decision is to compute the volume of sediment contained above the lowest measured bed elevation in the reach. This minimum bed level typically occurs in a scour hole; for example, at the outside of a bend or in a constriction. It is assumed that sediments below this level are inactive and do not take part in erosion or deposition processes. Over time, the quantity of sediment in the active channel and floodplain reservoirs may change. For example, if the river is systematically widening over time the volume of sediment in the active channel reservoir will increase.

A special case of sediment transfer and transport has been described by Dietrich et al., (1982). In this equilibrium case the volume of the sediment reservoirs will be constant over some time period and furthermore, the inflow and outflow will be

equal. Under these particular conditions the transfers between floodplain and channel must balance so that:

$$\Delta S_c + \Delta S_f = 0$$

The "age", average "transit time" and the "turnover time" are commonly used to define the time scales of a sediment reservoir (Dietrich et al, 1982). The "age" ( $T_a$ ) refers to the time that the sediments have spent in the reservoir since their introduction.

$$T_a = 1/M_o \int t * dM(t) \quad \text{where;}$$

$M_o$  is the total mass of the sediments in the reservoir;

$dM(t)$  is the incremental mass of sediments having age  $t$

The "transit time" ( $T_t$ ) represents the age of the sediments when they leave the reservoir.

$$T_t = 1/F_o \int t * dF(t) \quad \text{where;}$$

$F_o$  is the total flux of sediment through the reservoir;

$dF(t)$  is the increment flux passing out of the reservoir after time  $t$ .

Therefore, the average age is weighted with respect to mass while the average transit time is weighted with respect to flux.

The "turnover time" ( $T_o$ ) is defined simply as the ratio of the total mass of sediment in the reservoir to the flux through the reservoir:

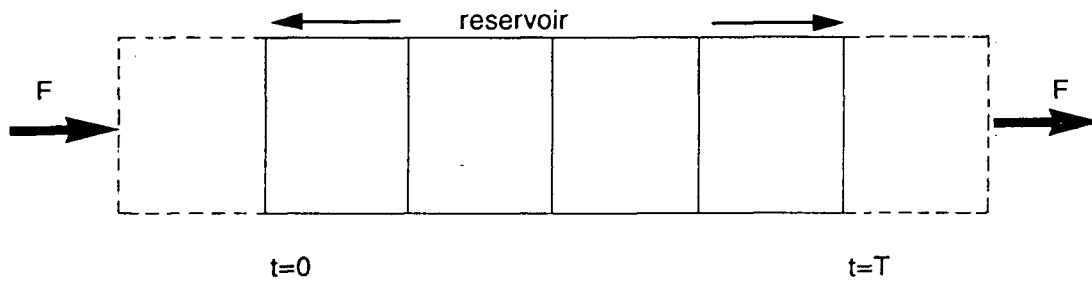
$$T_o = M/F$$

The case of a reservoir of mass  $M$  with a flux  $F$  under a steady state equilibrium condition has been used to represent a wide range of hydrologic and meteorological processes. This is mainly because the case is amenable to simple mathematical analysis. The work of Eriksson (1963) and later Bolin and Rodhe (1973) provide a means to assess the average transit time and average age of sediments in a natural channel or floodplain reservoir. For the steady state condition, the average transit time  $T_t$  will be equal to the turnover time (Bolin and Rodhe, 1973). However, the average age of the material in the reservoir may be greater than, equal to or less than the transit time.

The simplest steady state model of sediment movement through a single reservoir is illustrated in Figure 2.2. In this case sediment enters the reservoir at the upstream end and exits  $T$  years later. The movement is somewhat analogous to transport on a "conveyor belt". The average transit time of the sediments is  $T$  years and the average age of the sediments in the reservoir is  $T/2$  years.

However, for comparison, consider the case of two sediment sources to the reservoir of equal flux. However, for source 1 the sediment requires  $T_1$  years to pass through

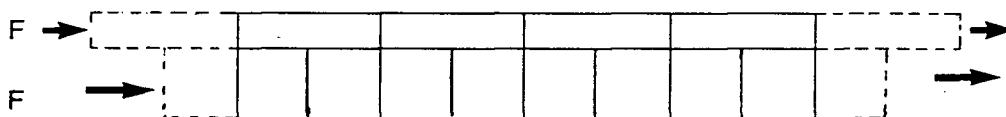
Case 1. Simple conveyor belt model of sediment transport



the average age of sediments in the reservoir =  $T/2$

the transit time for sediments passing through the reservoir =  $T$

Case 2. Simple model with multiple sediment inputs



the sediment flux from each source is equal

the travel times associated with each source are different

Figure 2.2 Representation of travel times through a sediment reservoir



the reservoir while the sediments from source 2 require  $T_2$  years. In this case the average transit time will be;

$$T_t = (F \cdot T_1 + F \cdot T_2) / 2 \cdot F = (T_1 + T_2) / 2$$

The average age of the sediments will be:

$$T_a = 1/2 \cdot (T_1^2 + T_2^2) / (T_1 + T_2)$$

For this case the average age will be less than the average transit time. Dietrich et al (1982) have pointed out that the assumption of steady state conditions in most sediment reservoirs is probably not very realistic when considered over a few years. However for the case of lowland rivers where most sediment transfers result from ongoing bank erosion and deposition, a steady state assumption may be reasonable when considered over a few decades. In general, the time interval required to meet the assumption of steady state conditions will be directly proportional to the transit time.

### 2.3 Relation between Sediment Transfers and Sediment Transport

Neill (1971) was one of the first to quantify the relation between sediment transport and morphologic change. His analysis considered the case of a regular down-valley migration of meanders and related the amount of bank erosion along the concave

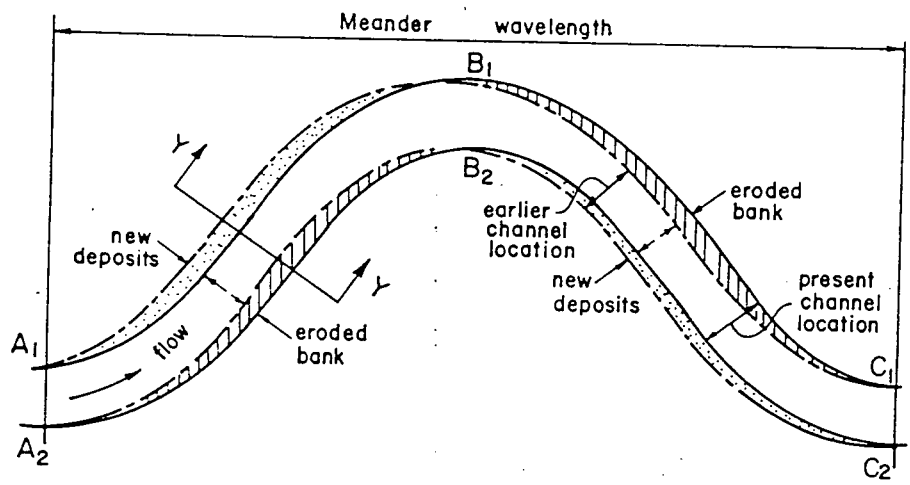
outer bank to the quantity of sediment transported past an arbitrary cross section (Figure 2.3). Citing laboratory experiments from Friedkin (1945) he assumed that material eroded from the receding bank on one side of the bend was deposited in the form of a point bar on the accreting bank of the next bend downstream. After deposition, it was assumed the sediments became incorporated into the floodplain and were not eroded again until the entire pattern had shifted one wave length down-valley. The average length of travel of sediment along the channel ( $L_e$ ) was assumed to be half of the length of a full meander bend. The volumetric transport rate, ( $Q$ ), was estimated to be:

$$Q = L_e * h * de/dt \quad \text{where :}$$

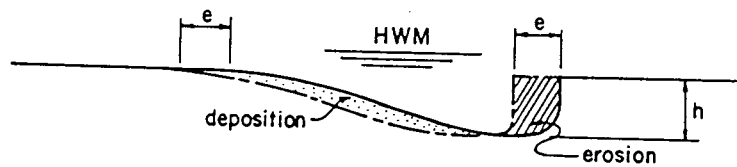
$h$  is the average bank height ;

$de/dt$  is the average bank recession rate.

Neill was careful to point out that this transport rate may correspond to a lower bound value since some sediment may move through the reach without taking part in the exchange process. For example, some artificially stabilized bends have adjusted their geometry so that sediment can pass directly through the reach without being deposited on the river bank of the bend. If morphologic methods are to be of use for predicting the actual bed load rate, then the quantity of sediment that behaves as "through put" will have to be small relative to the amount of material that is being transferred between morphologic features.



PLAN OF MEANDER LOOP MIGRATING DOWN-VALLEY



CROSS — SECTION Y-Y

Figure 2.3 Simplified meander sweep process in natural rivers assumed by Neill

Neill's analysis did not consider the time scale over which the morphologic change took place. For example, once sediment is eroded from a bank, the travel time that elapses before it goes back into storage could be several years. Under this condition the total quantity of erosion and deposition will not balance on a year to year basis. Instead, the channel migration may consist of an irregular "accordion" pattern of shifts with first one bank migrating rapidly and then stalling and remaining stable until deposition at the opposite bank produces sufficient accretion for it to "catch up". Such a pattern of behaviour has been noted previously by Nanson and Hickin (1983).

Under this condition the average rate of transport can be expressed as:

$$Q = h * dA * C_b / L_e \text{ where;}$$

$h * dA$  represents the volume of sediment eroded in the reach  $L_e$ ;

$C_b$  is the average celerity of the sediment moving through the reach;

The appropriate time scale for estimating an average transport rate would be at least  $L_e / C_b$ . Using this form of the equation, the method can be applied to other stream types provided that an appropriate step length,  $L_e$  can be defined. For the case of a "wandering" channel type, this should be feasible provided the pattern or style of morphologic change can be identified and a long history of changes can be compiled. However, it should be recognized that in some channel types there may be multiple step lengths (for example, see Figure 2.4) or the step lengths may not be

easily defined. Different step lengths may also occur in a reach as a result of differences arising in stage changes. For example, during low discharges the river could flow within a number of relatively narrow distributary channels, each of which has a different characteristic step length. During flood flows the river may have only a single wide channel with a much larger characteristic step length.

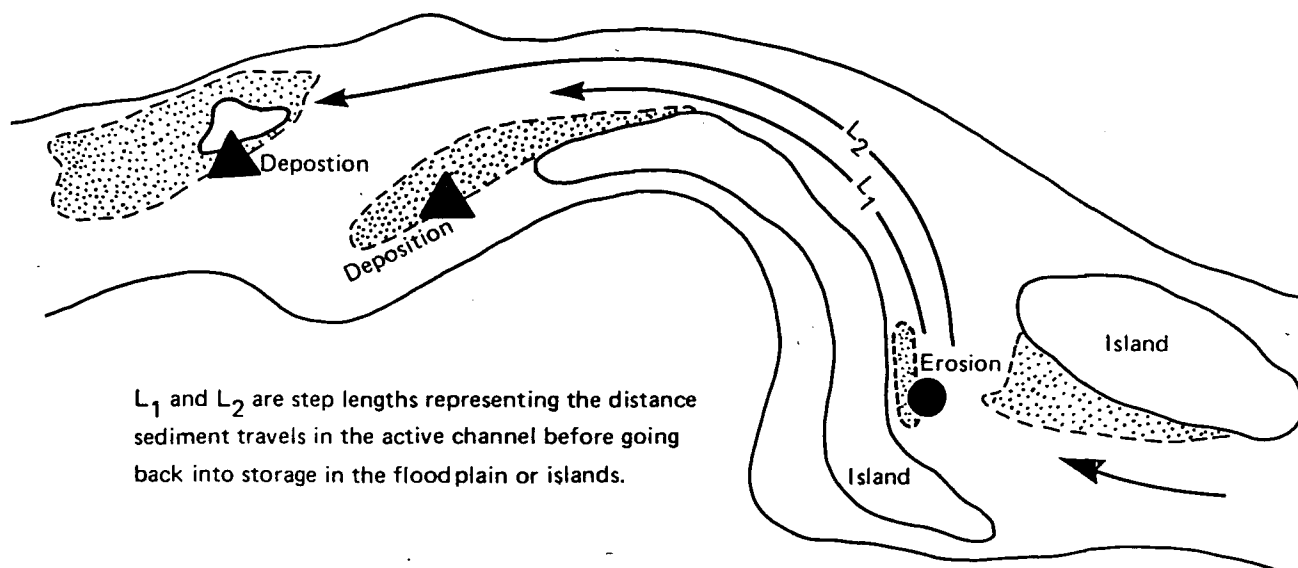


Figure 2.4 Sediment step lengths in a wandering river

### **3.0 AVAILABLE DATA**

#### **3.1 Morphologic Data**

The primary data available for assessing morphologic changes and channel pattern evolution of the lower Fraser River are the maps and air photos that have been produced over the last century. A compilation of available historical data is given in Church et al (1984).

In this study the earliest maps judged adequate for assessing morphologic change were the legal township surveys of 1876 - 1902. In these surveys the banklines of the river channel and islands were determined with particular care. The earliest air photos of the river were taken in 1928. Additional air photo coverage of the entire study reach was obtained from the survey agencies (federal and provincial) at approximately 5 to 10 year intervals after this date.

Air photo sets for analysis were selected in order to closely match discharge conditions (and hence river stages) between flights. All photos (except for the 1928 flight) were taken during the low water season between December and March and the range of discharges was very small. As a result, any apparent changes introduced by variations in bar and channel exposure will be very small.

### 3.2 Topographic Data

The earliest comprehensive channel survey in the study reach was conducted in the 1880's. The original maps were destroyed in the New Westminster fire of 1898 and no other copies have been located (Public Works Canada, 1962). The next comprehensive survey of the river was completed in 1952 by the Department of Public Works. This survey extended over a length of 120 km from Barnston Island to Yale and included measurement of approximately 1,500 river cross sections. Floodplain and island topography were mapped photogrammetrically. The river topography was compiled on 18 map sheets at a scale of 1:4,800. Less extensive river surveys were also carried out in 1963 as part of river control studies in the 10 km Agassiz to Carey Point Reach (Public Works Canada, 1964).

A complete re-survey of the river from Agassiz to Mission was carried out by the writer in 1984 with the co-operation and assistance of Environment Canada. The 50 km extent of this survey defines the main reach for the sediment budget analysis described in Chapter 7. The main field work that was completed in 1984 is described in Appendix A. The survey included establishment of 110 horizontal and vertical control points along the river and 62 temporary mapping control points. Based on this control, 400 main channel cross sections were surveyed over a 38.5 km length of river using an automated hydrographic survey system (Durette and Zrymiak, 1978). Conventional hydrographic methods were used to survey an additional 65 main channel cross sections and 18 km of side channel. Terrestrial



surveying methods were used to map exposed bars, bank lines and island topography. Approximately one man year of effort was spent completing the field component of this survey, with additional time required for data reduction and map generation. Final results from this work have been summarized on a set of 13 map sheets at a scale of 1:5,000.

### 3.3 Channel and Floodplain Sediments

The size distribution of the sediments in the channel and river banks was required in order to develop a quantitative budget of the gravel sediments. Particle size data were also required in order to assess sorting processes along the river. The sediment sampling program was directed towards two main types of information. First, sediment samples were taken from the mobile sediments in the active gravel bars along the river between Hope and Sumas Mountain. The sediments from these sites were assumed to be representative of bed load that is stored within the active channel zone. Second, samples were taken from actively eroding floodplain and island banks. This information was used in conjunction with calculations to estimate the quantity of gravel sediments that are being supplied to the channel from bank erosion. Volumetric (bulk) sampling methods were used in this study; other methods, such as surface sampling using a tape or grid would not have provided representative estimates of the composition of the deposits. In total, approximately 8 tonnes of sediment were manually field sieved at 85 sites along the river during the 1983 field season.

Additional bed material samples also have been collected from the main channel by Water Survey of Canada at the gauging station cross sections near Hope, Mission and Agassiz. Between 1965 and 1983 WSC collected 165 bed material samples at Mission with a U.S. BM54 sampler. The samples were collected from five locations across the channel. The BM54 sampler collects only a very small sample (less than 1 kg) so that the individual measurements are too small to adequately represent the coarsest material (16 mm - 32 mm) found in the river bed (ISO, 1977; Church et al., 1982). However, the composite of all samples collected in a year should provide a reasonably representative measurement. It should also be noted that the BM54 sampler penetrates only the top 50 mm of the bed and therefore provides essentially a surface sample. A few bed material samples were collected by WSC at Agassiz in 1978 and 1979. However, based on current standards (ISO, 1977) it is clear that these samples were much too small (less than 10 kg) to provide any useful information about the coarse gravel sediments in this reach. Therefore, these data were not used in this investigation.

### 3.4 Sediment Transport Measurements

The first sediment transport measurements on the Fraser River were collected by Johnston (1921) at New Westminster. Later on, a systematic program of measurements was carried out between 1950 and 1952 at Hope (Kidd, 1953). These data were used by Mathews and Shepard (1962) to estimate the long term sedimentation rate at the Fraser delta. In 1965 Water Survey of Canada began a

comprehensive program to measure the suspended load and bed load at several locations along the main stem and on some tributaries. Since this time bed load and suspended load have been measured periodically at Port Mann, Mission and Agassiz. Only suspended load data have been collected at Hope. A summary of the available sediment data resulting from this program is given in Table 3.1. Some early results from these measurements were analysed by Tywoniuk (1972) and by Pretious (1972). More recently the data have been reviewed by Western Canada Hydraulics Laboratories Ltd. (1978) and an overview of the program was prepared by Kellerhals (1984). However, for the most part, the data have received very little systematic or critical analysis.

#### **3.4.1 Suspended Load**

Figures 3.1 and 3.2 show the frequency of suspended sediment sampling by Water Survey of Canada at Mission and Agassiz. Daily suspended sediment concentrations and loads have been published by WSC for Hope (1965 - 1979), Agassiz (1966 - 1986) and Mission (1965 - 1988). These daily loads include estimated values for days when samples were not collected. In addition the actual instantaneous measured values are adjusted to estimate the daily averages. The actually observed depth-integrated or point-integrated concentrations and particle size data are also reported. This information was all available on computer tape, which made manipulation of the relatively large amount of data simple.

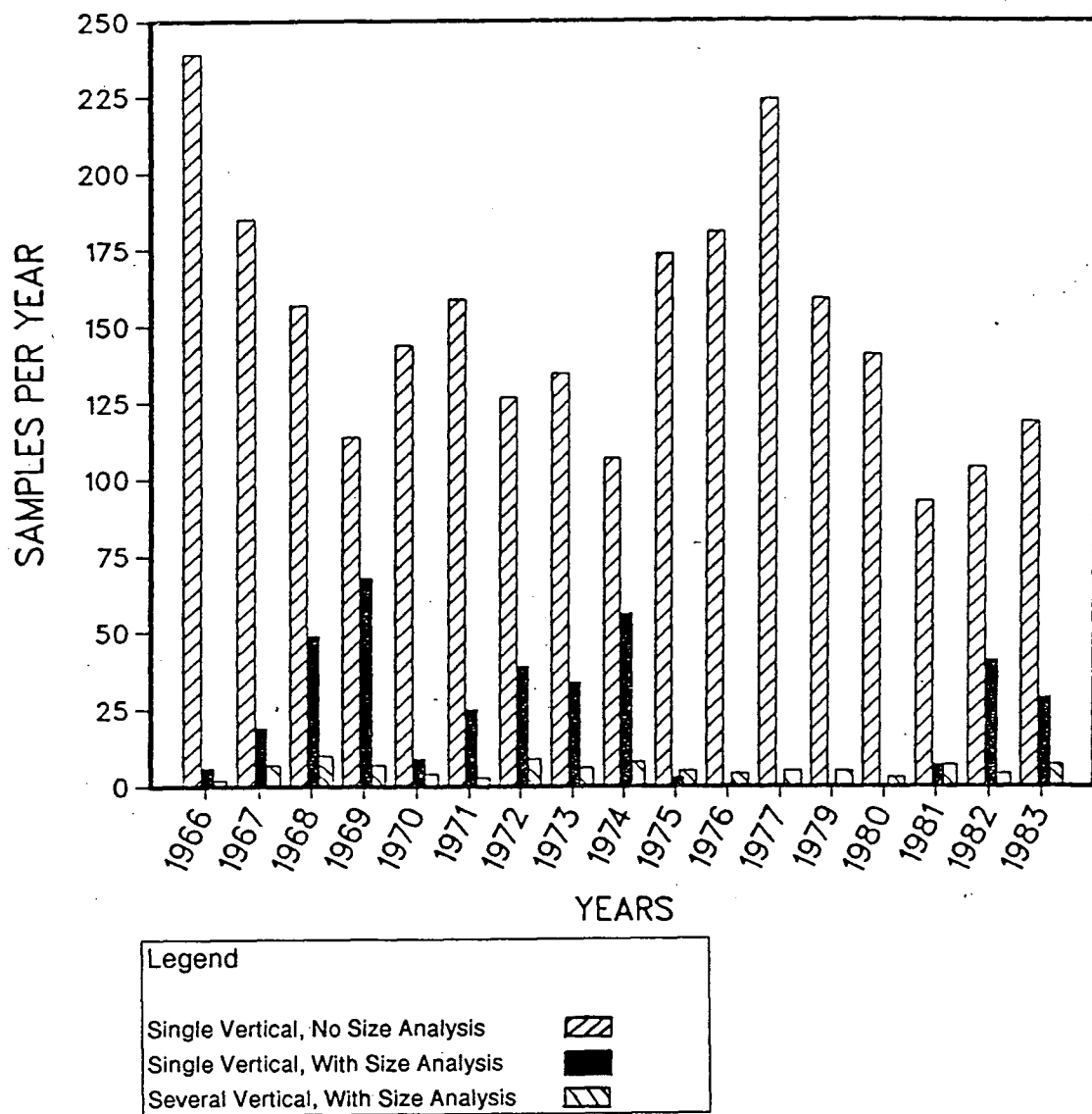


Figure 3.1 Suspended load sampling frequency at Mission

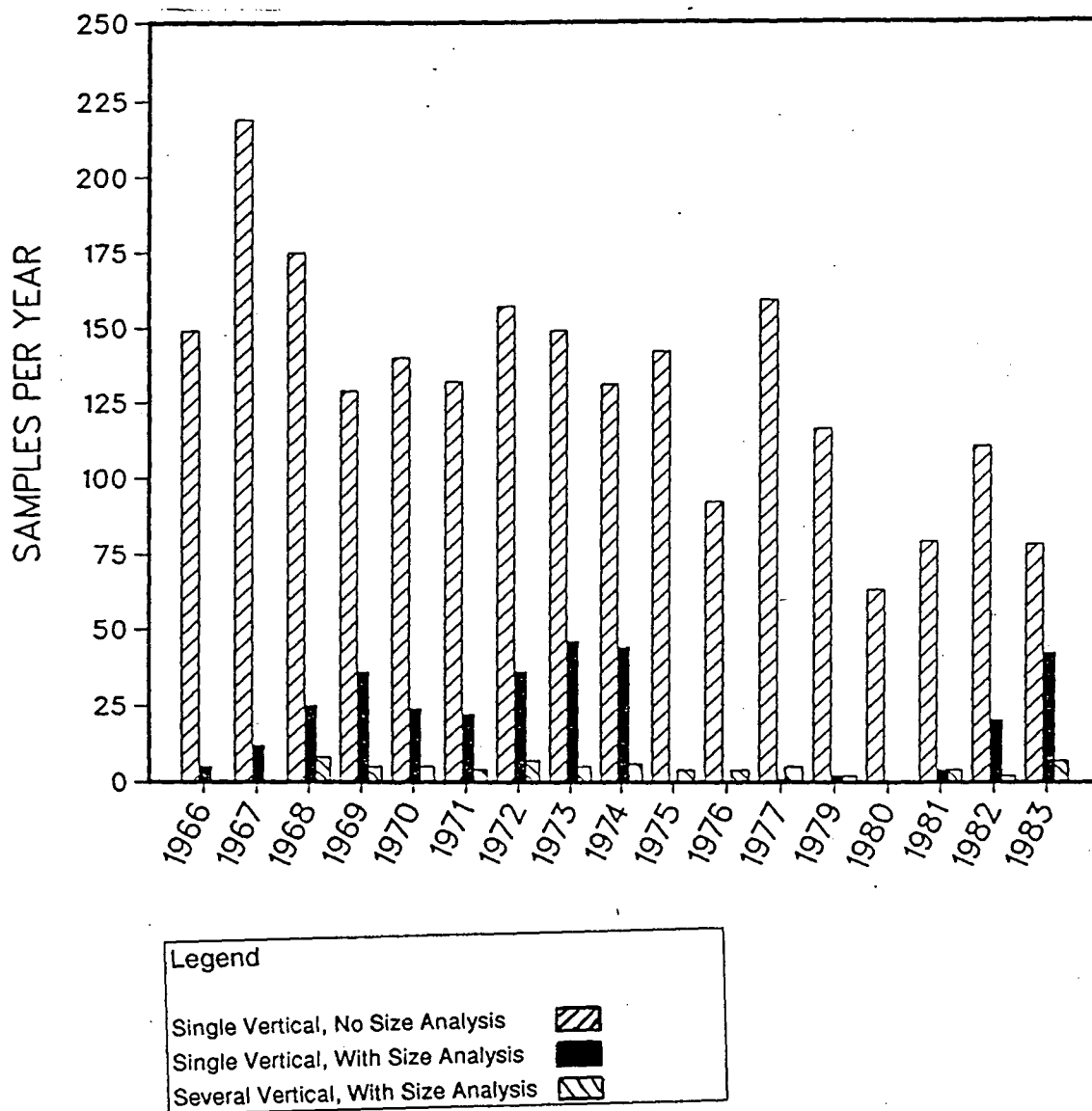


Figure 3.2 Suspended load sampling frequency at Agassiz

TABLE 3.1

LOWER FRASER RIVER HYDROMETRIC STATION SUMMARY  
(HOPE TO MISSION)

Station	Name	Drainage Area (km <sup>2</sup> )	Location	Suspended Load				Bed Load Particle Size	Bed Material Particle Size	Remarks
				Sediment Yield	Type of Observation	Particle Size PI	Particle Size DI			
08MF005	Hope	217,000	49 22 50 121 27 05	1965	MS	1965	1965			REG 52
				1966-69	MC	1967-68	1966-69			
				1970-79	MC	1970-78	1970-78			
08MF035	Agassiz	217,870	49 12 16 121 46 35	1966	MS	1966				REG 52
				1967-69	MC	1968	1967-69			
				1970-72	MC	1970-72	1970-72	1970		
				1973-79	MC	1973-79	1973-78	1973-79	1978-79	
				1980-86	MC	1981-86	1980-86	1980-86		
08MH024	Mission	228,000	49 07 39 122 18 08	1965	MS	1965	1965		1965	REG 52
				1966-71	MC	1966-68	1966-71		1966-71	
				1972-80	MC	1972-79	1972-80	1973-80	1972-80	
				1981-	MC	1981-	1981-	1981-	1981-	

Notes: M – manual sampling  
C – continuous operation  
S – seasonal operation  
REG – regulated flow

PI – Point Integrating Sample  
DI – Depth Integrating Sample

### 3.4.2 Bed Load

Bed load measurements were made at Agassiz between 1968 and 1986, and at Mission from 1966 to the present. Owing to uncertainties in the measurements, the data have not been published (except for the bed load size distribution). For this study the data were extracted from the work book files stored at the New Westminster office of Water Survey of Canada. All of the available measurements from Agassiz between 1968 and 1976 were reviewed on a point by point basis. Measurements at Agassiz after 1976 could not be included in the analysis as the data have not yet been reduced by WSC and were not made available. At Mission, only data from 1968, 1969, 1970, 1972, 1974, 1976 and 1979 have been fully analysed in this report. These measurements provide a good representation of the complete data set and include a large proportion of the high flow observations.

### 3.5 Channel Hydraulics

Estimates of the hydraulic conditions at the time of the sediment observations were obtained from the hydrometric measurements at Hope, Agassiz and Mission. Discharge measurements have customarily been carried out 12 to 15 times each year. These measurements have usually coincided with depth integrated or point integrated suspended load sampling and bed load sampling. At Mission, the hydrometric measurements have coincided with the point integrated sampling and

some of the bed load measurements. These data have not been published but were made available from the WSC work files.

### 3.6 Water Temperature

Based on experiences reported from other rivers, it is believed that the range in water temperatures on the Fraser River is sufficiently large to produce a measurable effect on the suspended sediment concentrations (Shen et al., 1978). Water temperatures have been recorded at Hope, Agassiz and Mission at one week or two week intervals in the winter and virtually daily during the May - August freshet period.

### 3.7 Water Surface Profiles

Surveys of water surface profiles are useful for estimating the slope of the river and for assessing hydraulic characteristics such as the bankfull capacity of the channel. Although some estimates of the water surface slope can be obtained from occasional high water profiles that have been surveyed along the river, regular slope measurements have not been made in the study reach. In addition, the existing hydrometric stations are too far apart to estimate the local slopes near the stations. In 1983 and 1984 surveys were carried out on four occasions to estimate the water surface slope at Mission and Agassiz. The slope at Mission was determined by establishing several temporary staff gauges along the south bank over a distance of 3 km. At Agassiz, the slope was estimated from an 8 km long profile.



## 4.0 BACKGROUND INFORMATION

### 4.1 Physical Setting

The Fraser River basin drains 232,000 km<sup>2</sup>, or about one quarter of British Columbia. Its total length from headwaters to the sea is about 1,360 km. The physical setting of the basin has been described by Holland (1976) while the basin hydrology is summarized by Slaymaker (1972).

The Fraser River drains portions of the Rocky Mountains, Cariboo Mountains and Fraser Plateau (Figure 4.1). Downstream from Quesnel the river becomes deeply incised below the surface of the plateau. Below Big Bar the river leaves the plateau country and flows through more mountainous terrain, being confined by the Camelsfoot and Pacific Ranges of the Coast Mountains on the west and the Marble, Hozameen and Skagit Ranges of the Cascade Mountains on the east. For most of this reach the river is confined in a narrow, steep walled canyon by bedrock, slide debris or high terraces, with the overall channel alignment being largely structurally controlled. Below Yale, the river leaves its narrow canyon and flows for 190 km over its alluvial plain across the lower Fraser Valley. This reach includes the portion of the river investigated in this study. At the lower end of Sumas Prairie, near Mission, the river abruptly changes from a wandering gravel bed channel to a single thread, sand bed channel. The head of the modern delta commences below New Westminster, 40 km from the sea.

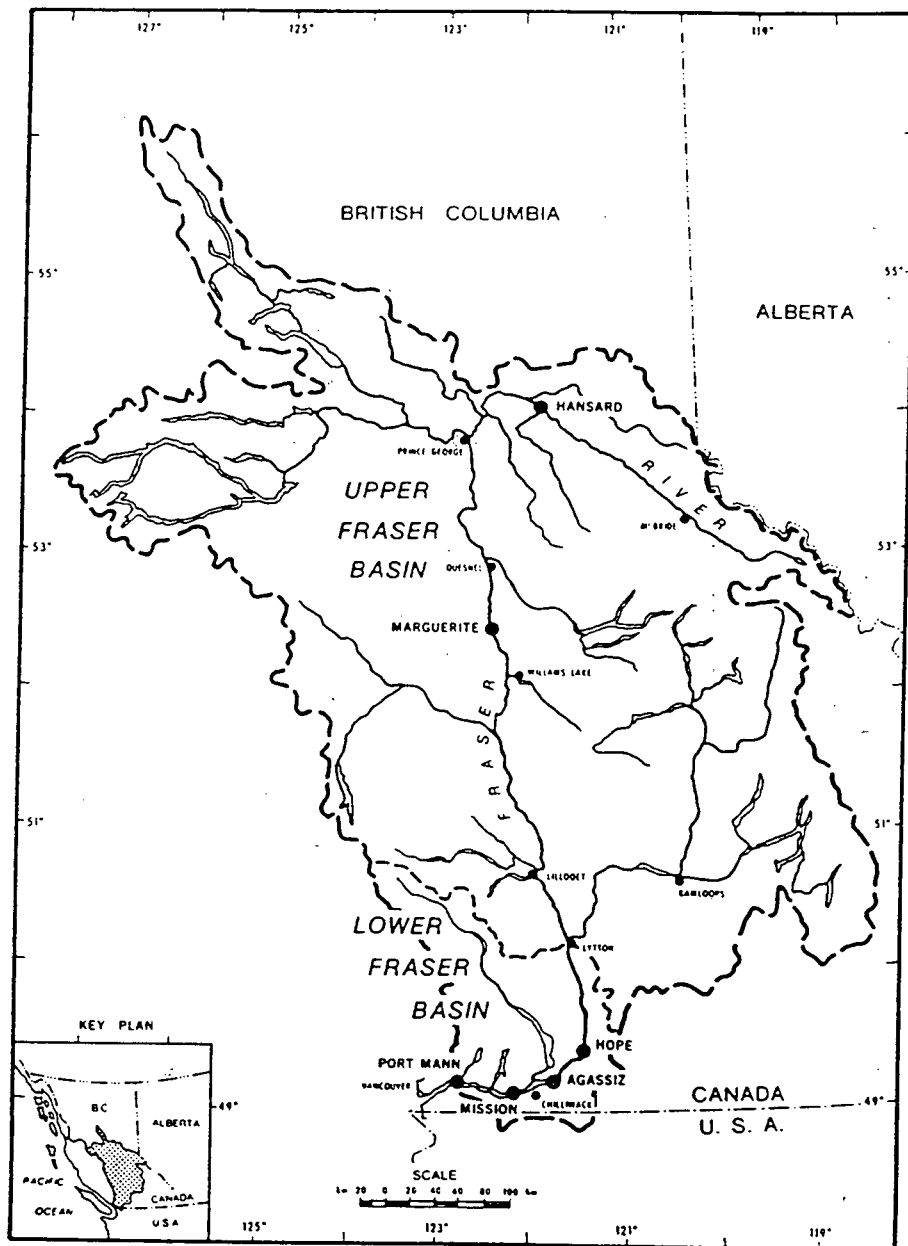


Figure 4.1 Fraser River drainage basin

The Fraser River basin was intensely glaciated during the Pleistocene Epoch and thick deposits of glaciolacustrine, glacio-fluvial and glacial deposits have been left behind in the main trunk valleys. These sediments were laid down during and shortly after deglaciation when the upland areas became ice-free and remnants of ice blocked portions of the trunk valleys (Fulton, 1969). In post-glacial times the Fraser and its tributaries have incised into these sediments. Ongoing erosion and mass wasting of these valley fills still provides an important sediment source to Fraser River (Church et al, 1989).

The Holocene evolution of the western Fraser Valley and the delta has been studied since the turn of the century. However relatively little information has been published on the Valley east of Chilliwack. The following brief summary is based mainly on the reports of Armstrong (1981) and Clague and Luternauer, (1982). The Lower Fraser River occupies a late glacial and post-glacial valley up to 5 km wide and 300 m deep. The Fraser Valley west of Pitt Meadows (Km 50) became ice free about 13,000 years ago and was subsequently invaded by the sea. However it is believed that a piedmont glacier (Sumas Glacier) occupied the eastern Fraser Valley about 11,400 years ago. The Fraser River probably established itself in a meltwater channel west of Chilliwack about 11,000 years B.P. (Armstrong, 1981). Disintegrating remnants of the Cordilleran Ice Sheet supplied meltwater and sediment to the Fraser River until about 10,000 years B.P. when ice finally disappeared from the British Columbia Interior (Clague and Luternauer, 1982). During this time the basins vacated by glacier ice in the eastern Fraser Valley were

filled with fluvial and deltaic sediments. It is believed that the Fraser River floodplain was continuous east of Pitt Meadows by 10,500 years B.P. (Armstrong, 1981).

Figure 1.1 illustrates the extent of the modern floodplain, and Figure 4.2 indicates sites where the river encounters non-alluvial sediments in the main study reach (km 80 to 165). It can be seen that the floodplain is quite restricted, mainly as a result of the river being confined by bedrock along Sumas Mountain, Chilliwack Mountain and the flanks of Mount Cheam near Hope. In addition, remnant Pleistocene age deposits and/or non-alluvial materials impinge on the modern channel at several locations in the Fraser Valley. These locations include rockfall and slide debris which confines the north bank of the river downstream of Hope near the head of Seabird Island, glacial drift or outwash which confines the south bank of the river upstream of Rosedale, and extensive terraces of glacio-fluvial materials which confine the river downstream of Mission.

#### 4.2 Hydrologic Regime

At Mission, the most distal long term hydrometric station on the Fraser River, the total annual runoff averaged  $108 \text{ km}^3$  over the period 1966 to 1984. This corresponds to a water yield of about 50 cm over the entire basin. The greatest water yield (171 cm) is produced from the Coast Mountains between the Agassiz and Mission stations, which is drained by the Lillooet and Harrison River system which

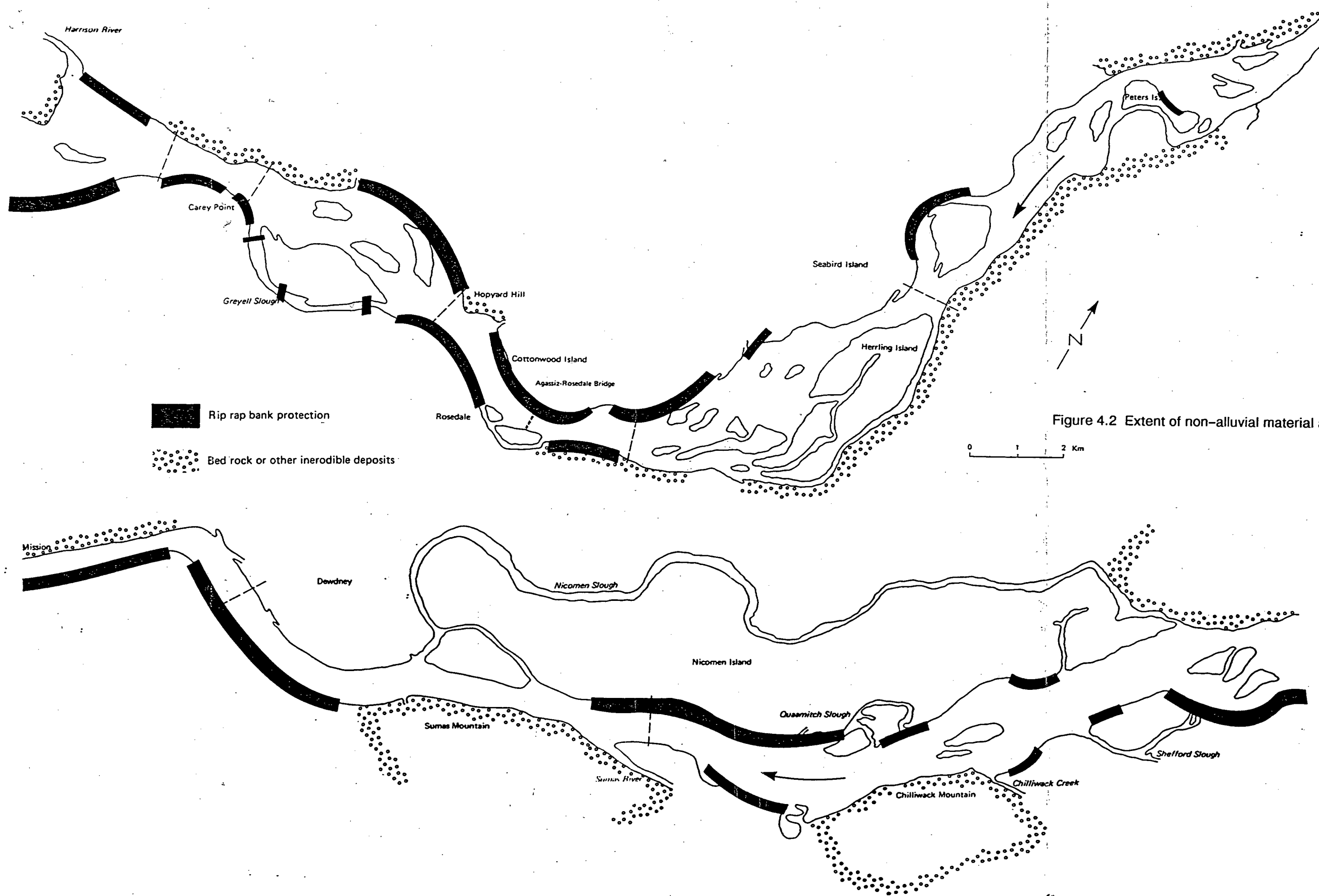


Figure 4.2 Extent of non-alluvial material along lower Fraser River

is tributary to the Fraser in the main study reach. The lowest water yield (27.9 cm) is produced from the Chilcotin region of the Fraser Plateau between Marguerite and Texas Creek.

The Fraser River has a nival flow regime so that the annual snowmelt generated freshet forms the dominant hydrological process on the river. As a result, the river typically rises in early April and peaks in the first weeks of June. This pattern is very consistent along most of the river's course.

The pattern in long term flow variations on the Fraser River was first investigated by Slaymaker (1972). Figure 4.3 illustrates time series plots of mean annual discharge and annual maximum daily discharges at Hope between 1912 and 1982. The Hope records shows persistent periods of lower than average flows from the mid-1930's to the mid-1940's and persistently higher than average flows throughout the late 1940's into the mid-1970's. This increase in runoff occurred in spite of the operation of Kenney Dam which, since 1952 has effectively reduced the drainage area of the basin by 14,000 km<sup>2</sup>.

Figure 4.4 summarizes the pattern of daily discharge at Hope, near the upstream limit of the study area. Some key discharge statistics from gauging stations in the lower Fraser Valley at Hope, Agassiz and Mission are summarized in Table 4.1. The only significant tributaries between Hope and Mission are the Harrison and Chilliwack Rivers, both entering downstream from Agassiz. During the summer

TABLE 4.1

## DISCHARGE SUMMARY FOR LOWER FRASER RIVER

STATION	WSC REF	PERIOD	DRAINAGE AREA km <sup>2</sup>	MINIMUM DAILY FLOW m <sup>3</sup> /s	MEAN ANNUAL FLOW m <sup>3</sup> /s	MEAN JUNE FLOW m <sup>3</sup> /s	MEAN ANNUAL FLOOD m <sup>3</sup> /s	FLOOD OF RECORD m <sup>3</sup> /s
HOPE	08MF005	1912-84	217000	340	2730	7030	8766	15200
HOPE	08MF005	1966-84	217000	527	2826	7215	8586	12900
AGASSIZ	08MF035	1966-84	217870	470	2880	7180	8760	13100
MISSION	08MF024	1966-84	228000	648	3350	8140	9790	14400

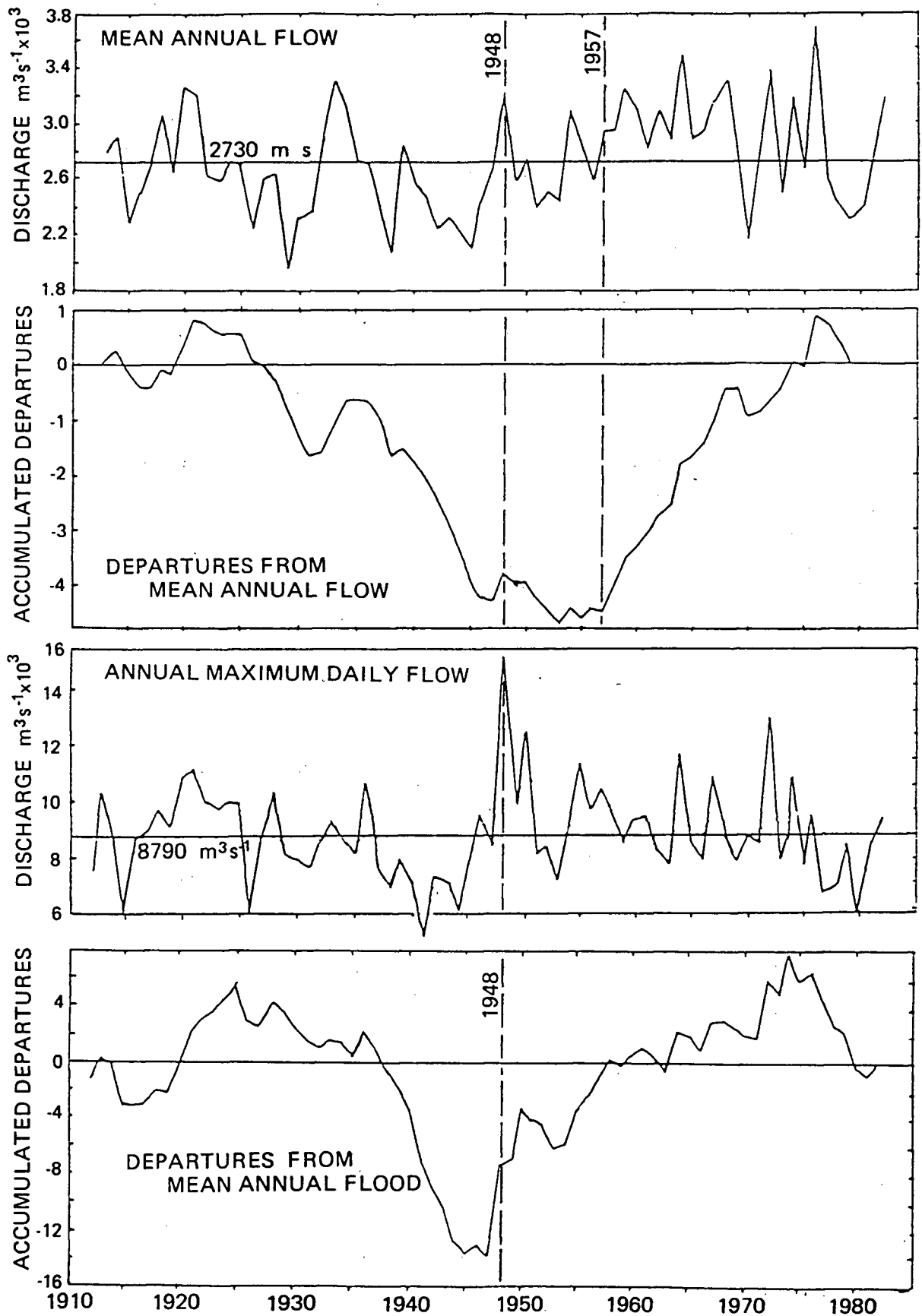


Figure 4.3 Longterm trends in runoff, Fraser River at Hope



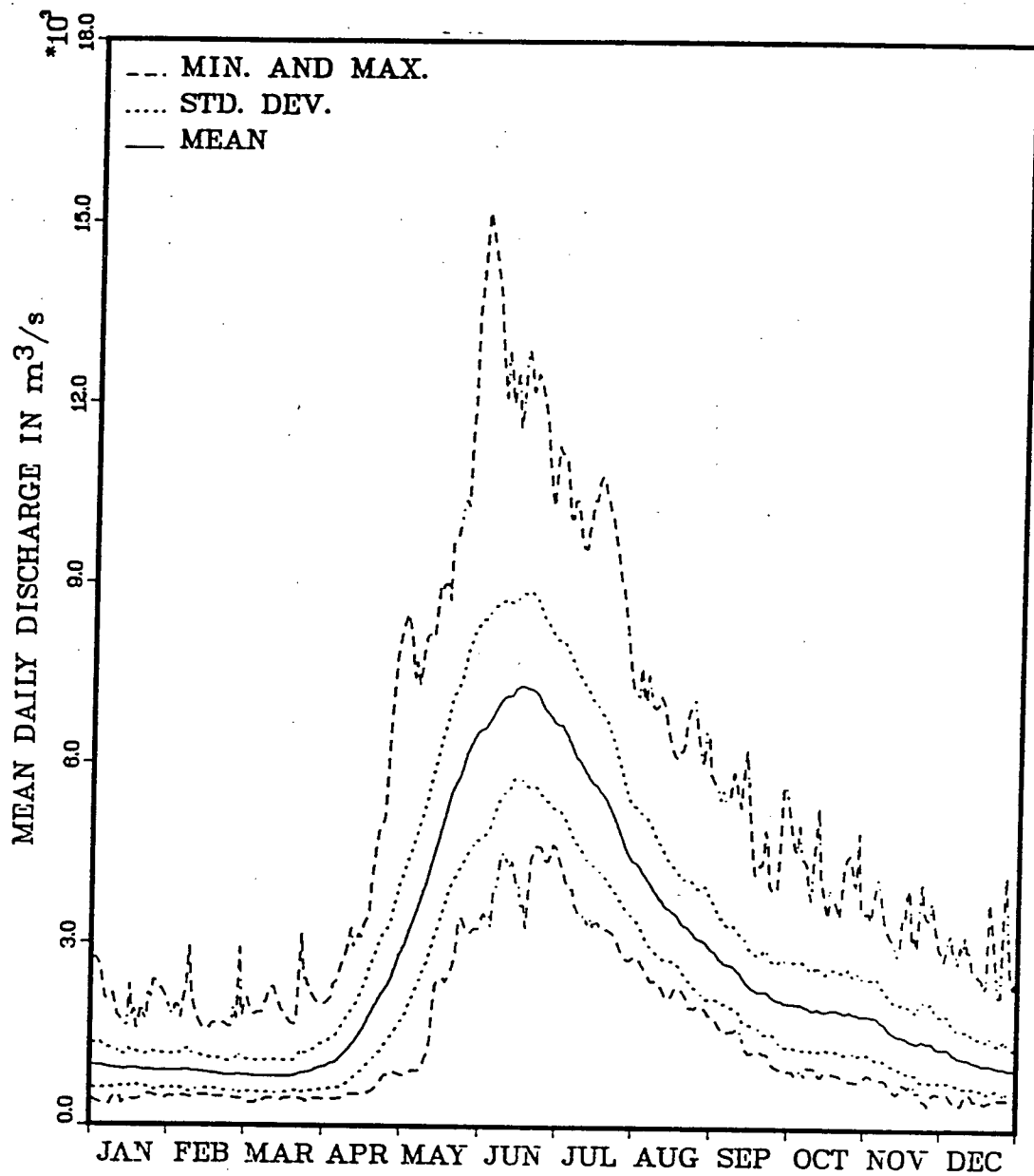


Figure 4.4 Seasonal distribution of runoff; Fraser River at Hope

freshet, tributary inflows have increased the annual maximum daily flows on Fraser River by 5% to 15% between Hope and Mission. During the autumn and winter seasons, localized rainstorms in Fraser Valley may result in tributary inflows accounting for up to 45% of the total discharge at Mission.

There have been two major floods documented since European settlement in the Fraser Valley - in 1894 and 1948. Figure 4.5 shows frequency plots of annual maximum daily discharge, June monthly discharge and mean annual discharge at Hope.

Characteristics of the ten largest historical floods at Mission and Hope are summarized in Table 4.2. The record flood of 1894 exceeded the 1948 peak stage at Mission by over 0.3 m. The return periods of the 1894 and 1948 flood stages at Mission were estimated to be 160 years and 60 years respectively. In comparison, the return period of the 1948 flood at Hope is at least 100 years using the 75 years of daily discharge records that are available between 1912 and 1986. The different estimates of the return period for the 1948 flood at Mission and Hope probably reflect the longer flood record at Mission: several major floods occurred before the gauging station at Hope commenced operations. Inflows from the Harrison River in 1948 may also have substantially augmented the flows at Mission.

The flood of 1972 is the highest measured discharge at Mission and the second highest at Hope. However, based on the historical waterlevel data at Mission, the

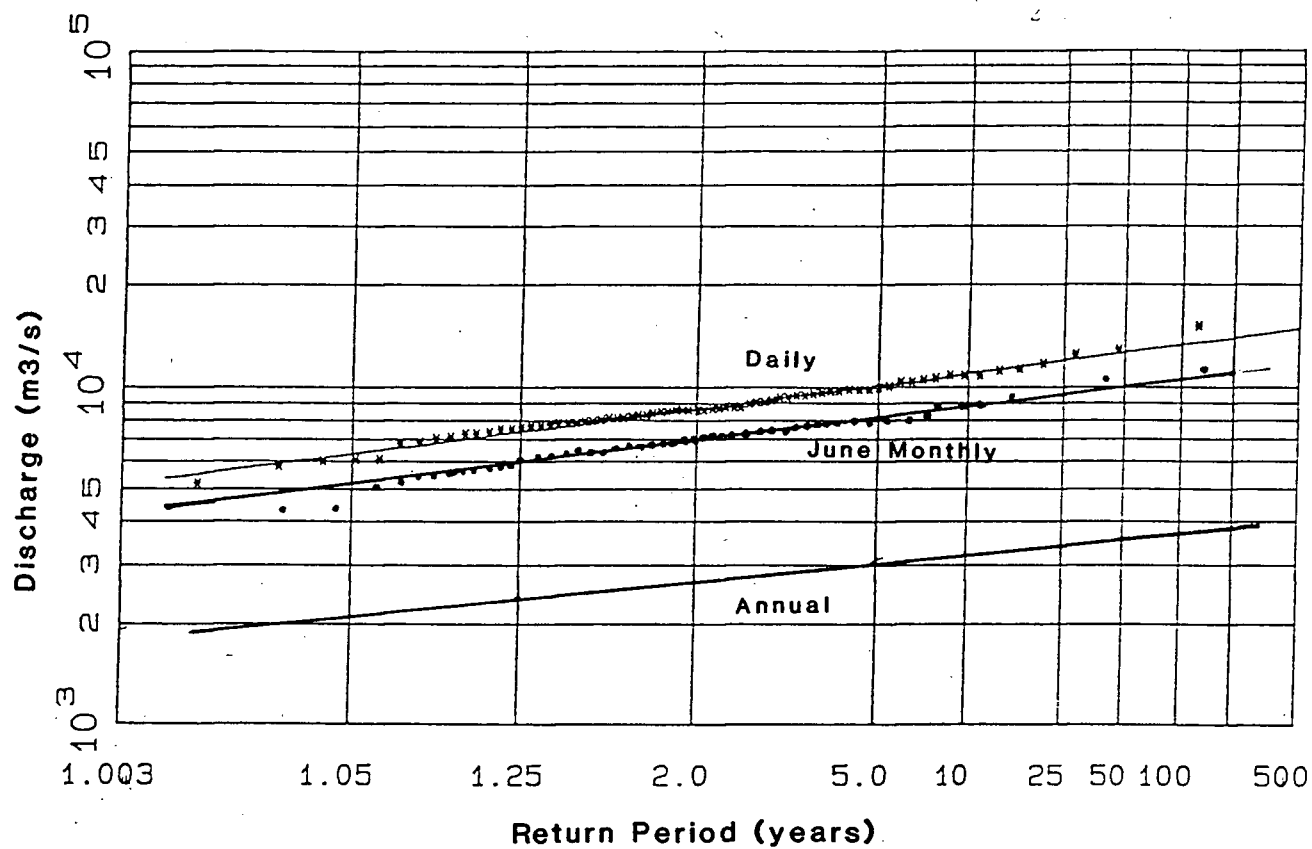


Figure 4.5 Flow frequency distribution; Fraser River at Hope

TABLE 4.2

## HISTORICAL FLOOD OCCURRENCES AT HOPE AND MISSION

MISSION 08MH024: (1896 to 1984 or present)

YEAR	MAXIMUM DAILY DISCHARGE				JUNE MONTHLY DISCHARGE	MEAN ANNUAL DISCHARGE
	RANK	WL (m)	DISCHARGE (m <sup>3</sup> /s)	RETURN PERIOD (years)	(m <sup>3</sup> /s)	(m <sup>3</sup> /s)
1894	1	7.92	18600	160-330		
1948	2	7.61	16700	60-100	12000	
1950	3	7.45	15700	35-40	9900	
1882	4	7.34	15200	25-35		
1972	5	7.15	14400	17-20	12400	4030
1964	6	7.01	13700	12-13	12900	
1876	7	7.00	13700	12-13		
1936	8	7.00	13600	11-12	8100	
1967	9	6.97	13500	10-11	11800	3900
1903	10	6.93	13400	9-10		

HOPE 08MF005: (1912 to present)

YEAR	MAXIMUM DAILY DISCHARGE			JUNE FLOW	RANK	MEAN ANNUAL DISCHARGE
	RANK	DISCHARGE (m <sup>3</sup> /s)	RETURN PERIOD (years)	(m <sup>3</sup> /s)		(m <sup>3</sup> /s)
1948	1	15200	120-500	10700	2	3230
1972	2	12900	25-50	10800	1	3390
1950	3	12500	20-35	8800	6	2730
1964	4	11600	12-17	10200	3	3490
1955	5	11300	10-14	7950	12	2820
1921	6	11100	9-12	9320	5	3210
1974	7	10800	7.5-8.5	8430	8	3180
1920	8	10800	7.5-8.5	7240	28	3270
1967	9	10800	7.5-8.5	9960	4	3160
1936	10	10600	6-8	7170	29	2700

1972 flood was only the 5th largest in the period of record, being exceeded in 1894, 1948, 1882 and 1950.

The average monthly June flow has exceeded 10,000 m<sup>3</sup>/s at Hope and 12,000 m<sup>3</sup>/s at Mission on a number of occasions. The years with the highest monthly flows do not always correspond with the years of highest daily flows. For example, the June 1964 flow at Mission probably exceeded the monthly flows in 1972, 1948 and 1950 even though the 1964 daily maximum was only the 6th largest on record.

#### 4.3 Sediment Yield

This section summarizes some characteristics of the suspended sediment transport regime of the Fraser River. Discussion of the bed load transport data has been postponed entirely to Chapter 9. This separation of topics is justified since the gravel bed load transport forms one of the central subjects of this thesis and the available data have required a substantial amount of analysis and interpretation before any meaningful results could be obtained. Furthermore, it has been clearly demonstrated that the bed load accounts for only a very small fraction of the basin's total sediment yield (Tywoniuk and Stichling, 1973; McLean and Church, 1986).

There are only two long term operating sediment stations on the Fraser River upstream of Hope. These stations are situated at Hansard, upstream of Prince George and at Marguerite, downstream of Quesnel in the Fraser Plateau. About

66% of the annual load is produced from the upper half of the basin upstream of Marguerite and 13% of the load is supplied from upstream of Hansard. The average sediment yield decreases from 0.44 T/day/km<sup>2</sup> at Hansard, to 0.25 T/day/km<sup>2</sup> at Marguerite and to 0.21 T/day/km<sup>2</sup> at Hope or Agassiz. The relatively constant sediment yield between Marguerite and Hope indicates that there are important sediment sources along the river in this reach so that the rate of sediment production increases more or less in proportion to the increase in drainage area. The most important source of sediments today probably is erosion of the Quaternary terraces and slopes that confine the river in much of this reach (Church et al, 1989).

#### **4.3.1 Total Suspended Load Characteristics**

Table 4.3 summarises the annual suspended loads at Hope, Agassiz and Mission between 1966 and 1986. Over the period 1967 - 1979 when measurements were made at all three stations, the mean annual loads were virtually identical. A paired t-test on the annual differences between Hope - Agassiz, Agassiz - Mission and Mission - Hope confirmed that the loads at the three stations are not significantly different statistically.

TABLE 4.3

ANNUAL TOTAL SUSPENDED LOADS ON LOWER FRASER RIVER  
(loads in tonnes/year)

YEAR	MISSION	AGASSIZ	HOPE
1966	19273000		19746000
1967	26071000	25333000	23437000
1968	20927000	21359000	23626000
1969	13928000	12769000	13171000
1970	11499000	12392000	12003000
1971	17531000	18023000	16308000
1972	30954000	28029000	29061000
1973	12220000	13839000	16151000
1974	24938000	24134000	23230000
1975	11975000	11238000	12031000
1976	24883000	25808000	27637000
1977	14535000	12745000	12415000
1978	12297000	10651000	8993000
1979	15008000	14721000	15539000
1980	10908000	9497000	
1981	12366000	12048000	
1982	25562000	23329000	
1983	8093000	8735000	
1966-83	17387000		
1967-83	17276000	16744000	
1966-79	18289000		18096000
1967-79	18213000	17772000	17969000

The average loads at Agassiz and Hope agree to within 1% over the period 1967 to 1978. This agreement is to be expected since there are no obvious sediment sources that would affect the suspended sediment load in this 40 km reach. The difference is close to the expected result if the annual loads were identical at the two sites but could be measured with a precision 5% (McLean & Church, 1986). This provides some indication about the reliability of the suspended load measurement program on the river.

The data in Table 4.3 also illustrates that the range in annual loads has been relatively small over the last 18 years, varying between 30 million tonnes/year in 1972 and 8 million tonnes/year in 1983. The variation in daily transport rates at Agassiz and Mission over the period of station operation is summarized in the load-duration curves in Figure 4.6. The maximum observed daily loads have reached 956,000 tonnes/day at Mission and 823,000 tonnes/day at Agassiz.

The seasonal variations in sediment loads are illustrated in Figure 4.7 for the measurements at Agassiz and Mission. Virtually identical results were found for the measurements at Hope and Agassiz. Approximately two thirds of the annual load is transported in May and June while the period between October and March accounts for less than 6% of the total.



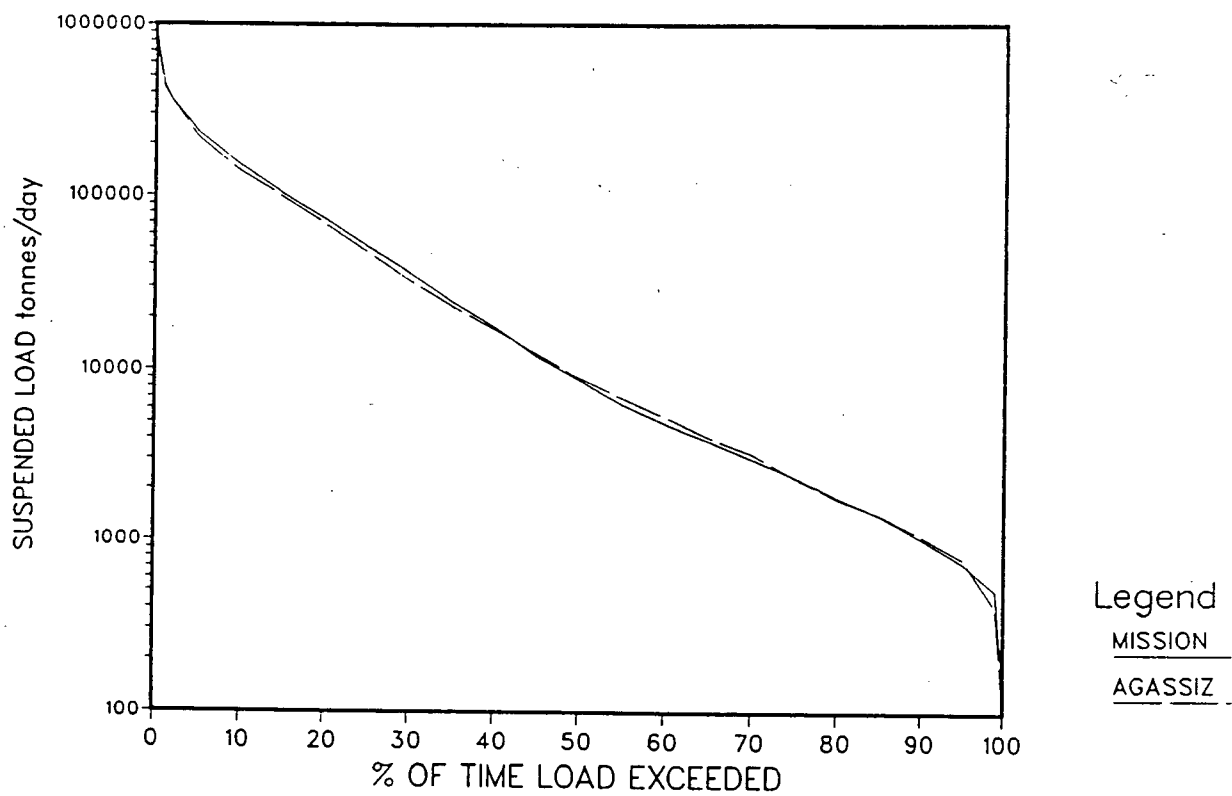


Figure 4.6 Suspended load durations - Mission and Agassiz

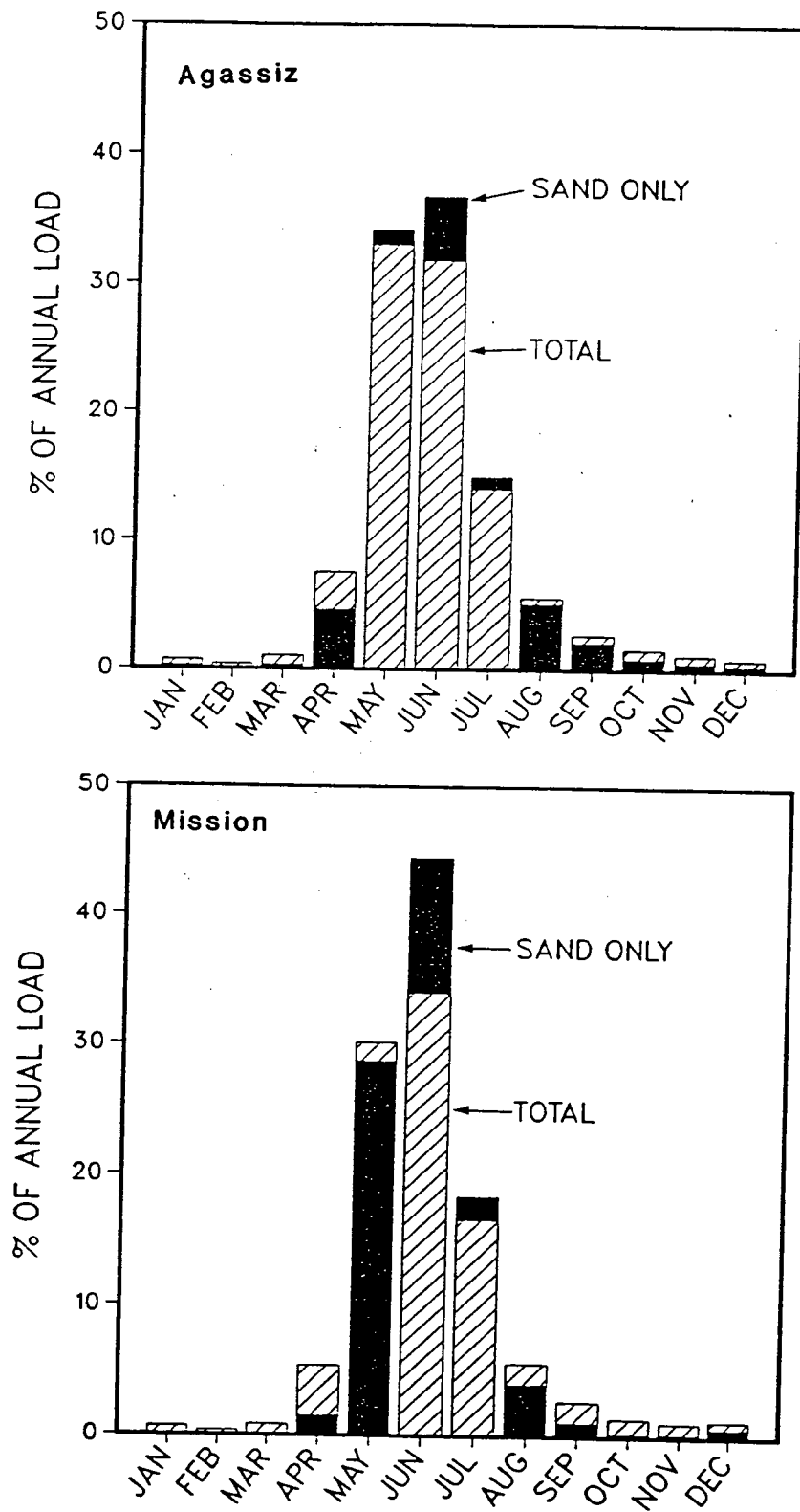


Figure 4.7 Seasonal distribution of suspended load at Mission and Agassiz

The fraction of the annual load transported by various discharges was computed from the daily concentration and discharge data at Hope, Agassiz and Mission.

Results for Agassiz and Mission are shown in Figure 4.8. This analysis shows that the flows contributing the largest fraction of the sediment load are between 8,500 and 9500 m<sup>3</sup>/s.

These discharges correspond to about the 1.5 year flood at each of the sites. In comparison, discharges above 10,000 m<sup>3</sup>/s (5 year return period at Agassiz or Hope) accounted for only about 12% of the long term sediment load. It is apparent that over the long term the relatively frequently occurring, moderate freshet flows account for the greatest proportion of the river's annual sediment load while the very high flows occur so infrequently that the actual quantity of sediment contributed is relatively small. This result is in accordance with findings on many other streams (Wolman and Miller, 1960).

The daily and monthly sediment loads display a very characteristic hysteresis over the year as illustrated on the hydrograph in Figure 4.9 and the sediment rating curves in Figure 4.10. These figures show that the sediment load is substantially higher on the rising limb than on the falling limb, indicating that the sediment supply becomes exhausted over the freshet season. This hysteresis has been described previously by Kidd (1953), and by Whitfield and Schreier (1981), amongst others. In examining

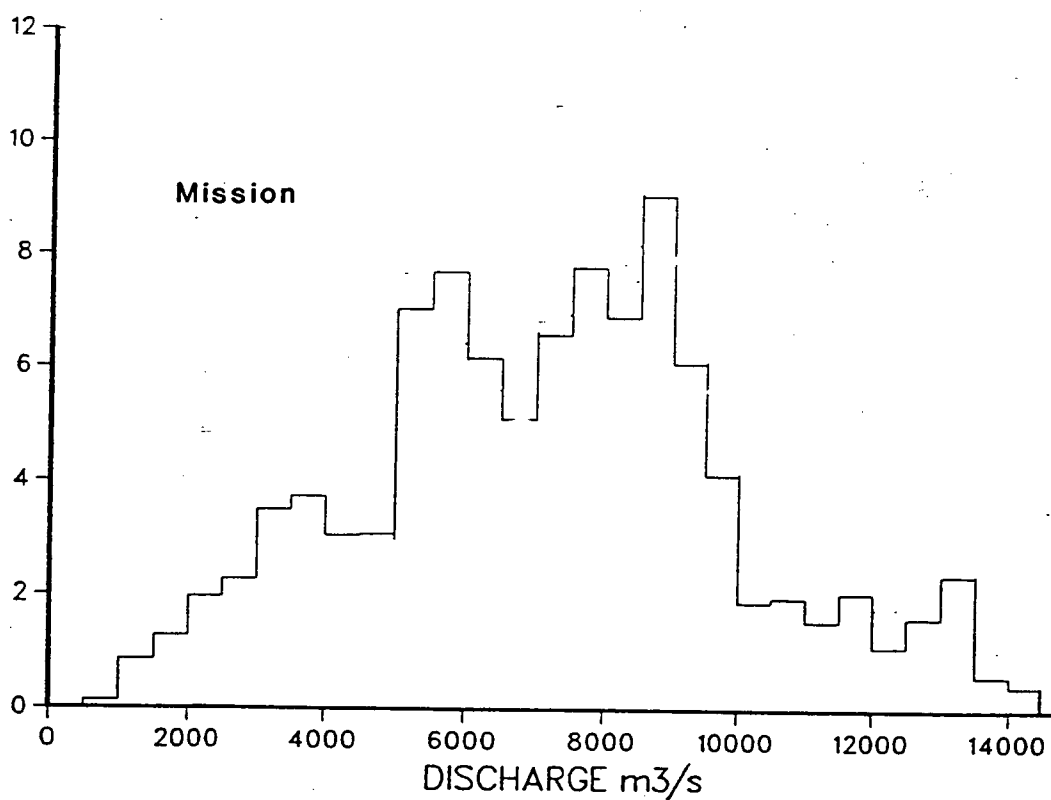
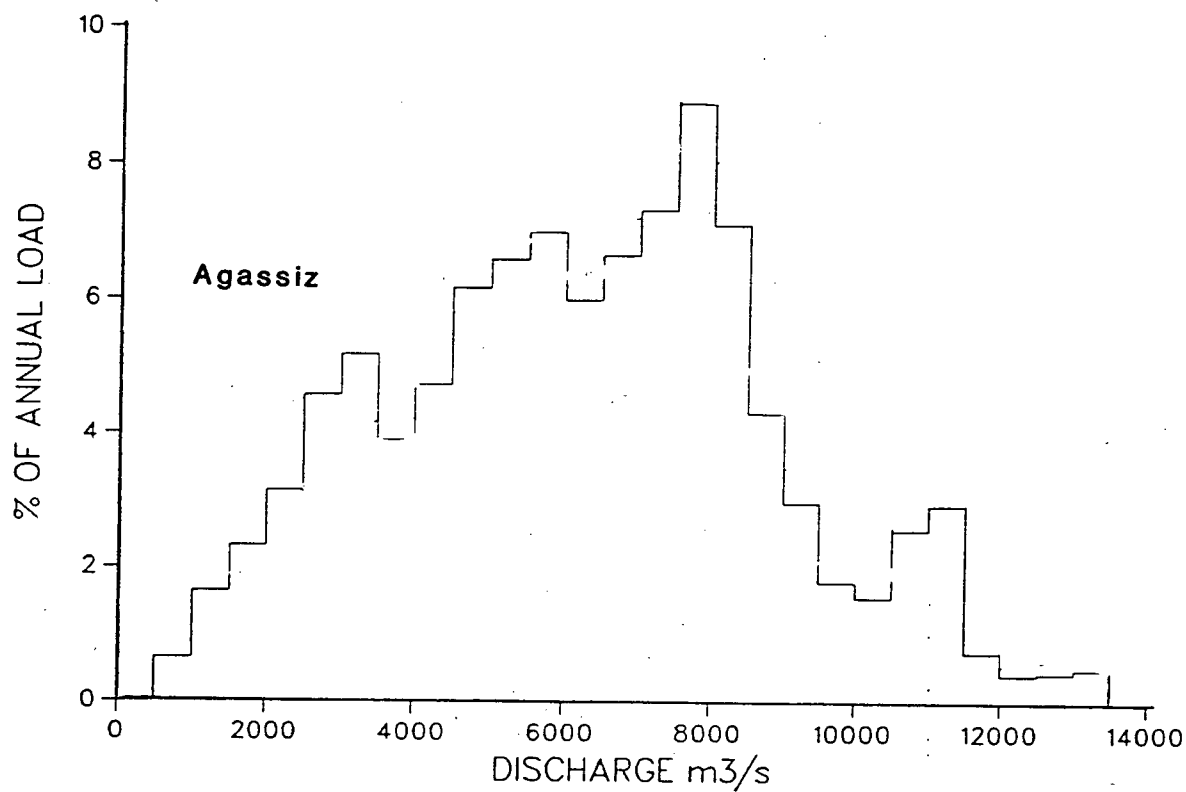


Figure 4.8 Fraction of annual suspended load transported by different flow ranges at Mission and Agassiz

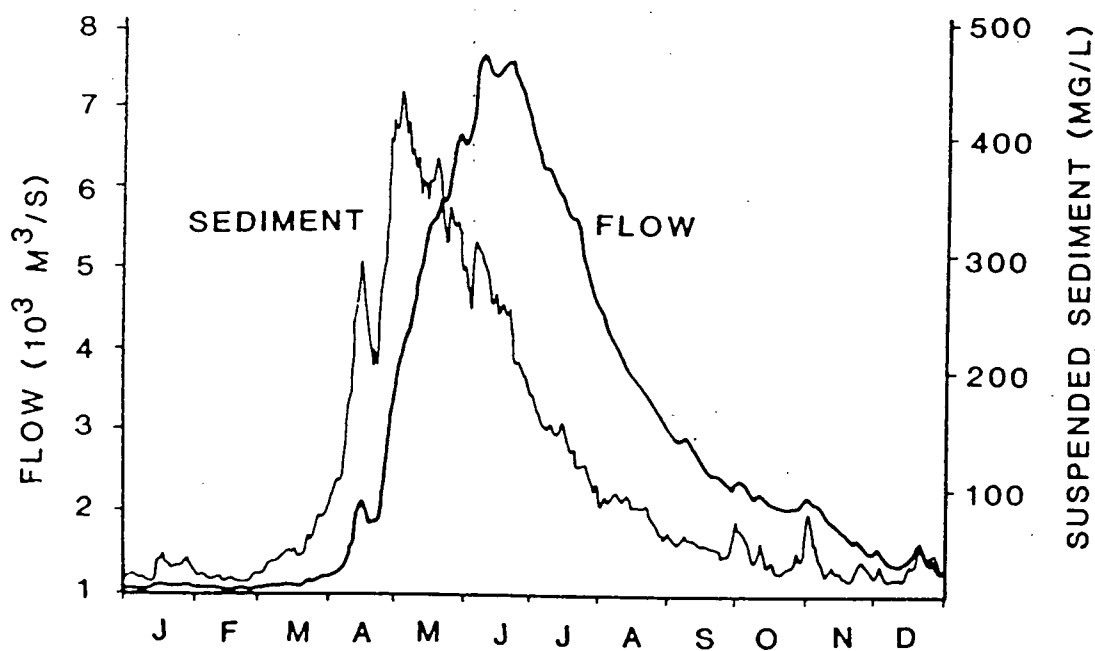


Figure 4.9 Annual flow and sediment transport hydrographs at Agassiz, 1972

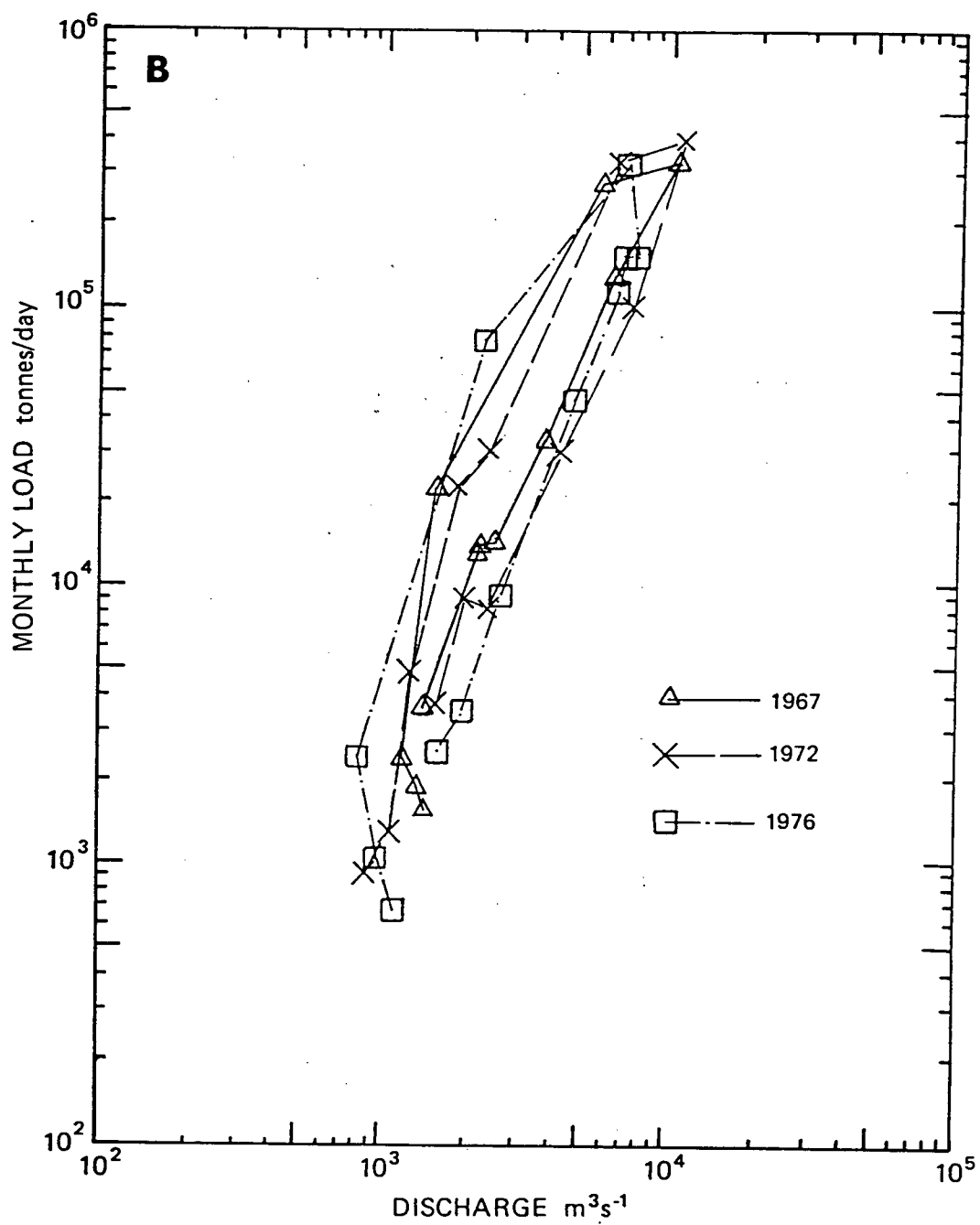


Figure 4.10

Seasonal hysteresis of sediment transport at Agassiz, 1972

the daily sediment load rating curves it is apparent that three distinct periods can be identified:

- an early rising limb period when the sediment loads follow a well defined relation with discharge;
- a supply exhaustion period, which usually begins on the rising limb of the hydrograph; in this period the sediment concentration is virtually independent of discharge and rapidly declines with time;
- a falling limb period when the flows are receding and a second well defined relation exists between sediment concentration and discharge;

This hysteresis greatly complicates the predictions of daily sediment loads.

#### 4.4 History of Improvements on Lower Fraser River

Since the start of European settlement in the 1860's there have been three main types of developments in the study reach that may affect the channel morphology and hydraulics of the river. The earliest and most important developments are related to the construction of dykes along the floodplain to control the extent of overbank flooding, and the placement of bank protection works such as rip rap revetments along channel banks to control bank erosion.

#### **4.4.1 Dyke Construction**

Dyke construction along the Fraser River dates back to about 1892 with the damming of Hope Slough and Camp Slough near Chilliwack (Sinclair, 1961). By 1923 dykes had been constructed between Chilliwack Mountain and Sumas Mountain as part of the reclamation of Sumas Lake. This early dyking and river training work has been described by McLean (1980). Following the flood of 1948 a major program of dyke construction and upgrading was initiated by the Fraser Valley Dyking Board.

By 1960, 117 km of dykes were in place between Mission and Agassiz (Fraser River Board, 1963). A second program of dyke upgrading and construction took place following the Federal-Provincial Flood Control Agreement of 1968. This work was substantially completed by 1975.

Since virtually all dykes have been set back from the main channel of the Fraser River, their direct impact on the channel has been relatively limited. On the other hand, the dykes have cut off a number of major sloughs (particularly Maria Slough and Camp Slough), which has had a major impact on the back channels on the floodplain. These changes, which have involved mainly infilling by fine sediments and vegetation encroachment, have not been investigated in detail in this study.



#### 4.4.2 Erosion Control Structures

Construction of revetments and rip rap river training structures has been carried out since the 1920's in an attempt to control bank erosion and to prevent direct river attack on the dykes. Most modern revetments typically consist of a layer of angular stone (median size 300 - 400 mm) placed on a prepared slope from the top of bank and extending down to the anticipated scour level. River training by construction of groins or spurs has generally been applied in only a few special cases in side channels. These structures have been used in Greyell Slough, Bateson Slough near Harrison Mills and the side channel east of Herrling Island.

There is relatively little documentation of early bank protection work along the river. The main source of information is contained in Public Works Canada (1949). Table 4.4 lists the main early bank protection work along the river.

A major program of bank protection construction took place following the Federal-Provincial Flood Control Agreement of 1968. Table 4.5 compares the extent of bank protection along the river before and after the program. Before the start of the program there were approximately 36 km of revetment in-place along the 65 km reach between Mission and Laidlaw.

Table 4.4  
History of Early Erosion Control

<u>Period</u>	<u>Work Carried Out</u>
1894-1910	Wing dam built at Chilliwack to prevent erosion.
1894-1910	Closure of small sloughs and upper end of Nicomen Slough by construction of earth dams.
1911-1948	Construction of bank protection along Nicomen Island. Erosion control was not effective in preventing bank erosion. Eventually river was diverted away from banks by dredging a channel through the severe bend that had developed as a result of the erosion.
1927-1939	Construction of gabion bank protection at Rosedale.
1929-1948	Construction of closely spaced pile groins and rock protection at Agassiz.

TABLE 4.5

## EXTENT OF BANK PROTECTION ALONG LOWER FRASER RIVER

REACH	EXTENT	REACH LENGTH (km)	BEFORE 1970 UPGRADING		AFTER 1970 UPGRADING	
			LEFT BANK	RIGHT BANK	LEFT BANK	RIGHT BANK
Mission	Km 86-91	5	4.4	0.0	4.4	0.0
Sumas	Km 91-101	10	2.0	2.1	2.0	5.8
Chilliwack	Km 101-12	19	5.5	3.8	5.9	5.8
Rosedale	Km 113-20	12	8.3	6.0	9.6	7.5
Cheam	Km 115-32	19	0.0	3.8	1.6	10.8
Total	Km 86-151	65	20.2	15.7	23.5	29.9

By the end of 1975, the total length of revetment was increased to approximately 54 km. As a result, nearly half of the banklines have been protected with riprap.

#### **4.4.3 Dredging and Gravel Mining**

The main dredging activity on the gravel-bed portion of the Fraser River within the study area has been carried out by industrial gravel mining operations. However some early dredging was carried out by Public Works Canada in order to provide channel improvements in selected areas. For example, 400,000 m<sup>3</sup> of sediment was dredged in the vicinity of Nicomen Island between 1914-1922 (Public Works Canada, 1949). However, since it is believed this material was disposed within the channel it is unlikely this type of activity would have a longterm impact on the sediment balance of the river.

Commercial gravel extraction from within the active channel has been regulated since 1974 by the Provincial government under the authority of the present Ministry of Crown Lands. This has involved issuing a permit for a specific operating site and then collecting a royalty on the net amount of material removed from the channel. This regulatory process provides a reasonably good basis for estimating the amount of material that has been extracted. Since 1980, the federal Department of Fisheries and Oceans has also become involved in regulating mining operations. At some sites, special monitoring programs have been carried out in order to verify that the volumes that have been removed were within the allowable limits set out in the

permits. These studies provide a means for checking the reliability of the gravel mining records.

In 1987 Kellerhals Engineering Services Ltd. prepared an overview of past gravel mining activities on the river and summarized all available information on historical rates of gravel mining between Hope and Mission. These data have provided the basis for the quantities used in this present analysis. Table 4.6 lists the known sand and gravel extractions from the Lower Fraser River between 1973 and 1986. The total amount of material removed from the river has averaged about 120,000 m<sup>3</sup>/year since 1973 and has reached up to 230,000 m<sup>3</sup>/year in 1982. About 80% of the past gravel mining activity has been carried out by two operations on the Minto side channel in the vicinity of Minto Landing near Chilliwack. These operations, and their effects on the side channel have been documented in McLean and Mannerstrom (1985) and Kellerhals Engineering Services Ltd (1987).

Table 4.6

Summary of Gravel Mining Quantities from the Channel of  
Fraser River, Hope to Mission

## Quantities in Cubic Metres per Year

Site	1973	1974	1975	1976	1977	1978	1979	1980	1981	1982	1983	1984	1985	1986	
Strawberry Island		2,800	2,800	2,800	2,800	2,800	2,800	2,800							approx 76,000 removed in 1969 between 23,000—46,000 removed annually 1966–72 removal began in 1971/72
Heppner Bar		800													
DS Cattermole		2,300													
US Cattermole											3,800	2,300		3,800	
DS Chilliwack Mtn															
Minto Channel – Vosco	60,000	60,000	60,000	60,000	0	0	0	0	34,000	46,000	54,000	61,000	76,000	76,000	
Minto Channel – Rempel	49,000	49,000	49,000	49,000	49,000	49,000	49,000	49,000	15,000	23,000	23,000	23,000	23,000	23,000	
Minto Bar															
Foster Bar		73,000	73,000	38,000	31,000	15,000									
Gill Island Bar									69,000	138,000					
Gill Island Bar								15,000							gravel stockpiled on island  approx 19,000 m <sup>3</sup> /yr removed, some returned to river  approx 100,000 removed in 1965/66
Gill Island Bar							92,000								
Hamilton Rd						1,500	1,500	800							
Rosedale Bridge		92,000													
DS end Herring Island						34,000									
Opposite Seabird Island							54,000								
Wahleach Island Trap					19,000	92,000									
Ruby Creek	76,000														
Katz															
Croft Island		5,400	5,400	5,400	5,400	5,400	5,400	5,400	5,400	5,400	5,400	5,400	3,800	3,800	
Total, Mission to Hope	185,000	285,300	190,200	155,200	107,200	199,700	204,700	73,000	123,400	235,400	109,200	91,700	102,800	106,600	
Sub-total Mission to Agassiz–Rosedale Bridge	109,000	187,900	184,800	149,800	82,800	68,300	145,300	67,600	118,000	230,000	103,800	86,300	99,000	102,800	

## 5.0 CHANNEL MORPHOLOGY

### 5.1 Principal Morphological Sub-Division

Between Hope (km 167) and Laidlaw (km 150) the river flows in an irregular single channel and is nearly continuously confined by bedrock walls, slide debris, or Pleistocene terraces (Figure 5.1). The channel is composed of cobbles, gravel and sand and displays riffles and lateral bars.

The wandering gravel bed reach, which is the main focus of this study, extends from Laidlaw to the Vedder River confluence (km 100.4) near Sumas Mountain. This reach displays many mid-channel islands that sub-divide the river into multiple gravel-bed channels. The islands are densely covered by cottonwood or, less frequently, cedar or maple, which are climax species. Island stratigraphy is mostly relatively simple, consisting of a basal gravel and sand layer overlain by 1 to 3 m of sand or silty sand. The most common gravel bars are relatively stable lateral bars that are attached to the upstream ends of islands or banks (Figure 5.2). In some cases bars may attach to either side of the island giving the resulting feature a very symmetrical appearance. Lateral bars tend to grow outwards or downstream from their point of attachment. The size of bed material in these bars is highly variable and they often contain large inner sloughs composed of sand or fine gravel. The bar heads are composed of gravel. Mid-channel bars are less common and are less stable. Often these migrate and become attached to islands or to lateral bars. Mid-

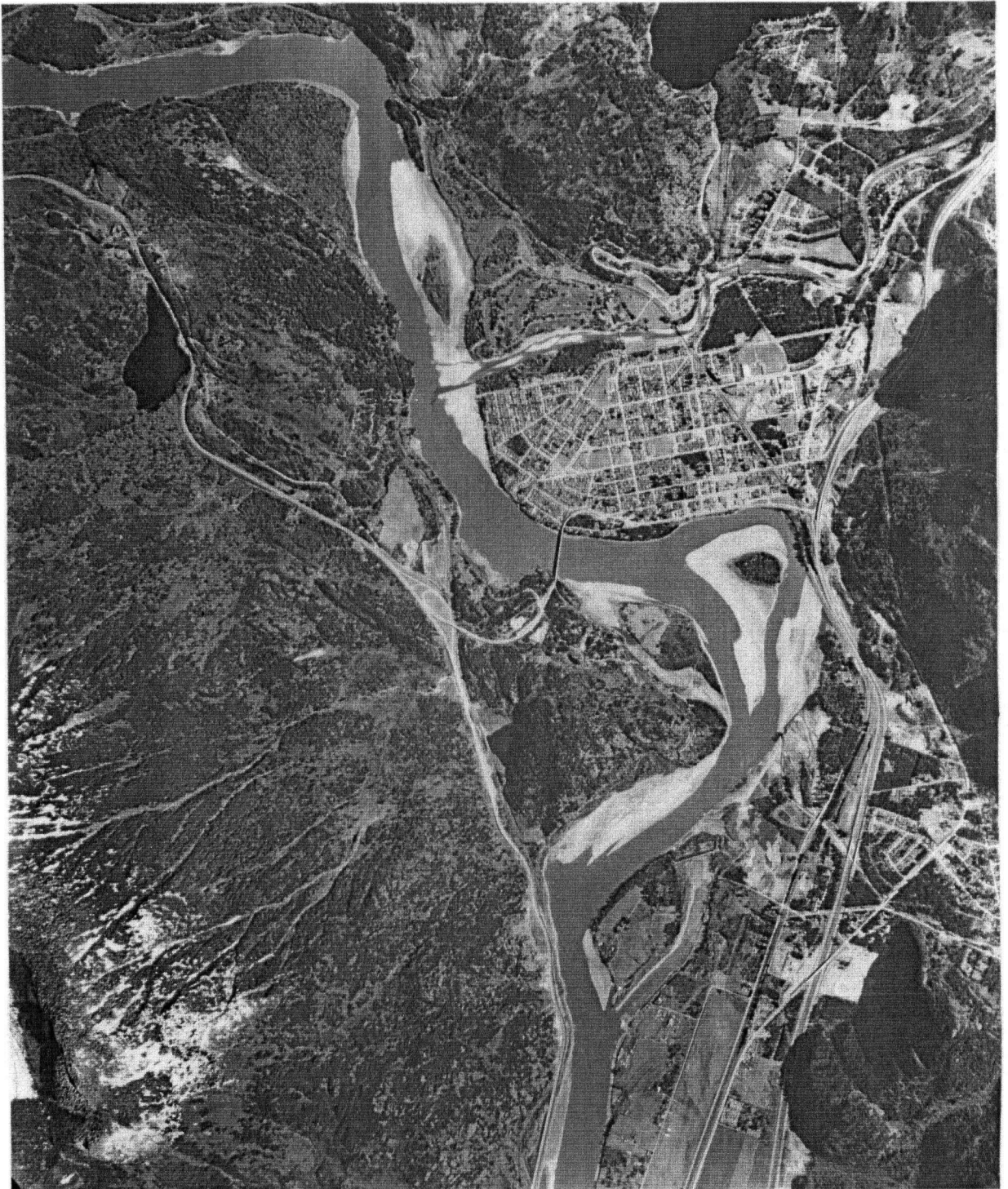


Figure 5.1 Confined channel pattern between Hope and Laidlaw





Figure 5.2 Typical bar and island morphology in the "wandering reach" between Peters Island and Sumas Mountain

channel bars generally consist of gravel and sand sheets having a coarse gravel head and a finer tail.

Between the Vedder River (km 101) confluence and Matsqui Prairie (km 91) the river changes from a wandering gravel bed channel to a single sand bed channel. This transition is very abrupt: the last gravel bar in the river is located at km 92 near the head of Sumas Mountain (Figure 5.3). However, the thalweg of the main channel is composed primarily of sand as far upstream as Nicomen Slough (km 97).

Downstream of Sumas Mountain, the single, sand-bed channel is confined by glacial outwash terraces which deflect the channel in a series of abrupt bends (Figure 5.3). Farther downstream below Fort Langley it becomes more regularly sinuous. The extensive meander scars and scroll patterns along Nicomen Island and Matsqui Prairie, as well as the ancient meander that forms Hatzic Slough, indicate that the lateral activity of the river was greater in the past than at present.

## 5.2 Channel Characteristics & Dimensions

### **5.2.1 Water Surface Profiles**

Water surface profiles have been surveyed between Hope and Mission in 1972 and 1974 by Environment Canada and between Agassiz and Mission in 1984 by U.B.C. (Figures 5.4 to 5.6). The water surface slope decreases from  $5.5 \times 10^{-4}$  near Hope



Figure 5.3 Transition from gravel-bed to sand-bed reach near Sumas Mountain



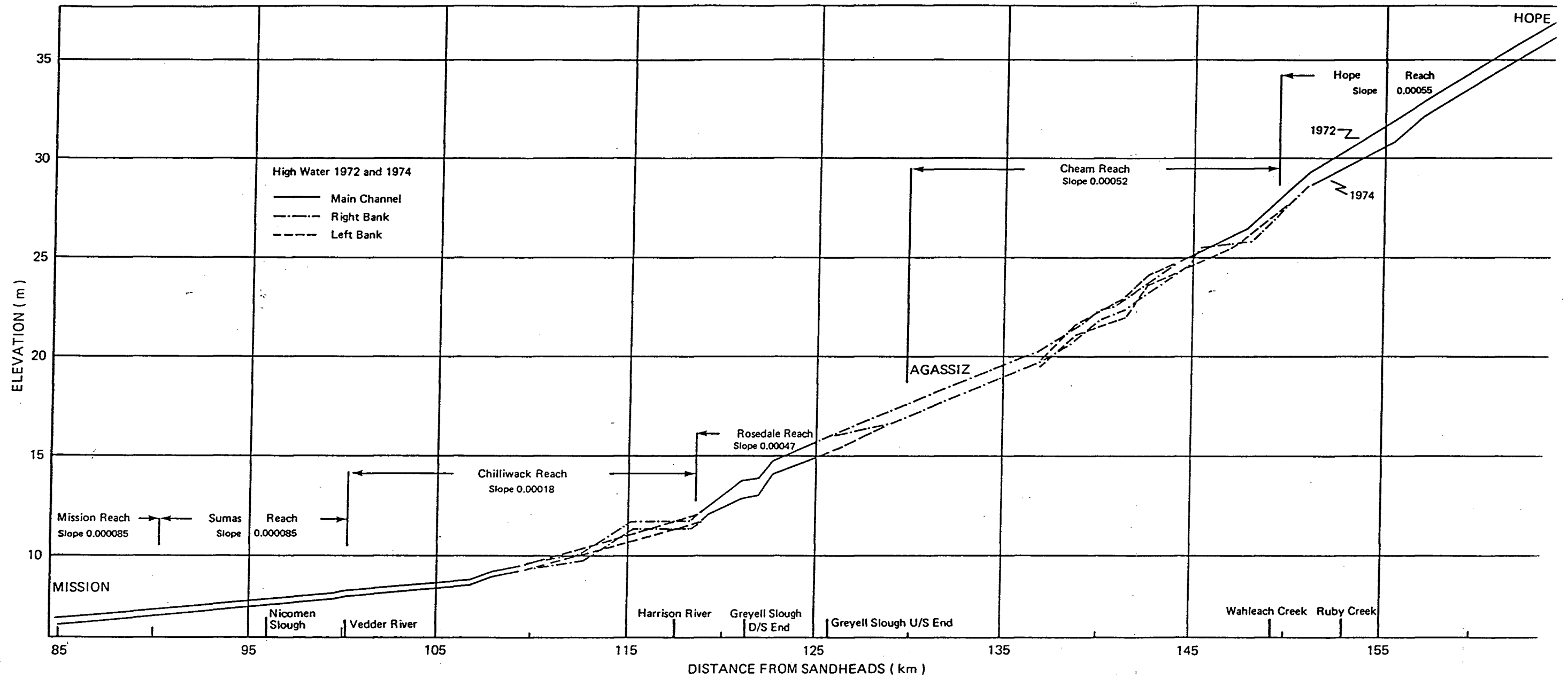


Figure 5.4 Water surface profiles of 1972 and 1974 flood profiles between Hope and Mission

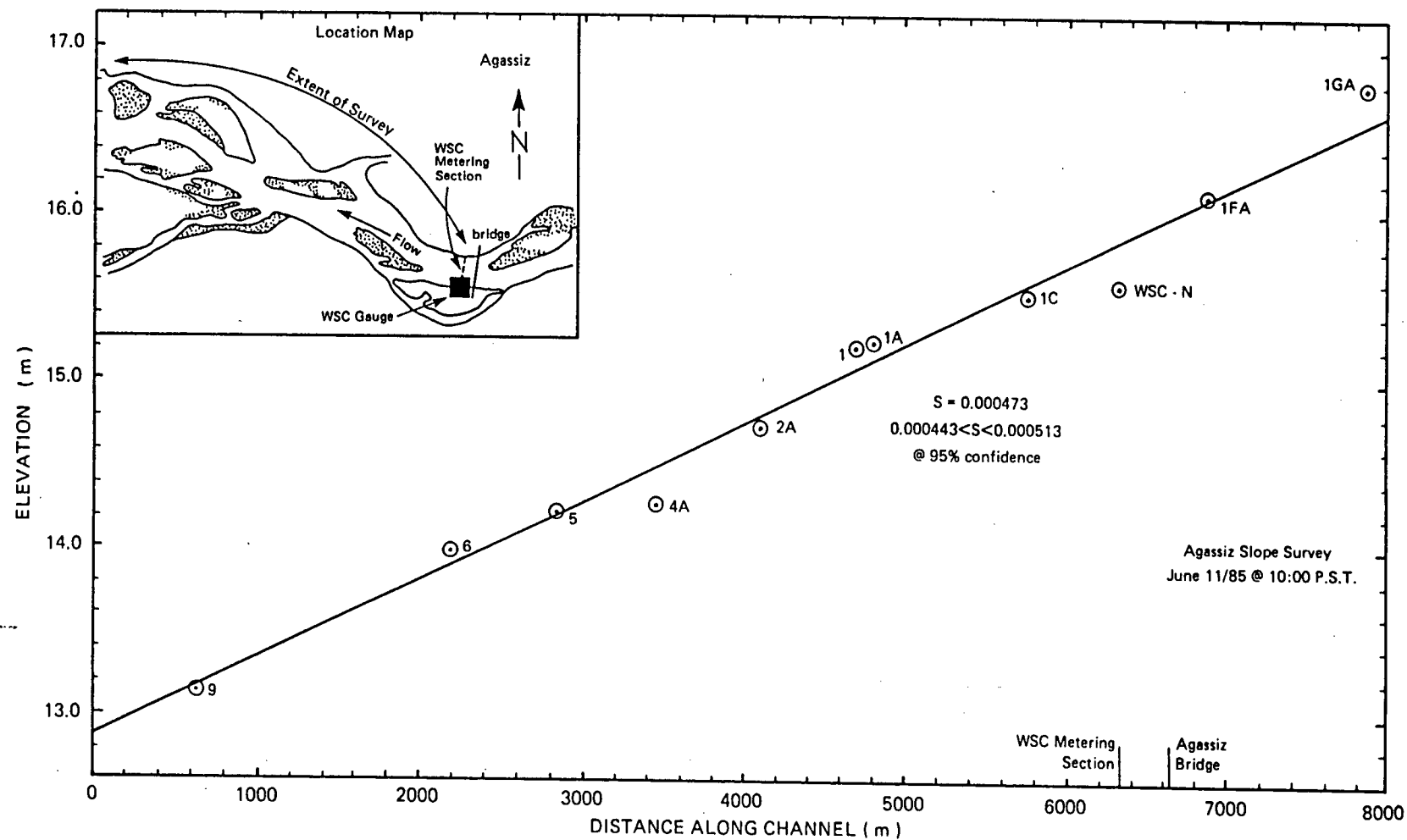


Figure 5.5 Water surface profile downstream of Rosedale bridge

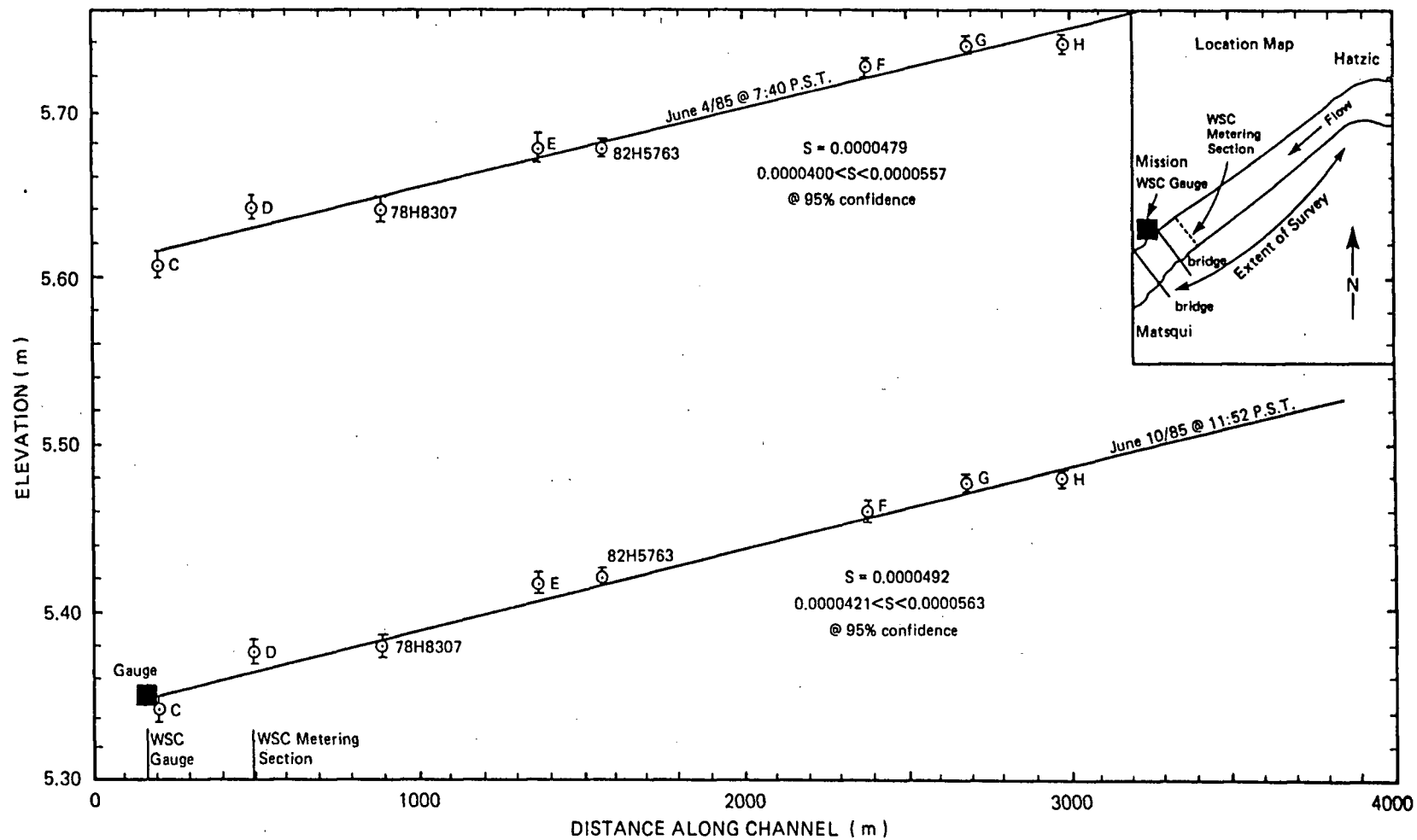


Figure 5.6 Water surface profile upstream of Mission

to  $4.7 \times 10^{-4}$  near Carey Point. Downstream of Chilliwack the slope flattens appreciably, averaging about  $8.5 \times 10^{-5}$  in the Mission-Sumas Mountain reach.

During the 1984 freshet a number of water level profiles were surveyed between Agassiz and Sumas Mountain to estimate bankfull discharge. These profiles were surveyed at a Hope discharge of  $7770 - 8100 \text{ m}^3/\text{s}$ , which corresponds to a return period of about 1.25 to 1.5 years. During the surveys it was apparent that bankfull stage varied considerably along the river and was strongly related to the island and floodplain stratigraphy, and to the age and species of vegetation present. Along areas covered with very old cottonwoods (one dated at 140 years) or maple and cedar, bankfull stage was 1.0 m to 2.0 m above the 1.5 year flood level. In these areas the banks were capped by 2.0 to 3.0 m of sandy or silty sand sediments. Areas covered with relatively young cottonwood (10 to 30 years old), such as recently stabilized islands, generally had less than 1 m of silty and sandy sediments overlying the basal gravels. In these areas bankfull stage was only 0.1 m to 0.5 m above the 1.5 year flood stage (Figure 5.7). Therefore it is not appropriate to specify a single estimate of bankfull discharge along the Fraser River. Instead, bankfull discharge was estimated for several island and floodplain classes (Table 5.1). The discharge at bankfull stage was estimated by transferring the Agassiz rating curve along the river using the 1984 high water profile as a reference stage (after Neill and Galay, 1967).

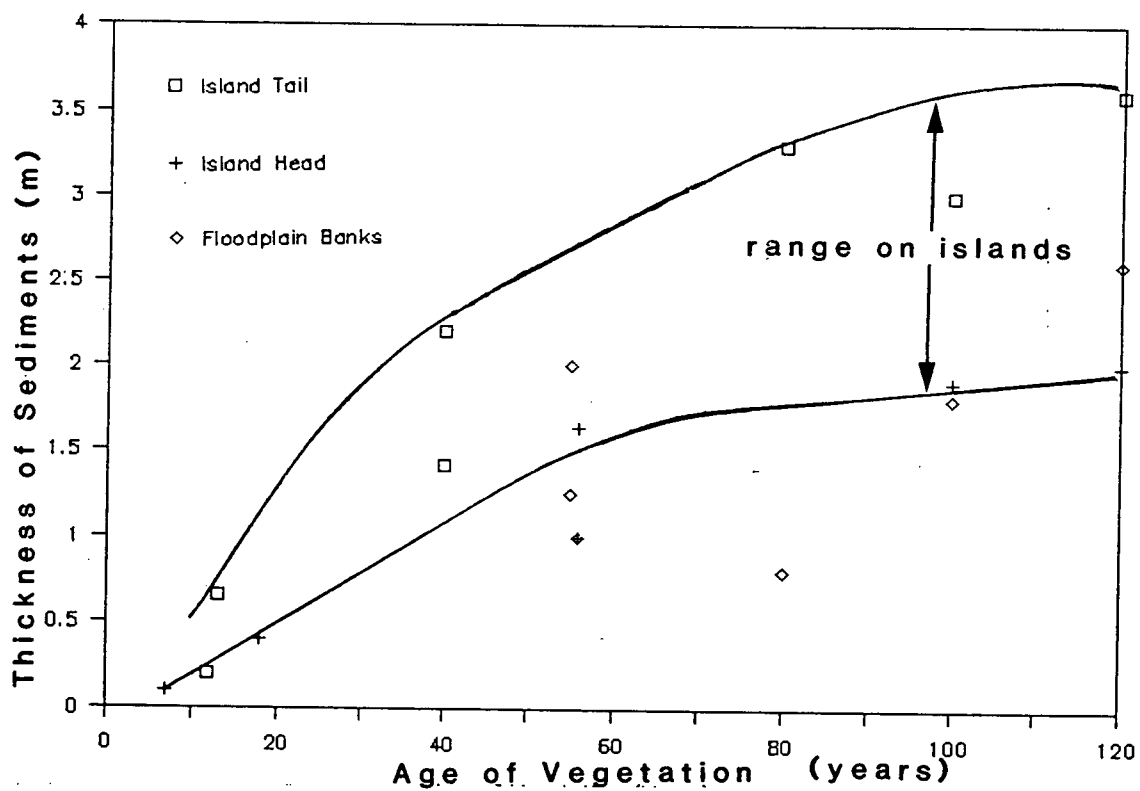


Figure 5.7 Thickness of floodplain sediments on islands and banks as a function of vegetation age



TABLE 5.1

## BANKFULL DISCHARGES: AGASSIZ TO SUMAS MOUNTAIN RACH OF FRASER RIVER

LOCATION	VEGETATION/AGE	OVERBANK SAND DEPTH (m)	BANKFULL DISCHARGE (m <sup>3</sup> /s)	RETURN PERIOD (years)
Floodplain/island	old growth cottonwood or cedar/maple	2-3	12000	20-25
Floodplain/island	overall average, all values	2	10900	7-10
Islands	cottonwood, willow < 30 years old	0.5-1.5	8500	2

### 5.2.2 Channel Dimensions and Hydraulics

Figure 5.8 shows some typical channel cross-sections along the river. These sections were located approximately 3 km apart between Mission (km 85.5) and Ruby Creek (km 153.4) and are intended to illustrate the variability of cross-sectional shapes and dimensions along the river.

Hydraulic properties were measured from the cross-sections and these results are summarized in Table 5.2. At the 2-year flood discharge the channel width and mean depth vary from 260 m and 10.2 m respectively near Hope to 1000 m and 3.3 m in the Rosedale Reach where the channel is split by wooded islands. Near Mission the channel averages approximately 880 m in width and 8.0 m depth at the 2-year discharge.

Several very deep scour holes occur along the river, typically at the concave side of bends, or at points where the river impinges directly against bedrock cliffs that project into the channel. These types of scour hole features are typical of other wandering gravel bed rivers (Neill, 1973). The deepest hole surveyed is downstream of the Harrison River confluence and reached a depth of 30.5 m at mean annual flow stage or roughly 34.5 m at 2-year flood stage. A second deep hole (29.1 m at mean annual flow stage) was measured in the Mission bend where the flow deflects off Pleistocene deposits along the right (north) bank.

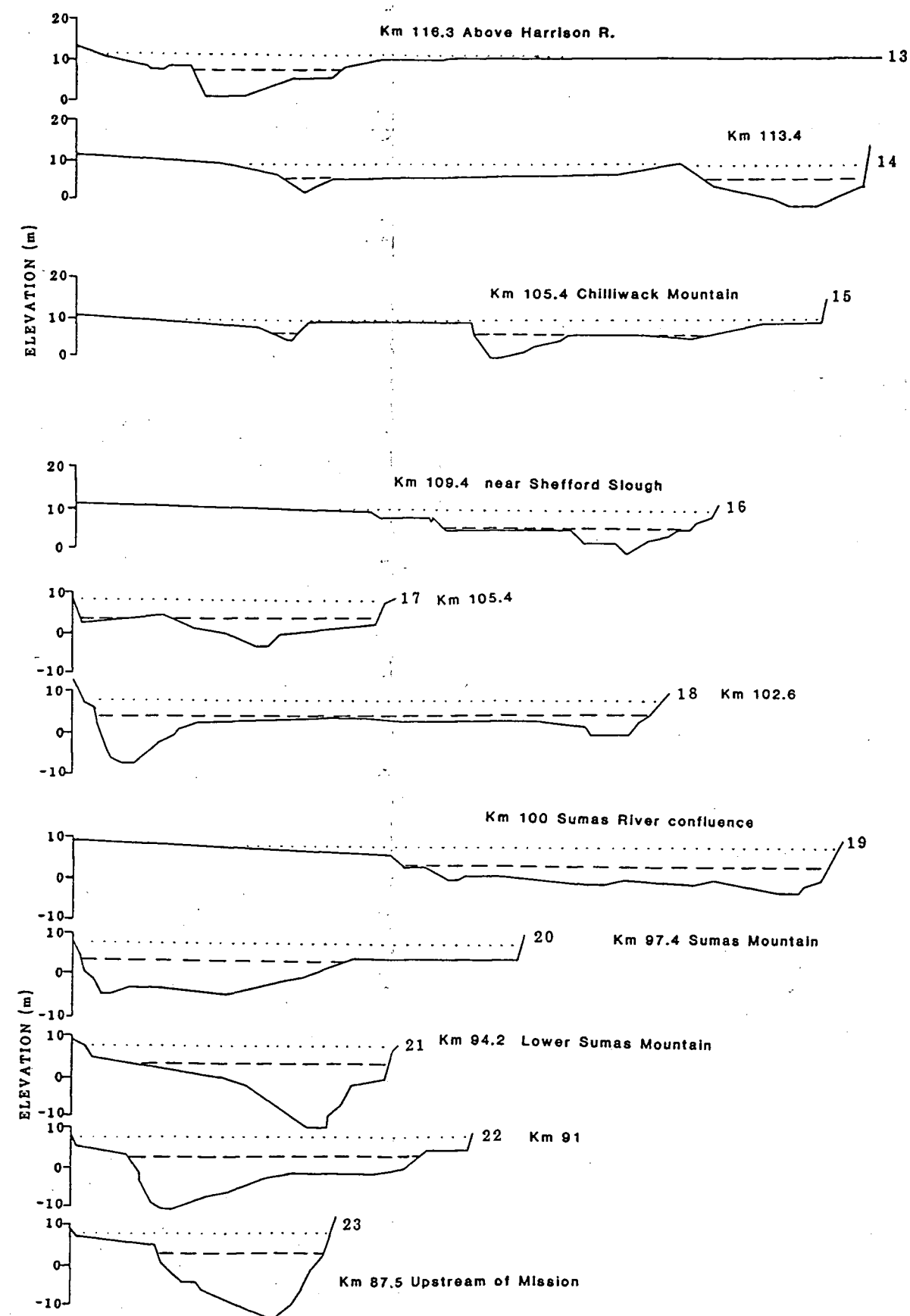
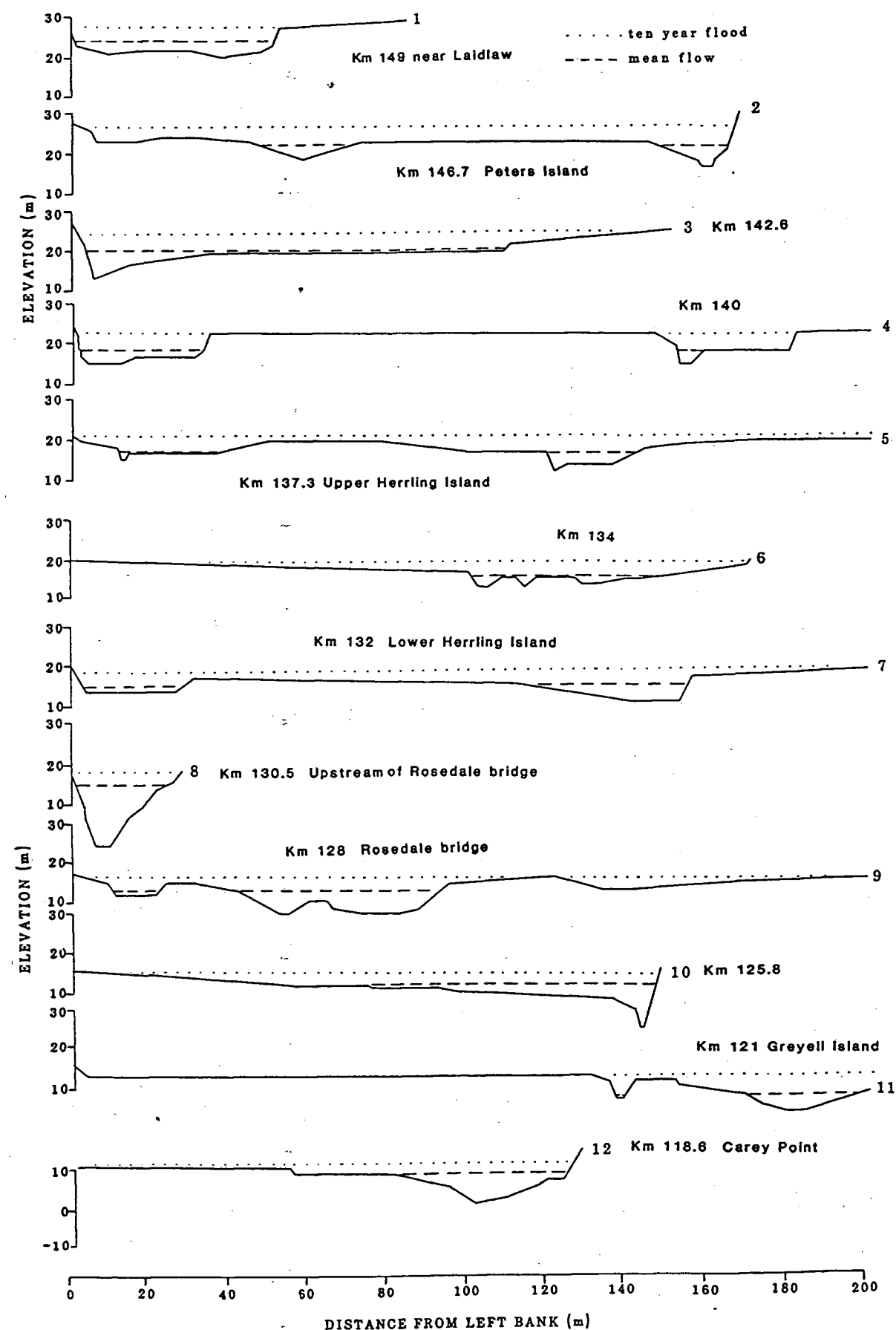


Figure 5.8 1952 channel cross sections between Laidlaw and Mission

TABLE 5.2

## MEAN HYDRAULIC GEOMETRY

REACH	# OF SECTIONS	Q (m <sup>3</sup> /s)	AREA (m <sup>2</sup> )	WIDTH (m)	MEAN VELOCITY (m/s)	MEAN DEPTH (m)	SLOPE AVERAGE
Mission-Sumas	4	LTM 3400	4154	615	0.82	6.75	.000085
		2 YR 10500	7000	880	1.50	7.95	
Chilliwack	7	LTM 3400	2476	930	1.37	2.66	.00018
		2 YR 10100	6213	1361	1.63	4.57	
Rosedale	5	LTM 2900	1612	527	1.80	3.06	.00047
		2 YR 8600	3353	1007	2.56	3.33	
Cheam	7	LTM 2900	1292	726	2.24	1.78	.000519
		2 YR 8500	3964	1353	2.17	2.91	
Hope	1	LTM 2830	1890	240	1.50	7.85	.00055
		2 YR 8560	2674	263	3.20	10.2	

LTM = long term mean flow

2 YR = 2 year recurrence interval flood

Table 5.3 summarizes the channel dimensions and hydraulic properties at the Hope, Agassiz and Mission hydrometric stations. Figure 5.9 shows the channel cross sections at the three gauging lines. The measured at-a-station hydraulic geometry relations are plotted in Figure 5.10.

### 5.3 Bed Materials

#### **5.3.1 Sampling Objectives**

The bed material sampling program was directed towards characterizing the bed sediments between Hope and Mission, with particular emphasis on the reach downstream of Agassiz. Since the information was required for constructing the sediment budget of the river, volumetric sampling procedures were used. In most cases, the bed samples were collected from the head of gravel bars. This decision was made to ensure that morphologically similar sites were sampled along the river (Kellerhals and Bray, 1973). Samples were obtained from virtually every gravel bar in the 40 km reach between the Agassiz - Rosedale bridge and lower Sumas Mountain. In addition, samples were collected from selected sites between Hope and Agassiz. Since each sample weighed in the order of 100 to 300 kg the coarse gravel fraction of the deposits was sieved in the field. The finer fraction was split and retained for laboratory analysis.

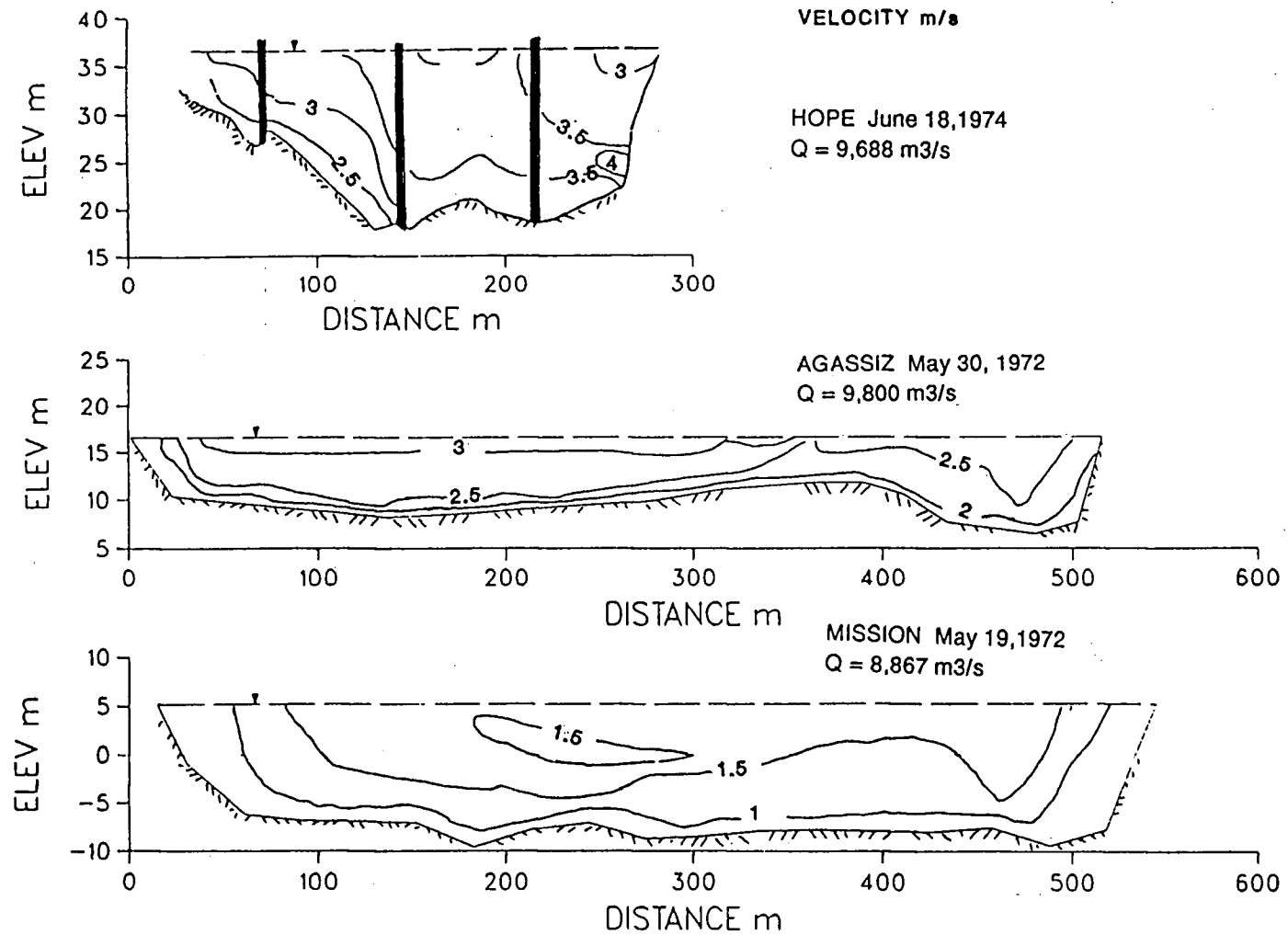


Figure 5.9 Channel cross sections at Hope, Agassiz and Mission gauging stations

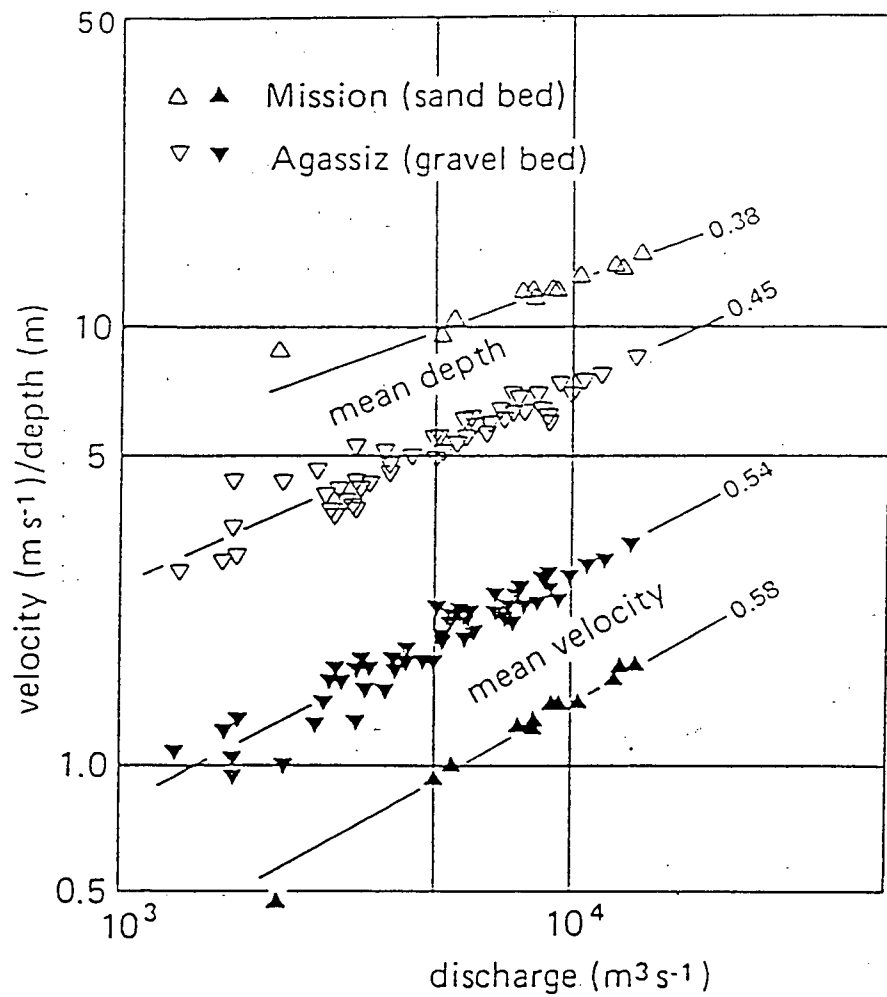


Figure 5.10 At a station hydraulic geometry measured at Agassiz and Mission hydrometric stations

TABLE 5.3

## CHANNEL CHARACTERISTICS AT GAUGING SITES

STATION	INDEX #	FLOW	Q m <sup>3</sup> /s	V m/s	d m	W m	SLOPE	BED MATERIAL		
								Surface mm	Subsurface mm	
Hope	08MF005	LTM	2830	1.5	7.9	240	.0006	D90	180	128
		mean June	7030	2.8	9.7	258		D75	130	60
		MAF	8766	3.2	10.1	268		D50	100	30
		5 yr	10200	3.5	11.1	270		D25	75	7
		10 yr	11500	3.7	11.5	270		D10	40	1
		1972 flood	12900	4.0	11.7	275				
Agassiz	08MF035	LTM	2880	1.4	4.1	500	.00048	D90	80	80
		mean June	7180	2.3	6.1	509		D75	56	50
		MAF	8760	2.6	6.6	512		D50	42	25
		5 yr	10300	2.8	7.1	513		D25	30	8
		10 yr	11600	3.0	7.5	515		D10	20	2
		1972 flood	13100	3.2	7.9	516				
Mission	082H024	LTM	3410	0.7	9.4	518	.00005	D90	8	8
		mean June	8140	1.3	12.0	530		D75	0.5	0.5
		MAF	9790	1.5	12.6	540		D50	0.38	0.38
		5 yr	11500	1.6	13.2	550		D25	0.20	0.20
		10 yr	13000	1.7	13.7	552		D10	0.15	0.15
		1972 flood	14400	1.9	14.1	555				

Notes: LTM = Long term mean discharge  
 MAF = Mean Annual Flood  
 Flow statistics for period 1966-84

V = Mean velocity  
 d = Mean depth  
 W = Top width



A second set of samples was collected to illustrate the variation in sediment sizes within particular bars. These data were used to compare the variability of sediment sizes within a site to the variations along the river. These samples were also used to provide a means for estimating the volumes of gravel sediments contained in islands and bars. The sampling procedures were similar to those used for assessing downstream changes.

### **5.3.2 Variability of Sediments Within Bars**

Gravel bars typically display very large spatial variations in grain size. This variability has been described previously by Bluck (1979) and Wolcott (1984). In most situations the coarsest materials are found near the bar heads or outer sides of bars nearest the main channel. Often the sediments become progressively finer towards the bar tail or near inner sloughs on the landward side of the bars.

In this study the variability in sediment sizes was characterized on three bars:

- the most distal mid-channel bar on the river near Sumas Mountain (km 92);
- a side bar located near Chilliwack (km 110);
- a lateral bar near the Agassiz - Rosedale bridge (km 129).

Figure 5.3 illustrates the location of the mid-channel bar at Sumas Mountain. As this bar marks the end of the gravel bed reach, the size of the sediments in this bar

was finer than at most other sites. The largest clast had a b-axis size of 76 mm while most of the bar tail was composed of medium sand. A grid of 16 sample points was laid out over the 600 m long, 200 m wide bar. However, due to tidal variations over the period of sampling, volumetric samples were collected from only 13 of the sites. These data were presented earlier in Wolcott (1984). The results were pooled and compared with a single large volumetric sample from the head of the bar. Figure 5.11 illustrates the differences between the two size distributions.

It can be seen that the median ( $D_{50}$ ) size from the composite bar sample was about 25% smaller than the results from the bar head. Also, the overall composite bar sample contained more sand than the bar head (32% versus 23%).

Figure 5.12 shows the lateral bar downstream of the Agassiz - Rosedale bridge. Samples were collected from eight sites at approximately 50 m intervals along the axis of the bar. The sediments in this bar were substantially coarser than at the Sumas Mountain bar, with the largest clast reaching 175 mm (b-axis). The samples near Agassiz also contained substantially less sand. The composite sample over the bar contained about 22% less than 2 mm while the bar head sample contained 18%. However, the median particle size from the two samples agreed closely (25 mm at the bar head versus 20 mm for the composite sample).

Only three volumetric samples were collected from the side bar near Chilliwack. The approximate location of these sites is shown on Figure 5.13. The median size

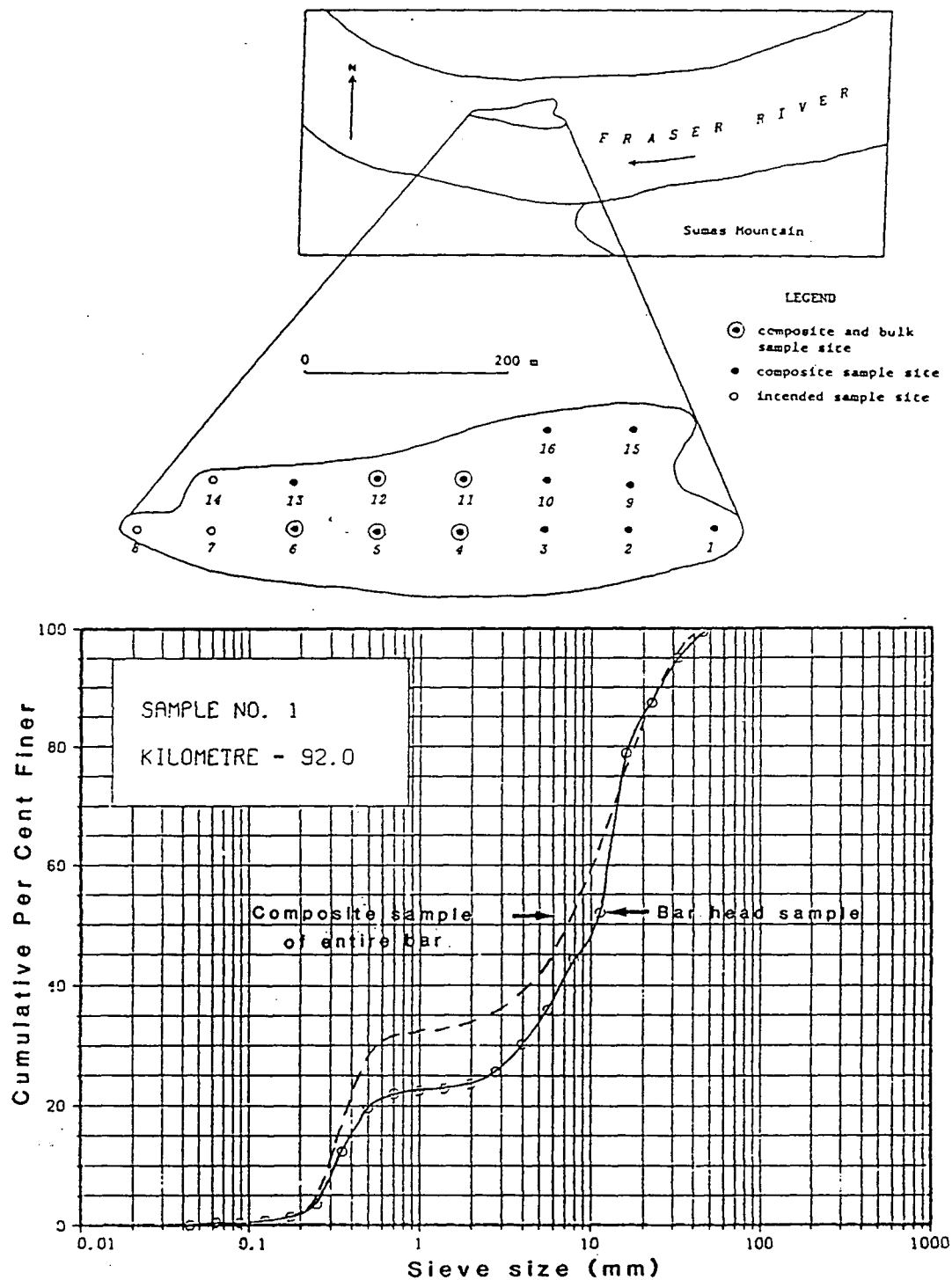


Figure 5.11 Comparison of a sub-surface bar head sample with a composite sample from the entire bar – near Sumas Mountain

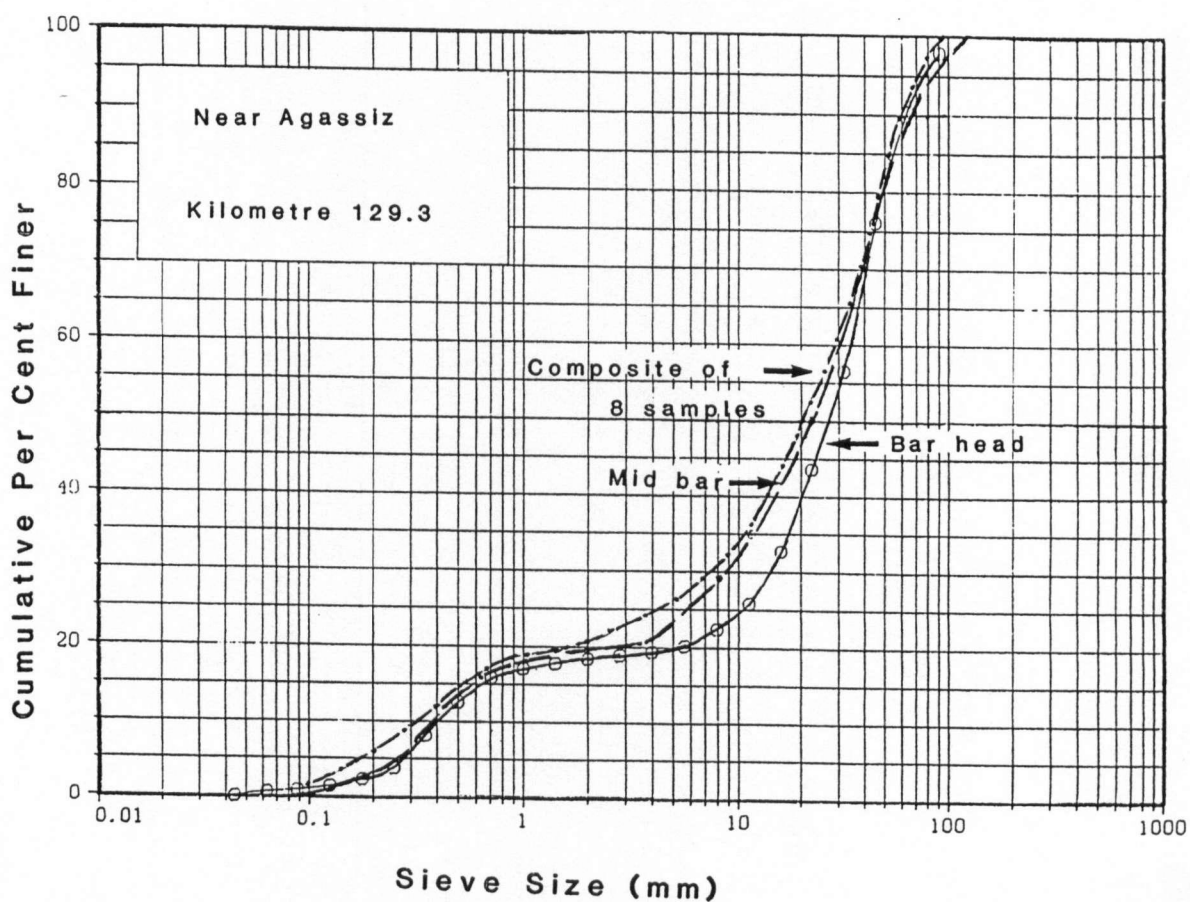
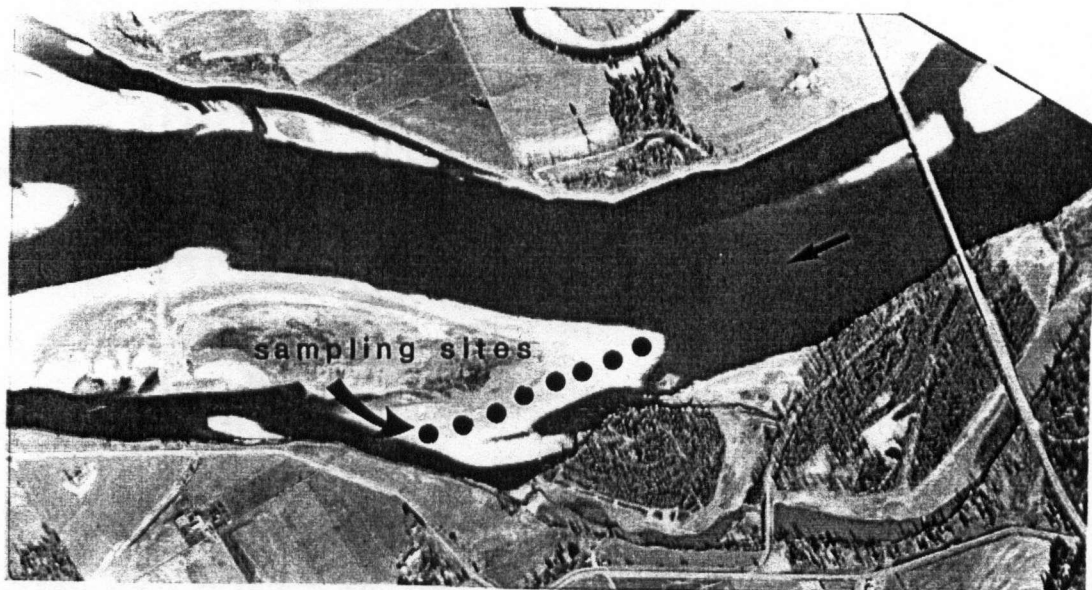


Figure 5.12 Comparison of a sub-surface bar head sample with a composite sample from the entire bar – near Rosedale bridge

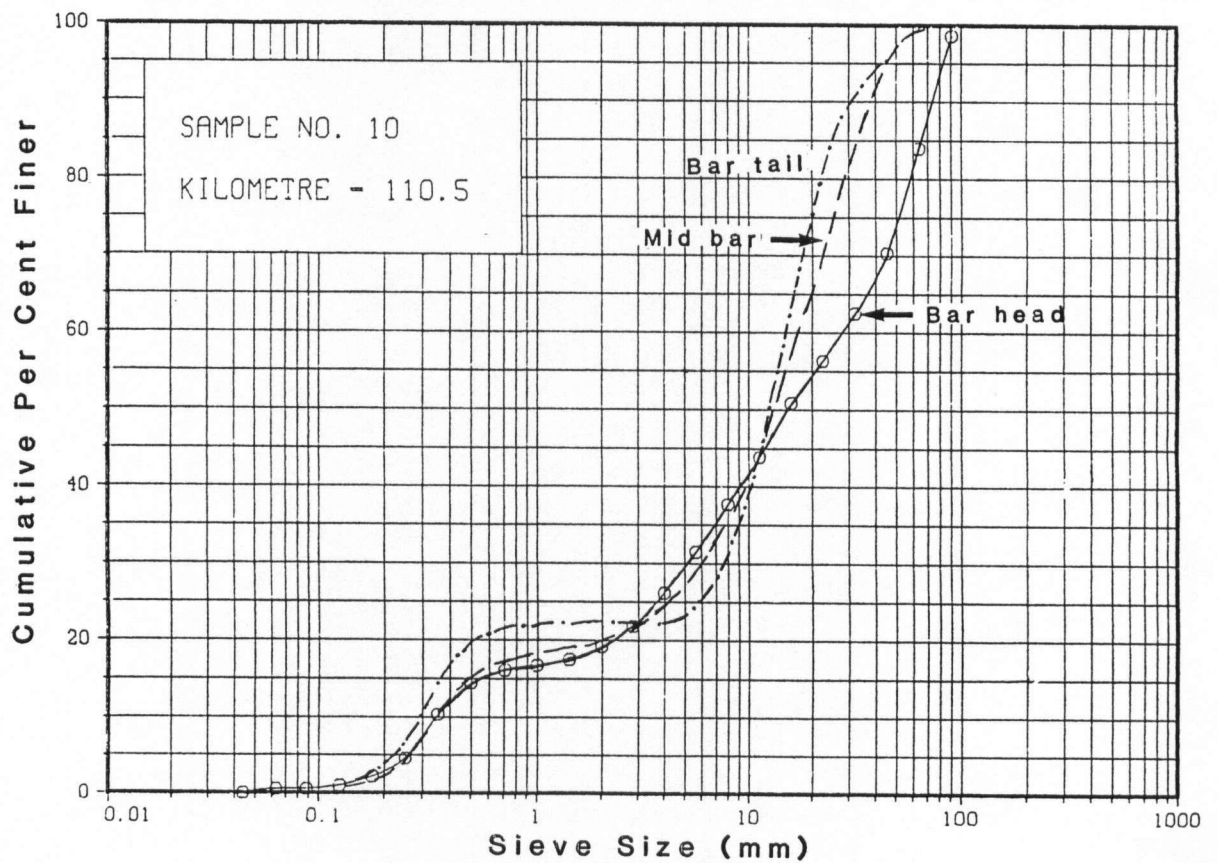
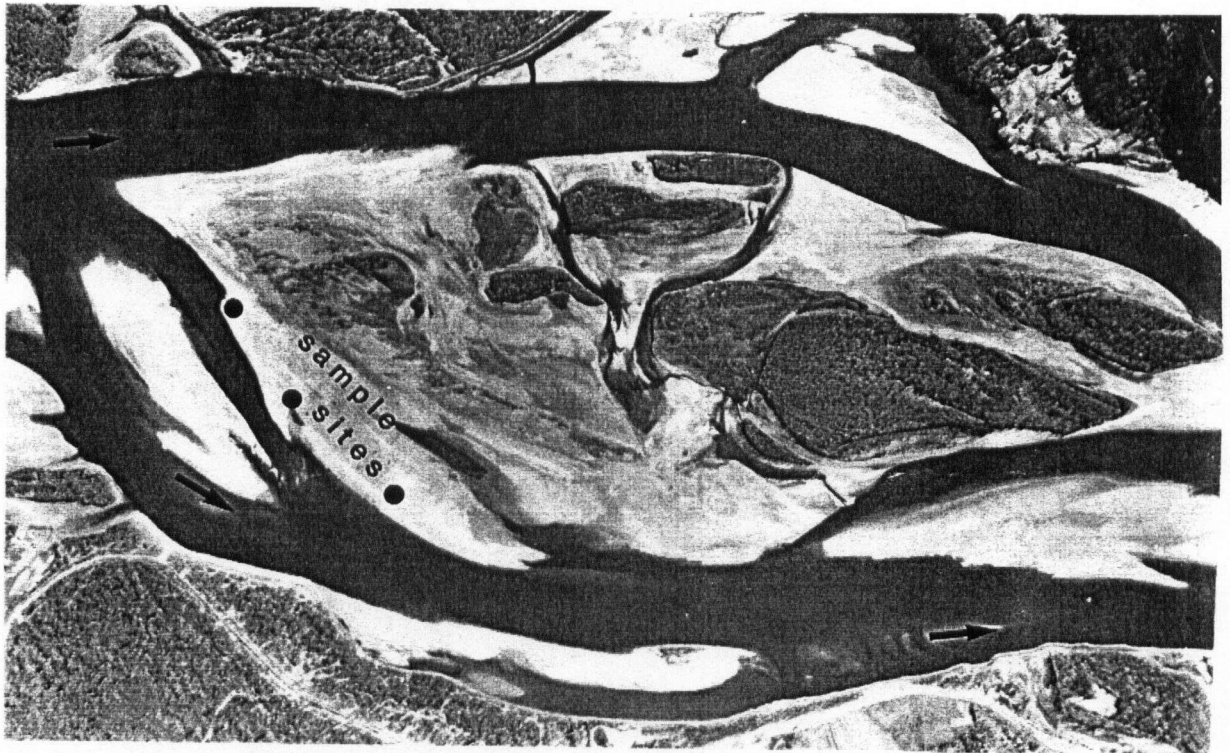


Figure 5.13 Comparison of three sub-surface samples from a gravel bar near Chilliwack

decreased from 16 mm at the bar head to 13 mm at the centre of the bar and 12 mm near the bar tail. The corresponding sand fractions at the three sites were 19%, 20% and 22%.

These results illustrate that the overall composition of the gravel bars was finer than the composition from samples taken at the bar head. Furthermore, the fraction of the bar composed of gravel sized sediments were slightly lower (between 88% and 95% for the three test sites) than in the bar head. For the purposes of producing the gravel sediment budget, a correction factor of 0.9 was applied to the results of the bar head samples along the river.

#### **5.3.4 Downstream Changes in Grain Size**

Figure 5.14 shows the location of all bed material sampling sites. Table 5.4 summarizes the size distribution of the sub surface bed sediments along the river between Hope and Mission. The downstream changes in the size distributions are summarized in Figures 5.15 and 5.16. The volumetric bar head samples show that there is a relatively consistent decrease in the size of the coarsest particles in the bed (as measured by the  $D_{90}$  size) along the river downstream of Hope. For example, the  $D_{90}$  size decreases from 130 mm near Hope to only about 60 mm near Agassiz, 40 km downstream. Near Sumas Mountain 65 km downstream from Hope the  $D_{90}$  size was reduced to only about 25 mm.

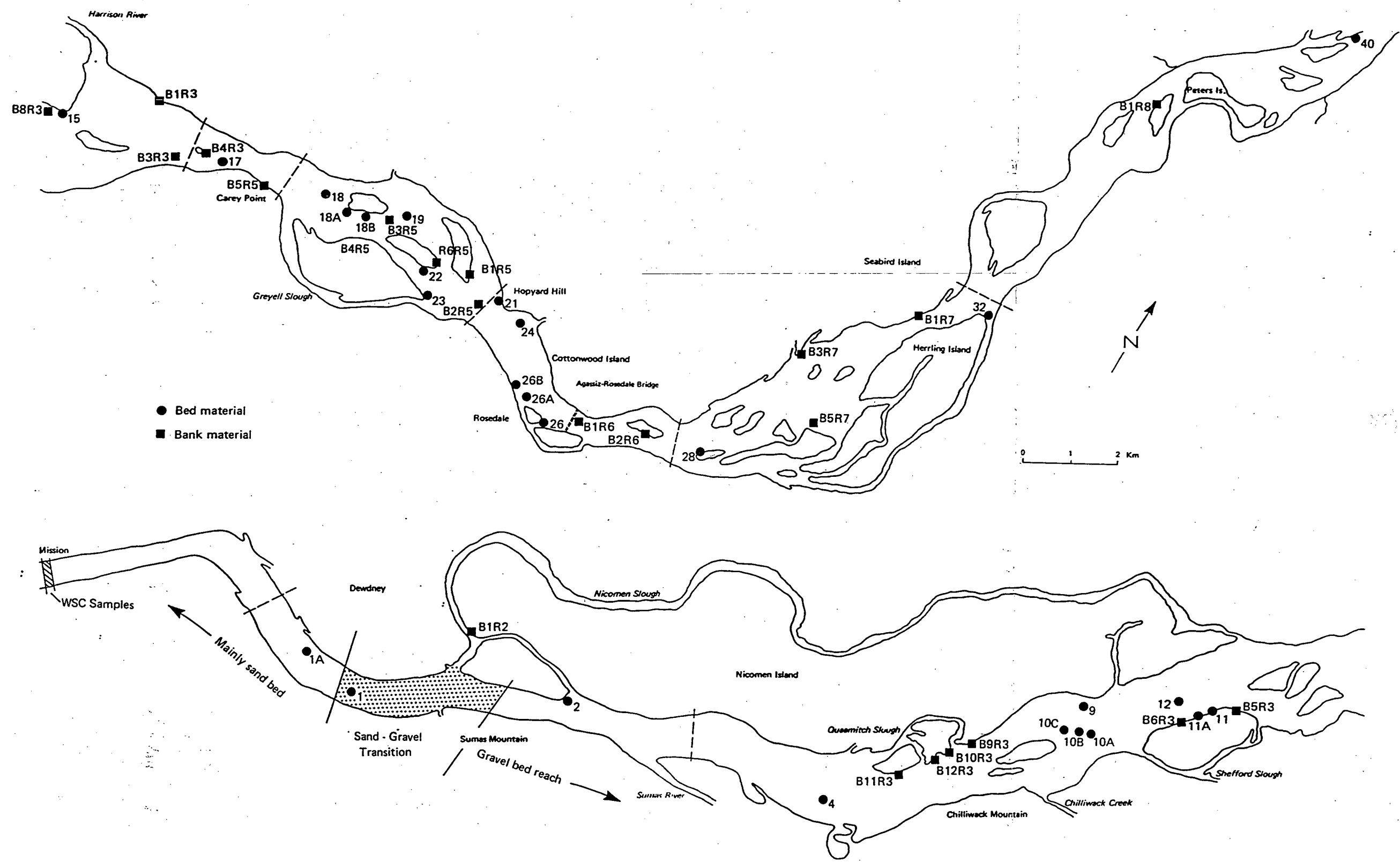


Figure 5.14 Location of bed and bank material samples that were collected in 1983 and 1984

**TABLE 5.4**  
**BED MATERIAL CHARACTERISTICS (mm)**

Site Name	Date	Ref. Distance (km)	Site Location	Morphologic Unit	Sample Location on Unit	Grain Size at Indicated Frequencies (mm)						% Gravel	% > 25 mm
						10%	25%	50%	75%	90%	100%		
WSC	composite	84	Mission	CHAN	THAL	0.18	0.22	0.34	0.5	8	84	14	0
1A	29/01/84	91	Hatzic slough	SB	MB	0.11	0.13	0.18	0.23	0.3	5.66	0	0
T1A	29/01/84	91	Lower Sumas Mtn	CHAN	THAL	all sand							
T2A	03/08/84	92	Lower Sumas Mtn	CHAN	THAL	0.27	0.33	0.42	0.53	0.9	32	7	2
D1	03/08/84	94	Lower Sumas Mtn	CHAN	THAL	0.25	0.3	0.33	0.4	0.5	8	1	0
D-2	03/08/84	94	Lower Sumas Mtn	CHAN	THAL	0.2	0.28	0.33	0.35	0.45	4	0.04	0
D-3	03/08/84	95	Lower Sumas Mtn	CHAN	THAL	poor recovery      gravely sand							
D-6	03/08/84	95	Lower Sumas Mtn	CHAN	THAL	0.2	0.37	0.52	0.6	24	32	33	0
D-7	03/08/84	95	Lower Sumas Mtn	CHAN	THAL	0.27	0.33	0.45	0.6	0.72	45	5	0.5
D-8	03/08/84	95	Lower Sumas Mtn	CHAN	THAL	0.2	0.37	0.7	15	28	32	28	12
D-9	03/08/84	95	Lower Sumas Mtn	CHAN	THAL	0.28	0.38	0.45	0.63	0.7	11	5	0
D-10	03/08/84	95	Lower Sumas Mtn	CHAN	THAL	poor recovery      gravely sand							
D-11	03/08/84	95	Lower Sumas Mtn	CHAN	THAL	0.25	0.32	0.41	0.5	0.66	32	4	1
D-12	03/08/84	95	Lower Sumas Mtn	CHAN	THAL	0.25	0.3	0.38	0.47	0.6	16	2	0
T-3	09/05/84	98	Strawberry Island	CHAN	THAL	no recovery      gravel							
T-4	09/05/84	98	Strawberry Island	CHAN	THAL	0.18	0.25	0.3	0.36	0.44	8	0	0
1	10/03/83	92	Lower Sumas Mtn	MCB	BH	0.3	2.7	10.5	15	28	64	78	12
2	05/02/83	98	Strawberry Island	SB	BH	0.32	0.42	5	15	25	45	54	12
4	02/02/83	102.5	US Vedder River	MCB	BH	0.35	4	12	21	32	64	78	18
9	02/02/83	109.8	Nicomen Island	SB	BH	0.6	6	17	34	55	90	86	35
10	16/08/83	110.5	Nicomen Island	LB	BH	0.35	3.8	15	50	73	90	81	43
10B	16/08/83	110	Nicomen Island	LB	MB	0.34	4.1	13	25	37	90	80	25
10C	16/08/83	109.5	Nicomen Island	LB	BT	0.31	6	13	20	30	64	78	15
11	12/08/83	112	Shefford Slough	SB	BH	0.56	3.2	11	25	37	64	80	25
11A	12/08/83	119.9	Shefford Slough	SB	MB	0.36	0.7	5.5	14	20	45	65	5
12	30/06/83	112.3	Nicomen Slough	LB	MB	0.4	3.2	14	40	65	128	80	38
15	01/07/83	118.6	Harrison River	ISLAND	BH	0.5	5.6	15	26	34	64	83	26
17	17/06/83	120	Carey Point	LB	BH	0.5	4	15	42	65	91	82	38
17A	22/06/83	119.8	Carey Point	SB	BT	0.4	9	23	40	58	91	84	47
18	18/08/83	122.7	Carey Point	LB	BH								
18A	19/08/83	123.3	Carey Point	MCB	MB	0.3	1	12	21	32	91	74	18
18B	23/08/83	124	Carey Point	MCB	BH	0.35	6.5	18	32	44	91	78	37
19	18/08/83	124.5	Hopyard Hill	MCB	BH	0.5	4.2	16	45	70	128	79	37
22	23/06/83	126	Greyell Slough	CHAN	BH	0.43	6.3	23	50	79	128	84	47
21	04/02/83	126.5	Hopyard Hill	SB	BH	0.43	7.8	24	52	73	128	86	49
23	16/03/83	126.7	Greyell Slough	CHAN	BH	0.5	7	22	42	72	128	86	46
24	27/07/83	128	Hopyard Hill	ISLAND	BH	0.3	11	25	41	60	128	82	50
26A	06/08/83	129.4	Agassiz Bridge	LB	BH								
26B	07/08/83	129.3	Agassiz Bridge	LB	BH	0.33	5.5	21	45	80	128	82	47
28	02/07/83	134	Herrling Island	CHAN	BH	0.38	3	17	40	65	128	78	
32	03/09/83	139.8	Herrling Island	ISLAND	BH	0.32	12	33	52	70	128	83	63
40	27/08/83	163.7		SB	BH	0.25	3	17	27	33	91	76	25
41	27/08/83	163.8	Seabird Island	LB	BH	0.4	7	25	60	130	181		

Notes:

Morphologic Units

Sample Location

CHAN = Channel

THAL = Thalweg

SB = Side Bar

MB = Mid-Bar

MCB = Mid Channel Bar

BH = Bar Head

LB = Lateral Bar

BT = Bar Tail



It is common to describe the downstream change in grain size (D) with distance along a channel (x) in terms of a simple exponential expression:

$$D = D_0 * \exp(-ax)$$

where a is a diminution coefficient

The basis for an exponential decrease in grain size has been discussed by several researchers (Shaw and Kellerhals, 1982). A regression between median particle size in logarithmic units and distance produced a diminution coefficient of  $0.024 \text{ km}^{-1}$ . However, as shown on Figure 5.16, there is a substantial scatter in the relation between grain size and distance along the river. In fact, the variability in sediment sizes within particular reaches is comparable in magnitude to the trend in sediment sizes along the channel.

This scatter is partially due to sheltering effects that can develop at individual sampling sites which results in finer sediments being deposited at the sites.

The apparent diminution coefficient is about 5 to 10 times greater than values reported from measurements along many Alberta gravel bed rivers (Shaw and Kellerhals, 1982). The Fraser River sediments are composed of a wide variety of lithologies but contain mainly relatively competent materials. Armstrong (1981) reported the main components of the gravel sediments are granites, metamorphics and some volcanics. Therefore it is unlikely that the rapid change in grain size

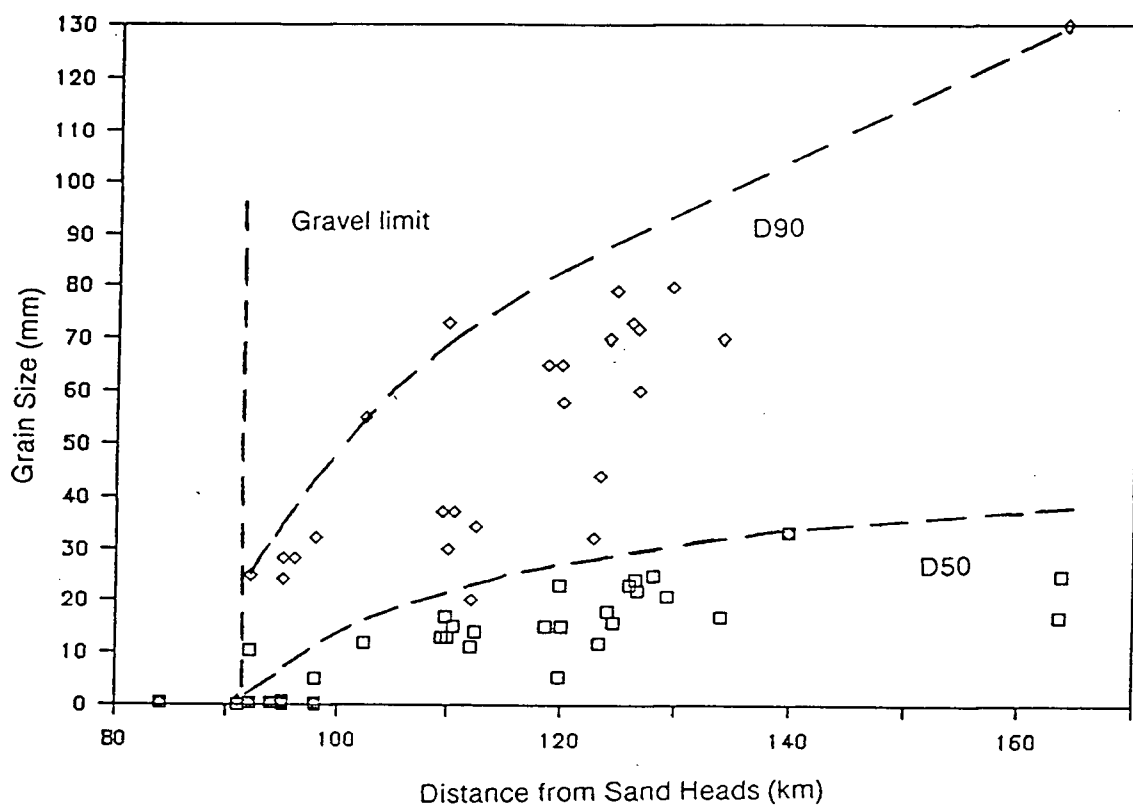


Figure 5.15 Downstream variation in sub-surface particle size between Hope and Mission

downstream of Hope can be attributed to abrasion of particles. The alternative explanation is that the coarsest sediments in the bed are undergoing differential sorting as a result of selective deposition along the river. It is also apparent from Figure 5.15 that an exponential relation does not fit the overall trend of the data very well. In fact, other functions such as a linear relation fit the data equally well.

The transition between the gravel-bed and sand-bed reaches below Sumas Mountain is apparently very abrupt. The most distal mid-channel bar near Sumas Mountain at km 92 contained about 68% gravel. Samples dredged from the main channel only 1 km downstream were composed of sand and contained less than 10% gravel. In fact, other samples from the main channel showed that the bed is composed primarily of sand nearly as far upstream as Nicomen Island. The actual gravel-bed/sand-bed transition was mapped on three different occasions: at low flow on January 29, 1984; on May 9, 1984 near long term mean flow conditions (discharge at Hope was  $2,940 \text{ m}^3/\text{s}$ ); and on August 3, 1984 after the freshet at a discharge of  $5,020 \text{ m}^3/\text{s}$  (at Hope). This work included dredging samples from the river and using an echo sounder to observe the formation of dunes in the sand portion of the channel. The dune profiles provided a means for interpolating the location of the gravel/sand interface across the channel since it was found that bed forms were absent in the gravel portion of the river. In most cases the transition between plane bed (gravel bed) and duned bed (mainly sand) was very abrupt and the interpretations agreed very closely with the results from the sediment sampling.

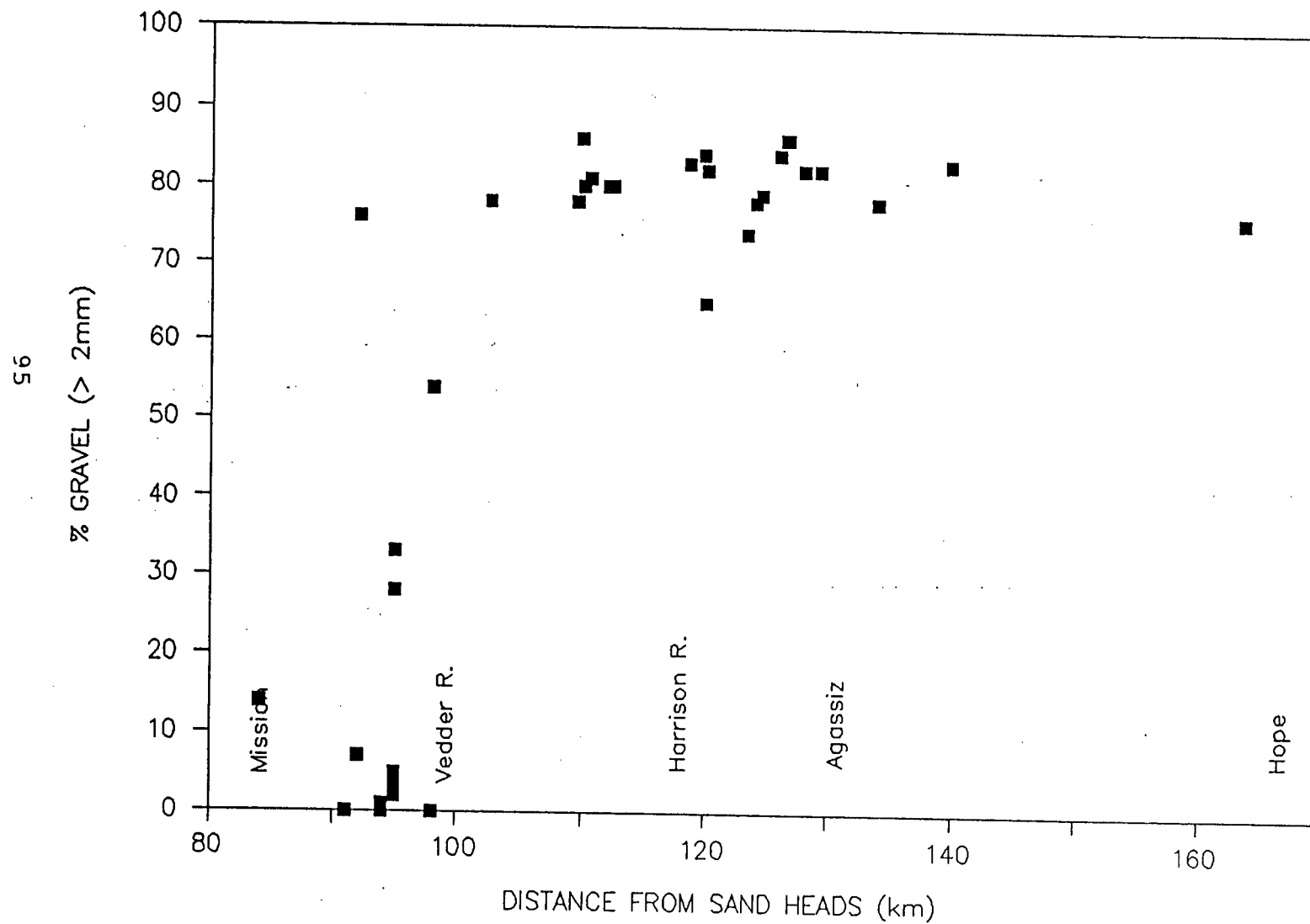


Figure 5.16 Downstream variation in the gravel content of sub-surface bed material samples

The thalweg samples collected in January contained finer sediments than the later samples. In fact, some samples from the thalweg immediately upstream of the mid-channel gravel bar contained a substantial amount of silt and very fine sand. However, in all three cases the sandy main channel deposits commenced just upstream of the lower end of Nicomen slough near km 94 (Figure 5.3). Therefore, the mid-channel gravel bar at km 92 is a relatively isolated feature and is not representative of the adjacent channel characteristics.

Figures 5.17 and 5.18 compare the size distributions of the sandy deposits below Sumas Mountain and at Water Survey of Canada's gauging line at Mission. The samples at Sumas show that the gravel fraction typically makes up less than 5% of the sediments, whereas at Mission the gravel fraction accounts for 16% of the material. In reviewing the bed material data collected by WSC it was found that the coarse gravels are exposed only on the north side of the channel. Since the data reported by WSC represent a composite of five samples across the channel, the local exposure of gravel skews the results of the combined sample. It is likely that the bed gravel at Mission is derived from bank erosion of the glacial-fluvial deposits that confine the north bank of the river. Therefore, these samples are not representative of the sand bed portion of the river.

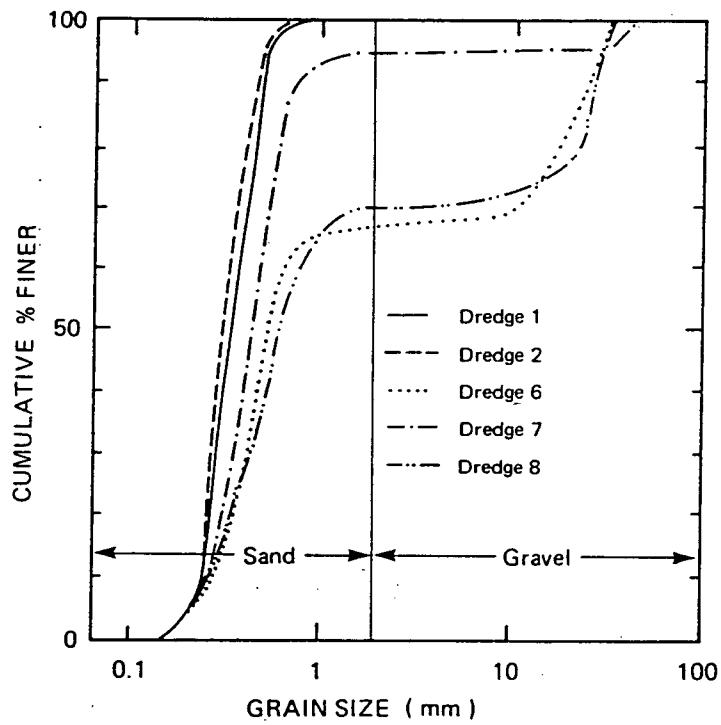


Figure 5.17 Volumetric bed material samples from the main channel near Sumas Mountain

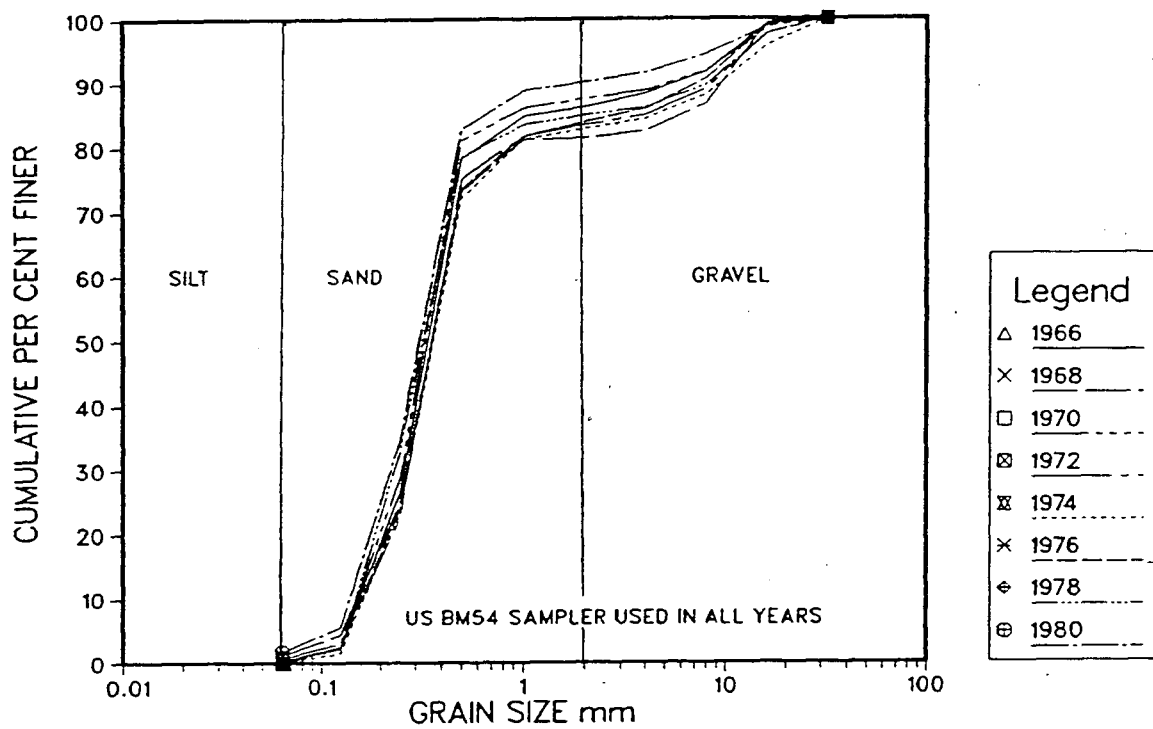


Figure 5.18 Bed material characteristics at Mission hydrometric station

#### 5.4 Bank Materials

The bank materials typically consist of a basal layer of poorly sorted gravel and sand deposits overlain by 1 to 3 m of finer sandy or silty floodplain sediments. The main emphasis of the sampling program was to determine the sizes of the sediments in the basal layer, and to identify and map the distribution of non-alluvial deposits along the river. The bank material samples were taken from actively eroding islands or floodplain areas. Table 5.5 summarizes the size gradations of the basal layer materials. Figures 5.19 and 5.20 show the variations in bank material sizes along the channel.

Over most of the river the composition of the alluvial basal layer deposits is very similar to the channel materials. This is not surprising since many islands have evolved from bar sites. In particular, these deposits show the same bimodal characteristics as the bed material. Figure 5.20 shows that the basal layer materials are typically composed of 75% - 80% gravel between Hope and Nicomen Island. The median size of the bank materials is about 25 mm at Agassiz and starts to decline noticeably downstream of the Harrison River confluence. Bank exposures of gravels are not found downstream of about km 105, near Yaalstrick Island. As discussed previously, the last active gravel bar extends to km 92, or 13 km further downstream from this site.



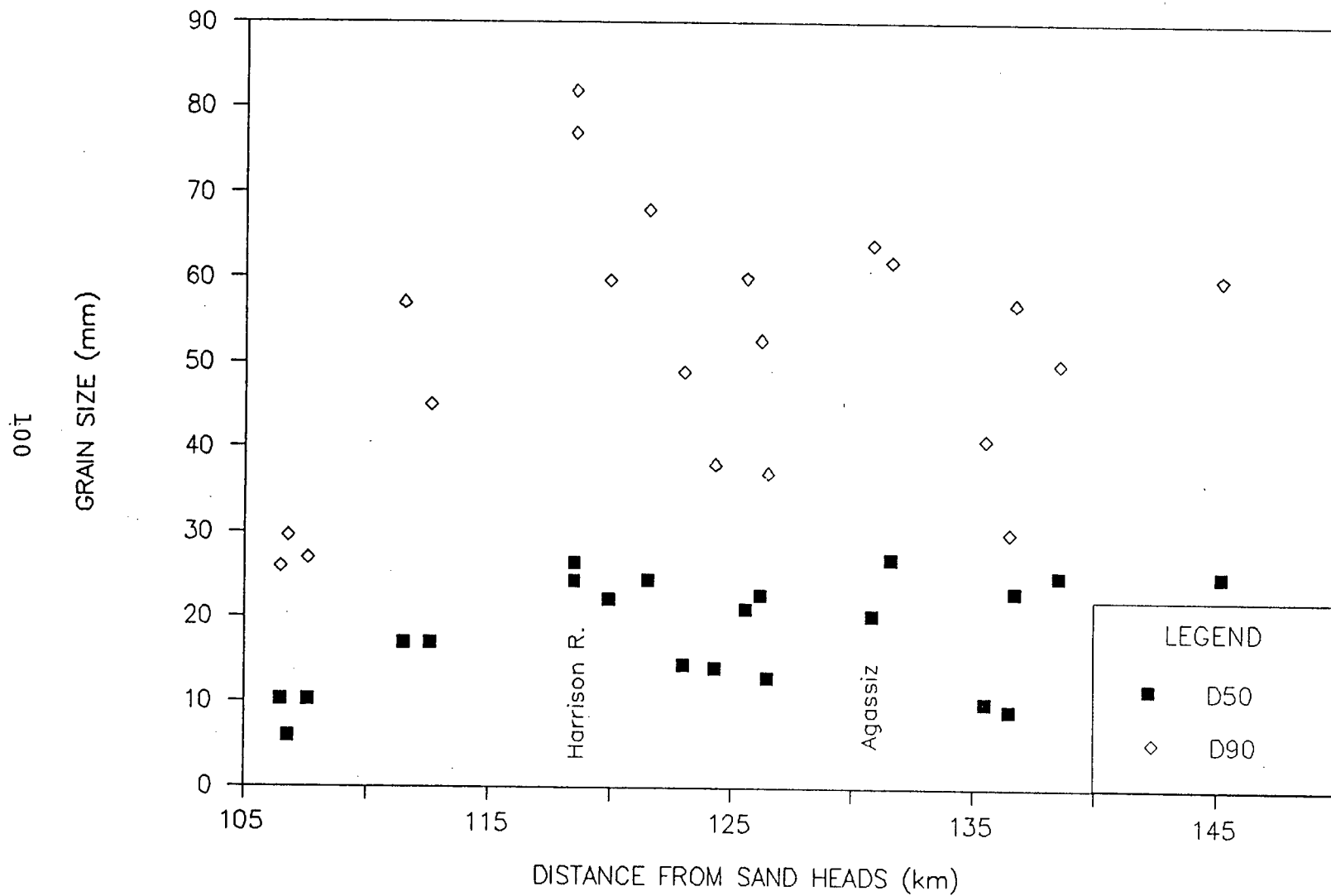


Figure 5.19 Downstream variations in bank material composition between Hope and Mission

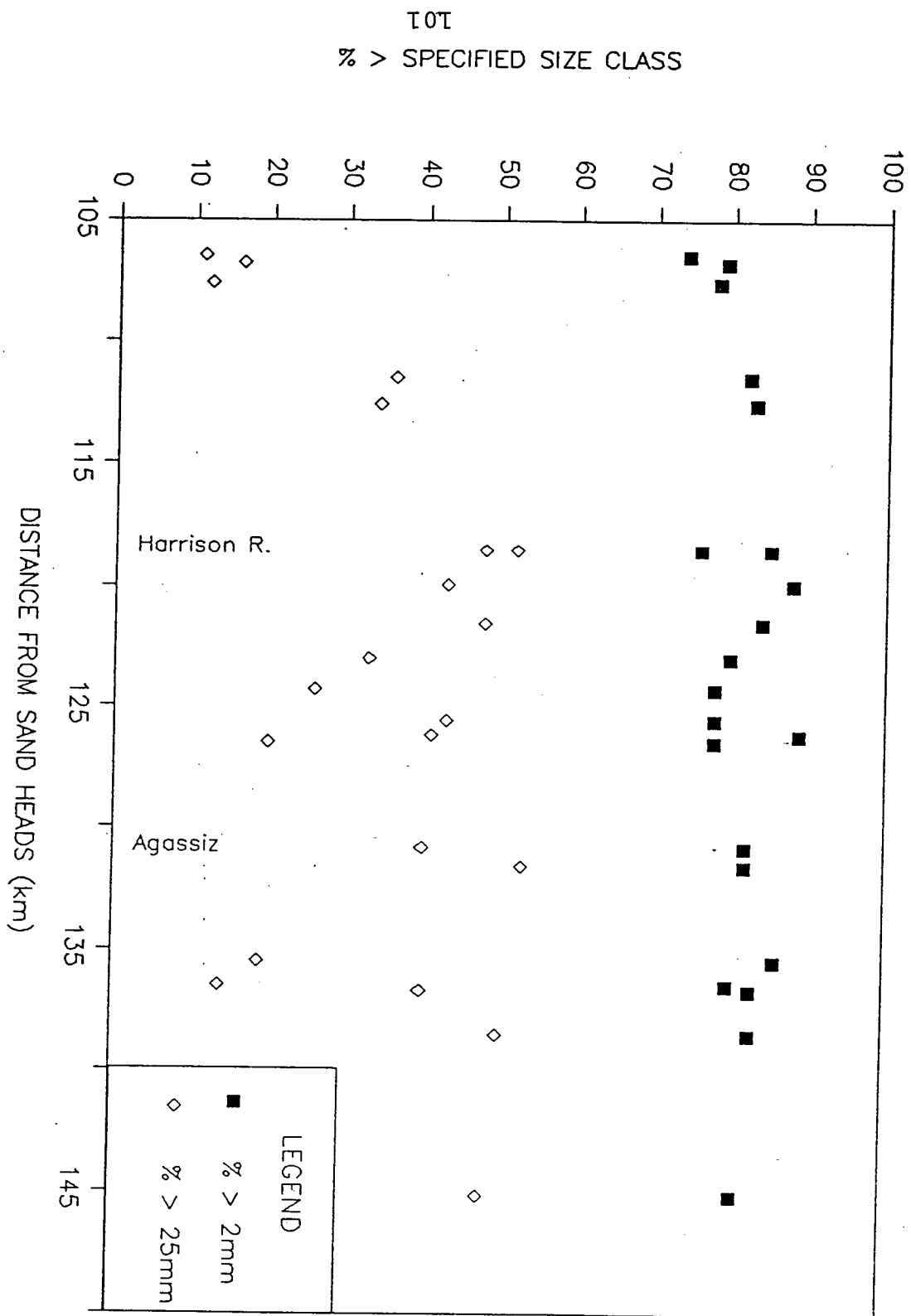


Figure 5.20 Downstream variation in the gravel content of bank materials between Hope and Mission

TABLE 5.5

## BANK MATERIALS (BASAL LAYER)

SITE NAME	DATE	REF. DIST. (km)	LOCATION	MORPHO-LOGIC UNIT	SAMPLE LOCATION ON UNIT	HEIGHT (m)		Grain Size at Indicated Cumulative Frequencies (mm)						Per Centage	
						BASAL LAYER	TOP LAYER	10%	25%	50%	75%	90%	100%	Gravel	>25 mm
R3-B12	31/08/83	106.5	Yaalstrick Island	Island			0	0.3	1.1	10.3	19	26	50	74	11
R3-B10	31/08/83	106.8	Yaalstrick Island	Island	MID	1.4	2	0.38	4.1	5.9	20	29.6	64	79	16
R3-B9	31/08/83	107.6	Yaalstrick Island	Island	US	2	0.4	0.4	3.4	10.3	18.1	27	91	78	12
R3-B6	22/06/83	111.5	Nr. Shefford Slough	Island	MID	1	1.9	1.9	4.3	17	35	57	128	82	36
R3-B5	22/06/83	112.6	Nr. Shefford Slough	Island	US	0.75	1.3	1.3	5.8	17	31	45	91	83	34
R3-B7	30/06/83	118.5	Nr. Harrison River	Island	US	1.5	0.1	0.1	9	26.5	51.3	82	128	85	52
R3-B8	01/07/83	118.5	Nr. Harrison River	Island	US				3	24.3	50.9	77	128	76	48
R3-B4	21/06/83	119.9	Nr. Nelson Slough	Island	DS	0.8	0.65	0.65	10.1	22.2	40.5	59.7	128	88	43
R3-B10															
R5-B5	19/08/83	121.5	Carey Point	FP				0.42	6.2	24.4	49.5	68	128	84	48
R5-B4	19/08/83	123	Greyell Island	Island	DS	2.4	0.8	0.32	3.8	14.4	32	49	91	80	33
R5-B3	18/08/83	124.3	Nr. Mountain Slough	BAR	MID	1.7	0.1	0.31	4.2	14	25.8	38	64	78	26
R5-B6	23/08/83	125.6	Nr. Greyell Slough	Island	MID	2.5	1	0.38	6.1	21	40.5	60	91	78	43
R5-B1	27/08/83	126.2	Nr. Hopyard Hill	Island	US	1.05	0.4	1.5	10	22.6	35	52.7	128	89	41
R5-B2	27/07/83	126.5	Nr. Hopyard Hill	Island	DS	0.85		0.34	4.9	12.9	27	37	91	78	20
R6-B1	09/07/83	130.8	US Agassiz Bridge	Island	DS	7	0	0.47	5	20.3	40	64	128	82	40
R6-B1A	09/07/83	130.8	US Agassiz Bridge	Island	DS	7	0								
R6-B2	16/07/83	131.6	US Agassiz Bridge	Island	US	0.45	1.25	0.4	10	27	43	62	128	82	53
R7-B5	03/09/83	135.5	Herrling Island	Island	MID	1.7	0.2	0.65	4.4	10	21	41	91	86	19
R7-B2	03/09/83	136.7	Herrling Island	Island		0.6	1.42	0.4	7.3	23	38	57	91	83	40
R7-B3	02/09/83	136.5					2.2	0.4	3.1	9.1	18.5	30	64	80	14
R7-B1	02/07/83	138.5	Seabird Island	Island	MID	1.3	1	0.42	15	25	38	50	91	83	50
R8-B1	16/07/83	145.2	Peters Island	Island	MID	1	0.1	0.3	11.6	25.1	40.2	60	128	81	48

In this reach the banks typically consist of massive, brown sands or silty sands or occasionally sandy silt. In some places such as near the lower end of Sumas Mountain the banks are composed of organic clay and silt with peat. This evidence suggests that the main channel has shifted laterally across the valley floor in relatively recent times and is now cutting across former backchannels or slackwater areas. This would imply that the former main channel was situated further north, in the vicinity of Nicomen Island. It is apparent that the features exposed in this section of the river are not a product of contemporary sedimentation processes.

## **6.0 PATTERNS OF CHANNEL INSTABILITY**

### **6.1 Introduction**

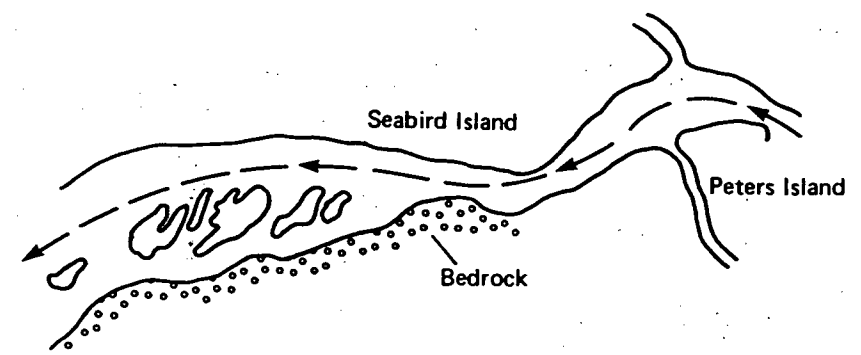
In this investigation, channel shifting and bank erosion processes were studied by comparing historical maps and air photos. Channel-shift maps were prepared by superimposing 1:15,840 or 1:31,680 legal township maps of 1876-1906 and air photo maps from 1928 and 1943 onto 1:25,000 National Topographic maps of 1971. Additional photo maps were prepared to study specific channel areas using air photos from 1954, 1967, 1973, 1979 and 1982. Areas where erosion or accretion has occurred over the last century have been given a site number and are identified on Figure 6.1. The channel shift maps of individual reaches are summarized on Figures 6.2 to 6.6. Comparative air photos of the reaches are summarized in Appendix B.

### **6.2 Historical Channel Changes**

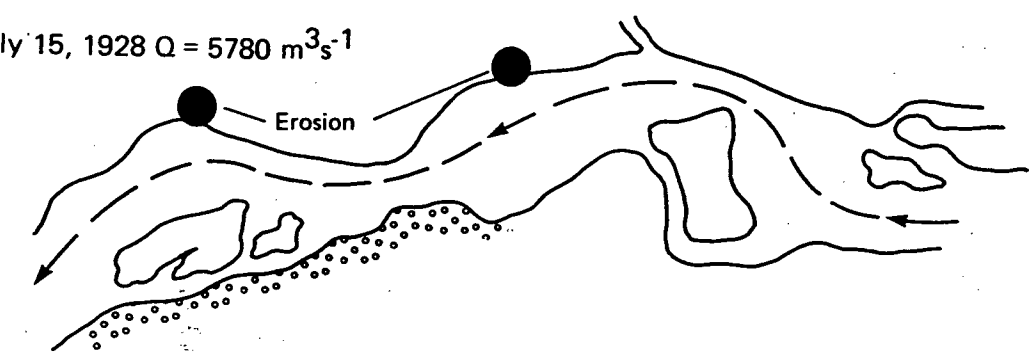
The overall channel pattern has remained remarkably stable over the last century. Most of the major island groups such as Peters Island, Herrling Island, Greyell Island and Yaalstrick Island were mapped in the original township surveys. Vegetation evidence suggests that some islands have existed for considerably longer than a century. A cottonwood on Yaalstrick Island was dated at 140 years. Large cedars found on Greyell Island and near Maria Slough suggest that these areas have remained stable for even longer periods. However, large areas of floodplain have

Figure 6.1 In pocket at back of thesis

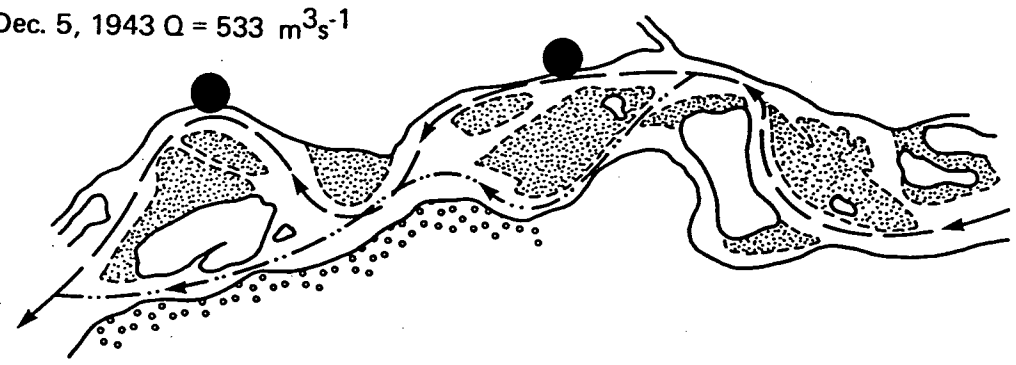
Township Survey 1878 - 1907



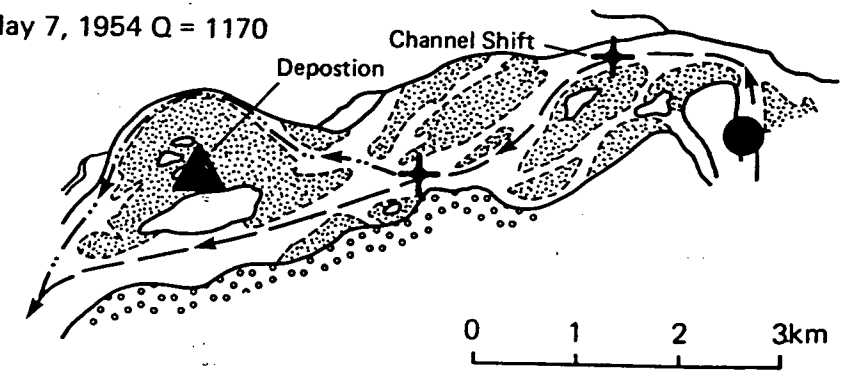
July 15, 1928  $Q = 5780 \text{ m}^3\text{s}^{-1}$



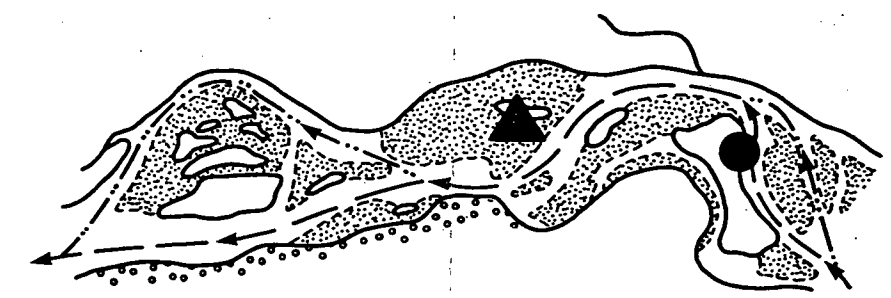
Dec. 5, 1943  $Q = 533 \text{ m}^3\text{s}^{-1}$



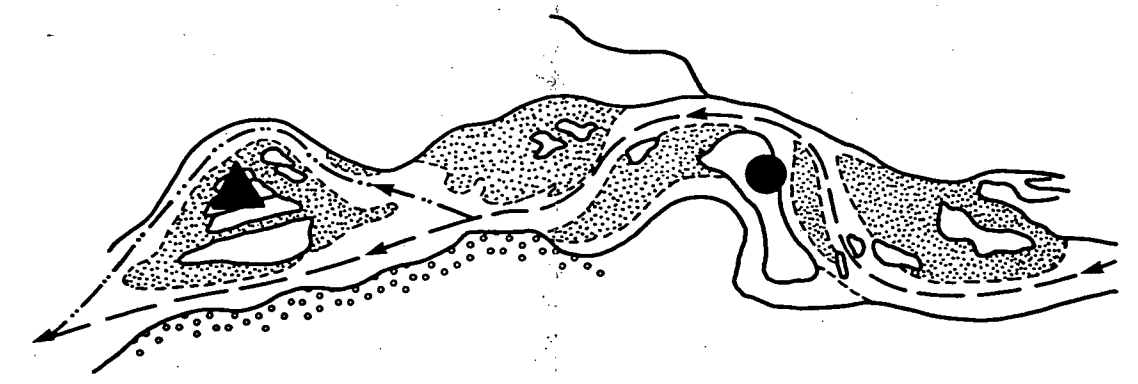
May 7, 1954  $Q = 1170$



April 11, 1967  $Q = 1120 \text{ m}^3\text{s}^{-1}$



March 18, 1971  $Q = 799 \text{ m}^3\text{s}^{-1}$



March 22, 1979  $Q = 1010 \text{ m}^3\text{s}^{-1}$

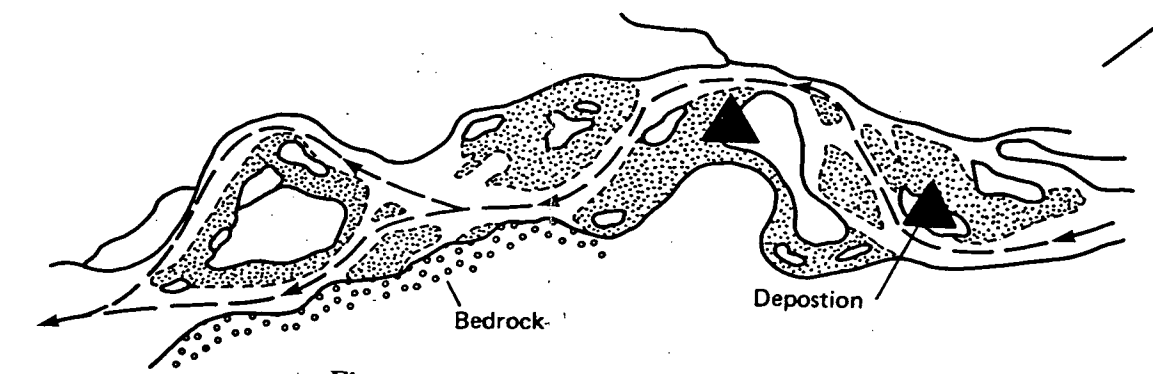
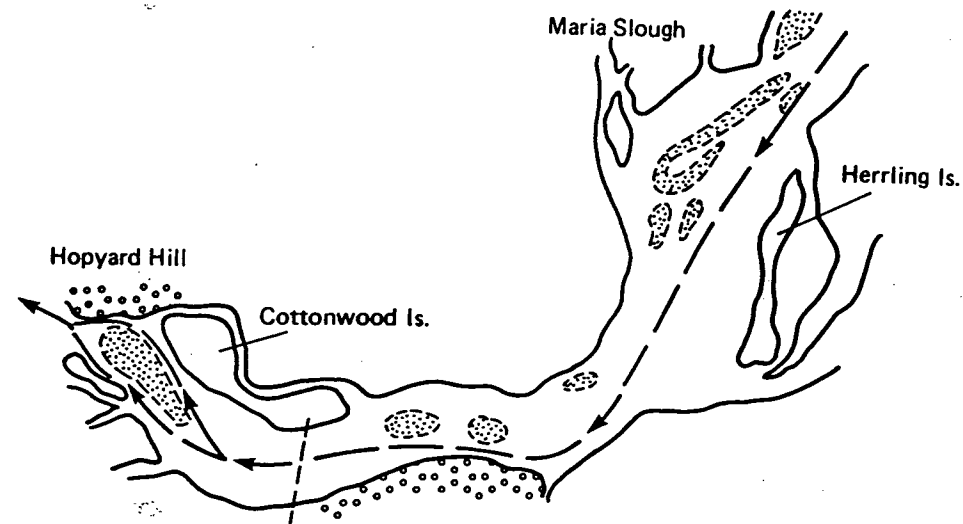
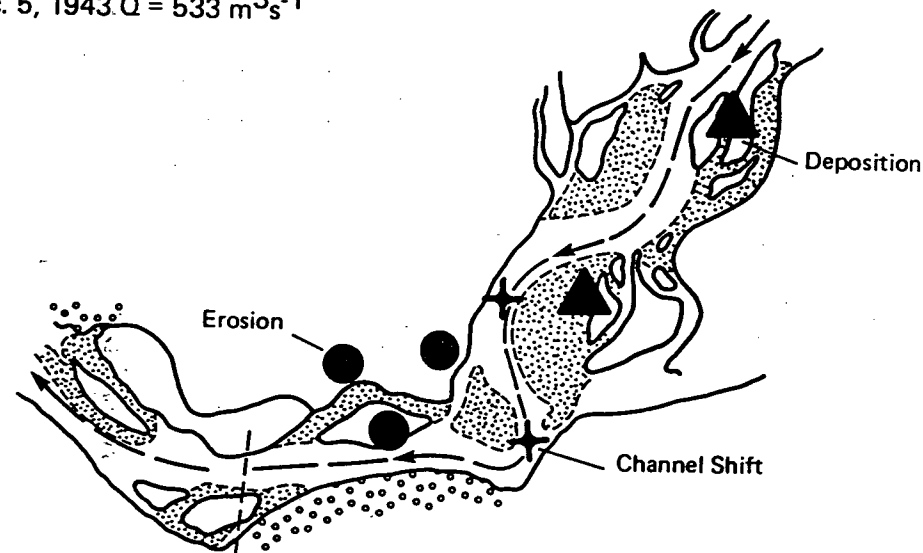


Figure 6.2 Channel changes, Peters Island - Herrling Island

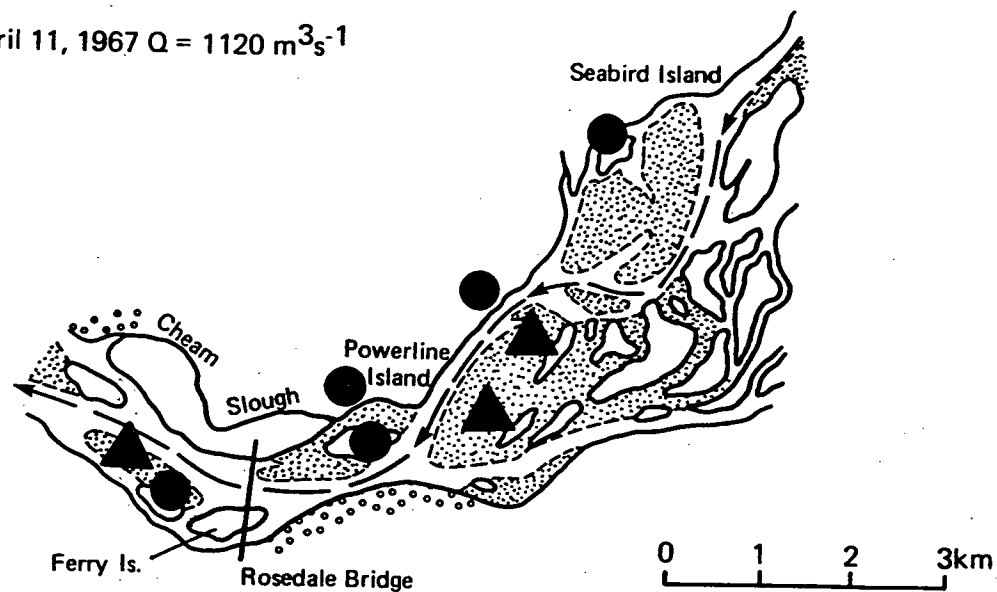
Township Survey 1872 - 1902



Dec. 5, 1943  $Q = 533 \text{ m}^3\text{s}^{-1}$

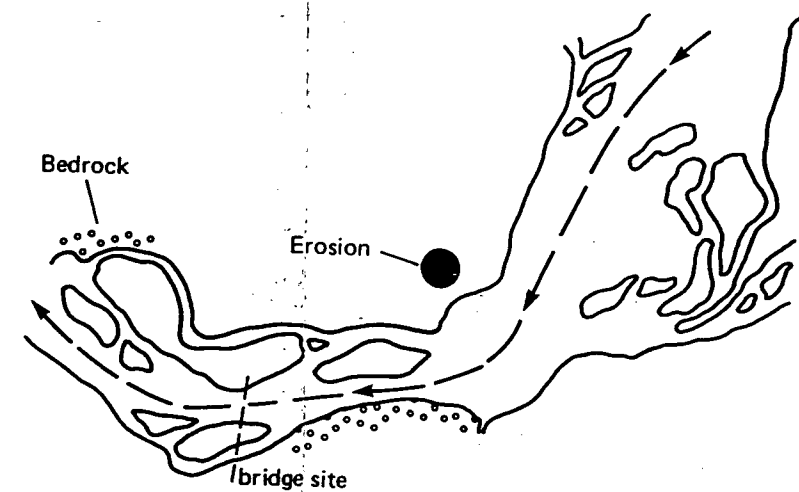


April 11, 1967  $Q = 1120 \text{ m}^3\text{s}^{-1}$

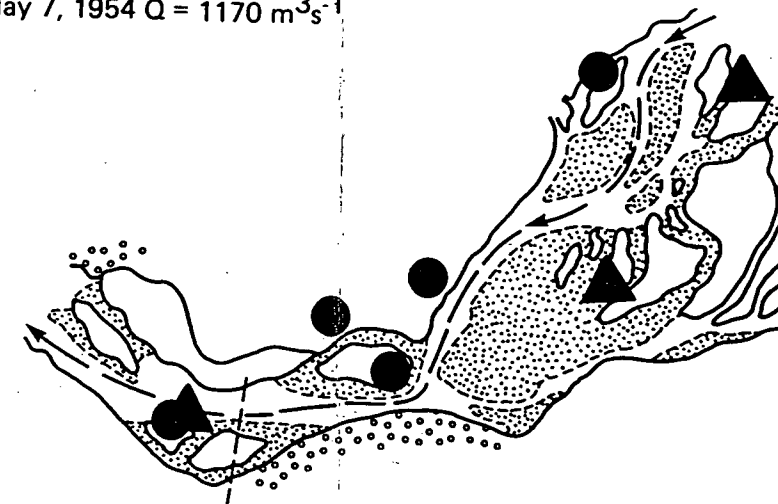


0 1 2 3km

July 15, 1928  $Q = 5780 \text{ m}^3\text{s}^{-1}$



May 7, 1954  $Q = 1170 \text{ m}^3\text{s}^{-1}$



March 22, 1979  $Q = 1010 \text{ m}^3\text{s}^{-1}$

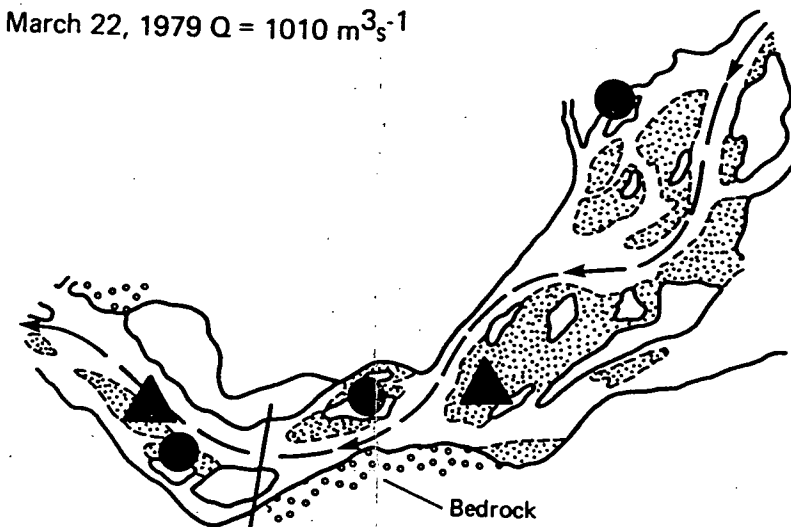


Figure 6.3 Channel changes in the Herrling Island - Rosedale bridge reach



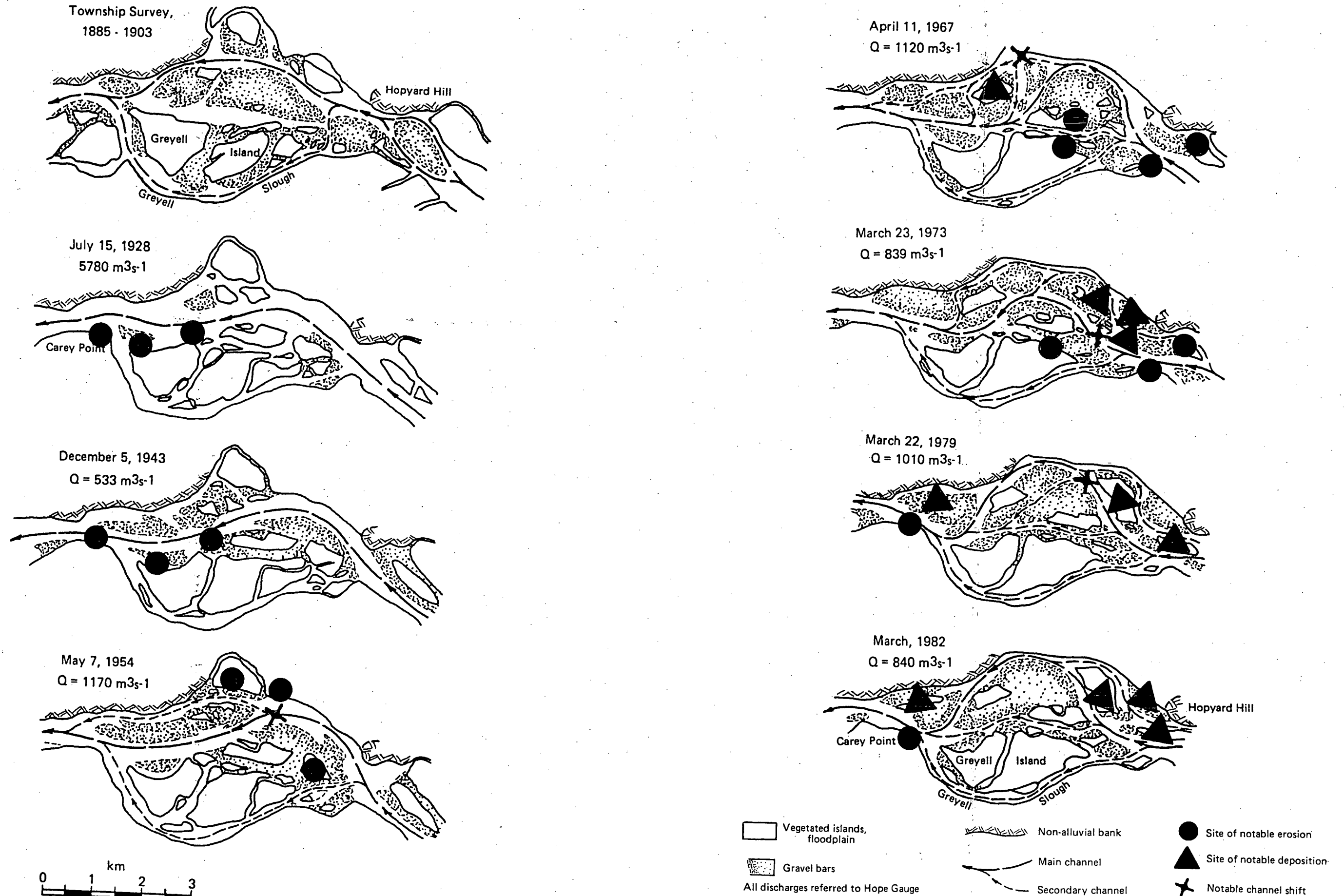


Figure 6.4 Channel changes in the Greyell Island - Carey Point reach

Township Survey 1885 - 1903

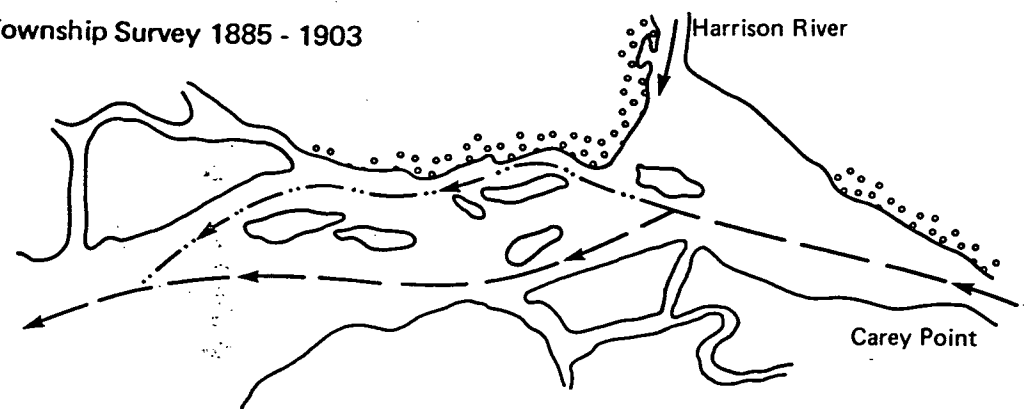
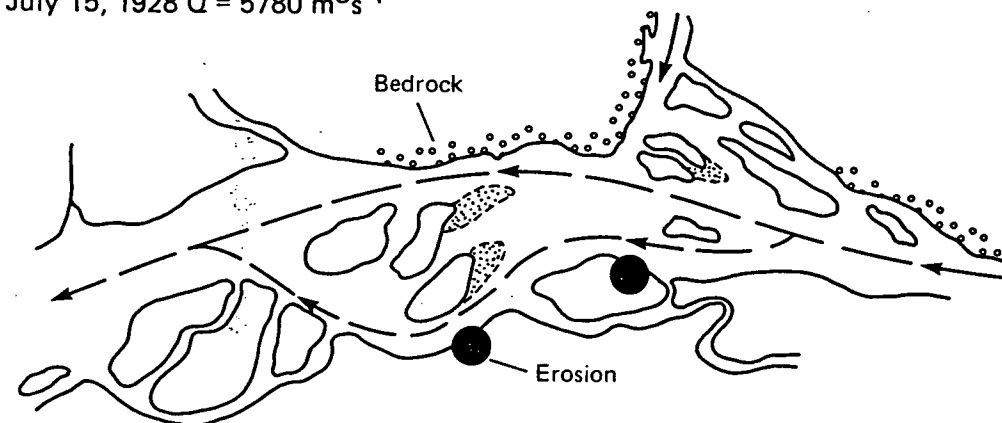
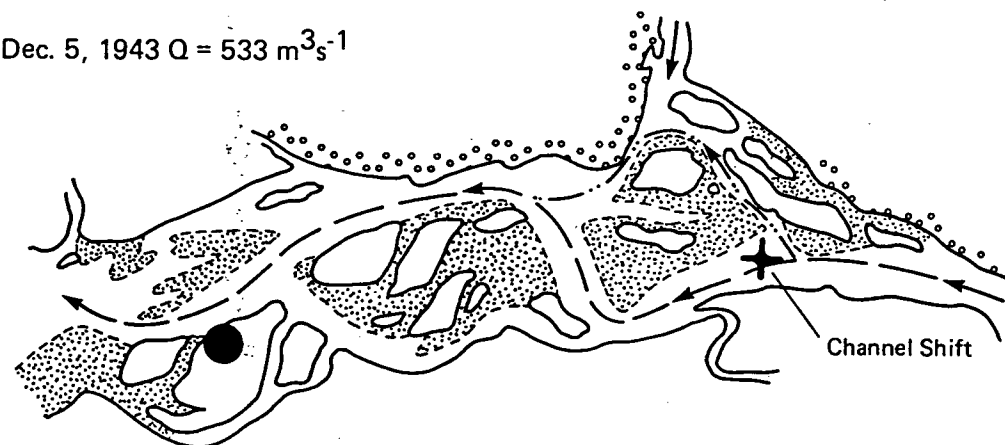
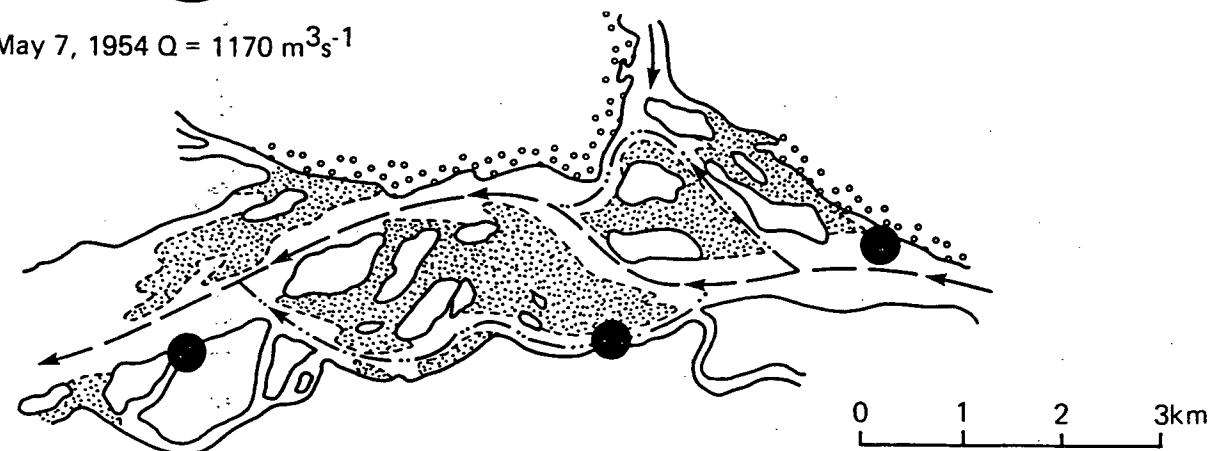
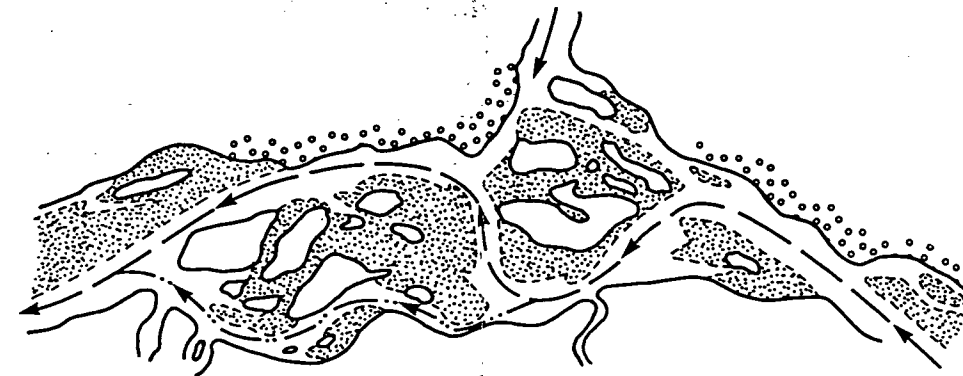
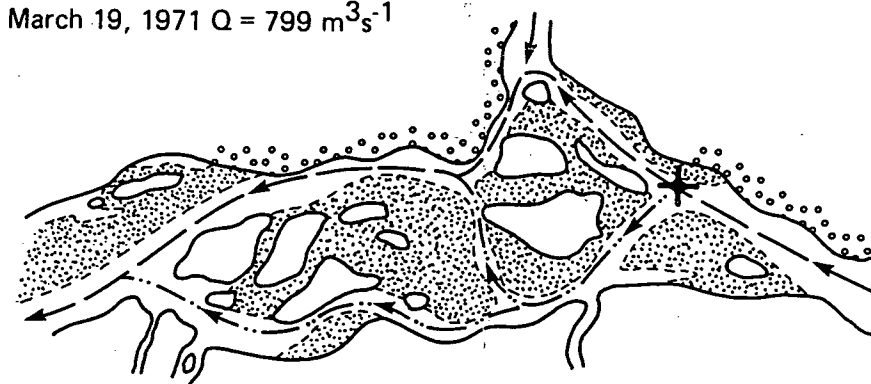
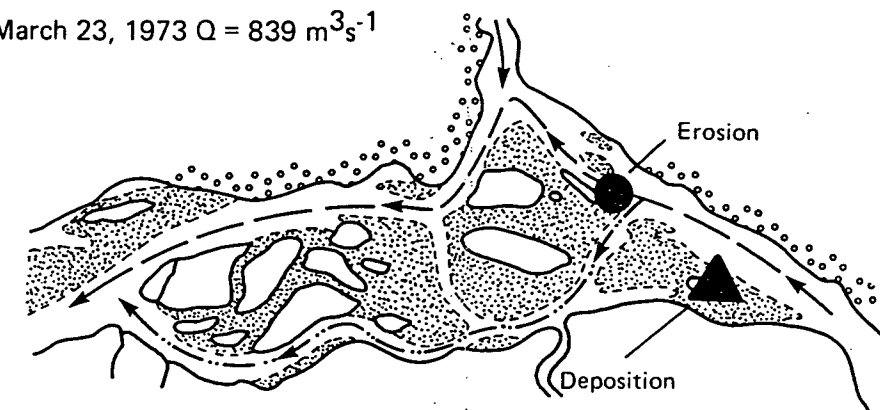
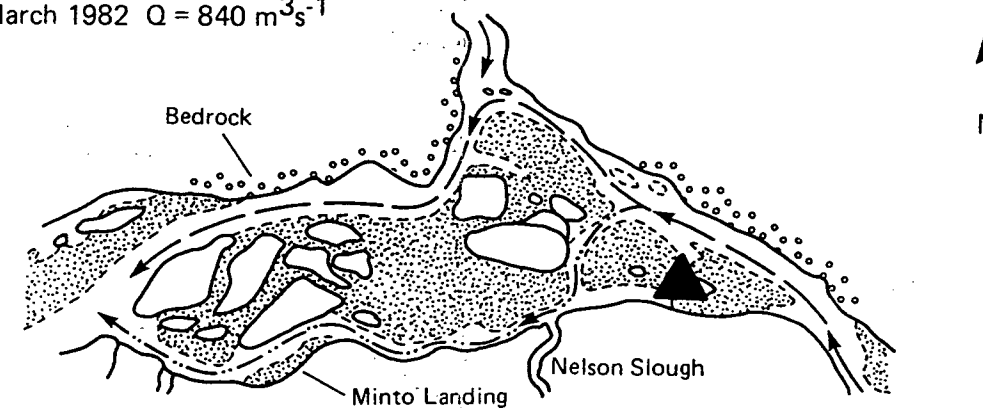
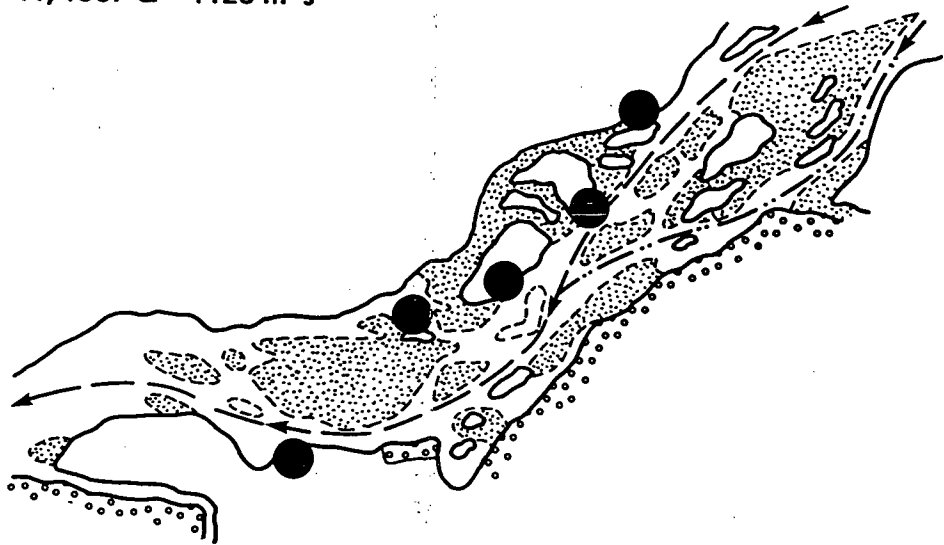
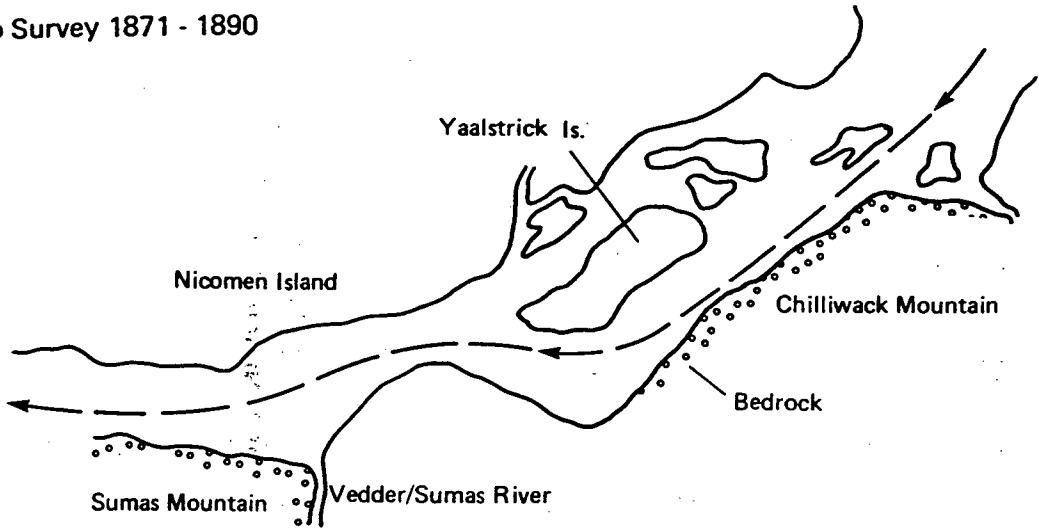
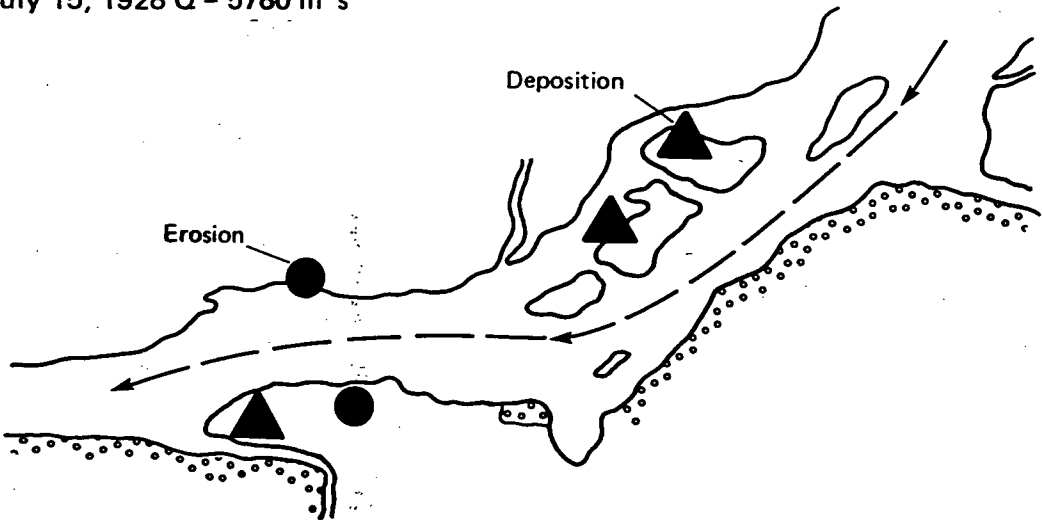
July 15, 1928  $Q = 5780 \text{ m}^3\text{s}^{-1}$ Dec. 5, 1943  $Q = 533 \text{ m}^3\text{s}^{-1}$ May 7, 1954  $Q = 1170 \text{ m}^3\text{s}^{-1}$ April 11, 1967  $Q = 1120 \text{ m}^3\text{s}^{-1}$ March 19, 1971  $Q = 799 \text{ m}^3\text{s}^{-1}$ March 23, 1973  $Q = 839 \text{ m}^3\text{s}^{-1}$ March 1982  $Q = 840 \text{ m}^3\text{s}^{-1}$ 

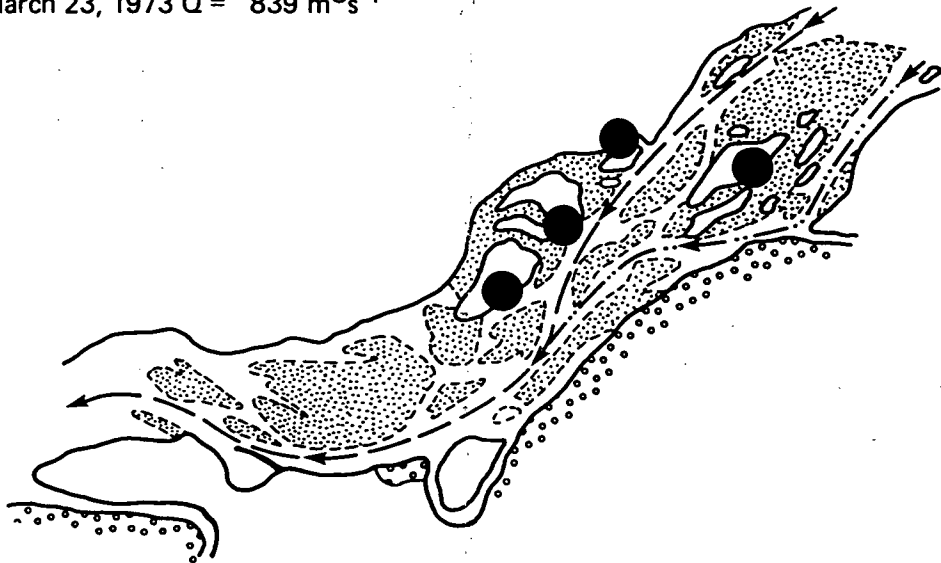
Figure 6.5 Channel changes in the Carey Point - Harrison River reach



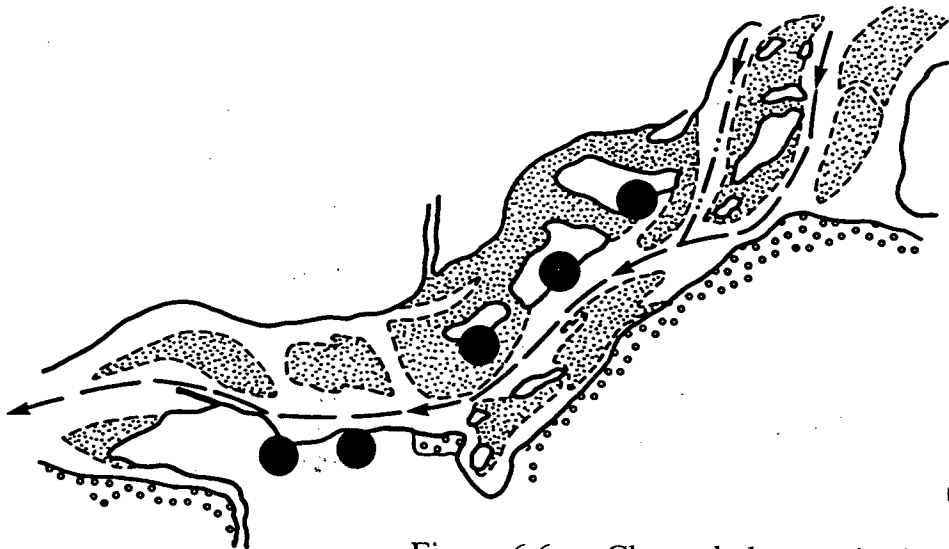
July 15, 1928  $Q = 5780 \text{ m}^3\text{s}^{-1}$



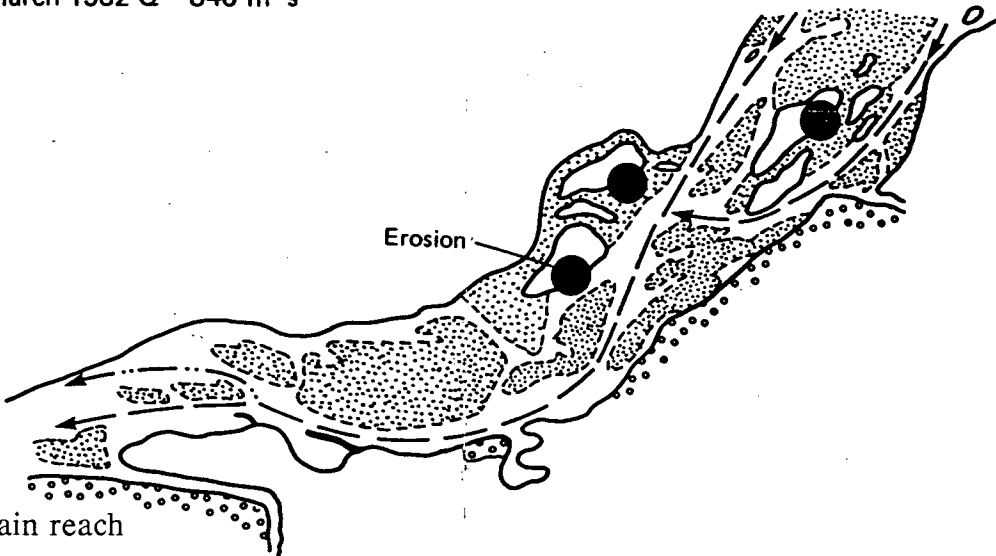
March 23, 1973  $Q = 839 \text{ m}^3\text{s}^{-1}$



Dec. 5, 1943  $Q = 533 \text{ m}^3\text{s}^{-1}$



March 1982  $Q = 840 \text{ m}^3\text{s}^{-1}$



0 1 2 3km

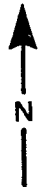


Figure 6.6 Channel changes in the Chilliwack Mountain - Sumas Mountain reach

been eroded since the turn of the century with major erosion occurring near Seabird Island, Maria Slough, Shefford Slough and upper Nicomen Island.

Channel instability was greatest in the first half of the century in the Cheam, Chilliwack and Sumas Reaches, but greater in the latter half in the Rosedale Reach. Major deposition zones include Lower Herrling Island, Vedder River confluence and Lower Nicomen Island. The Township Surveys which commenced in the late 1870's showed many sloughs along the river as actively flowing side channels. The largest side channels included Nicomen Slough and its tributaries Zaitscullachan and Quaamitch, Camp Slough and Nelson Slough near Chilliwack, Greyell Slough, Maria Slough around Seabird Island and Wahleach Channel around Herrling Island. All of these channels, with the exception of Greyell, Cheam and Wahleach were dammed or closed off by the turn of the century. Cheam Slough was subsequently shut off sometime between 1928 and 1943. These channels have apparently narrowed and infilled with finer sediment after being shut off from the main channel.

The following sections present a brief history of the channel changes that have occurred along the river over the last century.

#### Peters Island to Herrling Island

Comparison of the original township plans with later maps shows that approximately 150 ha of erosion occurred between 1890 (approx) and 1943 along Seabird Island

(sites E-47 to E-50 on Figure 6.1). This erosion resulted in substantial widening of the channel (up to 500 m) and promoted deposition in the zone of flow expansion downstream of Peters Island. Deposition also took place along the north side of the prominent mid-channel island (D-22 Figure 6.1) which reduced the extent of the island's western channel. As a result, the main channel eventually shifted to the eastern side of the river between 1943 and 1954.

Since 1954, the most noticeable change in this reach has been associated with bank erosion along Peters Island (Site E-50) and subsequent deposition immediately downstream. This pattern of erosion and deposition is related to the formation of the highly sinuous bend in the side channel across from Peters Island, with erosion along the outer, concave portion of the bend and deposition around the inner, convex bar. Therefore, this reach is one that can possibly be used to estimate bed load rates from observed rates of morphologic change. The infilling along the convex bank eventually resulted in the abandonment of a side channel in this reach. This shift has produced an overall change in the flow alignment further downstream, with the result of directing the main flow back into the northern side channel.

#### Herrling Island to Rosedale

The channel changes downstream of Herrling Island have proceeded relatively independently of events further upstream. Extensive bank erosion took place between the turn of the century and 1943 along the north side of the river between

Maria Slough and Cheam Slough (Site E-37). This period of erosion was accompanied by island construction along Lower Herrling Island. Bar deposition in the widened channel promoted the development of a very sinuous main channel which caused further erosion near the south bank. Between 1943 and 1954 the alignment straightened out and the main channel shifted to the north side of the river. The new alignment and additional erosion along the north bank (at site E-37) initiated rapid erosion after 1954 at Powerline Island (E-35, 36) just upstream of the Agassiz-Rosedale bridge. This erosion occurred in response to changes in flow alignment as a result of the northward shift in the main channel.

The erosion along the upstream end of Powerline Island was accompanied by deposition along its downstream side. As a result of the deposition, the main channel of the river shifted over towards the south. This shift was not anticipated by the designers of the Agassiz-Rosedale bridge before its construction in 1952. As a result, the main navigation span was situated over the north side of the channel which was in the process of turning into an island!

A second cycle of upstream erosion along Herrling Island and downstream deposition near the bridge commenced about 1974. The erosion has occurred along the outside of a bend over a 2 km length of Lower Herrling Island. Shortly after this erosion commenced, a mid-channel bar began to form downstream of the bridge in a reach including Water Survey of Canada's gauging section. By 1984 about 4 m of deposition had occurred, which has caused the river to develop a split channel. This

deposition eventually interfered with the hydrometric and sediment measurements and contributed to the termination of the sediment program at the station in 1986.

### Agassiz-Rosedale Bridge to Carey Point

The pattern of erosion and deposition between Herrling Island and the bridge initiated a sequence of channel shifts over the 10 km reach to Carey Point. Eroded material from the Cheam Reach (probably mainly from Powerline Island and site E-37) was deposited in a prominent lateral bar that became attached to Ferry Island about 1954. This bar grew rapidly throughout the 1960's and gradually forced the main channel toward the north side of the river. As a result, flow was directed towards a large, formerly stable island near Hopyard Hill (site E-32). This island was rapidly eroded between 1961 and 1979, which eventually led to major channel changes further downstream. Sediment eroded from Hopyard Hill Island (Site E-32) was deposited immediately downstream in the main channel. By 1971 this deposited material forced the channel southwards towards the head of Greyell Island (site E-30) and by 1973 the main channel had completed a major southward shift. Sediment eroded during this shift appears to have been redeposited 1.5 km downstream, which plugged the channel and forced a second shift between 1973 and 1979 back toward the north side of the river. This latest change in alignment has forced the river to attack Carey Point (site E-21), which has experienced rapid bank erosion in recent years.

Figure 6.7 shows a map of bank changes near Carey Point over the period 1979 - 1986. The bankline changes were measured from direct surveys or, for the case of the 1979 positions, by photogrammetric means using low level air photos. The most rapid erosion took place between 1979 and 1982 after the last avulsion when a low "wave like" gravel sheet became attached to the island complex north of Carey Point. This gravel wave forced the river to impinge against the erodible banks at Carey Point and initiated the erosion. As the wave propagated through the reach the locus of erosion also shifted downstream, the channel curvature decreased and the rate of erosion slowed.

#### Carey Point to Harrison River

There have been two major changes in channel alignment near the mouth of Harrison River over the last century. The first major channel avulsion took place along the south side of the river near the mouth of Shefford Slough (Site E-14) between 1890 and 1943. It is not clear whether this shift is related to any upstream controls. By 1943 the main channel had developed a sinuous alignment which directed the flow southward toward Hog Island then northwards toward Harrison Hill. This pattern was not significantly affected by the flood of 1948. However by 1954 a lateral bar began to develop on the south bank downstream of Carey Point (Site D-12). By 1967 the growth of this bar directed the main channel towards a group of formerly stable islands upstream of the Harrison River (Sites E-17, 18, 19, 20). By 1971 these islands had been severely eroded and the main channel shifted



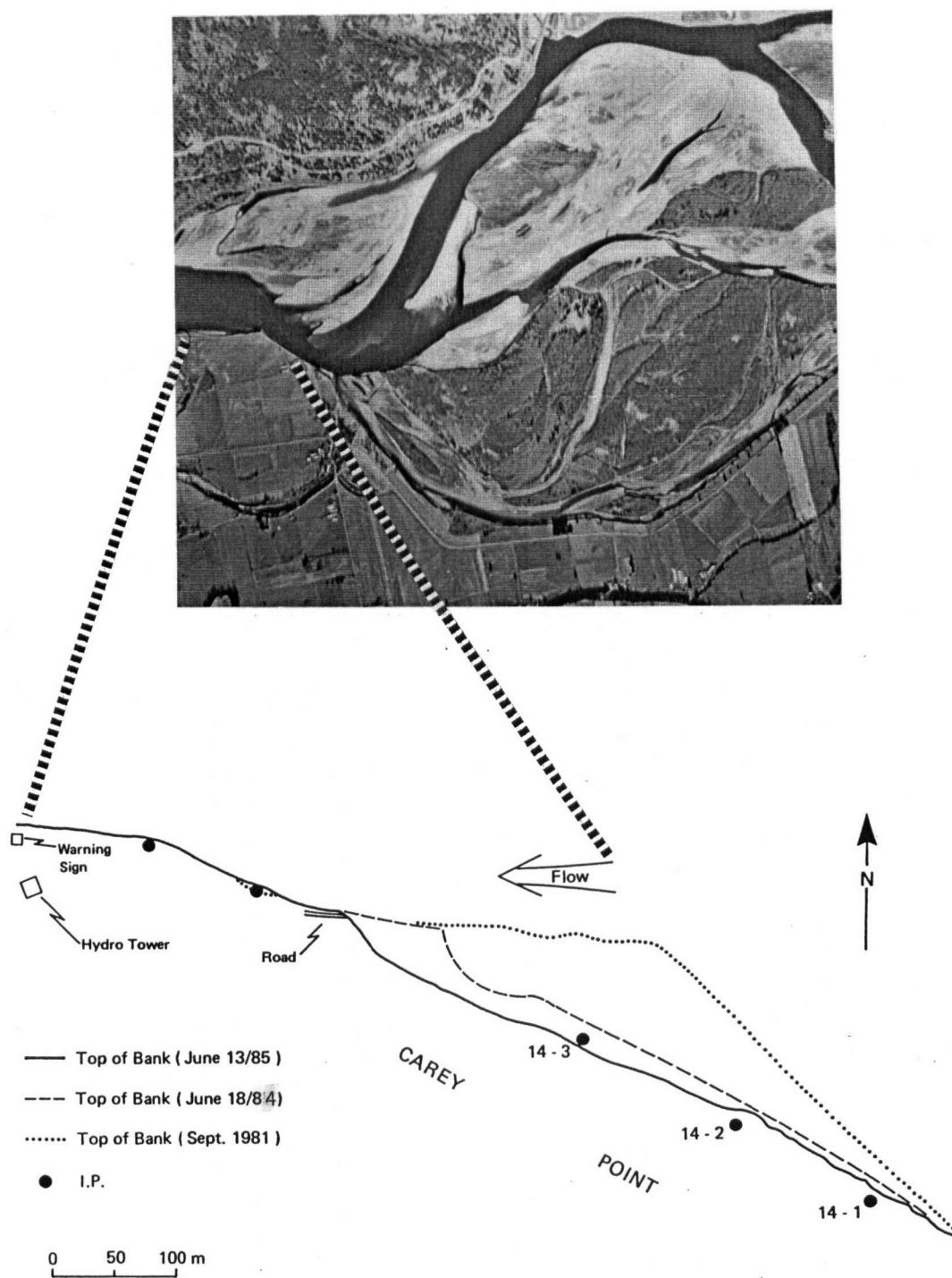


Figure 6.7 Comparative surveys of bankline changes near Carey Point

to the north side of the river around Harrison Hill. By 1979 the old main channel on the south side of the river was completely infilled.

### Chilliwack Mountain to Sumas Mountain

The bankline changes and rapid erosion along Shefford Slough and Chilliwack Creek that took place between 1928 and 1954 appear to have initiated another major channel avulsion opposite Chilliwack Mountain. The cause of the avulsion was a large gravel wave that migrated along a more stable lateral bar and eventually became attached to a group of wooded islands off Chilliwack Mountain. As a result, by 1962 an important distributary channel was completely filled in by the bar.

This infilling has caused more flow to be carried by the south side of the river along Chilliwack Mountain. Recently accelerated erosion along Yaalstrick Island has been a direct result of the change in flow distribution.

A second site of major channel instability occurred near the Vedder River confluence (Sites E-4, D-3 Figure 6.1). These changes are very likely to be related to the shift in Chilliwack River across its alluvial fan between 1875 and 1894. Based on the early Township surveys it appears that a large "slug" of sediment from the Chilliwack River was deposited at its confluence with the Fraser before 1928 (McLean, 1980).

### 6.3 Factors Governing Channel Instability

The bank erosion rate was about 25% higher in the period 1928-1943 compared to 1943-1971, this notwithstanding that between 1928 and 1943 the largest flood had a return period of only 5 years, whereas in the period 1943-1971 four floods had return periods exceeding 10 years (including the extreme flood of 1948). This decrease in erosion rate over time may reflect to some extent the effect of bank protection works that have been constructed since the 1940's. However, comparison of the channel shift maps shows that most of the channel changes along the river were governed by processes that developed over a number of years or decades and not during any single flood event. Therefore the appropriate time scales for considering channel instability processes on the Fraser River also are measured in years or decades. Extreme floods, such as in 1948 and 1972, were able to complete or "speed up" channel changes that were already underway. Large floods were also able to alter the flow alignment within the channel zone which later on initiated new patterns of channel instability. The change in flow alignment near Herrling Island between 1943 and 1954, and subsequent erosion at Powerline Island is an example of this type of process.

Much of the channel instability along the river has been related to relatively localized changes in flow alignment that developed as a result of earlier channel changes farther upstream. An important practical result would be to establish the

time required for channel instabilities to propagate along the river. For example if we consider the Rosedale Reach the following sequence developed:

1. 1943-1971: Powerline Island is eroded;
2. 1954: Ferry Island bar starts to grow and deflects river towards Hopyard Island;
3. 1954-1961: Hopyard Island is eroded 1 km;
4. 1961-1971: Sediment from Hopyard Island is deposited 1.5 km downstream causing main channel shift;
5. 1971-1979: Material eroded during the 1971 shift is deposited 1.5 km downstream and triggers a second shift;
6. 1979-1984: Carey Point erosion reaches its peak rate.

The disturbance (starting with the growth of the bar at Ferry Island) travelled 5 km downstream in about 25 years. During this period the lateral bar at Ferry Island grew about 2.0 km in length, giving the appearance that the channel disturbance can travel much faster than the sediment.

A second long sequence of inter-related events can be followed between Carey Point and Chilliwack Mountain:

1. 1928: Initial channel alignment downstream of Carey Point is very straight;
2. 1928-1943: Deposition off Nelson Slough produces avulsion and rapid bank erosion along south side of river. Extreme channel curvature develops;
3. 1943-1954: Bar growth off Queens Island triggers bank erosion downstream of Shefford Slough;

4. 1954-1962: Gravel wave migrates downstream from Shefford Slough site and shuts off distributary channel opposite Chilliwack Mountain;
5. 1962-1979: Sediment is flushed from the south channel along Chilliwack Mountain and this distributary captures main river flow;
6. 1982-1986: Enlarged distributary channel directs flow at Yaalstrick Island, initiating accelerated bank erosion along Island.

This disturbance propagated 7 km from Nelson Slough to Chilliwack Mountain in the 26 year period between 1928 and 1962, and about 10 km to Yaalstrick Island over the 54 year period ending in 1982.

Three main "styles" of channel shifting and instability can be discriminated from the historical records. The first type of instability is associated with the development of very sinuous distributary channels around islands or stable lateral bars. After these bends develop a high degree of curvature, the channel often shifted abruptly either by forming a classical "chute cutoff" or by cutting across the outer concave bank and forming a new secondary channel. In both cases the overall curvature of the channel will be reduced. The recent erosion at Peters Island and at Lower Herrling Island provide examples of this style of erosion. Figure 6.8 summarizes bend properties from all of the distributary channels between Peters Island and Sumas Mountain. The two parameters that were used to describe the bends were the radius of curvature  $R_o$  (measured through the convex side of the bend) and the average low water channel width ( $B$ ). It can be seen that most of the distributary channels have a ratio  $R_o/B$  of between 2 and 6. Furthermore, it appears that rapid instability or

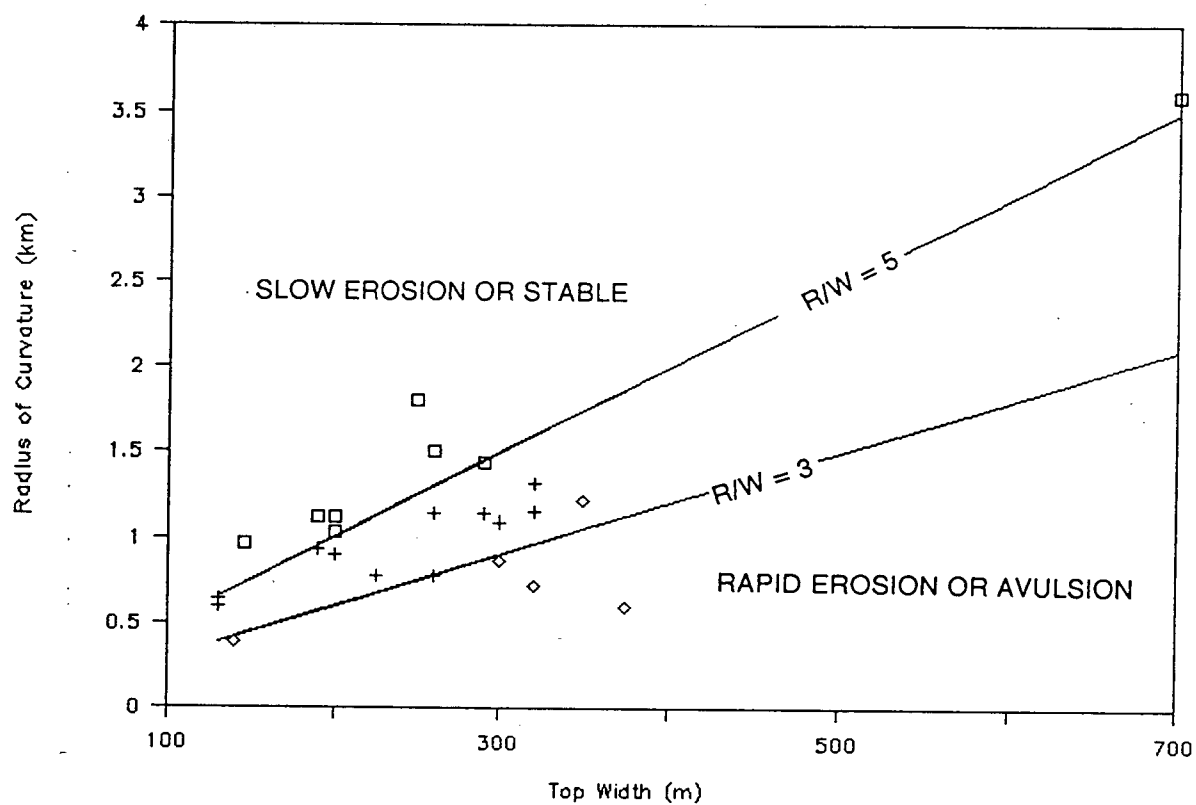


Figure 6. 8 Stability of channel bends in the wandering gravel bed reach

avulsion may be expected when this ratio is less than 2 or 3 (cf Hickin, 1974). This observation may provide some guidance in forecasting future instability along the river.

The second style of channel instability is associated with unstable gravel sheets or low amplitude, broad gravel waves that can migrate through a reach. Such features induce erosion during the low water season by direct flow impingement. They can also produce aggradation and local infilling of other channel features. The gravel sheets are usually formed when gravel is scoured from a channel cut. Therefore, some other external disturbance is required to initiate this type of process. The two best examples of these features were described previously at Carey Point and Chilliwack Mountain. Since these features can be identified readily on air photos it should be very easy to recognize when this type of instability is occurring.

The third style of instability that can be identified is associated with flow realignment by upstream controls. For example, upstream changes in flow alignment may cause the channel to impinge against formerly stable banks or islands. The major sequence of island erosion off Harrison River confluence is one example of this process.

In this case the main channel was re-directed towards the islands as a result of the growth of a bar just downstream of Carey Point.

Two contrasting styles of island formation were identified in the study reach. The most common mechanism involves a sequence of depositional processes, starting with formation of a mid-channel or lateral gravel bar, gravel aggradation up to a high water level, establishment of vegetation (such as alder), and eventually deposition of finer suspended load materials. Although many local variations occur to modify the pattern of island growth and development the basic depositional processes remain relatively similar. The time period for this sequence of development typically require between 10 and 30 years. The islands that have developed between Rosedale bridge and Carey Point are an example of this type of process.

The second style of island formation involves erosion of existing floodplain or island topography. These islands appear after periods of rapid channel migration or avulsion when former floodplain areas are cut off by newly created side channels. In this case the stratigraphy of the islands may be very different from the islands that have evolved from bar deposition. For example, many portions of the floodplain (former back channel and slough areas) are composed entirely of fine silty sand sediments. In this case the islands may be eroded very rapidly during subsequent flood events. The islands at the head of Minto side channel are examples of this style of formation.



## 7.0 SEDIMENT BUDGET OF THE LOWER FRASER RIVER

The observed morphologic changes that were described qualitatively in Chapter 6 can be re-interpreted quantitatively to estimate the bed sediment transfers along the reach. This current chapter describes the application of a sediment budget approach for relating measured volumetric channel changes to sediment transport rates at selected points along the river.

In Chapter 8, the sediment transport rates will be estimated on the basis of the observed patterns of sediment movement along the river and from estimates of bank and island erosion rates.

### 7.1 Methods

The methodology for constructing a sediment budget of the Lower Fraser River has been presented in Section 2.2. In this application, the sediment budget equation has been used to estimate the gravel bed load entering a reach ( $Q_i$ ) in terms of the net sediment transfers from islands and the floodplain within the reach ( $\Delta S_f$ ), the net channel changes ( $\Delta S_c$ ), and the amount of gravel leaving the reach ( $Q_o$ ). The net sediment transfers from islands and floodplain areas include both island and bank re-construction ( $D_f$ ) and erosion ( $E_f$ ). In the past, gravel has been removed from the channel as a result of commercial gravel mining operations. These quantities ( $V_d$ ) represent an additional outflow of sediment from the reach and must be

accounted for in the budget. Therefore the complete sediment budget equation can be written as:

$$Q_i = Q_o + (\Delta S_c + \Delta S_f + V_d)/\Delta t$$

The sediment sampling analysis presented earlier has demonstrated that the gravel load at the downstream end of the study reach near Mission is negligible. This information makes it possible to estimate the gravel inflows to any reach upstream of Mission. By sub-dividing the channel into a number of sub-reaches the inflows to one reach can be used as the outflows from the next upstream sub-reach. This provides a means for calculating the long term gravel bed load transport rate along the river.

The analysis was carried out using the bathymetric survey data collected in 1952 and 1984. Therefore, the sediment transport rates have been estimated over a 32 year time. The river was sub-divided into 25 sub-reaches or "cells" between Mission and the Agassiz - Rosedale bridge with each sub-reach being approximately 2 km in length. The locations of these cells are illustrated on Figure 7.1. The bank lines from the 1984 and 1952 surveys were overlaid to delineate areas of bank erosion and re-construction in each cell. The third region that was delineated included the common active channel area between the two dates. Each of these regions delineates a distinct term in the sediment budget equation. As a result, each term was analyzed separately. The bank erosion volumes were estimated by planimentering the areas

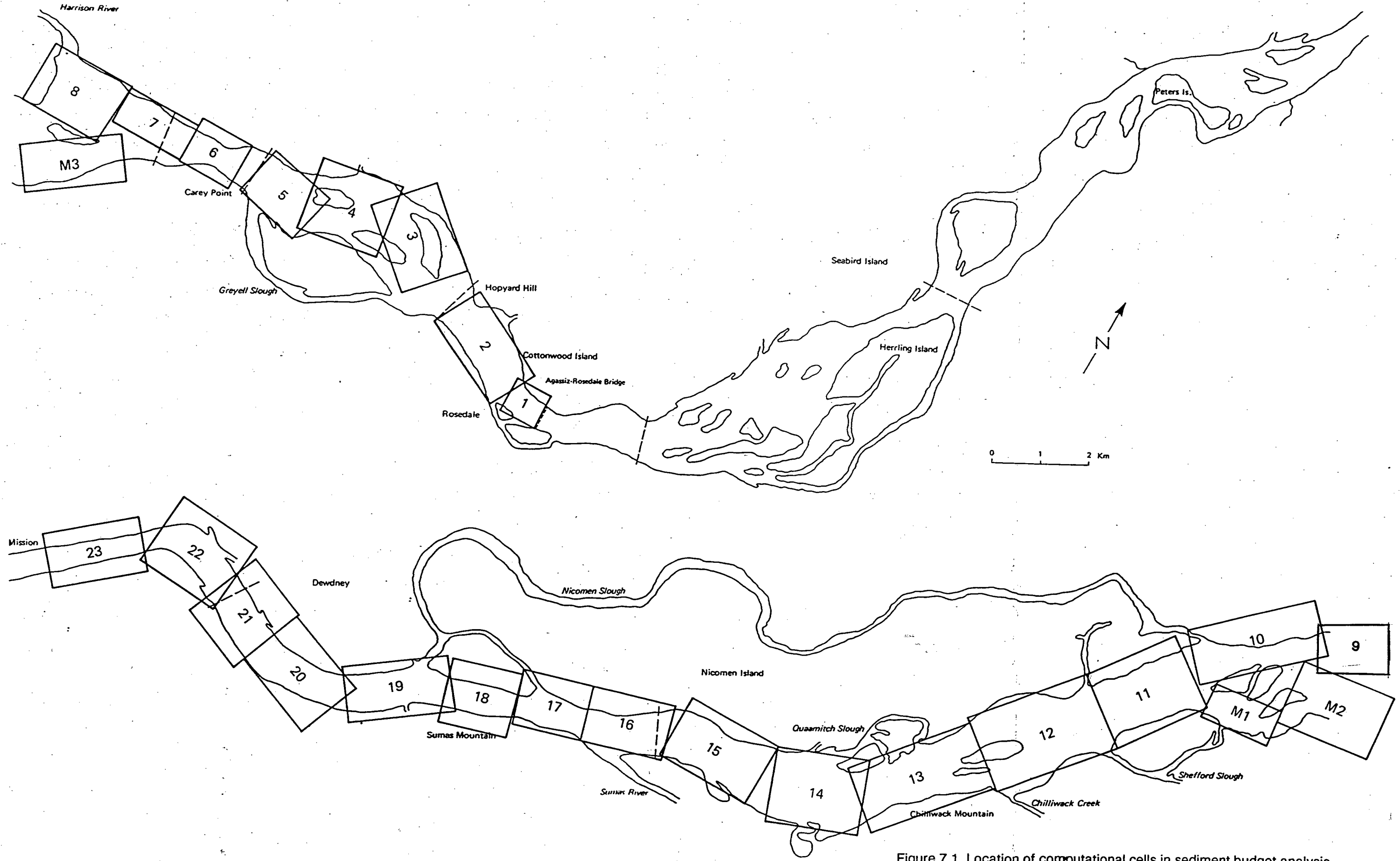


Figure 7.1 Location of computational cells in sediment budget analysis

and multiplying these areas by the estimated basal layer bank heights. The thickness of the overlying fine grained floodplain deposits was estimated for each site.

In most cases the thickness was estimated from direct measurements. At some sites entire islands have disappeared so the stratigraphy of the banks can only be inferred. In these cases the thickness of the floodplain deposits was estimated on the basis of the site's age using the criteria developed in Section 4.3. The historical map and airphoto data were used to determine the age of the sites.

The volumes of island or floodplain reconstruction were computed using basically similar procedures. However, in these calculations the thickness of the fine grained floodplain deposits was always determined from direct measurements.

A FORTRAN program was written to compare the 1984 and 1952 bathymetric survey data and to compute the volumes of net channel change. The sounding lines established in 1984 did not coincide with the lines surveyed in 1952. However, since a very dense network of sounding lines was used in both surveys (cross sections were typically spaced only 80 - 120 m apart) it was concluded that very reliable estimates of the net channel changes could still be determined. The method for comparing the two surveys was based on a digital terrain model (DTM). The general flow chart for the sequence of calculations that was performed is summarized in Figure 7.2.

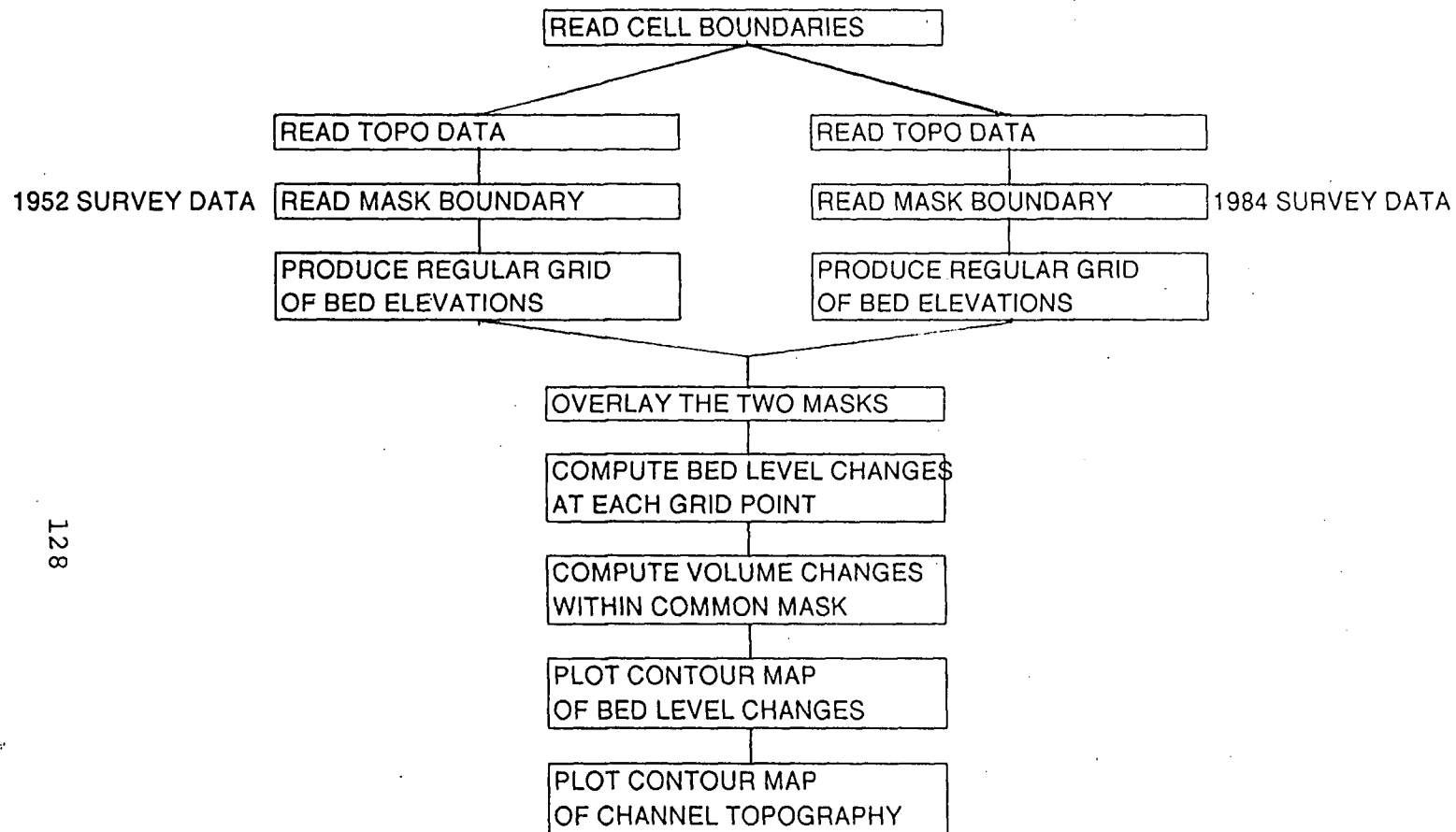


Figure 7.2 Flow chart of digital terrain model computing volumetric changes between successive surveys

The basis for the DTM is an algorithm that replaced the irregularly spaced survey points with a set of regularly spaced interpolated values. The interpolation subroutine CGRID1 was used for estimating the grid point elevations from the scattered survey data. This Fortran routine was developed at the University of Alberta Computing Centre and uses a combination of Laplacian and spline interpolation to estimate the grid point elevations. The relative degree of Laplacian or spline interpolation can be controlled by varying a coefficient. If only Laplacian interpolation is used, the surface tends to develop rather sharp peaks and dips. If only spline interpolation is used, the surface is smoother. With this approach the topographic surface resembles a lattice of flexible beams that are constructed to pass through each of the datum points. Therefore, preliminary calculations were required in order to determine the most appropriate method for representing the channel topography.

A "masking" subroutine was added to the DTM to screen out areas beyond the limits of the surveys and to prevent the model from incorporating data from regions that could distort the representation of the channel topography.

For example, artificial features such as rock groins or training works may introduce local discontinuities in the topography that are virtually impossible to represent with any interpolation procedure. The mask boundaries from the two successive surveys were overlaid in order to define the common overlapping region. The channel volume changes were then computed only within this common region.

The net volume change  $\Delta V$  was then estimated by summing up the volume increments at each grid cell in the region:

$$V = \sum (Z2_{ij} - Z1_{ij}) \Delta X * \Delta Y \text{ where;}$$

$Z1_{ij}$  is the bed level in 1952 at grid cell  $ij$

$Z2_{ij}$  is the bed level in 1984 at grid cell  $ij$

$\Delta X$  is the grid spacing in the X direction

$\Delta Y$  is the grid spacing in the Y direction.

In addition to these basic calculations three types of computer generated graphics were produced. These included contour maps of the 1952 and 1984 bed topography, a contour "isopach" map of bed level changes (scour or fill), and finally cross section plots of the 1952 and 1984 topography through any specified region. These plots were used to assist in interpreting the results of the analysis, for screening out errors in the data and for ensuring the topography was represented in a realistic fashion.

## 7.2 The Data

The channel surveys in 1984 used a combination of automated hydrographic surveying equipment, conventional sounding surveys and terrestrial ground mapping. The channel topography was represented by establishing cross sections at intervals of between 100 and 200 m along the river. In total, over 400 cross sections were surveyed in the 38.5 km reach between Mission and Agassiz - Rosedale bridge and

more than 44,000 elevation points were measured in the channel. This corresponds to a sounding density (planimetric area of channel divided by number of sounding points) of approximately  $625 \text{ m}^2/\text{point}$  or one measurement per  $25 \text{ m} \times 25 \text{ m}$  square.

The 1952 surveys were carried out by Public Works Canada and the soundings were compiled on 1:4,800 (1 inch = 400 feet) scale charts. In the 1952 surveys the active channel was surveyed with a fathometer. The elevations of the floodplain surface were determined photogrammetrically and plotted at 1.5 m (5 foot) contour intervals with 0.3 m (1 foot) spot elevations. All elevations were referred to geodetic datum. The horizontal control for the 1952 surveys was based on latitude and longitude. Since the 1984 surveys were all referred to UTM co-ordinates a BASIC program was written to establish a UTM grid on the 1952 charts. The computations that are required for this transformation are described in Davis et al, (1983).

The cross section spacing of the 1952 surveys typically varied from 50 m to 120 m. Over 300 cross sections were surveyed between the Mission bridge and the Agassiz - Rosedale bridge. This represents a substantial field effort considering that all surveys were carried out manually, without the benefit of automated data acquisition equipment. The sounding density over the area averaged  $2,000 \text{ m}^2/\text{point}$  which corresponds to one point per  $45 \text{ m} \times 45 \text{ m}$  square. The lower density of points in the 1952 survey is mainly due to the smaller number of points that were used to define each cross section - typically only 15 to 20 compared to between 30 and 50 points in the 1984 survey.



### 7.3 Accuracy of the Computations

Several different test computations were made to assess the precision of the volumetric calculations. Most of this effort was directed towards evaluating the reliability of the digital terrain model since this part of the computations generated most of the numerical results in the analysis. Furthermore, compared with the assessments of bank erosion or re-construction, this aspect of the work could not be verified easily by simple manual calculations.

Initial tests of the digital terrain model involved sensitivity calculations to determine the effect of varying the size of the grid spacing in the model. A 20 m square grid was selected as a reference case for comparing other schemes. In all cases the x axis of the grid was aligned parallel to the longitudinal axis of the channel. The mean bed level and channel volume in a 2 km long, 1 km wide reach was computed for each grid arrangement. Two examples of test comparisons are illustrated on Figure 7.3. The two test results shown on this graph were made on two different river reaches in the sand bed portion of the river near Mission. As expected, the computed mean bed level was not sensitive to the grid spacing that was used for the computations. This is because even the for the largest grid spacing that was used (80 m x 80 m), any single cell represents less than 1% of the total surface area in the test reach. This result also illustrates that the channel volumes computed by the model will not be overly sensitive to the grid size that is used.

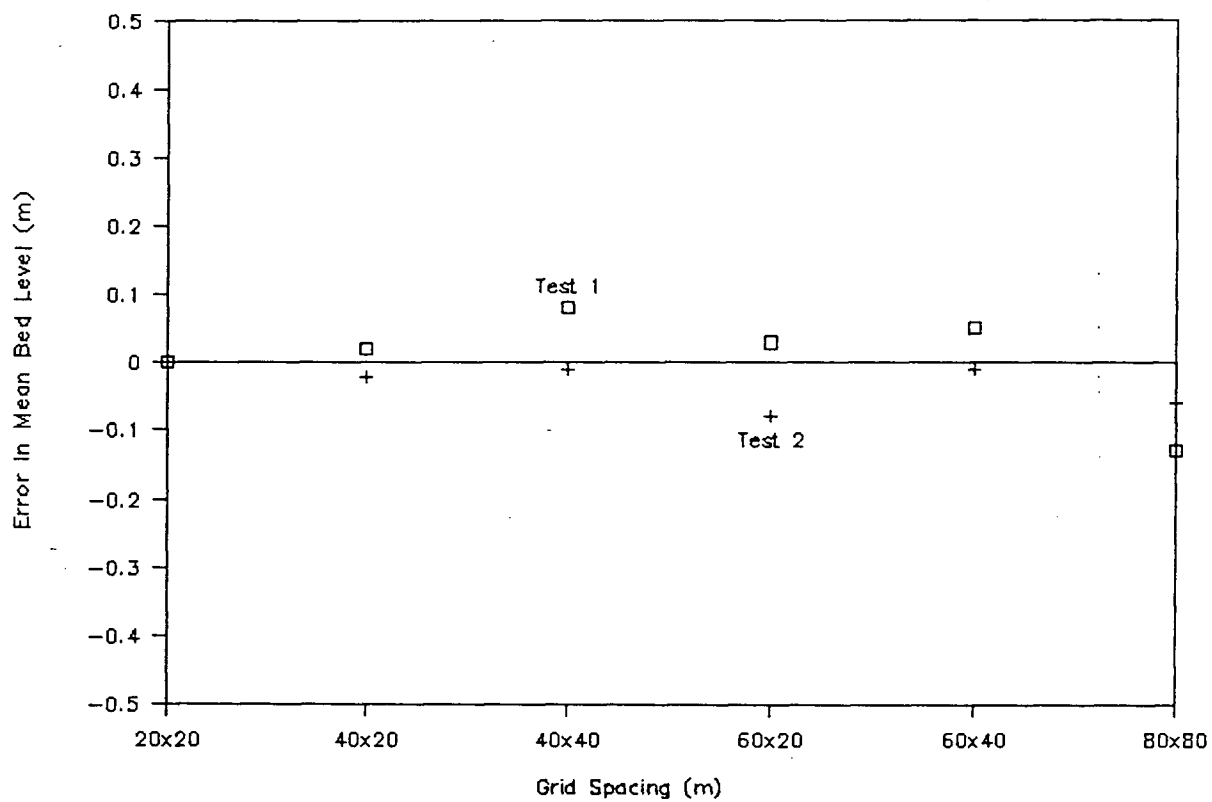


Figure 7.3 Comparison tests to evaluate the effects of grid spacing on the precision of the mean bed level in a 2 km long, 1 km wide reach

For example, even for the coarsest grid spacing (80 m x 80 m) the imprecision of the computed volume was less than  $\pm 50,000 \text{ m}^3$  per kilometre of channel, when compared with the volume computed using a 20 m x 20 m grid spacing. This corresponds to a nominal precision of  $\pm 5 \text{ cm}$  in the overall mean bed level.

Comparisons were also made between actual surveyed spot elevations and computed grid cell values. These comparisons could be made only in a few special cases since usually the grid cells and the surveyed points did not coincide. Even when a surveyed cross section line coincided with a grid line not all of the spot elevations would correspond to grid cell locations. For the purposes of these tests it was decided to accept any point that fell within a 2 m radius of the grid cell location. The precision of the DTM was estimated from the differences between the elevation of the actual sounding point and the calculated value. The RMS error of the grid point elevations was computed as :

$$E_z = \sum (Z_c - Z_a)^2 / N_c)^{1/2} \quad \text{where;}$$

$Z_c$  and  $Z_a$  are the computed and actual bed elevations;

$N_c$  is the number of points in the cross section.

The results of the comparisons are summarized in Table 7.1. In most cross sections the RMS error within any cross section ranged between 0.1 m and 0.3 m. In bends or scour holes where the channel bottom sloped very steeply the RMS error reached up to 0.5 m.

TABLE 7.1

## ROOT MEAN SQUARE ERROR IN SPOT ELEVATIONS

CROSS SECTION	GRID SPACING (m)		
	20 m x 20 m	40 m x 20 m	40 m x 40 m
0	0.12		
1	0.48		
2	0.22		
3	0.32		
4	0.18	0.18	0.24
5	0.16	0.18	0.41
6	0.26	0.25	0.53
7	0.32	0.26	0.31
8	0.16	0.17	0.19
average	0.21	0.21	0.34

An estimate of the precision of the volume changes between successive surveys can be made from the RMS errors of the grid points. For the case of a 40 m (x axis) by 20 m (y axis) the RMS elevation error of any grid point is 0.2 m and the RMS error of the elevation change at the grid cell will be:

$$E_{\text{diff}} = (0.2^2 + 0.2^2)^{1/2} = 0.28 \text{ m}$$

The RMS error of the mean bed level difference in a specified reach ( $E_{\text{av}}$ ) can be estimated as:

$$E_{\text{av}} = E_{\text{diff}} / N_r^{1/2} \text{ where;}$$

where  $N_r$  is the number of points in the region that is used to establish the average.

For the case of a 40 m x 20 m grid arrangement there are 676 grid cell points in a 1000 m long, 500 m wide channel reach. If the elevation change at each of these points can be considered as an independent quantity then the RMS error of the average elevation change in the reach will be approximately 0.01 m.

For this case the RMS error associated with the computed volume change between surveys will be  $0.01 \times 500 \times 1000 = 5,000 \text{ m}^3$  per kilometre of channel.

However, the assumption of independence is not strictly correct since the elevation at any grid cell will be influenced to some extent by the values at adjacent points.

This is because the elevation at any grid cell is computed by fitting a geometrical surface through the set of points contained in an area centred about the grid cell. The zone of influence about each grid cell is controlled by a parameter in the DTM. After some preliminary trial computations it was set to extend over a radius of four grid points. Therefore, within a 500 m wide by 1000 m long channel, there would be 36 independently determined points in the region. Using this number the RMS error of the mean bed level change is approximately 0.047 m and the expected imprecision in the computed channel volume changes will be approximately 23,000 m<sup>3</sup> per kilometre of river.

In order to assist in interpreting the results of the channel survey comparisons, a precision class was assigned to each sub-reach that was used in the sediment budget. The highest precision (Class 1) was assigned to reaches where full survey coverage was available from both the 1952 and 1984 surveys. Sub-reaches which contained areas that were not covered by channel surveys in either 1952 or 1984 were assigned the lowest precision (Class 3). Sub-reaches which contained areas where the cross section spacing exceeded 100 m were assigned an intermediate precision (Class 2). There were only two sites on the 1952 map sheets where the survey coverage could be considered sufficiently poor to require a Class 3 designation. In both cases the problem arose as a result of the river shifting into a back channel area that was probably too shallow to survey by boat and was mapped only photogrammetrically by widely scattered spot elevations.

Additional uncertainties in the sediment budget are introduced from the estimates of bank erosion and accretion along the river. These quantities were not computed with the DTM. Instead, specific sites where erosion or deposition has occurred were identified by comparing the two surveys and the banklines in these sites were digitized. Areas of erosion or deposition were computed for each site in the reach by using a BASIC planimetry program. The heights of the banks at each site were estimated from the available survey data and erosion or deposition volumes were computed by multiplying the area changes by the bank heights. The precision of the area calculations was assessed in a set of test runs by comparing the coordinates of the digitized bank lines with manually determined values from the 1:10,000 scale mylar prints of the 1952 maps. The error in the position of each point ( $E_{\text{dig}}$ ) was computed as:

$$E_{\text{dig}} = ((X_{\text{dig}} - X_{\text{man}})^2 + (Y_{\text{dig}} - Y_{\text{man}})^2)^{1/2} \text{ where;}$$

$X_{\text{dig}}$  and  $Y_{\text{dig}}$  are the digitized coordinates of the point,

$X_{\text{man}}$  and  $Y_{\text{man}}$  are the manually determined coordinates.

The imprecision of the bankline coordinates is affected by several factors, including scale distortions on the drawings as a result of paper stretch or shrinkage, distortions associated with the scale projection system of the 1952 maps, inaccuracies in transferring a UTM grid system onto the 1952 maps and, finally, random errors associated with digitizing the bank lines. In four separate tests the RMS error in the bankline coordinates averaged 13 m. It was found that in any particular test the

errors tended to be systematic rather than random. This suggests that the errors associated with the map grid system and scale distortions were more important factors than random errors in digitizing.

The uncertainty in the calculated areas of bank erosion or deposition ( $E_a$ ) can be estimated by the R.M.S. error of the apparent bankline changes:

$$E_a = L * (E_1^2 + E_2^2)^{1/2},$$

where L is the length of the bankline

$E_1$  and  $E_2$  are the errors associated with the bank positions mapped in 1952 and 1984.

Based on the results discussed above, these values were estimated to be 13 m.

The corresponding uncertainty in the volume of erosion or deposition ( $E_v$ ) will be;

$$E_v = (E_a^2 + E_h^2)^{1/2},$$

$E_h$  is the error term associated with the height of the banks.

There is no rigorous method to estimate the uncertainty in the estimates of the bank heights. Since the survey coverage extended over virtually the entire study reach, the uncertainties in the bank heights will be largely governed by the uncertainties in the bank elevations and adjacent bed topography. The 1952 surveys used photogrammetric methods to establish the bank elevations. As discussed previously,



these maps were produced with a 5 foot contour interval using horizontally and vertically controlled air photos. In photogrammetric mapping studies the precision of the ground elevations is frequently taken as half the contour interval (or about 0.8 m). However, there are other factors that will increase the uncertainty in the estimates of the bank heights. First, in order to use the erosion or deposition quantities in a sediment budget calculation, the basal gravel and sand sediments need to be distinguished from the overlying finer grained floodplain deposits. Therefore the stratigraphy of the banks must be quantified at each site. At many sites where the rate of erosion has been slow the stratigraphy of the banks was measured directly. At other sites entire islands or areas on the floodplain have been destroyed. In these areas the stratigraphy could be inferred only from the age of the sites and their morphology (see Section 5.2 and Figure 5.5). This estimation of the thickness of the floodplain deposits is not very precise, but probably within  $\pm 1$  m.

Three precision classes were assigned to the bank height calculations. The criteria were similar to those used in the channel survey analysis, with the additional complication that information on bank stratigraphy was needed. The highest precision (Class 1) was assigned to sites with direct measurements of bank stratigraphy and surveyed bank topography. The lowest precision (Class 3) was assigned to sites where the stratigraphy could not be documented and only planimetric information was available for defining the banklines. This latter condition arose at only two sites on the 1952 mapping when the bank positions were shown but no topographic information was provided. The intermediate precision

category (Class 2) was assigned to sites where adequate topographic mapping was available but stratigraphic information was lacking.

At sites in the highest precision category the nominal uncertainty in the sediment volumes was estimated to be 20,000 m<sup>3</sup> per lineal kilometre of bank while the value for the intermediate class was 30,000 m<sup>3</sup> per kilometre. Therefore, in a 2 km reach that is designated as Class 1, the uncertainty in the erosion volumes would be in the order of 80,000 m<sup>3</sup> if there were 4 km of bank lines in the reach. These quantities are in the same order as the uncertainties associated with the channel volume changes that are computed with the DTM.

Table 7.2 shows precision classes that have been assigned for each sub-reach in the sediment budget. These designations are subjective since within any reach erosion or deposition may have occurred at several different sites. The main purpose of this table is to identify reaches where the budget computations are weakest and the uncertainties in the results are greatest.

#### 7.4 Assumptions

In order to make quantitative estimates of the gravel transport rate along the river it has been assumed that the gravel transport past Mission is negligible.

TABLE 7.2

PRECISION CLASSES ASSIGNED TO EACH SUB-REACH IN THE  
SEDIMENT BUDGET

REACH NUMBER	REACH	REACH LIMITS (KM)	PRECISION ESTIMATES CHANNEL	BANKS
1	Agassiz	128.5 - 130	1	1
2	Hopyard Hill	126 - 128.5	1	1
3	Upper Greyell	124.5 - 126	1	1
4	Mid Greyell	122.8 - 124.4	1	1
5	Lower Greyell	120.8 - 122.8	1	1
6	Lower Carey	119.5 - 120.8	1	1
7	Upper Harrison	119 - 119.5	1	1
8	Harrison	117 - 119	3	1
9	Harrison Knob	115.3 - 117	1	1
10	Harrison Hill	113.5 - 115.3	1	1
11	Queens Island	110 - 113.5	1	1
12	Chilliwack Mountain	108 - 110	1	1
13	Chilliwack Mountain	106 - 108	2	1
14	Cannar	104 - 106	1	1
15	Upper Sumas	101.7 - 104	1	1
16	Sumas River	100 - 101.7	1	1
17	Strawberry Island	97.8 - 100	1	1
18	Cox	96.5 - 97.8	1	1
19	Sumas Mountain	94.8 - 96.5	1	1
20	Hatzic Upper	91 - 94.8	1	1
21	Hatzic Lower	89 - 91	1	1
22	Mission Bend	87 - 89	1	1
23	Mission Bridge	85 - 87	1	1
SIDE CHANNELS				
C1	Chilliwack Mountain	107.5 - 108.5	2	1
C2	Chilliwack Mountain	108.5 - 109.5	3	1
M1	Lower Minto Landing	113 - 114	2	1
M2	Minto Landing	114 - 115	2	3
M3	Hog Island	115 - 116.5	2	3

This assumption is reasonable since gravel sediments ( $>2$  mm) typically make up only a small fraction (typically less than 5%) of the channel bed material below Mission. Coarse gravels ( $>25$  mm) are virtually absent below Mission except in local areas where non-alluvial materials outcrop in the channel. Table 7.3 shows the assumed composition of the bed and bank materials that was used to characterize the sediments in each sub-reach. These values were based on the results of the sediment sampling program that was described in Section 5.3. Upstream of Chilliwack Mountain (km 110) the reach averaged size distributions of the bed and basal gravel bank materials were assumed to be identical. However, between Chilliwack Mountain and Sumas Mountain the sediment size in the banks was shown to be substantially finer than the bed material. Therefore, these differences had to be accounted for.

Estimates of sediment quantities removed by gravel mining were based on the data compiled in Section 4.3. Only material that has been permanently removed from the channel has been included in the sediment budget.

Channel maintenance dredging or other types of channel improvement operations have been excluded since these activities return the gravel back into the channel so there is no net impact on the budget. The data indicate that  $1.6 \times 10^6$  m<sup>3</sup> of gravel have been permanently removed from the channel since 1971 when annual records were first kept. About 80% of the gravel mining has taken place in a single side channel of the river near Minto Landing. Unfortunately, these records are likely to

TABLE 7.3

ASSUMED COMPOSITION OF BED AND BANK MATERIALS  
IN EACH SUB-REACH IN THE SEDIMENT BUDGET

REACH NUMBER	REACH	REACH LIMITS (KM)	CHANNEL BED COMPOSITION		BANK COMPOSITION	
			% > 2 mm	% > 25 mm	% > 2 mm	% > 25 mm
1	Agassiz	128.5 - 130	84	50	84	50
2	Hopyard Hill	126 - 128.5	83	50	83	50
3	Upper Greyell	124.5 - 126	83	47	83	47
4	Mid Greyell	122.8 - 124.4	82	45	82	45
5	Lower Greyell	120.8 - 122.8	82	42	82	42
6	Lower Carey	119.5 - 120.8	82	41	82	41
7	Upper Harrison	119 - 119.5	82	38	82	38
8	Harrison	117 - 119	81	35	81	35
9	Harrison Knob	115.3 - 117	81	33	81	33
10	Harrison Hill	113.5 - 115.3	81	30	81	30
11	Queens Island	110 - 113.5	81	29	81	29
12	Chilliwack Mountain	108 - 110	81	28	81	25
13	Chilliwack Mountain	106 - 108	81	26	81	20
14	Cannar	104 - 106	80	25	80	10
15	Upper Sumas	101.7 - 104	80	20	80	10
16	Sumas River	100 - 101.7	80	17	50	5
17	Strawberry Island	97.8 - 100	75	15	0	5
18	Cox	96.5 - 97.8	65	12	0	0
19	Sumas Mountain	94.8 - 96.5	40	10	0	0
20	Upper Hatzic	91 - 94.8	20	0	0	0
21	Lower Hatzic	89 - 91	5	0	0	0
22	Mission Bend	87 - 89	5	0	0	0
23	Mission Bridge	85 - 87	5	0	0	0

be incomplete and do not extend back to the date of the earliest survey in 1952. However, interviews with local residents and gravel mining operators indicate that the amount of material removed for commercial extraction prior to 1971 was small compared to recent times.

Therefore, only the post 1971 data were used to estimate the total amount removed. This assumption will introduce a bias into the sediment budget analysis, since an underestimation of the gravel extraction quantities will cause the estimates of the sediment inflows also to be underestimated. The impact of this problem on the final results is discussed further in Section 7.6.

## 7.5 Results

The overall gravel sediment budget for the reach between Agassiz - Rosedale bridge and Mission is summarized in Table 7.4. Between 1952 and 1984 there was an apparent net gain in storage ( $\Delta S_c + \Delta S_b$ ) of  $3.5 \times 10^6 \text{ m}^3$  of sediments coarser than 2 mm. This represents a net aggradation of approximately  $10^5 \text{ m}^3/\text{year}$  of gravel sediment within this reach.

The net change in channel storage ( $\Delta S_c$ ) amounted to  $7.5 \times 10^6 \text{ m}^3$ , which was about twice the magnitude of the net change in bank storage ( $\Delta S_b$ ). After accounting for the amount of gravel extracted from the river ( $1.3 \times 10^6 \text{ m}^3$ ) the total gravel inflow at the Agassiz - Rosedale bridge was estimated to be  $5.1 \times 10^6 \text{ m}^3$ . This corresponds

Table 7.4

## OVERALL RESULTS OF SEDIMENT BUDGET ANALYSIS, 1952 TO 1984

All volumes measured in  $10^6 \text{ m}^3$ 

GRAIN SIZE (mm)	NET CHANNEL CHANGE	NET BANK CHANGE	TOTAL GRAVEL MINING	TOTAL GRAVEL INFLOW @ ROSEDALE
> 2	7.5	-4.0	1.6	5.1
> 25	2.4	-0.7	0.6	2.3

TABLE 7.5

Bed and Bank Changes by Sub-Reach, 1952 to 1984

all volumes in million cubic metres

REACH NUMBER	REACH	REACH LIMITS (Km)	CHANNEL CHANGES		BANK CHANGES	
			>2mm	>25mm	>2mm	>25mm
1	Agassiz	128.5 - 130	0.139	0.083	-0.245	-0.146
2	Hopyard Hill	126 - 128.5	0.774	0.467	0.973	0.586
3	Upper Greyell	124.5 - 126	0.491	0.278	0.501	0.284
4	Mid Greyell	122.8 - 124.4	-0.204	-0.112	-1.003	-0.550
5	Lower Greyell	120.8 - 122.8	1.357	0.695	0.142	0.073
6	Lower Carey	119.5 - 120.8	0.130	0.065	0.000	0.000
7	Upper Harrison	119 - 119.5	-0.130	-0.060	0.000	0.000
8	Harrison	117 - 119	0.000	0.000	-1.183	-0.511
9	Harrison Knob	115.3 - 117	-0.377	-0.154	0.000	0.000
10	Harrison Hill	113.5 - 115.3	0.261	0.097	0.000	0.000
11	Queens Island	110 - 113.5	-0.203	-0.073	0.243	0.087
12	Chilliwack Mountain	108 - 110	1.372	0.474	-0.496	-0.153
13	Chilliwack Mountain	106 - 108	1.098	0.353	-1.652	-0.408
14	Cannar	104 - 106	-0.179	-0.055	-0.309	-0.039
15	Upper Sumas	101.7 - 104	0.708	0.177	-0.635	-0.079
16	Sumas River	100 - 101.7	0.717	0.152	-0.208	-0.021
17	Strawberry Island	97.8 - 100	0.568	0.114	0.000	0.000
18	Cox	96.5 - 97.8	-0.159	-0.029	0.000	0.000
19	Sumas Mountain	94.8 - 96.5	0.140	0.035	0.000	0.000
20	Hatzic Upper	91 - 94.8	0.027	0.000	0.000	0.000
21	Hatzic Lower	87 - 89				
SIDE CHANNELS						
C1	Chilliwack Mountain	107.5 - 108.5	0.198	0.063	0.000	0.000
C2	Chilliwack Mountain	108.5 - 109.5	-0.261	-0.084	0.000	0.000
M1	Lower Minto Landing	113 - 114	-1.053	-0.429	0.178	0.073
M2	Minto Landing	114 - 115	-0.405	-0.165	0.000	0.000
M3	Hog Island	115 - 116.5	1.493	0.608	-0.112	-0.046



to a gravel transport rate of roughly  $1.4 \times 10^5 \text{ m}^3/\text{year}$ . If the actual amount of gravel mining was twice the estimated value then the actual gravel inflows at Agassiz-Rosedale bridge averaged  $2.1 \times 10^5 \text{ m}^3/\text{year}$ . Therefore, the overall results of the budget are reasonably insensitive to the assumed gravel mining quantities.

The overall net channel and bank changes for the coarse fraction of the gravels ( $> 25 \text{ mm}$ ) totalled  $+1.7 \times 10^6 \text{ m}^3$  between 1952 and 1984. This quantity represents the net aggradation of coarse gravel sediments in the reach between Rosedale and Sumas Mountain. After accounting for the past gravel mining, the average annual coarse gravel inflow at Rosedale bridge was estimated to be  $7.2 \times 10^4 \text{ m}^3/\text{year}$ .

Figure 7.4 illustrates the reach by reach sediment budget and the estimates of the gravel transport along the river. The budget illustrates that three main gravel transport zones exist along the river. The most distal zone is the depositional reach that extends from Chilliwack Mountain to Sumas Mountain. This zone corresponds to the river's transition from a gravel bed to a sand bed channel. There is also a noticeable change in water surface gradient in this reach - from  $1.8 \times 10^{-4}$  above Vedder River confluence to less than  $8.5 \times 10^{-5}$  below Sumas Mountain. In this 11 km reach the average annual gravel transport rate decreased from approximately  $4 \times 10^4 \text{ m}^3/\text{year}$  to virtually zero. The net aggradation in the reach totalled roughly  $1.2 \times 10^6 \text{ m}^3$  between 1952 and 1984. This deposition rate is very low, representing an average accumulation of only 0.2 m of sediment in 32 years.

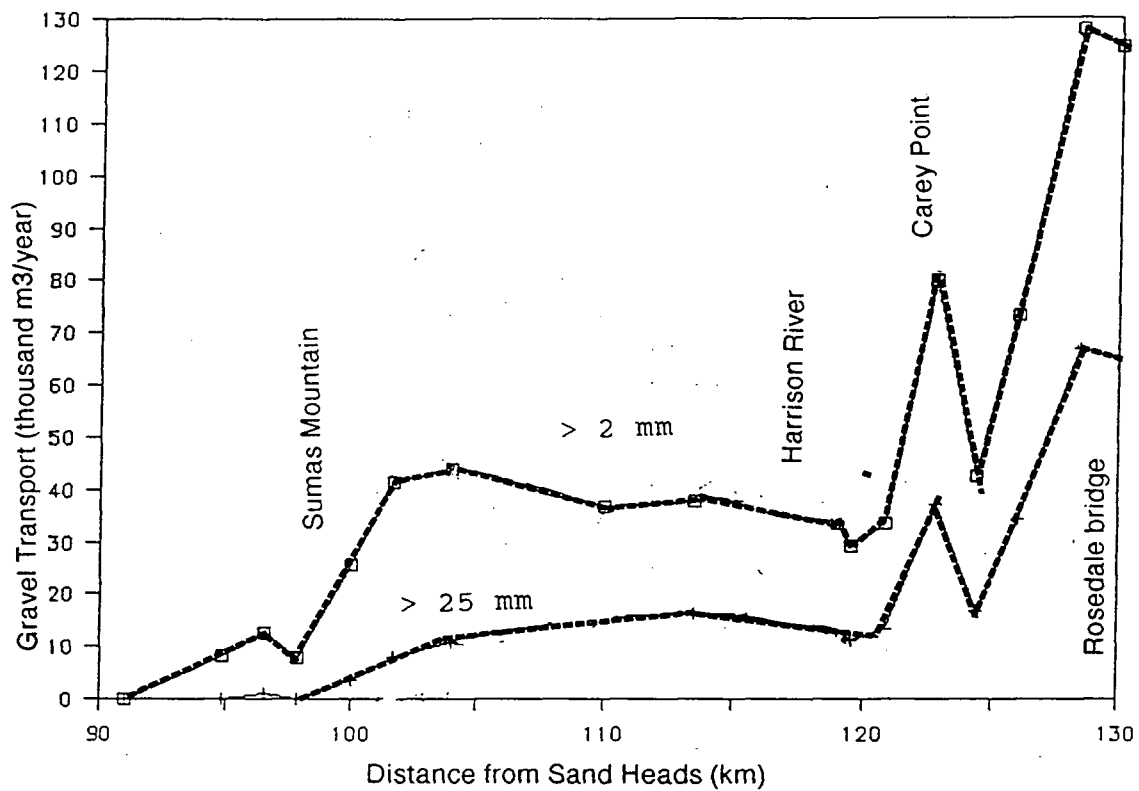


Figure 7.4 Average gravel transport between Rosedale bridge and Mission over the period 1952 to 1984

The second transport zone extends 20 km from upstream of Chilliwack Mountain to near km 120, upstream of the Harrison River confluence. Within this reach the average annual gravel transport rate was relatively constant, averaging about  $5 \times 10^4 \text{ m}^3/\text{year}$ . This reach can be considered in overall equilibrium since the incoming and outgoing gravel loads were approximately equal over the 32 year period.

However, although the overall net change ( $\Delta S_c + \Delta S_f$ ) was close to zero, neither the change in channel storage ( $\Delta S_c$ ) nor the change in floodplain storage ( $\Delta S_f$ ) term was near zero. The net bank erosion and channel deposition within this reach reflects the major changes (extensive island erosion near Harrison River and bar deposition near Chilliwack Mountain) that took place between 1952 and 1984.

The third transport zone extends from Carey Point up to the Agassiz - Rosedale bridge. This 10 km zone is another depositional reach. The average annual gravel transport decreased from  $1.2 \times 10^5 \text{ m}^3/\text{year}$  at the bridge site to  $5 \times 10^4 \text{ m}^3/\text{year}$  downstream of Carey Point. In total, approximately  $2.2 \times 10^6 \text{ m}^3$  of gravel sediments were deposited within this reach between 1952 and 1984. This aggradation corresponds to the major sequence of island re-construction and gravel bar deposition that was described in Section 6.2.

Based on the evidence described in Chapter 6, it is likely that the 32-year period of the sediment budget is on the same scale as (or shorter than) the time scale for most

morphologic changes to develop. A rough estimate of the time scale for gravel transport through the reach was made by estimating the turnover time ( $T_o$ ) for gravel sediments within the active channel zone. Using the 1984 survey data, the lowest general bed scour level in this reach was estimated to be at El. - 15 m. The total volume of gravel sediments within this reach lying above this level was computed from the DTM to be  $1.2 \times 10^8 \text{ m}^3$ . Assuming a gravel flux of  $5 \times 10^4 \text{ m}^3/\text{year}$  the corresponding turnover time for the gravel sediments in the channel is 2,400 years. This type of calculation helps to confirm the notion that many channel adjustments on a river the size of the Fraser River develop over relatively long time scales and that the present channel may not be in equilibrium with its present flow and sediment input regime.

## 8.0 SEDIMENT TRANSFERS AND MORPHOLOGIC CHANGE

### 8.1 Assumptions

This section of the report assesses the feasibility of estimating sediment transfers and ultimately sediment transport rates from morphologic changes that can be measured from planimetric maps and air photos. Bank erosion and deposition areas were planimetered from the 1:25,000 scale channel shift maps described in Section 6. These maps provide the channel alignment in 1890, 1928, 1943 and 1971 so that the channel changes between surveys have been measured over periods of 15 to 38 years. The overall net channel changes have been computed for a period spanning more than 80 years. Quantities of materials eroded from islands and the floodplain were estimated by multiplying the eroded areas by the estimated bank heights at each site. These estimated bank heights were determined from the available channel surveys in 1952, 1964 and 1984. Deposition volumes were not calculated from the areas of known deposition since it was not possible to estimate the thickness of the deposits from the planimetric maps. The stratigraphy of the banks and islands was estimated from observed present day conditions. For most of the alluvial sections in the gravel bed reach it was assumed that the banks were composed of a basal gravel and sand layer overlaid with a layer of finer sands and silts. The thickness of these finer floodplain deposits was estimated from the existing exposures along the river (see Section 4.2). This provided a means for estimating both the gravel transfers and the transfers of the finer suspended load sediments to the channel over the last century.

## 8.2 Long Term Sediment Transfers Along Fraser River

The overall pattern of erosion and deposition along the river has been governed, to some extent, by the lateral confinement along the valley. Major erosion and deposition zones are situated in the wide, unconfined sections (such as near Herrling Island) while more stable reaches have been located in the narrower, confined sections (such as the reach downstream of Carey Point). This pattern makes it useful to sub-divide the wandering reach between Laidlaw and Sumas Mountain into seven different sub-reaches. These sub-reaches, along with the single channel reaches from Hope to Laidlaw and from Sumas Mountain to Mission are illustrated on Figure 8.1. This figure also summarizes the general pattern of past erosion and deposition along the river.

Figure 8.2 shows the distribution of erosion along the channel over the three time periods. The basal layer bank erosion volumes have totalled 750,000 to 938,000 m<sup>3</sup>/year along the 50 km reach between Laidlaw and Vedder River. In total, approximately 67.5 million m<sup>3</sup> (108 million tonnes) of predominantly gravel sized sediments have been eroded from the islands and floodplain of the river between 1890 and 1971. Table 8.1 summarizes the erosion quantities in individual reaches.

The highest erosion rates have generally occurred between Laidlaw and the Agassiz - Rosedale bridge. The lowest erosion rates occurred downstream of Chilliwack.

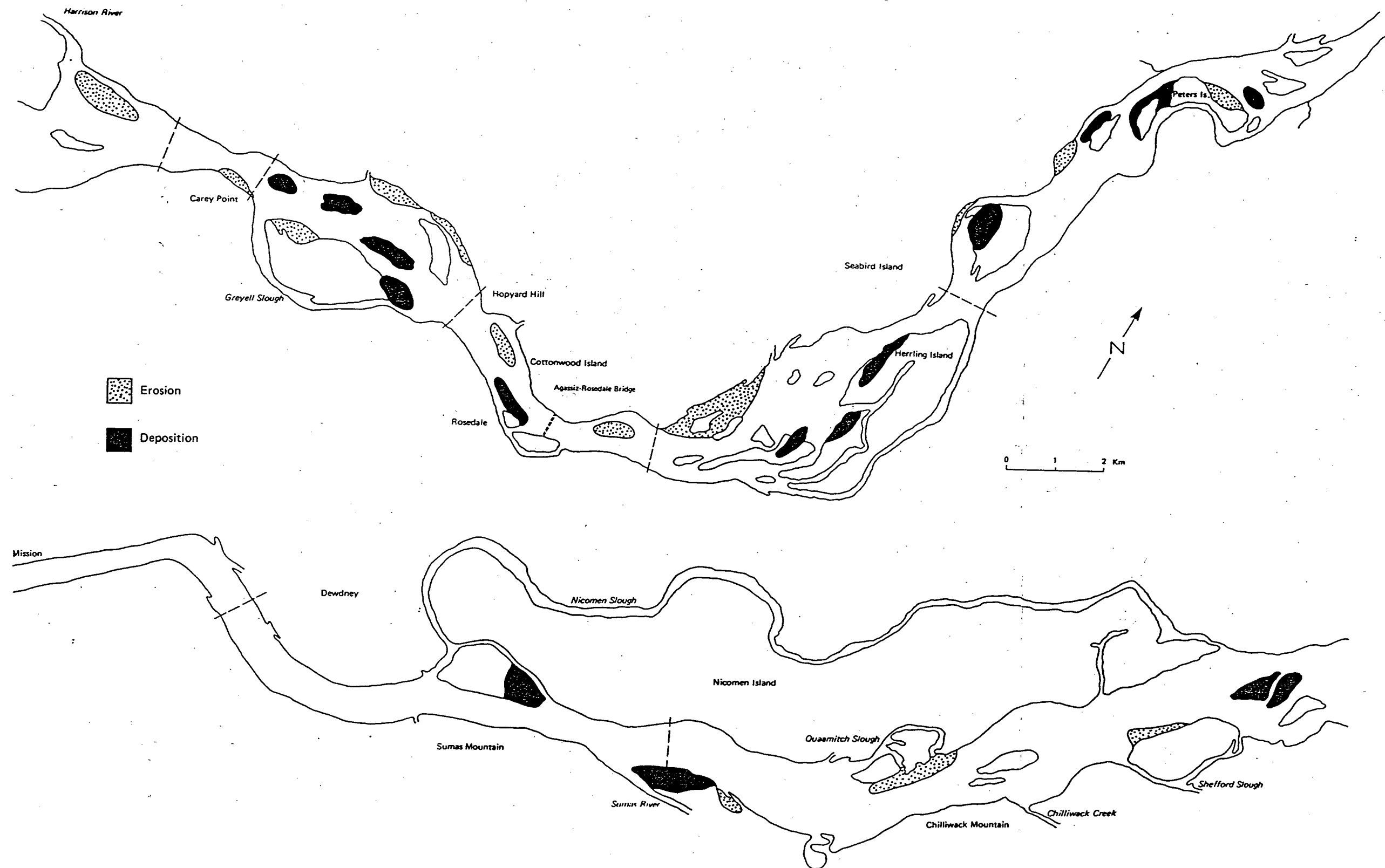


Figure 8.1 Overall pattern of deposition and erosion in historic times along lower Fraser River

# Gravel Sediments Only

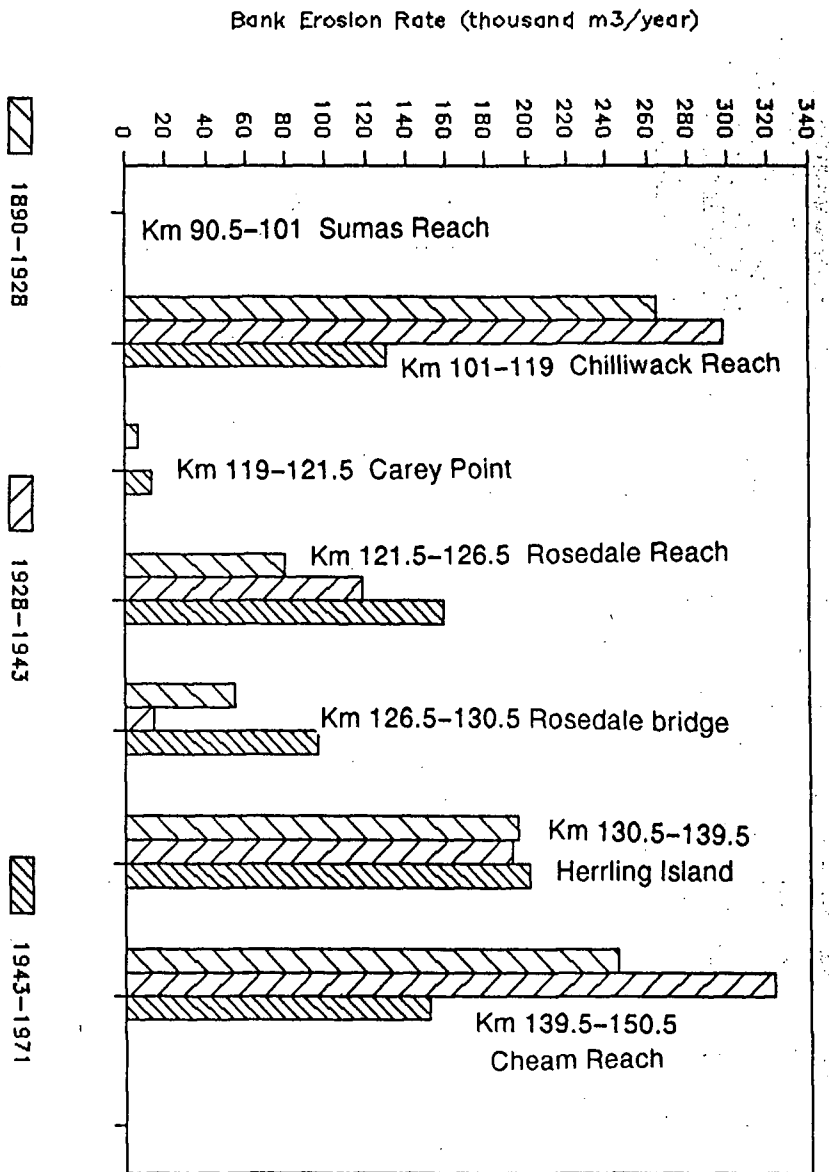


Figure 8.2 Distribution of historical bank erosion rates along the wandering reach



TABLE 8.1

## SUMMARY OF BANK EROSION RATES ALONG LOWER FRASER RIVER

REACH	LENGTH (km)	EROSION AREA (ha)	SEDIMENT VOLUME million cubic metre	ANNUAL EROSION million cubic metre/year
Period 1890 (approx.) - 1928				
Sumas	10.5	88		
Chilliwack	17.5	410	10.1	265
Rosedale	12.2	162	5.36	141
Cheam	21.0	<u>423</u>	<u>16.7</u>	<u>440</u>
Total		1083	32.16	847
Period 1928 - 1943				
Sumas	10.5	10		
Chilliwack	17.5	173	4.47	298
Rosedale	12.2	372	1.94	129
Cheam	21.0	<u>170</u>	<u>7.67</u>	<u>511</u>
Total		725	14.08	938
Period 1943 - 1971				
Sumas	10.5	21		
Chilliwack	17.5	177	3.68	131
Rosedale	12.2	153	6.25	223
Cheam	21.0	<u>264</u>	<u>11.15</u>	<u>398</u>
Total		615	21.08	752

Note: Annual erosion volumes do not include fine sandy and silty floodplain deposits.

The bank erosion rate was about 25% higher in the period 1928 - 1943 compared to 1943 - 1971. This occurred even though the flows during the period between 1928 and 1943 were well below the long term average. For example, the largest flood in this period had a return period of less than 5 years. During the period 1943 - 1971 four floods had return periods in excess of 10 years, including the 1948 flood which had a return period of over 100 years. As described previously, the morphologic changes along the Fraser River have generally evolved over a long period of time (several years to decades) and so are not affected greatly by individual flood events. The decrease in bank erosion rate over time may be partly accounted for by the influence of bank protection works that have mainly been constructed since the 1950's.

Figure 8.3 shows the cumulative bank erosion rate by grain size fraction for the period 1943 - 1971. The volumes of gravel coarser than 2 mm and gravel coarser than 25 mm were computed in each sub reach by using the basal layer bank material size data reported in Section 5.4. The total quantity of gravel ( $> 2$  mm) that has been transferred to the channel during this period averaged slightly over  $600,000 \text{ m}^3/\text{year}$ , which represents 83% of the total sediment transfers from the basal layer. The total quantity of gravel coarser than 25 mm that was transferred to the channel during the same period averaged  $320,000 \text{ m}^3/\text{year}$  or 42% of the total quantity supplied from the basal layer. However, Figure 8.3 shows that virtually all of this coarse gravel was supplied from upstream of the Harrison River confluence

# Cumulative Bank Erosion Along River

1943-1971 Basal Gravel Layer Only

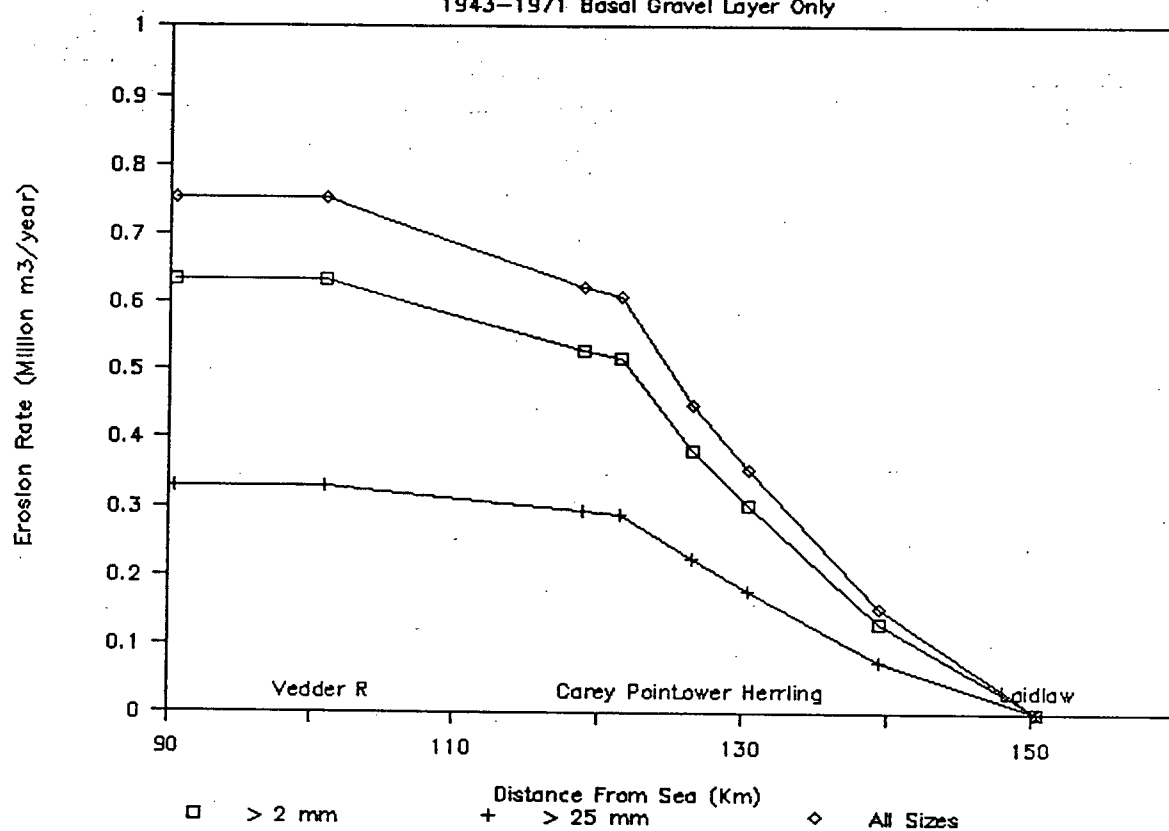


Figure 8.3 Cumulative distribution of gravel bank erosion along the river, 1943-1971

(km 120). This result also suggests that there is very little coarse gravel being supplied from bank erosion to the river below the Harrison confluence.

Figure 8.4 shows the estimated quantity of fine sand and silt floodplain sediments that has been supplied to the river by bank erosion. Approximately 40 million m<sup>3</sup> (64 million tonnes) of fine sediment was eroded from the banks between Laidlaw and Vedder River in the period between 1890 and 1971. An additional 11 million m<sup>3</sup> (17.5 million tonnes) was supplied from erosion downstream of the Vedder River. This quantity represents an average annual influx of 1 million tonnes/year of fine sediment or approximately 6% of the annual suspended sediment load measured at Hope or at Mission.

Figure 8.4 shows that the greatest supply of fine sediment in historic times has been from the reach downstream of Carey Point. The reach between Laidlaw and Carey Point has contributed between 20% and 40% of the total supply. The relatively small contribution of fine floodplain sediments from the reach upstream of Carey Point is due to several factors. First, virtually all of the actively eroding banks upstream of Carey Point are composed primarily of a basal gravel layer. There are virtually no exposures of massive fine grained deposits, which are common downstream between Harrison River and Sumas Mountain. Furthermore, the top capping of floodplain sediments found overlying the basal gravels tends to be thinner upstream of Carey Point. This is probably because the "turnover time" for islands is

# Fine silty sandy floodplain materials

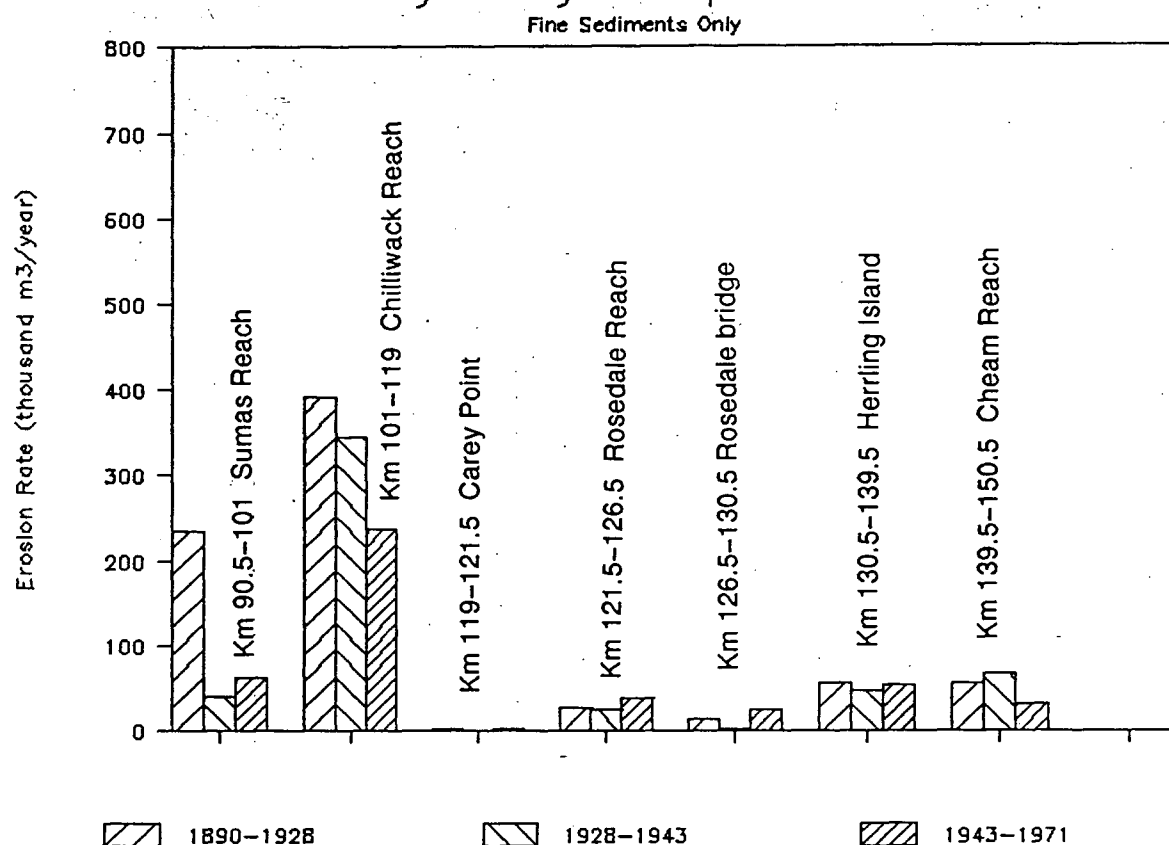


Figure 8.4 Cumulative distribution of sandy-silty floodplain sediment bank erosion quantities in three time periods

shorter in the upstream reaches of the river. As a result, there is less fine sediment deposited on top of the basal gravels.

### 8.3 Estimating Bed Load Transport Rates

#### **8.3.1 Sediment Transfers and Sediment Loads**

The portion of the bed load that is exchanged between major morphologic features along the river can be estimated from the quantities of bank erosion, provided a representative step length can be identified. For the case of a regularly meandering river, Neill (1967) claimed that the step length corresponds to half the meander wave length. Leopold and Wolman (1957) showed that the meander wave length scales linearly according to the width of the channel; the ratio of meander length to channel width was reported to average about 10. The major morphologic feature associated with meanders is the sequence of alternating diagonal bars or "riffles" and deep pools. The spacing between the bars also scales linearly with the channel width, and since there are two diagonal bars per meander, the diagonal bar spacing will be half of the meander wave length. This scaling was presented by Keller and Melhorn, (1978) and Church and Jones, (1982). These results indicate that the step lengths between these morphologic features is in the order of five times the channel width. On rivers where the channel alignment is straight, it is common for a regular pattern of alternating side bars to develop. It has been reported that the development of these alternating bars represents the first stage in the formation of

meanders (Lewin, 1976). The spacing between these features shows a relation similar to that of the diagonal bars in classical meanders.

Individual sub-channels in the wandering gravel bed reach typically have incised widths of 300 to 500 m. The total cross section width, measured at bankfull stage is typically 700 m to 900 m in most unconfined alluvial reaches. This suggests that the characteristic step lengths along the Fraser River should be in the order of 3 to 5 km.

An alternative approach for assigning step lengths is to identify the major, active deposition zones along the river. The spacing between these zones must be analogous to a step length. The major sediment accumulation zones along the lower Fraser River were shown in Figure 8.1. The spacing between these zones ranges from 2.75 km (in the reach between Agassiz bridge and Carey Point) to 5 km (in the reach between Carey Point and Vedder River).

The key data that were used for estimating the annual gravel bed load that is associated with bank erosion are summarized in Table 8.2. The estimated bed load quantity was calculated as the product of the unit transfer rate and the average step length. The unit sediment transfer rates in each reach represent the average annual volume of bank and island erosion per km of channel. The volumes represent the amount of sediment that has been supplied to the channel each year as a result of bank erosion. The average step length corresponds to the distance between major

TABLE 8.2

## SUMMARY OF SEDIMENT TRANSFERS AND BED LOAD TRANSPORT RATES

Period	Laidlaw Agassiz Bridge Reach Length = 20 km Transfer Length = 3.5 km			Agassiz Bridge - Carey Point Reach Length = 9 km Transfer Length = 2.75 km			Carey Point - Vedder River Reach Length = 18 km Transfer Length = 5 km		
	Total Erosion	Unit Transfer Rate	Bed load Transport Rate	Total Erosion	Unit Transfer Rate	Bed Load Transport Rate	Total Erosion	Unit Transfer Rate	Bed Load Transport Rate
	$10^3 \text{ m}^3/\text{yr}$	$10^3 \text{ m}^3/\text{yr}/\text{km}$	$10^3 \text{ m}^3/\text{yr}$	$10^3 \text{ m}^3/\text{yr}$	$10^3 \text{ m}^3/\text{yr}/\text{km}$	$10^3 \text{ m}^3/\text{yr}$	$10^3 \text{ m}^3/\text{yr}$	$10^3 \text{ m}^3/\text{yr}/\text{km}$	$10^3 \text{ m}^3/\text{yr}$
1890-1928	441	22.1	77.2	134.7	15.0	41.2	265.4	14.7	73.7
1928-1943	515	25.8	90.1	119.0	13.2	36.4	298.2	16.6	82.8
1943-1971	353.6	17.7	61.9	255.3	28.4	78.0	131.3	7.3	36.5



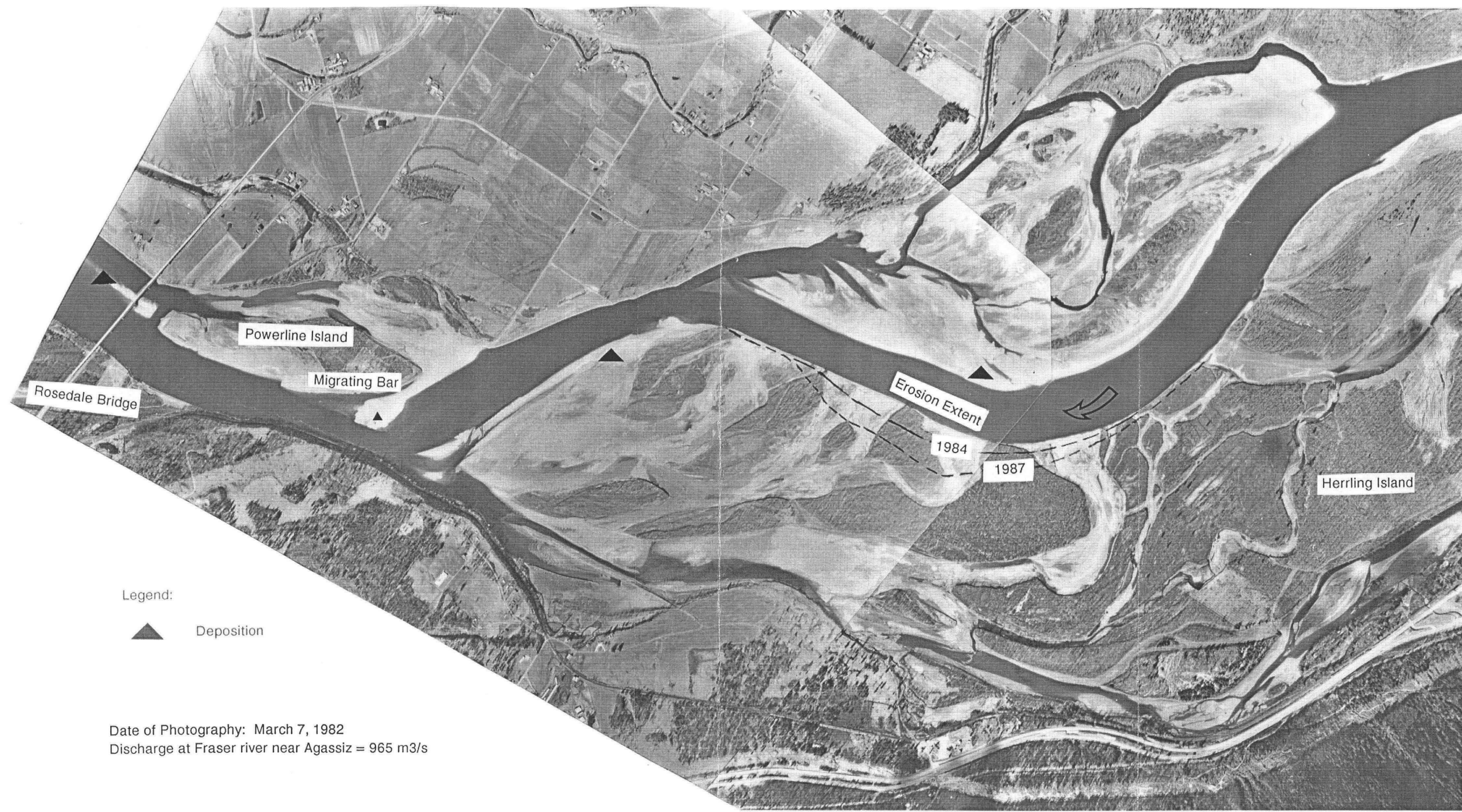
sediment storage zones along the river. The average step length per year is a measure of the velocity of travel of bed load along the channel. The computed loads typically range from 60,000 to 90,000 m<sup>3</sup>/year for the reach upstream of Agassiz and from 37,000 to 83,000 m<sup>3</sup>/year in the reach downstream of Carey Point. The variations in sediment loads along the river are consistent with the observed pattern of instability that has been described in each reach of the river. For example, upstream of Agassiz, the estimated loads were highest in the period 1928 to 1943 and lowest in the period 1943 to 1971. However, between Agassiz Bridge and Carey Point the opposite trend was observed - the highest loads occurred in the period 1943 to 1971 and the lowest loads occurred between 1928 and 1943.

### **8.3.2 Test of Neill's Approach**

The bend along the lower end of Herrling Island is the one of the few sites where the bed load rate can be estimated by using the approach described by Neill (1967). The evolution of this bend was described in Section 6.2 and is illustrated in the historical air photos on Figure 6.12. Over the last 20 years the pattern of sediment transfer at this site has included bank erosion along the lower end of Herrling Island, lateral migration of the channel to the south and deposition of gravel sediments in the reach immediately downstream of the Agassiz - Rosedale bridge. Using Neill's approach the estimated bed load passing the Agassiz - Rosedale bridge should correspond to the quantity of gravel material eroded from Lower Herrling Island.

The bank erosion areas were computed by constructing channel shift maps from sequential air photos flown in 1979, 1982, 1984, 1986 and 1987. The bankline changes have been superimposed on Figure 8.5. The height of the eroded banks was estimated from surveys that were carried out in July, 1983. These surveys involved measuring the longitudinal profile in the channel along the base of the eroding banks over the entire 5 km length of the island. Partial channel cross sections extending out from the banks showed that the water depths dropped off very sharply to between 3 and 4 m and then flattened out and sloped down more gradually towards the main channel thalweg. The height of the banks above the waterline was estimated at the time of the surveys. The estimated bank heights will be representative of conditions around the time of the surveys. Unfortunately, other surveys from the 1960's or 1970's are not available. Therefore, estimated erosion volumes during these earlier time periods may be less reliable than the estimates in the 1980's.

Figure 8.6 shows the historical variation in erosion rates at lower Herrling Island. It can be seen that the highest bank erosion rates occurred between 1967 and 1971 and between 1982 and 1987. The erosion rate has also varied closely with the degree of bend curvature, with very low rates of erosion occurring when the bend radius to channel width ratio approached a value of five. This relation, as well as the historical air photography illustrate that rapid bank erosion can commence very abruptly - for example the erosion rate jumped from 10,000 m<sup>3</sup>/year between 1979 and 1982 to 180,000 m<sup>3</sup>/year between 1982 and 1984.



Date of Photography: March 7, 1982  
Discharge at Fraser river near Agassiz = 965 m<sup>3</sup>/s

Figure 8.5 Test reach for estimating gravel transport from meander sweep progression

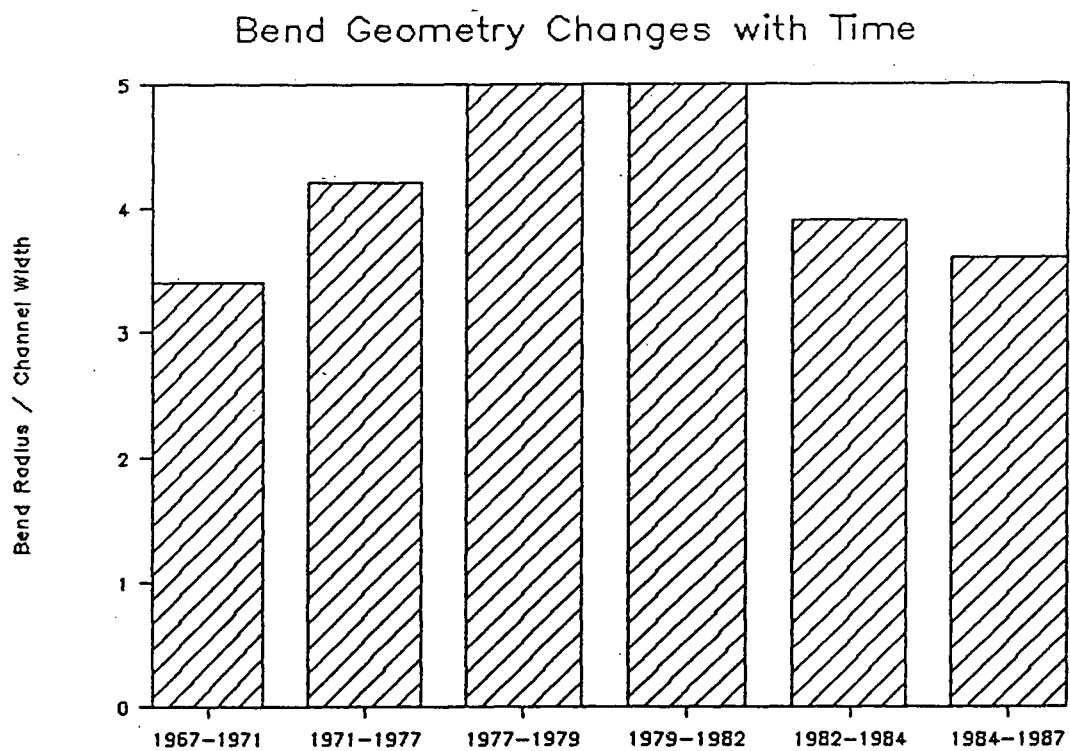
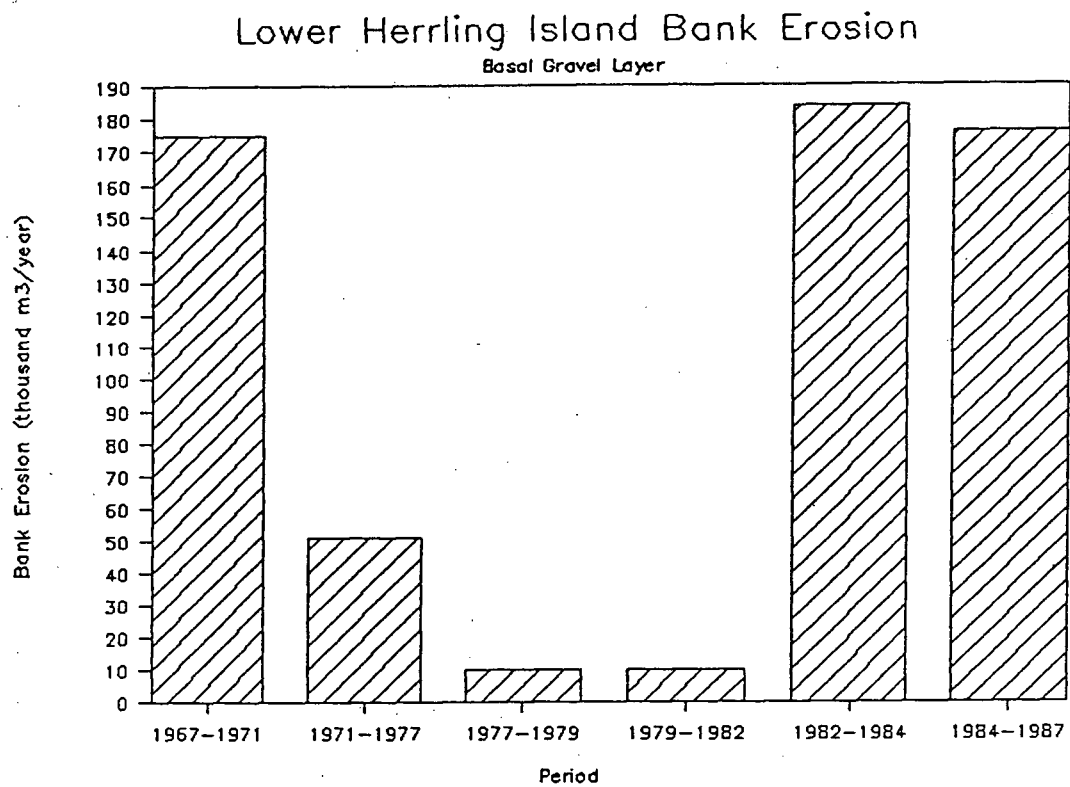


Figure 8.6 Historical variations in sediment transfers and bank erosion at lower Herrling Island

It is useful to relate the sediment inflows to observed channel changes immediately downstream of this eroding reach. The overall pattern of morphologic changes in this area was described in Section 6.2. It is apparent that during the period between 1977 and 1982, when bank erosion rates were low, sediment was accreting along the convex side of the bend. Some of this accretion took the form of low amplitude sheets or waves that became attached to the more stable point bar features and the lateral bar on Powerline Island. Therefore, it is clear that even though the erosion rate from the outer bank was very low during this period sediment was moving through the channel zone in discrete, migrating gravel sheets. These sheets may not have gone into permanent storage in the floodplain or islands, however they clearly had an impact on the bar morphology in the reach. This accretion may also have been the major reason for the sudden increase in bank erosion after 1982.

There is photographic evidence that one of these discrete gravel sheets migrated along the edge of Powerline Island and was deposited below the Agassiz - Rosedale bridge during the period 1982 to 1986. It is interesting to note that substantial bank attack and undermining due to channel scour took place around this time along the base of the steep terrace that confines the river along its south bank just upstream of the bridge. It is likely that this suddenly accelerated erosion resulted from the passage of the migrating gravel sheet as it directed the flow towards the south bank. This erosion is another example of the kind described previously at Carey Point.

A second gravel sheet was generated as a result of the bank erosion along Herrling Island since 1982 and became attached to the most distal convex side of the bend. During this period the mid-channel bar below the Agassiz - Rosedale bridge continued to expand.

The channel changes below the Agassiz - Rosedale bridge during this period have been documented by two different means. First, the regular discharge metering carried out by Water Survey of Canada provides one source of data for measuring the channel changes over time. The location of the gauging cross section line in relation to the highway bridge was shown in Figure 4.3. In the period of interest, the cross section was typically surveyed between four and six times each year by measuring the point depths at approximately 20 points across the channel. These data were plotted and compared to assess the channel changes over time. Figure 8.7 shows some typical channel changes between 1980 and 1986. In addition to these data, detailed bathymetric surveys of the bar were completed by the author in 1984 and 1986. This involved surveying channel cross sections at 100 m intervals along the channel. The 1984 survey extended from the upstream end of Powerline Island. The 1986 survey was less extensive, but included 2 km of channel downstream of the highway bridge (Figure 8.8).

These data show that the mid-channel bar aggraded about 0.5 m at Water Survey of Canada's gauging line between 1980 and 1984. The repeat surveys in 1984 and 1986 showed that the greatest aggradation has occurred upstream of the gauging line.

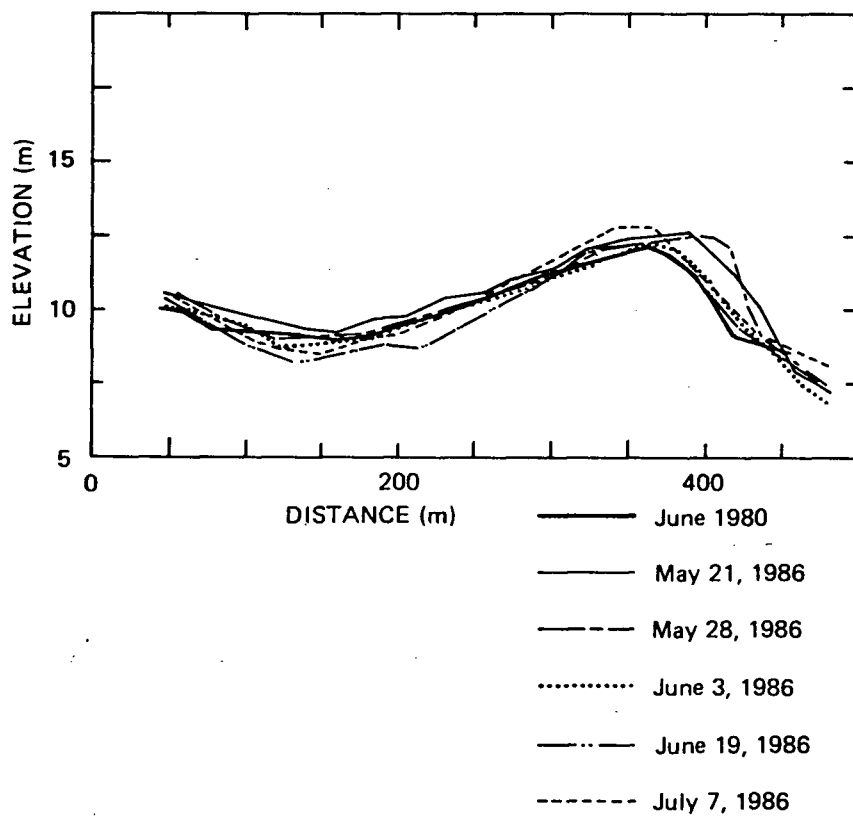


Figure 8.7 Historical Channel Changes at Agassiz Gauging Station

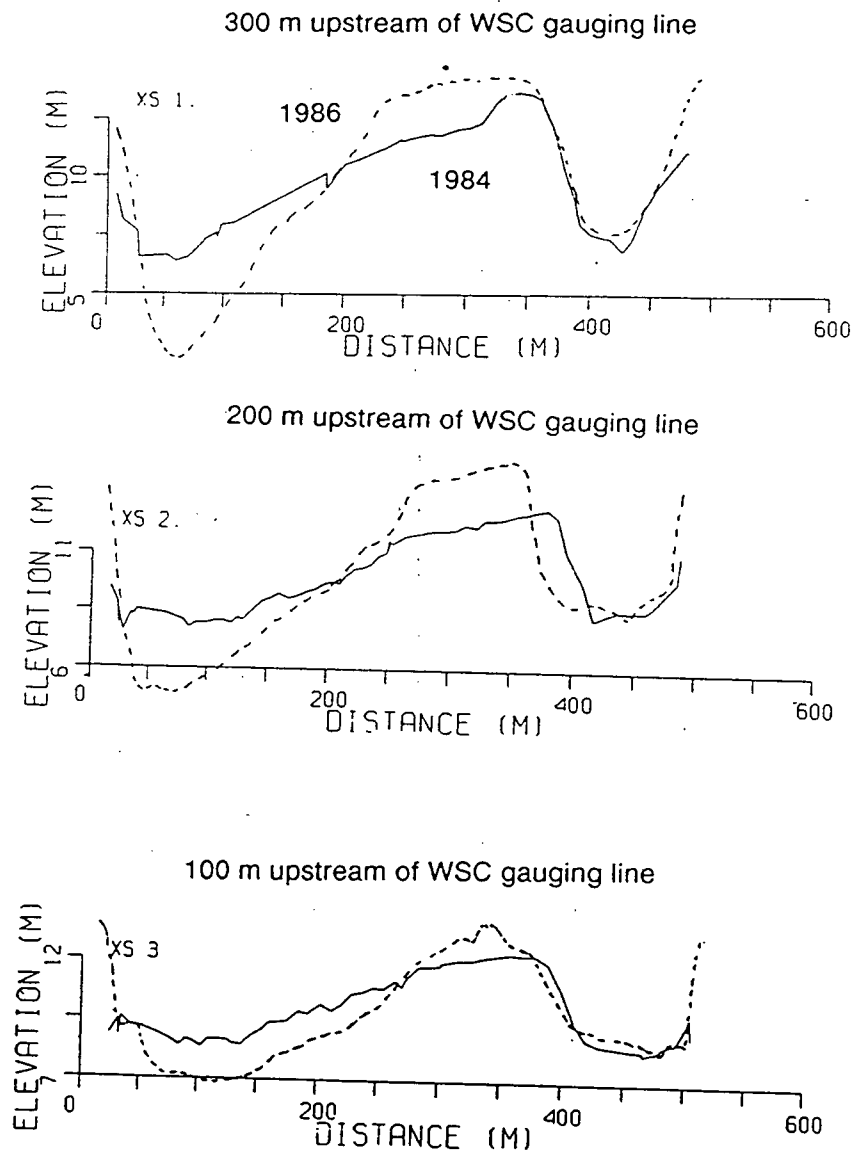


Figure 8.8 Channel aggradation at mid-channel bar downstream of Rosedale bridge



This amounted to up to 2.5 m over a width of 125 m. Approximately 160,000 m<sup>3</sup> of gravel deposition occurred at this bar between 1984 and 1986. However, deposition on the bar top has been accompanied by up to 3 m of scour in the thalweg downstream of the bar. This scour appears to have developed as a result of the changes in channel alignment upstream of the bridge. Also, the growth of the mid-channel bar below the highway bridge has produce a southward shift in the flow.

In summary, the pattern of sediment exchange observed along this reach does not follow the simple exchange process described by Neill. There are two scales of sediment transfers occurring in this reach:

- low amplitude gravel sheets that can migrate through other more stable bar and island features. The migration of these features will affect the active channel zone and may control the commencement of erosion or deposition at other, more stable morphologic features;
- transfers of sediment from islands and the floodplain as a result of large scale channel evolution processes such as meander migration.

For rivers that are characterized by migrating wave-like features it may be appropriate to treat these features like bed forms and estimate the bed load from their migration rate and geometry. This hydrographic approach is commonly used for estimating bed load in sand bed rivers (de Vries, 1973).

## **9.0 SEDIMENT TRANSPORT MEASUREMENTS**

### **9.1 The Bed Load**

The purpose of this chapter is to estimate the bed material load at Agassiz and Mission from direct measurements by Water Survey of Canada. These results provide an independent check on the sediment budget calculations and the morphologic estimates of sediment transport.

#### **9.1.1 Measurement Procedures**

Between 1968 and 1976, 110 bed load measurements were collected at Agassiz with the sampling frequency ranging from 23 measurements/year in 1968 to only 9 in 1976. Unfortunately, only 62 measurements were collected during the freshet season (May-July) when virtually all of the bedload movement takes place. The measurements were collected with a half size VUV sampler (Novak, 1957) and a basket sampler (Ehrenberger, 1931) at the higher flows (generally above  $7,500 \text{ m}^3/\text{s}$ ). The VUV sampler has an opening width of 225 mm and a height of 115 mm. This pressure difference type sampler is designed so that the water and transported bed material enter the sampler with the same velocity as the undisturbed flow. The WSC basket sampler is based on early Swiss designs from the 1930's and has an opening width of 610 mm, a height of 255 mm and a basket mesh size of 6 mm. Due to the coarse mesh size the finer gravel and sand will not be retained in the sampler.

The sampling times for both the VUV and basket measurements were usually two to three minutes and sample catches usually ranged from a few hundred grams up to 1 or 2 kg in the VUV sampler and up to 10 to 20 kg in the basket sampler.

The Agassiz bedload measurements were collected at six or fewer verticals from a WSC boat on the gauging section line (Figure 9.1). Typically only two or three repetitive samples were collected at each vertical making a total of 12 to 18 samples in each measurement.

The bed load measurements at Mission were made with a BTMA Arnhem sampler (Schaank, 1937; de Vries, 1973). This sampler is a pressure difference sampler with an intake opening 85 cm wide and 5 cm high. The Arnhem sampler was designed for measuring bedload in the Rhine River in the Netherlands where the bed material consists of coarse sand and fine gravel. The samples were collected at five verticals from a WSC boat on the gauging section line upstream of the Mission Railway bridge. Normally 3 to 5 replicate samples were collected at each vertical, with individual sample catches ranging from a few grams to a few hundred grams. In some of the early years a complete measurement was often repeated two or three times in the day so that the daily load could be estimated from 50 to 75 samples. For later years, the daily load must usually be estimated from about 15 samples.

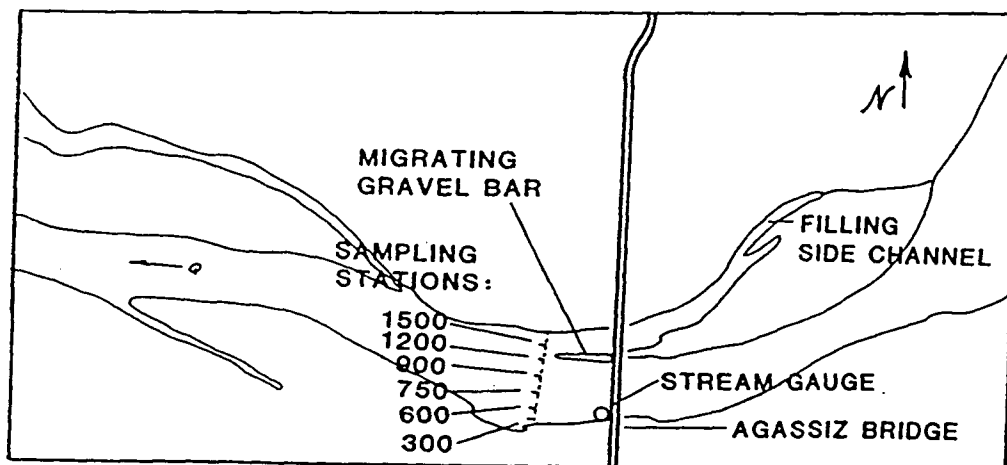
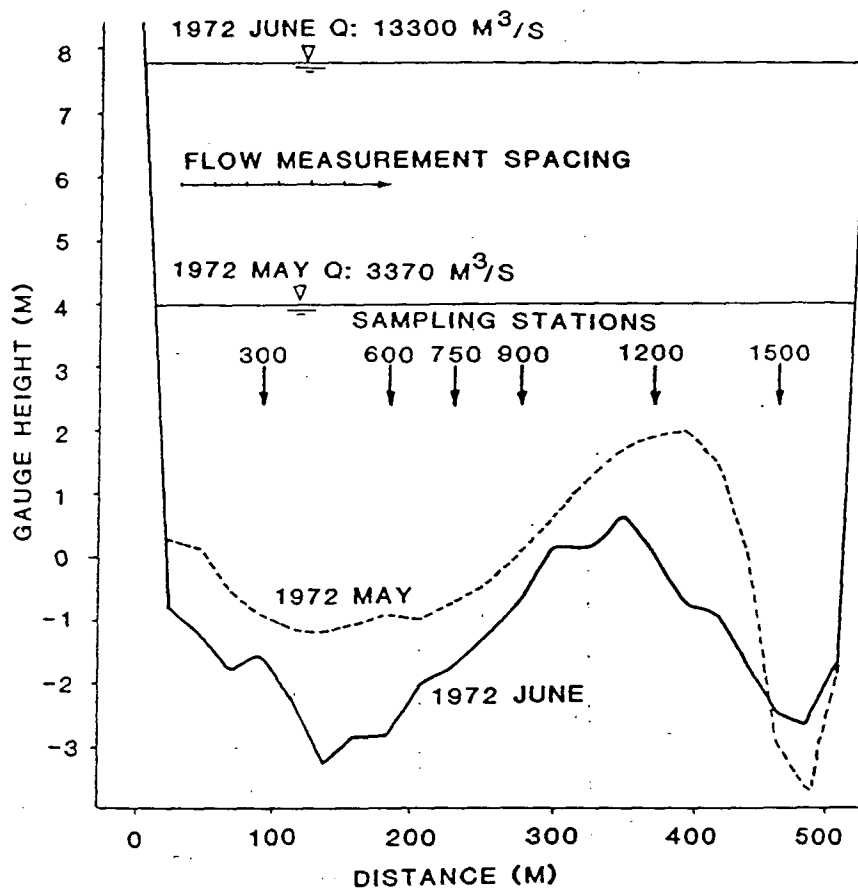


Figure 9.1 Sediment sampling verticals at Agassiz hydrometric station

### **9.1.2 Data Adjustment: Sampler Efficiency**

None of the daily bedload data has been published by WSC and all of the data in the work files is considered preliminary and subject to revision. Also, much more information is available for estimating the efficiency of the samplers at this time than when the data were first collected. Therefore, it was decided that all of the bedload data should be re-calculated. These revised estimates were compared against WSC's preliminary values in order to identify any significant discrepancies or calculation errors.

The efficiencies of the basket and VUV samplers were estimated from recent laboratory calibrations performed at the Canada Centre for Inland Waters (Engel, 1982, 1983). These studies, as well as results from previous investigations (Gibbs, 1973), indicated that the efficiency of the basket sampler is about 33% for the hydraulic conditions at Agassiz. However, this efficiency factor does not account for any loss of fine sediment through the coarse mesh of the basket. In all laboratory studies the model bed material was always coarser than the screen size. However, at Agassiz a considerable portion of the bedload is finer than the 6 mm wire mesh and was not retained in the sampler. This feature was very apparent when the size distributions of the basket samples were compared with those of the VUV samples. The missing portion of the sample can be estimated approximately by assuming that at high flows the bedload size distribution is similar to the sub-surface bed material size distribution (Einstein, 1950; Parker et al., 1982). The bed material samples

near Agassiz indicated that about 15% of the sediment was finer than 6 mm. Therefore the overall correction factor adopted in this study was estimated as:

$$K = 1/0.33 \times 1/0.85 = 3.5$$

Early studies suggested that the VUV sampler has an efficiency of 60 - 70% (Novak, 1957; Gibbs and Neill, 1973). More recent studies have shown that the efficiency may vary between 60% and 30%, depending on the hydraulic conditions and sampling times (Engel, 1983). For the hydraulic conditions at Agassiz and for sampling times of 2 to 3 minutes the efficiency of the half size VUV sampler was estimated to be about 33% (identical to that of the basket sampler). This estimated efficiency is surprisingly low compared to the results from previous laboratory studies.

The efficiency of the Arnhem sampler was determined from a series of model tests carried out in the 1930's at the ETH laboratories in Zurich (Meyer-Peter, 1937). The efficiency was found to decrease as the sampler filled with sediment, varying between 90% and 50%. However, WSC carried out field calibrations of the Arnhem sampler in 1968 at Mission by comparing bed load catches with estimates from tracking dune migration (WSC, 1970). In most of these tests the actual movement of the dunes was only 2 or 3 m, which is probably at the limit of the accuracy of the surveys. Based on these field tests, WSC estimated that the trap efficiency of the Arnhem was only 23%, or about one third of the value normally quoted. Some

preliminary flume experiments by the author suggested that the fine mesh bags used in the Arnhem sampler could become clogged when subject to relatively high suspended sand concentrations (McLean and Church, 1986). However, more definitive laboratory studies will have to be carried out to assess the most appropriate efficiency factor for the sampler when it is used on a sand bed river. For this study, WSC's efficiency factor of 0.23 was adopted. This meant that the measured loads were multiplied by a factor of 4.4 in order to estimate the actual transport rates.

### **9.1.3 Reliability of the Measurements**

Due to the sporadic nature of bed load movement and the physical difficulties involved in sampling, measurements of bed load are usually considered to be less reliable than measurements of suspended load. The problem of bed load sampling reliability has been discussed by de Vries, 1973; Csoma, 1973; Gibbs and Neill, 1973; Hubbell, 1987 and McLean and Tassone, 1987). The approach has generally been to collect replicate samples at a single vertical in the cross section and then to compare the load determined from only a few samples to the actual average load determined from the full set of measurements.

The most thorough study has been provided by Hamamori (1962) and de Vries (1973) who investigated the fluctuations in bedload rates caused by the passage of dunes and ripples along a sand bed channel. On the basis of this work and field

measurements from the Rhine River, de Vries (1973) recommended that a minimum of 10 samples should be collected at each vertical.

Measurements on the gravel bed portion of the Danube River showed that the probability distribution of transport rates varied across the channel, with the bedload rates being more widely distributed where the transport rates were highest (Csoma, 1973). In this case the Hamamori relation was found not to apply.

Einstein (1937) had earlier described the distribution of bedload transport movement by assuming that bedload particles moved in a series of steps and rests, with the rest periods being much longer than movement times. The related problem of describing the distribution of sediment volumes caught in a bedload sampler after a specified sampling time was also considered. The probability density function describing the volume of sediment trapped in a given sampling time implies that the distribution of bedload transport rates will depend on the duration of sampling and the intensity of transport, which is in agreement with Csoma's observations. This type of model appears to be more appropriate for estimating the reliability of measurements in gravel rivers.

A preliminary test of this model, using repetitive measurements at Agassiz is described by McLean and Tassone (1987). The replicate measurements at Agassiz were made by WSC on June 11, 1985 with the half size VUV sampler at a discharge of approximately  $7,700 \text{ m}^3/\text{s}$ . Twenty repeat samples were collected at two verticals



and 14 samples were collected at the third vertical. Figure 9.2 illustrates the large fluctuations in sample catches that were observed and the frequency distribution of the transport rates. The most important feature of these results is that individual measurements could reach up to six times the overall mean transport rate.

Furthermore, the distribution of transport rates was very non-symmetrical, with nearly 70% of the samples having loads less than the average and only 30% of the samples having loads greater than the average. These results should make clear that the normal practice of estimating the mean bedload rate with only two or three samples could result in substantial errors. In reviewing the past measurements at Agassiz it was found that in 30% of the daily measurements between 1968 and 1976 the range in transport rates at a single vertical exceeded the computed average at the vertical by a factor of two. As a result, the precision of the computed averages must be very low.

Three sets of repeated bedload measurements were collected at Mission in 1972 and 1974 under flow conditions that ranged from 10,800 m<sup>3</sup>/s to 6,570 m<sup>3</sup>/s. On these three dates between 20 and 25 bedload samples were collected at a single vertical (Vertical 900) over a period of three to four hours. The variation in transport rates that was observed is summarized in Figure 9.2. The 1972 data showed that individual bed load measurements varied between 0.1 and 4 times the average rate estimated from all samples. The frequency distribution of transport rates from the two sets of measurements in 1972 fit the theoretical Hamamori distribution much more closely than the 1974 measurements. The actual distribution of transport rates

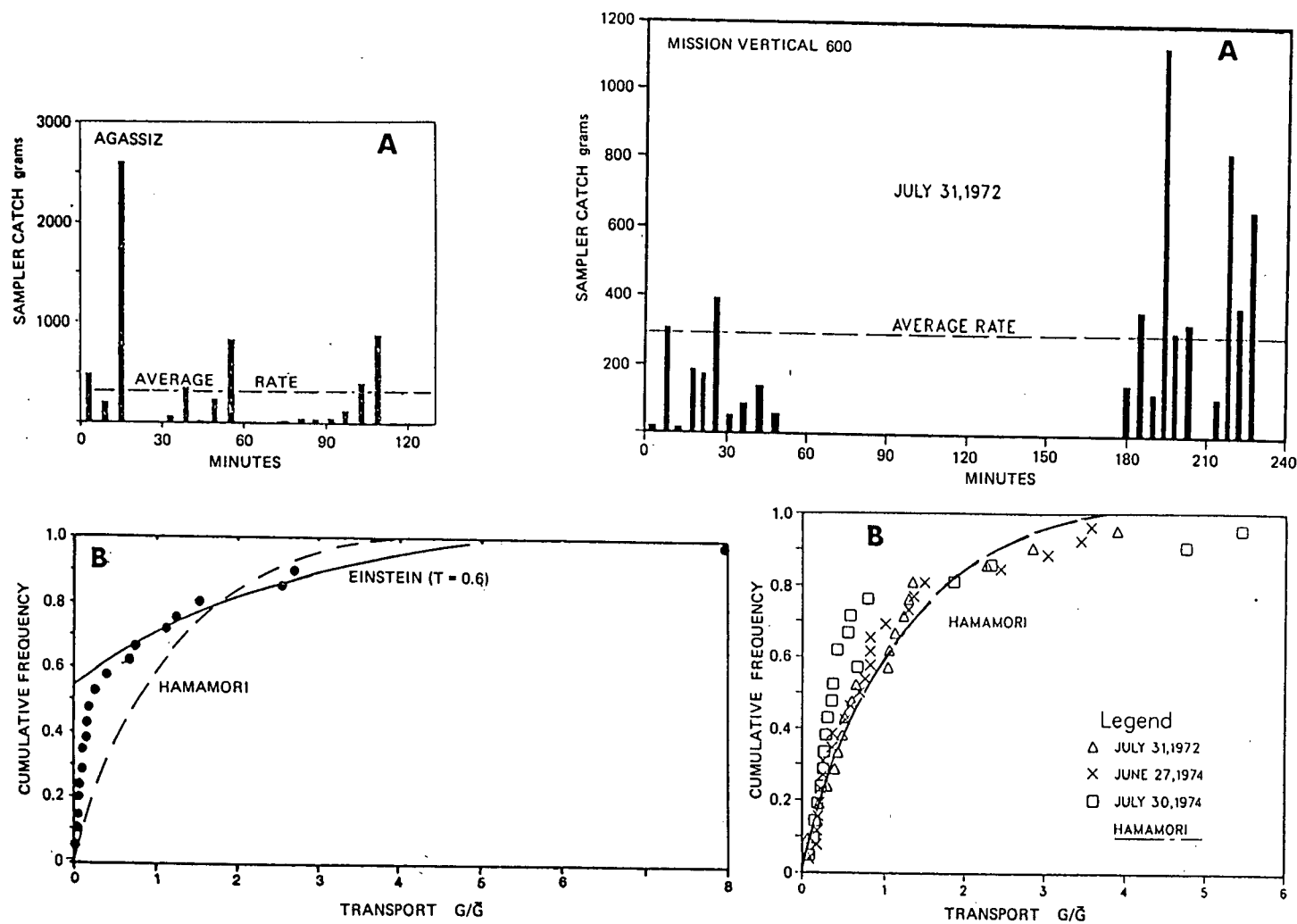


Figure 9.2 Replicate sampling to measure variations in bed load transport rate at Agassiz and Mission

in sand bed channels will be affected by the characteristics of the bedforms that are present.

Unfortunately, longitudinal profiles were not surveyed at the time of the bed load measurements in 1972 or 1974.

Given the distribution of transport rates at a point, the reliability of estimates of the true mean bedload rate from an n-sample average can be determined. In this study, the precision of the computed average bed load rates was estimated by using the Monte Carlo simulation technique in conjunction with the measured bed load probability distributions to generate a large number of n-sample averages. The precision of these synthesised measurements was then expressed as a coefficient of variation of the mean rate (standard deviation of the estimated means/mean bedload rate). The calculations were performed with a FORTRAN program that used a random number generator to produce 100 consecutive n-sample averages from the assumed bedload probability distribution (McLean and Tassone, 1987). This approach was first used by de Vries (1973) to estimate the number of measurements required on the sand bed portion of the Rhine River. The results of simulations using the measured probability distributions at Agassiz and Mission are illustrated in Figure 9.3. It was found that the precision of the measurements was substantially lower at Agassiz than at Mission. For a three sample average at a vertical the relative error (CV of the mean) was 84% at Agassiz and 50% at Mission. At least 10 repeat samples would be required at Agassiz before the relative error was less

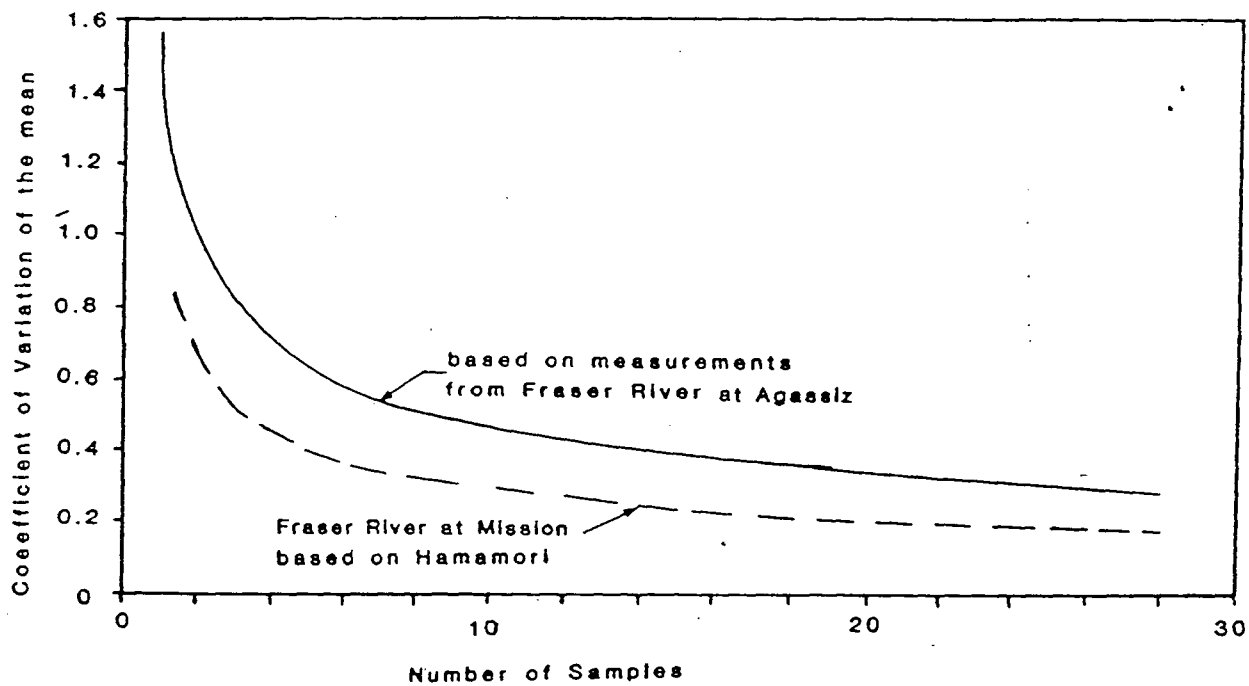


Figure 9.3 Precision of n-sample bed load measurements at a single vertical at Agassiz and Mission

than 50%. These values represent the expected error at a single vertical and not the error in total bedload rate at the cross section.

In order to estimate the error in the total bed load rate some information on the spatial variability of the bedload rates across the channel would be required. A field assessment of this problem would require collecting a minimum of 10 samples at 10 to 20 verticals across the section and then comparing the total rate with the estimate from the 5 verticals that are normally used. This exercise would involve a substantial field effort and has not been carried out.

Recently, Hubbell (1987) extended the Monte Carlo approach by allowing the mean transport rate to vary across the channel section so that the error in estimating the total bed load rate from a limited number of verticals and samples could be made. Hubbell considered the case in which the bedload rate could have only two possible values and used Hamamori's probability distribution for estimating the variation of transport rates at a point. After reviewing the data at Agassiz and Mission it was considered that it would be more realistic to allow the transport rates to vary continuously across the channel. Several different assumed lateral variations were tested including uniform, triangular, bell-shaped quadratic and bell-shaped exponential. Furthermore, the Einstein probability model was used for computing the frequency distribution of transport rates at a point. The model parameters in Einstein's equation were computed by the method of moments to reproduce the measured bedload transport distributions at Agassiz and Mission. In this second

simulation program the precision of the total bedload rate was computed for different sampling strategies by varying the number of verticals in the cross section and the number of repeat samples at each vertical. The simulations showed that when the spatial variability of the transport rates was less than the temporal variations at a single point, then the relative error in the total bedload rate was less than the relative error in the average at any single point.

A lower bound estimate for the error of the total loads can be made by assuming that the actual mean bedload rate is uniform across the channel. For the normal sampling procedures on the Fraser River (5 verticals, 3 samples/vertical) the relative error (CV of the mean) was found to be 40% at Agassiz and 26% at Mission. In examining the measured rates across the sections at Agassiz and Mission it was noted that the maximum rate at a vertical (estimated from 3 samples) seldom exceeded three times the mean rate at the cross section. For the case of a "bell shaped" exponential distribution and a maximum to mean ratio of three, the relative error increased to 58% at Agassiz and 34% at Mission. These values could probably be considered upper bound estimates of the errors in the measured total bed load rates.

#### **9.1.4 Analysis of Agassiz Bedload Data**

Some preliminary interpretations of the bed load data at Agassiz are contained in Mannerstrom and McLean (1985). Significant gravel transport begins to occur at about 5000 m<sup>3</sup>/s. Most VUV bedload samples collected below this flow consisted

of sand or granules in the 2 mm to 8 mm size range. The abrupt change from sand transport to gravel transport probably represents the threshold condition for mobilising the local armoured surface layer (Parker et al., 1982). After this condition was exceeded the grain size distribution of the bedload became similar to that of the sub-surface bed material.

Figure 9.5 shows that there is only a poorly defined relation between bedload transport rate and discharge. A large portion of the scatter may be attributed to the low precision of the bedload measurements.

In examining the bedload discharge plots it was noticed that the data sometimes display an apparent seasonal hysteresis. However, the direction of the hysteresis was not consistent from year to year. In some years the rising limb bed load rates were systematically higher than the falling limb rates. In other years the reverse situation was observed. In an attempt to explain some of these effects multiple regression techniques were used in order to include a number of independent variables such as hydraulic parameters (mean velocity, depth), flow parameters (rate of change of discharge, discharge on the day preceding measurement) and suspended sediment parameters (total concentration, sand concentration). Finally the data were split into rising limb/falling limb categories and separate regressions were developed for each group. None of these efforts consistently improved the estimation of the transport rates. After this exercise it was concluded that the seasonally variable behaviour most likely is related to erosional and depositional events along the channel upstream, and follows no consistent fashion.

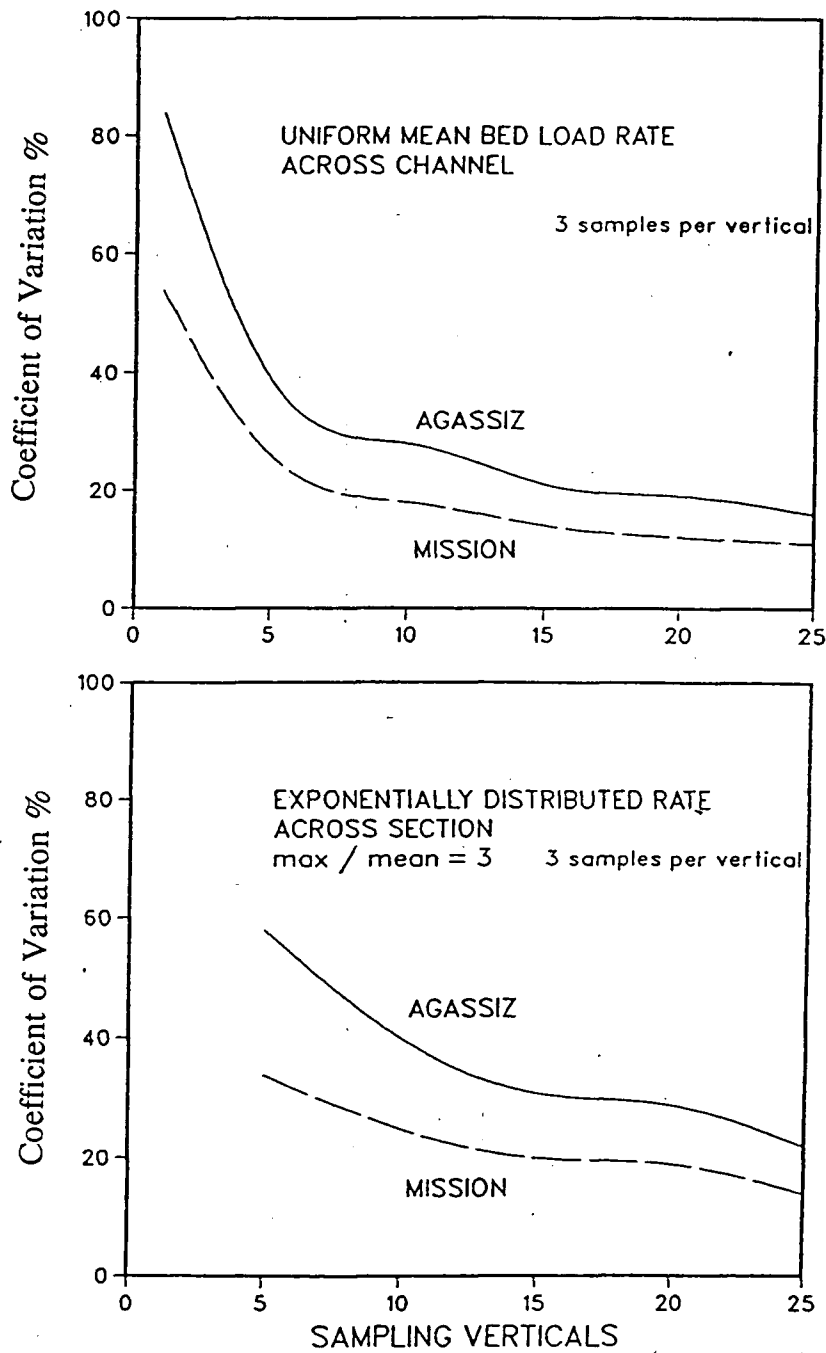


Figure 9.4 Precision of 3 sample per vertical bed load measurements in a hypothetical river cross section



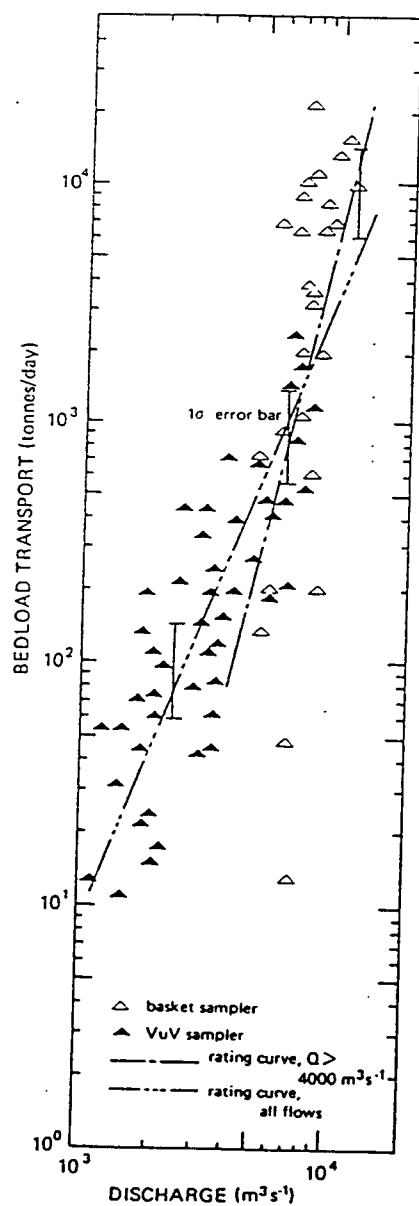


Figure 9.5 Bed load rating curve at Agassiz hydrometric station, 1966 to 1976

On the basis of these findings, the bedload rates were estimated using simple one variable regressions between discharge,  $Q$  and daily transport rate,  $g_b$ , having the form:

$$g_{bi} = a \cdot Q_i^d$$

This model assumes that a linear relation exists between the log transformed variables. The log transformation introduces a bias into the predictions which will result in a systematic under prediction of the loads (Ferguson, 1986). The magnitude of this bias will depend on the error variance of the regression  $s^2$ , and can be eliminated by applying a bias correction factor  $\exp(s^2/2)$  to the predicted values.

Separate rating curves were developed for the loads measured above and below a discharge of  $4,000 \text{ m}^3/\text{s}$ . This distinguished the predominantly sand transport at low flows from the predominantly gravel transport at higher flows. Furthermore, this separation ensured that the predicted transport rates at the low flows were based on the VUV measurements while the predictions at high flows were based primarily on the basket measurements. The two rating curves intersect at a discharge  $7,000 \text{ m}^3/\text{s}$ .

Figure 9.6 illustrates the range in annual bedload transport at Agassiz between 1966 and 1982, as estimated from the daily rating curves. The annual bedload rate averaged 170,000 tonnes/year between 1967 and 1982, and varied from 520,000 tonnes/year in 1972 to 60,000 tonnes/year in 1978. The size distribution of the

## FRASER RIVER NEAR AGASSIZ 1967 – 1982

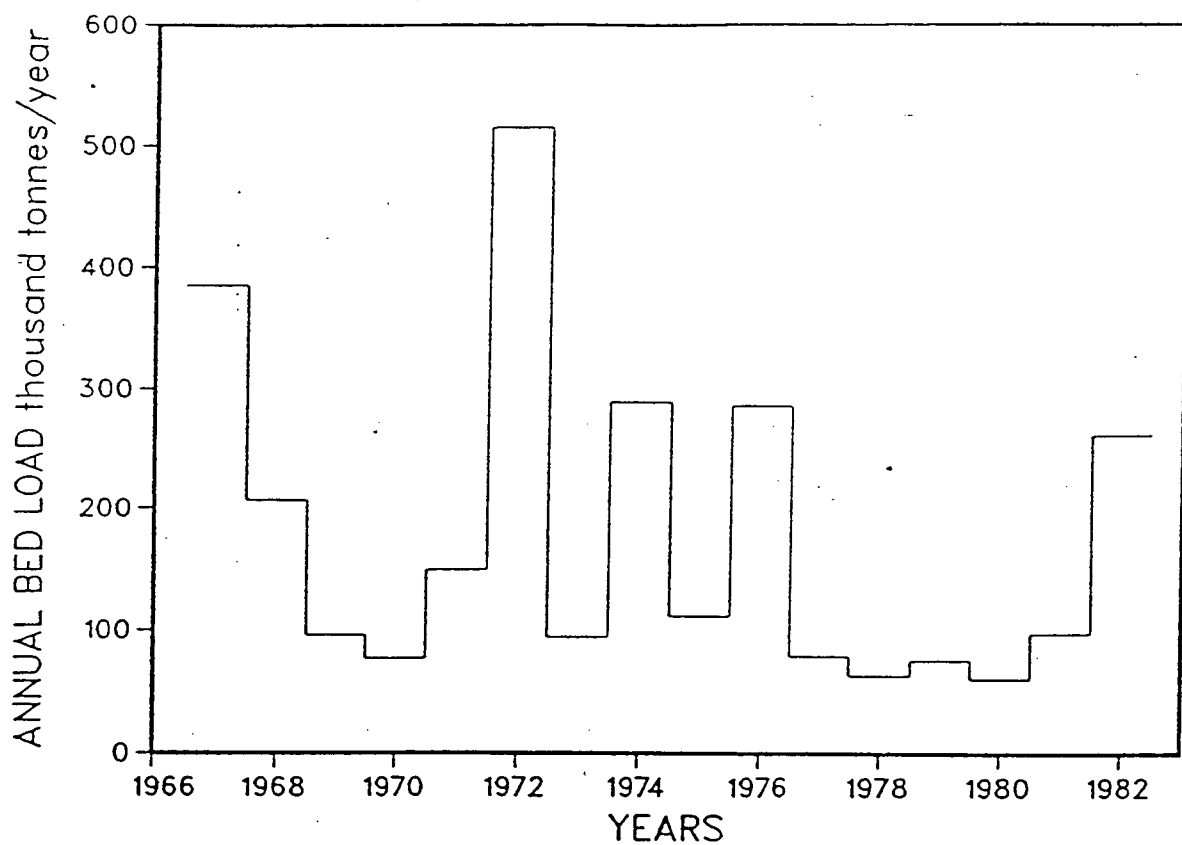


Figure 9.6 Variations in annual bed load transport rates at Agassiz, based on rating curve estimates

bedload was assumed to be similar to the size distribution of the volumetric bed material samples taken from the bars near Agassiz. This assumption is reasonable since the bar deposits represent bed load material in storage. Based on this assumption it was estimated that about 15% of the bedload consists of sand (primarily in the 0.25 - 1.0 mm size range) and 85% consists of gravel (primarily in the 16 - 45 mm range). It remains possible that the VUV sampler traps a minor proportion of suspended sediment near the bed, which may inflate the bedload transport estimates slightly.

One estimate of the precision of the annual loads was presented in McLean and Church (1986). The precision of the annual load was computed from the confidence limits on the bedload rating curve regression lines. The confidence interval on the "true" position of the rating curve can be expressed as:

$$y \pm t * SEE * (1/n + (x - \bar{x})^2 / ((n-1) * S_x^2))^{1/2}$$

SEE is the standard error of the regression

t is the t-statistic with n-2 degrees of freedom

Since the rating curves were based on power law regressions, x and y are the log transforms of the discharge and sediment transport rate.

The one standard error confidence limits on the rating curve line varied from +17.5% to -15% at a flow of 7,500 m<sup>3</sup>/s and from +30% to -23% at 14,000 m<sup>3</sup>/s.

The uncertainty in the annual load was estimated as follows:

1. The confidence interval (measured in per cent) on the rating curve estimate,  $E_i$ , was computed for flows ranging from 3,000 m<sup>3</sup>/s to 15,000 m<sup>3</sup>/s;
2. The fraction of the total annual load in each flow interval,  $Q_i$ , was computed to produce a weighting factor,  $W_i$ ;
3. The relative error in the annual load was then estimated as the sum of the weighted errors in each flow interval,  $\sum W_i E_i$ .

This calculation indicated that the estimated annual loads could be specified within  $\pm 20\%$  with a one standard error confidence interval or to within  $\pm 40\%$  with a two standard error confidence interval. This can be restated by saying there is a 68% chance that the "true" annual bedload rate will be within 20% of the estimated value and a 95% chance that the "true" rate will be within 40% of the estimate. By comparison, the one standard error confidence intervals on the daily bedload measurements ranged from  $\pm 40\%$  to  $\pm 58\%$  using the Monte Carlo simulations.

Figure 9.7 shows the fraction of the total bedload transported by different discharges over the period 1967 to 1982. This histogram reveals that the flows near 8,000 m<sup>3</sup>/s

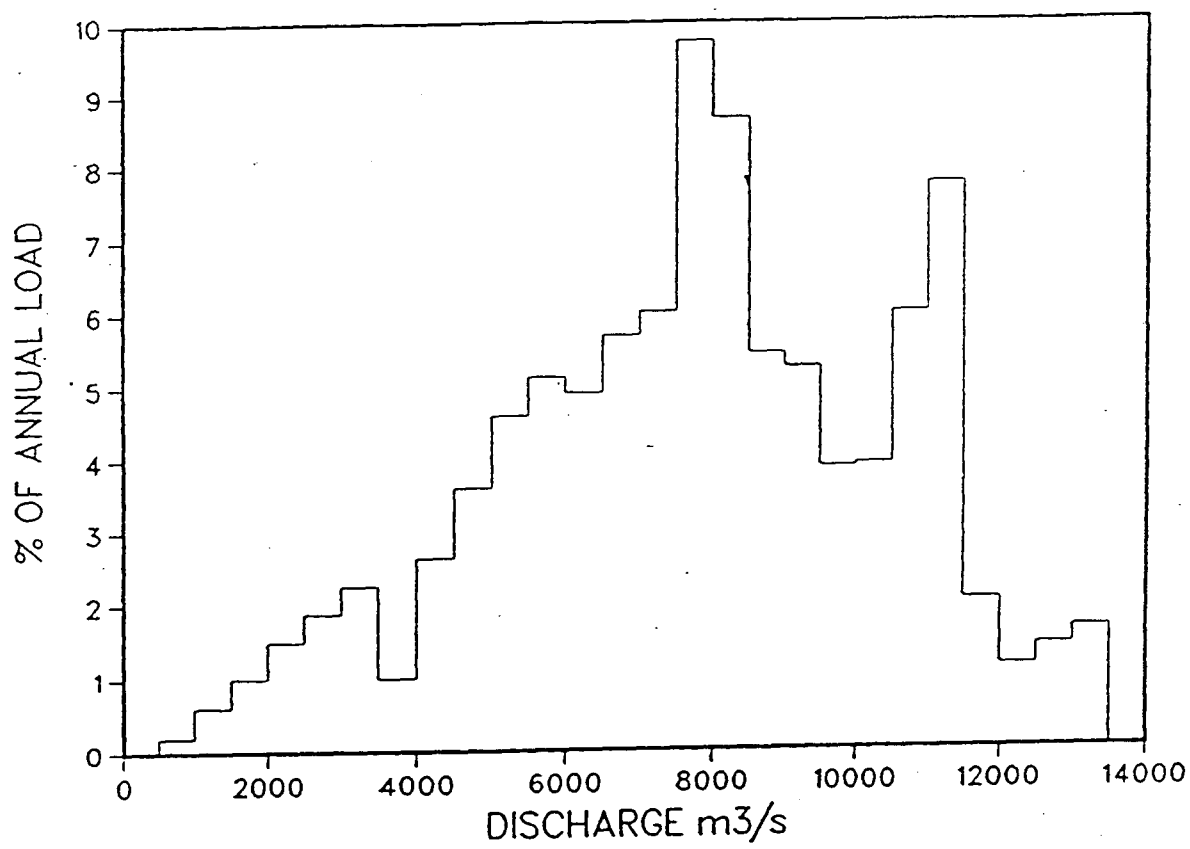


Figure 9.7 Fraction of annual bed load transported by various discharge ranges

accounted for the largest fraction of the total bedload transport over the 16 year period. Discharges over  $10,000 \text{ m}^3/\text{s}$  (approximately a 5 year flood) accounted for 24% of the total bedload. Therefore, the relatively frequent, moderate flood flows account for the largest proportion of the total bedload transport. Based on the hydraulic measurements at the gauge site, the shear stress at a flow  $8,000 \text{ m}^3/\text{s}$  was found to be only about 50% higher than the critical shear stress required for mobilizing the surface armour (Parker et al., 1982). This illustrates that the greatest proportion of the transport takes place when the bedload movement is weakly established. At conditions near threshold, minor changes in the state of the bed (such as the surface size distribution, extent of imbrication) can induce very large relative changes in the transport rate. Therefore, for most of the annual load, the bedload transport rates will not show a very systematic relation with local hydraulic conditions.

#### **9.1.5 Estimation of Bed Load by Formulae**

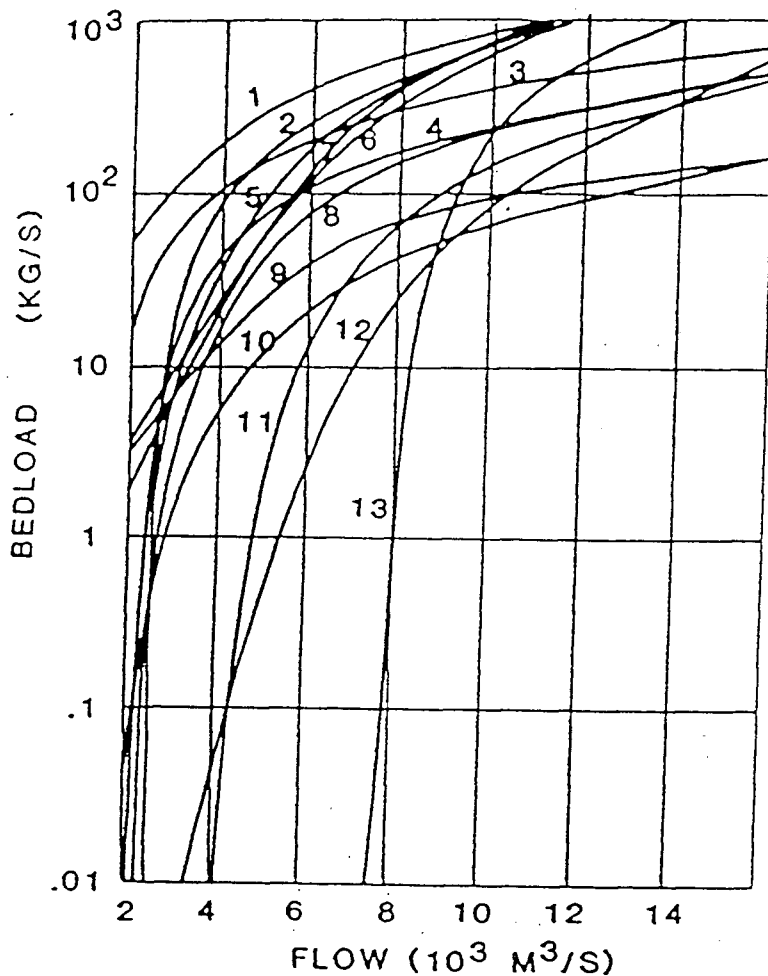
Two earlier studies investigated the feasibility of estimating the bed load transport at Agassiz by using sediment transport equations. These studies compared the measured and predicted transport rates (Mannerstrom and McLean, 1985) and assessed the limitations to theoretical predictions that may arise due to the sensitivity of the equations and error propagation (McLean, 1985). Since these studies have been published previously, the results of this work will be discussed only briefly.

The transport calculations utilized hydraulic data from WSC's hydrometric measurements at the Agassiz gauging station. Estimates of water surface slope and bed material size were based on the measurements described in Chapter 5.

A comparison of bed load formulae predictions with field measurements is shown in Figure 9.8. For flows above  $8,000 \text{ m}^3/\text{s}$  the predictions range over one order of magnitude. Below  $8,000 \text{ m}^3/\text{s}$  the range of predictions was even greater, reflecting the extreme sensitivity of most equations near threshold conditions.

A FORTRAN program was written to compute the annual loads in the period 1966 to 1986 when daily discharge measurements are available. This involved reading the daily discharges from a WSC data tape, estimating the hydraulic geometry using at-a-station regression relations, and then computing the corresponding daily load. The predicted annual loads ranged over an order of magnitude, from  $1.1 \times 10^5$  tonnes/year using the Meyer-Peter & Muller equation to over  $1.6 \times 10^6$  tonnes/year using the Ackers-White relation. Some of the relations that have been developed for use on gravel bed streams (Meyer-Peter & Muller, Einstein, Parker et al, 1982) produced estimates that ranged between  $1 \times 10^5$  and  $2 \times 10^5$  tonnes/year. However, the sensitivity of the predictions to small changes in data such as bed material size, or mean hydraulic geometry was found to produce some very large changes in transport rates. Therefore, it was concluded that the equations were potentially very unreliable without specific calibration data.





1. Einstein-Brown; 2. Du Boys-Straub; 3. Schoklitsch '34; 4. Schoklitsch '43; 5. Ackers-White; 6. Ackers-White-Day; 7. Ackers-Sutherland; 8. Meyer Peter; 9. Yalin; 10. Bagnold; 11. Parker; 12. Einstein (modified); 13. Meyer-Peter-Müller.

Figure 9.8 Range in bed load transport predictions at Agassiz from theoretical formulae using at-a-station hydraulic geometry

### 9.1.6 Analysis of Mission Bedload Data

Figure 9.9 shows the bedload rating curve that was established at Mission using data from 1968, 1972, 1974, and 1979. The Mission bed load data show considerable scatter; in 1974 the transport rates varied over a factor of five (i.e.  $\pm 67\%$ ) under virtually constant discharge conditions.

The scatter is greater than the expected  $\pm 25\%$  to  $\pm 40\%$  sampling errors associated with spatial and temporal variations in transport rate discussed in Section 9.1.3. This analysis implied that about half of the scatter on the bed load plots can be associated with measurement imprecision. Additional field studies would be required to explain the nature of the additional scatter.

The daily bed load transport rates at Mission were estimated from a single variable power law rating curve of the form:

$$G_{bi} = a * Q_i^d$$

The annual loads were computed by summing up the daily loads in each year. The annual loads averaged  $2.9 \times 10^5$  tonnes/year and ranged from only  $1.2 \times 10^5$  tonnes/year in 1978 to  $6.6 \times 10^5$  tonnes/year in 1972.

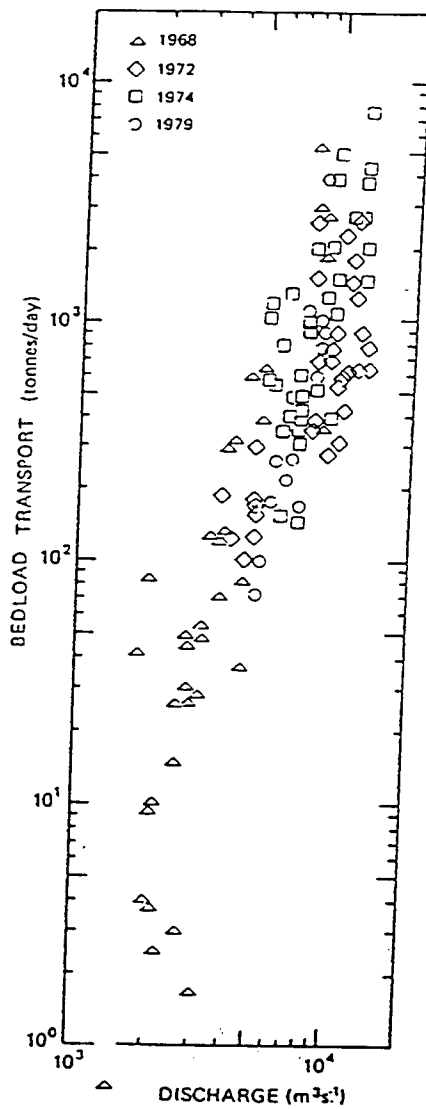


Figure 9.9 Bed load rating curve at Mission hydrometric station, 1968 to 1979

Table 9.1 lists the annual bed load transport rate by size fraction. These results were computed by applying the average bed load size distribution data to the annual bed load estimates. Figure 9.10 shows the average particle size composition from all bed load samples that have been collected at Mission using the Arnhem sampler.

The annual gravel transport rate (load coarser than 2 mm) past Mission amounts to only 3,000 tonnes/year or about 2% of the gravel load at Agassiz. Most (75%) of the bed load at Mission consists of medium sand between 0.25 to 0.50 mm.

## 9.2 The Suspended Sand Load

### **9.2.1 Analysis of Mission data**

So far the main part of this study has focused on gravel bed load transport. This is justified since over most of the study reach, the suspended load (including the sand) can be considered as wash load. However, at some point in the reach, presumably near the start of the sand bed reach at Sumas Mountain, a portion of the sand load will begin to behave as bed material load. In this sand bed reach the bed material load will be made up of two components - the sediments moving strictly as bed load (in the form of dunes or sand waves) and suspended bed material load which travels by intermittent suspension and saltation near the bed. This bed material load will be composed mainly of sand. In fact, a detailed review of all bed material samples from the sand bed portion of the river shows that there is virtually no sediments finer

Table 9.1

## Estimated Annual Bed Load at Mission

loads by grain size fraction (tonnes/year)

Year	0.125 mm 0.25 mm	0.25 mm 0.5 mm	0.5 mm 1.0 mm	1.0 mm 2.0 mm	2.0 mm 4.0 mm	Total
1966	88000	185000	24000	2000	1000	300000
1967	159000	332000	42000	4000	2000	539000
1968	115000	240000	31000	3000	1000	390000
1969	71000	148000	19000	2000	1000	241000
1970	44000	92000	12000	1000	1000	150000
1971	88000	185000	24000	2000	1000	300000
1972	195000	406000	52000	5000	2000	660000
1973	53000	111000	14000	1000	1000	180000
1974	133000	277000	35000	3000	2000	450000
1975	71000	148000	19000	2000	1000	241000
1976	133000	277000	35000	3000	2000	450000
1977	44000	92000	12000	1000	1000	150000
1978	35000	74000	9000	1000	0	119000
1979	44000	92000	12000	1000	1000	150000
1980	44000	92000	12000	1000	1000	150000
1981	53000	111000	14000	1000	1000	180000
1982	106000	222000	28000	3000	1000	360000
1983	50000	105000	13000	1000	1000	170000
1984	71000	148000	19000	2000	1000	241000
1985	88000	185000	24000	2000	1000	300000
1986	103500	216000	27900	2700	900	351000
Average	85167	178000	22757	2081	1138	289143

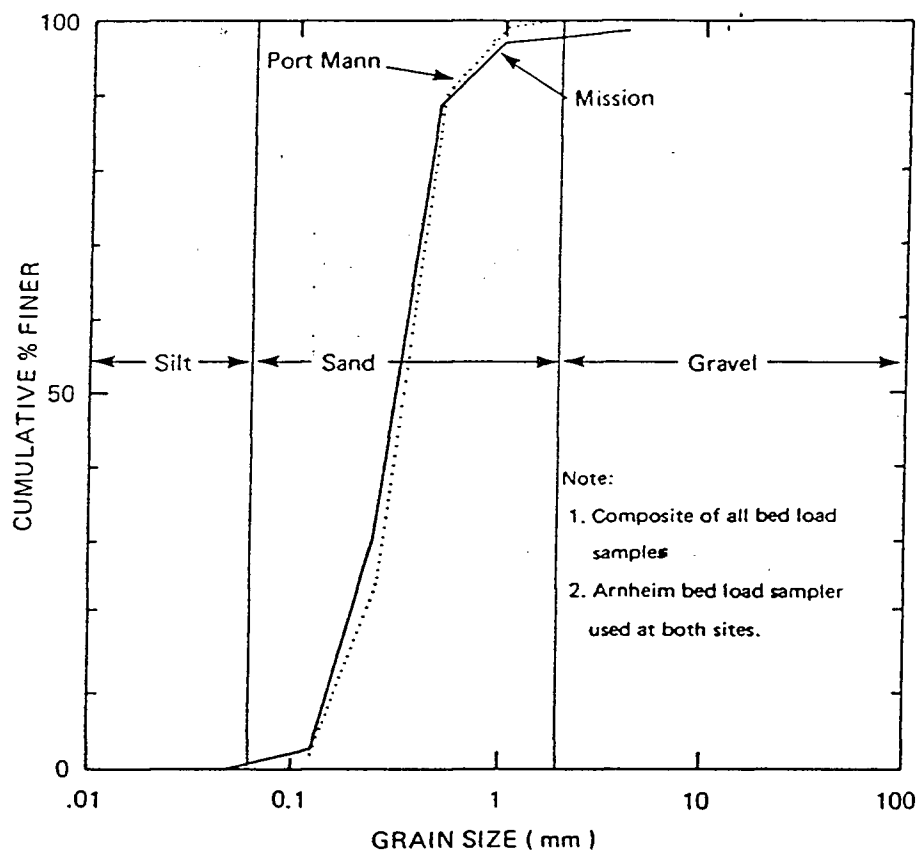


Figure 9.10 Average particle size distribution of bed load trapped at Mission

than 0.177 mm in the main channel of the Fraser River. This provides a reasonable choice for distinguishing the bed material load from the wash load in the sand bed portion of the river.

An approximate estimate of the river's annual suspended bed material load can be made by multiplying the long term mean total suspended load ( $17.7 \times 10^6$  tonnes/year at Hope) by the average fraction of the suspended load that is coarser than 0.177 mm (approximately 15%). This provides an estimated sandy bed material load of  $3 \times 10^6$  tonnes/year. However, the size distribution of the load can change appreciably with discharge and with the season due to the hysteresis effects noted previously. Therefore, any method of estimating the size distribution of the load should account for these factors. The approach used in this study is an extension of the methods that were presented in McLean and Church (1986).

First, the miscellaneous depth integrated particle size data collected by WSC were sub-divided into two fractions - a fine component consisting of clay, silt and very fine sand (0.063 - 0.125 mm), and a coarse component consisting of sand coarser than 0.125 mm. The rationale for using the 0.125 mm size fraction in the analysis is strictly operational convenience, since this size fraction is included on WSC's data tapes. A better choice would have been to use the 0.177 mm sieve break which was selected to distinguish the bed material load from the wash load. However, since this size fraction was not included on WSC's data tape some additional work would have been required to retrieve this information. A least squares regression program

was used to develop rating curves for the coarse fraction of the load. The rating curve expressed the concentration of the coarse fraction ( $C_{125}$ ) as a function of the recorded daily discharge ( $Q$ ) and the recorded total concentration ( $C_{tot}$ ). This relation was expressed as:

$$\text{Ln } C_{125} = a + b \cdot \text{Ln } Q + c \cdot \text{Ln } C_{tot}$$

The rating curve proved to be a good predictor of the coarse fraction of the load, providing a coefficient of determination ( $r^2$ ) of 0.89 and a standard error of 0.3 (Ln units). This standard error indicates that the actual concentration could range from 42 mg/l to 78 mg/l at a nominal value of 60 mg/l. An analysis of variance test showed that the daily discharge was the most important variable in the relation. However, the total concentration reduced the unexplained variance in the relation by 12% and was also found to be statistically significant. At first, it was thought that the influence of  $C_{tot}$  was spurious, since these values will include both the fine component and the coarse component of the load. This was tested by repeating the regression analysis by using the discharge and wash load concentration (fine component less than 0.125 mm) as the dependent variables. The regression equation in this case was:

$$C_{125} = a + b \cdot \text{Ln } Q + c \cdot \text{Ln } C_{wash}$$



An analysis of variance test confirmed that the wash load concentration has a statistically significant effect on the coarse fraction of the load. The relation showed that for the same discharge, higher wash load concentrations will be associated with higher coarse sand concentrations. A similar effect has been noted on the Missouri River (Shen et al, 1985).

The rating curve method was used to compute the sand load coarser than 0.125 mm in each month over the period 1966 to 1986. The monthly loads were then subdivided further into size fractions by using the monthly particle size data listed in Table 9.2. The load coarser than 0.177 mm was then interpolated between the 0.125 mm and 0.25 mm size fractions. The results of these calculations are tabulated in Table 9.3. The computations show that the mean annual suspended bed material load (coarser than 0.177 mm) has averaged  $2.84 \times 10^6$  tonnes/year over the period 1966 to 1986. The load has ranged from a high of  $7.3 \times 10^6$  tonnes/year in 1972 to a low of  $1.6 \times 10^6$  tonnes/year in 1983. Therefore, the suspended bed material load at Mission is approximately 10 times greater than the bed load.

Table 9.2

Average Monthly Size Distribution of the Suspended Load

Mission 1965 - 1986

<u>Month</u>	<u>Clay</u>	<u>Silt</u>	<u>&gt;.063</u>	<u>&gt;.125</u>	<u>&gt;.250</u>	<u>&gt;.50</u>	<u>&gt;1.0 mm</u>
March	22.0	61.0	17.0	4.0	0	0	0
April	22.7	62.7	14.6	4.6	0.7	0.1	0
May	16.5	56.9	26.7	12.9	4.7	1.2	0
June	14.1	45.4	40.6	25.5	11.8	3.5	0.3
July	16.0	46.2	37.7	25.2	12.8	4.4	0
Aug.	23.0	55.7	21.3	13.3	6.3	3.0	0
Sept.	21.7	60.3	18.0	7.3	2.7	0.7	0

Table 9.3

Mission Annual Suspended Load by Size Fraction

Tonnes/year

Year	Clay	Silt	0.063 mm 0.125 mm	0.125 mm 0.25 mm	0.25 mm 0.5 mm	0.5 mm 1.0 mm	1.0 mm 2.0 mm	Load > .125 mm	Load > .177 mm	Total
1966	3193239	9687333	2416234	2201851	1221193	534145	19446	3976635	2875709	19273441
1967	3742092	11591014	3124654	4115158	2428631	1010754	58391	7612934	5555355	26070694
1968	3352798	10218166	2582842	2591182	1498711	660061	22980	4772934	3477343	20926740
1969	2286037	6897813	1705985	1733445	920194	366043	18131	3037813	2171090	13927648
1970	1897260	5953992	1673774	1067649	631922	257214	17440	1974225	1440400	11499251
1971	1773990	6031324	1813957	4706323	2302057	881954	20989	7911323	5558160	17530594
1972	4204015	13104479	3554151	5531631	3180732	1306480	72179	10091022	7325210	30953667
1973	2055041	6365137	1632856	1210606	666224	279587	10884	2167301	1562000	12220335
1974	3824508	11734826	3076979	3409399	1987294	863734	41118	6301545	4596845	24937858
1975	1967092	5967168	1545994	1331563	794797	353263	16246	2495869	1829090	11976123
1976	3965609	12023131	2912497	3337441	1792611	834700	15684	5980436	4312720	24881673
1977	2666440	8015649	1995192	1035578	560398	252880	8977	1857833	1340045	14535114
1978	2194021	6674566	1754582	912903	522081	228336	10083	1673403	1216950	12296572
1979	2648110	8415200	2163030	986786	553145	232380	9610	1781921	1288530	15008261
1980	2064420	6072175	1391590	801385	409480	163720	5634	1380219	979530	10908404
1981	2127190	6572640	1656830	1135370	607820	255790	10730	2009710	1442030	12366370
1982	4125415	12633160	3344840	2943120	1723135	759990	32676	5458921	3987370	25562336
1983	1360185	4080960	1030555	893480	502760	215510	8950	1620700	1173960	8092400
1984	2130380	6289040	1620930	1213200	740155	336510	14584	2304449	1698110	12344799
1985	2388920	7489360	1942080	2169500	1132490	432415	21442	3755847	2671100	15576207
1986	2615000	8117830	2267245	2337900	1385180	551115	41465	4315660	3146710	17315735
Mean	2694370	8282617	2152705	2174546	1217191	513171	22745	3927652	2840393	17057344

### 9.2.2 Comparisons with Agassiz and Hope

As discussed in Section 4.3 the mean annual total suspended load at Hope, Agassiz and Mission is virtually identical. Figure 9.11 shows that the size distribution of the sand load is also virtually identical. This graph was prepared by computing the average size distribution from all suspended sediment samples that were collected in the month of June. This month accounts for the greatest sediment transport in the season (about 35%). This suggests that the annual suspended sand load is also nearly constant along the river. This was confirmed by repeating the sand load analysis presented in Section 9.2.1 using the data at Hope and Agassiz. The analysis showed that the annual suspended sand load at Agassiz averaged about 5% less than the load at Mission. This difference is within the expected error of the calculations. The results indicate that over a time scale of years to decades, all of the incoming sand load at Hope and Agassiz can be transported past Mission.

## SAND LOAD SIZE DISTRIBUTIONS – JUNE

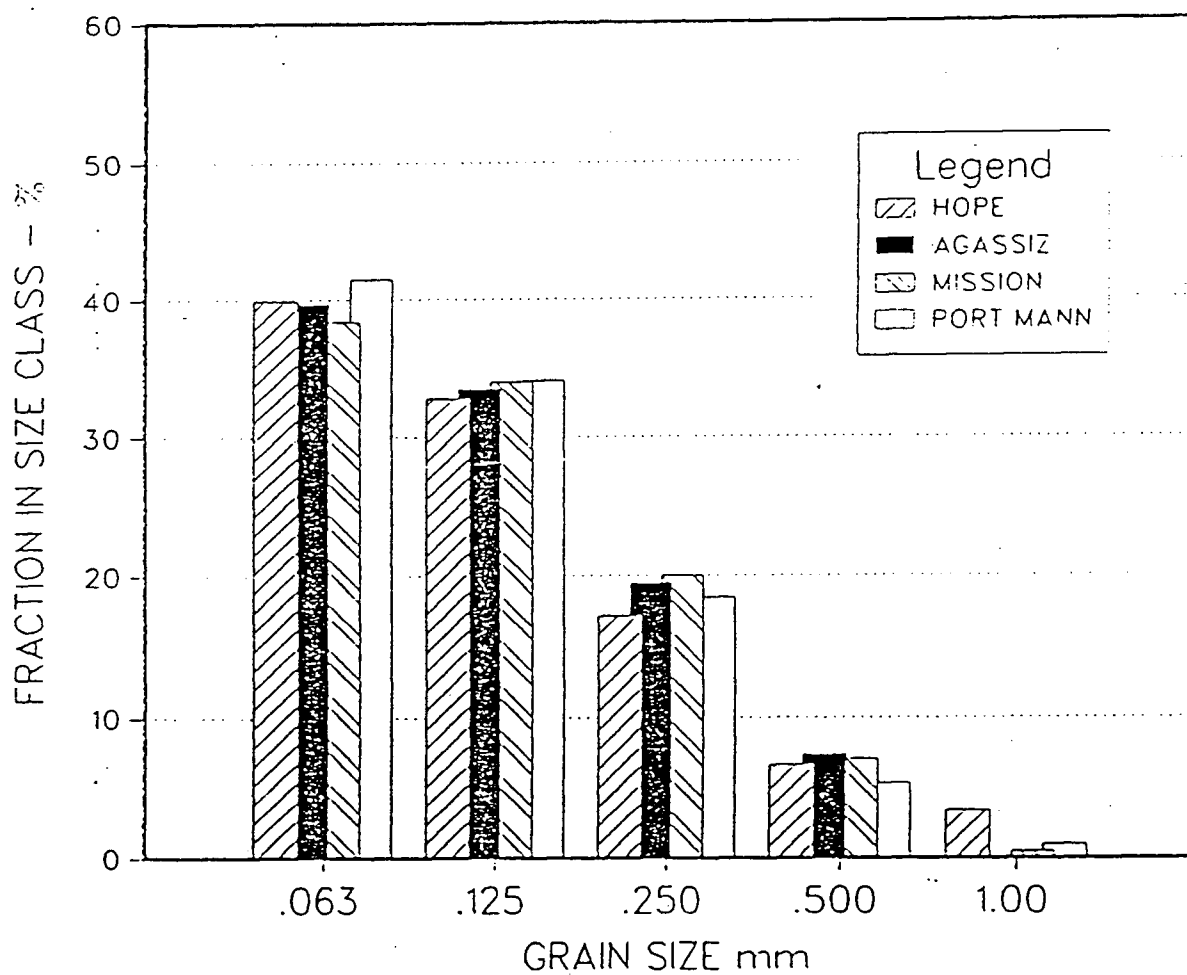


Figure 9.11 Average particle size distribution of depth integrated suspended sediment samples at Hope, Agassiz, Mission and Port Mann stations

## 10.0 COMPARISON OF BED LOAD ESTIMATES

### 10.1 Objectives

The purpose of this section is to draw together the results from the various methods that were used to estimate the annual gravel loads. An assessment is provided on the reliability of each method, on the data requirements; and on the amount of information that was generated. The comparisons also provide a means for developing a consensus on the best combination of techniques that should be employed in future investigations.

In this study, five different sets of calculations were performed to provide estimates of the annual gravel transport rate in the wandering reach between Peters Island and Sumas Mountain. These methods included:

- analyzing hydrographic surveys to produce a long term sediment budget;
- analyzing historical planimetric data to estimate rates of morphologic change and sediment transfer scales;
- using planimetric data in special test reaches and applying Neill's model of meander progression;
- analyzing direct measurements of gravel bed load transport from trap samples via rating curves;
- estimating the bed load from theoretical formulae.

The lower Fraser River is one of only a few rivers in the world where such a wide variety of techniques can be tested and compared. Therefore, it is hoped that the results of this assessment will be useful for developing procedures that can be applied on other rivers that do not have such an extensive historical record.

## 10.2 Assessment of Methods

### **10.2.1 Reliability of the Methods**

Table 10.1 compares the estimated mean annual gravel loads from the various methods. The comparisons have been made at two locations - the Rosedale bridge reach, and the reach between Carey Point and Chilliwack Mountain. One feature of these comparisons that makes interpretation of the results difficult, is that the time periods of the calculations vary. For example, the sediment budget was developed only for the period between 1952 and 1984, since the necessary survey data were available only for these dates. This may introduce some bias into the comparisons. In spite of this problem, the methods provide surprisingly consistent estimates of the long term gravel transport. For example, the estimated gravel load in the Rosedale bridge reach ranged between a high of  $1.5 \times 10^5 \text{ m}^3/\text{year}$  using the estimated bank erosion quantities at Herrling Island in Neill's approach to a low of  $7.8 \times 10^4 \text{ m}^3/\text{year}$  using the observed morphologic changes between the bridge and Carey Point. The estimates from the sediment budget and the results of the direct trap sampler

Table 10.1

Comparison of estimated gravel loads by different methods

Method	Period	Gravel transport rate $10^5 \text{ m}^3/\text{year}$	
		at Rosedale bridge	below Carey Point
sediment budget	1952-1984	1.2	.5
morphologic	1943-1971	.8	.4
Neill	1967-1987	1.5	---
WSC samples	1967-1984	1.0	---
Formulae:	1967-1984		
Ackers-White		1.0	---
Einstein		1.0	---
Meyer-Peter & Muller		0.7	---

Note: The Ackers - White and Meyer-Peter & Muller formulae were calibrated by adjusting the threshold for transport to agree with bed load sampler observations



measurements fell within this range. There is also reasonably close agreement between the sediment budget estimates and the morphologic estimates downstream of Carey Point. On the basis of these results it is reasonable to conclude that the long term annual gravel transport rate in the Rosedale reach has averaged approximately  $1 \times 10^5 \text{ m}^3/\text{year}$  and the average load between Carey Point and Chilliwack Mountain has averaged about  $5 \times 10^4 \text{ m}^3/\text{year}$ .

The issue of assessing the reliability of the estimates is difficult because there are sources of bias and imprecision in all of the calculations. For example, in the sediment budget analysis the nominal precision of the net channel changes (measured in terms of a standard error) was about  $85,000 \text{ m}^3$  for each 2 km long sub-reach. This means that apparent changes in transport rate within the reach of less than  $3,000 \text{ m}^3/\text{year}$  would not be significant. However, the sediment budget approach relies on a sequence of calculations where the incoming load from one sub-reach becomes the outflowing load from the next upstream reach. Therefore, systematic errors can be propagated through a sequence of reaches and induce biases in the computations that are much greater than the nominal precision. The reliability of the sediment budget is as good as its weakest link. In this case the greatest potential source of bias was related to the estimates of gravel mining. If the historical estimate of gravel extraction was underestimated by a factor of two (which is not unreasonable) then the annual load at Rosedale bridge will be underestimated by a factor of about 25%. However, near Carey Point where the load is substantially lower than at Agassiz, the load would be underestimated by at least 50%.

The main limitation associated with the morphologic methods is also related to introduction of biased results, rather than imprecision in estimating erosion volumes. The main source of error in this method is in assessing the sediment step lengths along the channel. These step lengths have a reasonably well defined geometrical representation on a regularly meandering stream but are ill defined on a wandering reach. Furthermore, on Fraser River the definition of step length seems to vary according to the time scale over which the channel changes are observed. Over short periods, (a few years) the dominant step lengths are related to major active bar features that are spaced along the channel. Over longer periods (years to decades) the step lengths are associated with major island features or deposition zones in the channel.

Furthermore, it is likely that in many low sinuosity reaches, the "throughput load" will represent an important component of the total bed load transport rate. As a result, the transport rate calculated from a morphologic method will represent only a lower bound of the total transport.

The main limitation of Neill's approach is that in the wandering reach there are only limited situations where a regular, downstream meander progression developed. In addition, since this approach is a morphologic method, it will provide only a lower bound of the total bed load transport rate.

The main limitation with the direct trap sample measurements is related to the very high temporal and spatial variability of bed load transport when observed over relatively short time scales. The replicate sampling program at Agassiz in 1985 demonstrated that the sampling effort would have to be much greater than in the past in order to achieve even a relatively low accuracy. For example, even if the sampling effort were tripled (from 15 samples per cross section to 45 samples per cross section), the coefficient of variation of the daily load would decrease only from 60% to 40%. The precision of the annual load estimates will depend on whether a reliable sediment rating curve can be developed. This is likely only if a relatively large number of samples can be collected over a number of years. Rating curves developed from a single year of measurements were not usually transferrable to other years.

The main limitation of the bed load formulae was in the sensitivity of the predictions to the input parameters and the wide variation in results that was obtained from the different equations. Based on these findings, it is doubtful that a reliable estimate could be made from transport formulae alone, without using other methods for verification and calibration. One approach that seems promising is to adjust the threshold conditions in the formulae to reproduce the observed threshold conditions determined from bed load sampling. Using this strategy, the Ackers-White formula provided longterm transport estimates that agreed closely to the results from the other methods (Table 10.1). The Meyer-Peter and Muller formula and Einstein bed load equation also provided comparable results.

### 10.2.2 Appropriateness of the Methods

It is useful to consider the generality and appropriateness of each method. There are three issues that arise in the sediment budget approach. First, the sediment budget method can be used to compute incoming sediment loads only if a boundary condition can be specified. If this boundary condition is not specified then only relative changes in transport rate (or net sediment transfers between floodplain and channel zones) can be evaluated. This type of information may still provide useful results for assessing rates of channel change, or rates of habitat creation and destruction.

The second issue relates to the appropriate time scale for developing a sediment budget. In most applications this time scale will be in the order of years to decades. The 32 year period on the Fraser River is probably longer than the optimum period. However, this time scale is at least in the same order as the scale for many of the major channel processes that develop on a river such as Fraser River. This is also the type of time scale that is of most interest in engineering and resource management issues. For example, the long term rate of gravel aggradation (or alternately, the rate of habitat re-construction) is probably a more important parameter to most river managers than a measure of the transport rate at any one instant in time.

The final issue that may limit the sediment budget method is that it has relatively large data requirements. For example, the hydrographic surveys in 1952 and 1984 required substantial field efforts and additional office time for data reduction and analysis. However, future advance in survey technology, and terrain modelling should reduce these efforts somewhat.

In general, the same types of issue that were discussed above are associated with the morphologically based estimates. The main difference is that these morphologic methods do not have such onerous data requirements as a complete sediment budget. In addition, since historical planimetric data is readily available in Canada (a 30 year air photo record of channel changes is available on virtually every major river in British Columbia) "hindcast" calculations can be made using the available information on hand. This advantage makes the morphologic methods by far the most generally applicable.

During the inception of this study, the trap sample measurements were believed to be the most important data that were available for assessing bed load movement on the river. However, issues related to measurement reliability, sampler calibration, as well as the tremendous spatial and temporal variability of bed load soon made it obvious that the bed load measurement program on the Fraser River was of limited usefulness except as a check on the other methods. The main limitations with the data were the low precision of the measurements and the fact that there was only a poor correlation between the load and the hydraulic conditions at the measurement

site. This latter problem makes it very difficult to integrate the short term transport measurements (hourly or daily) to determine the longer term loads (years or decades) that are required in most investigations. This implies that the time scale for the measurements is too short compared to the time scale of the processes and sediment movement patterns. It should be emphasized that the bed load data on Fraser River are as comprehensive as on any river in North America, and certainly far better than on any other large river in Canada. Therefore, the possibilities for interpretation of the data from other streams will probably be far more limited than on the Fraser River.

## 11.0 CONCLUSIONS

1. Three main "styles" of channel instability can be identified on the wandering gravel bed reach of lower Fraser River. Identifying morphologic features that are associated with these erosion patterns provides a means for diagnosing future occurrences of channel change.

One of the most frequent patterns of instability develops in sinuous meandering distributary channels around more stable islands or lateral bars. After these bends develop, the channel may shift very abruptly, either by forming a chute cutoff or by developing a new distributary channel with a lower sinuosity. It was found that the ratio of the radius of curvature of the bend to the distributary channel width provided a means for assessing the inception of rapid instability.

A second style of channel instability develops below local distributary channel avulsions which scour out a "slug" of gravel sediment. This sediment is deposited immediately downstream and travels through the reach as a low amplitude gravel wave or sheet. These wave-like disturbances pass through other more stable bar features (such as point bars or lateral bars) and may induce local changes in flow alignment which can initiate other sequences of erosion and deposition.

A third style of channel instability develops in response to flow re-alignment due to changes in upstream channel controls. The re-alignment of these upstream controls may be related to growth of lateral bars, or to changes in hydraulic geometry as a result of scour or erosion.

2. The erosion of sediments from floodplain and islands is part of an exchange process between sediment that is temporarily stored in inactive zones and the active channel zone. The distance sediment travels from the point where it enters the active channel to the point where it returns back into storage represents the "step length". The characteristic step length on a wandering river was inferred from the spacing of major morphologic features such as lateral bars, islands and other deposition zones. This length scale on the Fraser River was estimated to be in the order of 3 to 5 km.
3. Patterns of erosion and deposition in the wandering reach of the lower Fraser River evolve over periods of years to decades, which reflects the time scale for the sediment transfers and transport processes along the river. Channel changes may not show any correlation with short term flow conditions or local hydraulic parameters. This implies that the most appropriate time scale for assessing sedimentation processes and channel changes is also measured in years or decades.



4. Four different methods were used to estimate the annual gravel transport along the river. These approaches included using direct measurements with bed load traps, developing a sediment budget and relating changes in transport to the volumetric changes in the reach determined by survey, measuring planimetric channel changes from air photos and applying a simple morphologic model to relate sediment transport and sediment transfers in a reach, and finally using theoretical bed load formulae. The long term gravel transport rate below Rosedale was estimated to average in the order of  $1.5 \times 10^5 \text{ m}^3/\text{year}$ . The reliability and precision associated with each method is summarized in Chapter 10.
5. The study has demonstrated that the sediment budget and morphologically based estimates are the most generally applicable and most practical alternatives that are available for estimating long term gravel transport rates on wandering rivers. This is because the time interval that was used in these methods is comparable to the time scale of the major processes that govern the transport processes. In other words, more can be learned about the long term bed load transport processes along a river like the Fraser by examining the patterns of erosion and deposition that have occurred in the past than from an analysis of short term transport measurements at a single cross section. This is because at very short time scales, the patterns of sediment transport may not show any systematic relation with the local flow conditions. Furthermore, sediment transport measurements at a single point may not

Furthermore, sediment transport measurements at a single point may not reveal adequately the sedimentation phenomenon along the river.

6. There are three major bed load transport zones in the 30 km reach between the Rosedale bridge and Sumas Mountain:
  - a deposition zone between Rosedale and Carey Point in which gravels have been accumulating in the form of islands and mid-channel bars;
  - a transport zone, in between Harrison River and Chilliwack Mountain, where the net change in sediment storage along the reach has been approximately zero over the last 30 years;
  - a major deposition zone, between Chilliwack Mountain and Sumas Mountain, where channel aggradation has been occurring.
7. Two noticable morphologic changes occur in the depositional zone below Chilliwack Mountain. First, the river's slope decreases from approximately  $2 \times 10^{-4}$  to  $8 \times 10^{-5}$ . Secondly, the channel changes very abruptly from a predominantly gravel-bed to a sand-bed river. These features, and the observed aggradation all indicate that a "wedge" of gravel is slowly accumulating in this reach and slowly prograding downstream.

## REFERENCES

- Ackers, P. and White, W.R., 1973: Sediment Transport; New Approach and Analysis. Journal of Hydraulics Division, American Society of Civil Engineers, Vol. 99, HY11, p. 2041-2060.
- Andrews, E.D., 1983: Entrainment of Gravel from Naturally Sorted River Bed Material. Geological Society of American Bulletin, Vol. 94, p. 1225-1231.
- Armstrong, J., 1981: Post-Vashon Wisconsin Glaciation, Fraser Lowland, British Columbia, Geological Survey of Canada, Bull. 322. 34 pp.
- Bagnold, R., 1977: Bedload Transport by Natural Rivers, Water Resources Research 13, p. 303-312.
- Bluck, B.J., 1979: Structure of Coarse Grained Braided Stream Alluvium. Trans. Royal Society Edinburgh, 70, p. 181-221.
- Bolin, B. and Rodhe, H., 1973: A note on the concept of age distribution and transit time in natural reservoirs. Tellus 25, p. 58-62.
- Brayshaw, A., 1983: Bed Microtopography and Entrainment Thresholds in Gravel Bed Rivers, Geological Society of American Bulletin, V. 96, p. 218-223.

Church, M., 1972: Baffin Island Sandurs: A Study of Arctic Fluvial Processes. Geological Survey of Canada Bulletin, V. 216, 208 pp.

Church, M. and Jones, D., 1982: Channel bars in gravel-bed rivers. in Hey, R., Bathurst, J. and Thorne, C., Gravel Bed Rivers. Chichester, J. Wiley: pp 291-338.

Church, M. 1985: Bed load in gravel-bed rivers: observed phenomena and implications for computations. Canadian Society for Civil Engineering, 7th Hydrotechnical Conference, Saskatoon, P. 17-38.

Church, M. McLean, D.G. and Wolcott, J., 1987: River bed gravels: sampling and analysis. in Thorne, C., Bathurst, J., and Hey, R., editors, Sediment Transport in Gravel-Bed Rivers. International Workshop on Problems of Sediment Transport in Gravel-Bed Rivers. Colorado State University, Fort Collins, Chichester, Wiley, p. 49-89.

Church, M. Miles, M. and Rood, K., 1987: Sediment Transfer Along Mackenzie River: A Feasibility Study. Sediment Survey Section, Water Resources Branch, Environment Canada Report.

Church, M., Kellerhals, R. and Day, T., 1989: Regional clastic yield in British Columbia. Canadian Journal of Earth Sciences.

Clague, J.J., Luternauer, J.L., 1982: Late Quaternary Sedimentary Environments, Southwestern British Columbia, Excursion 30A: Eleventh International Congress on Sedimentology, McMaster University, Hamilton, Ontario. 167 pp.

Colby, B., 1957: Relationship of unmeasured sediment discharge to mean velocity. Transactions of the American Geophysical Union, vol. 38 no. 5, p. 707-717.

Csoma, J., 1973: Reliability of bed-load sampling. International Association for Hydraulic Research, International Symposium on River Mechanics, Bangkok, vol. B9, P. 97-107.

Davis, R., Foote, F., Anderson, J., Mikhail, E., 1983: Surveying, Theory and Practice. McGraw Hill Books, 983 pp.

de Vries, M., 1973: On measuring discharge and sediment transport in rivers. International Association for Hydraulic Research, Seminar on Hydraulics of Alluvial Streams, New Delhi, P. 1-9.

Dietrich, W.E. and Dunne, T. 1978: Sediment Budget for a small Catchment in Mountainous Terrain. Z. Geomorphol. Suppl. 29: p. 191-206.

Dietrich, W., Dunne, T., Humphrey, N. and Reid, L. 1982: Construction of sediment budgets for drainage basins. In Sediment Budgets and routing in Forested Drainage Basins. ed. Swanson, F., Janda, R., Dunne, T., and Swanston, D., United States Department of Agriculture Forest Service, Report PNW-141, p.5-23.

Durette, Y. and Zrymiak, P. 1978: HYDAC 100 - An Automated System for Hydrographic Data Acquisition and Analysis. Dept. of Environment, Inland Waters Directorate, Water Resources Branch, Technical Bulletin 105, 44 pp.

Ehrenberger, R., 1931: Direct bed-load measurements on the Danube at Vienna and their results to date. Die Wasserwirtschaft, Issue 34, p. 1-9, Translation No. 39-20, U.S. Corps of Engineers Waterways Experiment Station, Vicksburg.

Einstein, H.A., 1937: Bed Load Transport as a Probability Problem. Ph.d. Thesis in Sedimentation, Symposium to Honour Professor H.A. Einstein, edited by H.W. Shen, Fort Collins, Colorado, 99pp.

Einstein, H.A., 1950: The Bed-load Function for Sediment Transport in Open Channel Flows. Technical Bulletin 1026, U.S. Dept. of Agriculture, Soil Conservation Service, Washington, D.C., 70 pp.

- Engel, P., 1982: Characteristics of the WSC basket type sampler. Environmental Hydraulics Section, Canada Centre for Inland Waters, H81-3345, 19 pp.
- Engel, P., 1983: Sampler efficiency of the VUV bed-load sampler. Environmental Hydraulics Section, Canada Centre for Inland Waters, H82-377, 12 pp.
- Eriksson, E., 1963: Atmospheric Tritium as a tool for the study of certain hydrologic aspects of river basins. *Tellus* 15(3) p. 303-308.
- Ferguson, R., 1986: River loads underestimated by rating curves. *Water Resources Research*, 22, p. 74-76.
- Fraser River Board, 1963: Final Report on Flood Control and Hydro-Electric Power in the Fraser River Basin, Victoria, B.C., 106 pp.
- Friedkin, J.F., 1945: A Laboratory Study of the Meandering of Alluvial Rivers. Water Ways. Engineering, Experiment Station, Report 40 pp.
- Fulton, R.J., 1969: Glacial Lake History, Southern Interior Plateau, British Columbia,. Geological Survey of Canada, Paper 69-37, 14 p.
- Gibbs, C., 1973: Model study of the basket type bed-load sampler. M.Sc. thesis, University of Alberta, Dept. of Civil Engineering, Edmonton.

- Gibbs, C. and Neill, C.R., 1973: Laboratory testing of a model VUV bed-load sampler. Research Council of Alberta open file report 1973-29.
- Gomez, B. and Church, M., 1989: An Assessment of Bed Load Sediment Transport Formulae for Gravel Bed Rivers. Water Resources Research, Vol. 25, No. 6, p. 1161-1186.
- Griffiths, G. and Sutherland, A., 1977: Transport of Gravel Bed Load by Flood Waves. New Zealand Engineering, 15 January, p. 10-13.
- Hamamori, A., 1962: A Theoretical Investigation on the Fluctuations of Bed-Load Transport. Delft Hydraulics Laboratory Report R4.
- Hickin, E., 1974: The Development of Meanders in Natural Channels. American Journal of Science, 274, p. 414-442.
- Holland, S., 1976: Landforms of British Columbia, A Physiographic Outline. British Columbia Department of Mines and Petroleum Resources, Bulletin 48, 135 pp.
- Hubbell, D., 1964: Apparatus and techniques for measuring bed-load. U.S. Geological Survey Water Supply Paper 1748, 74 pp.



Hubbell, D., 1987: Bed-load sampling and analysis. in Thorne, C., Bathurst, J., and Hey, R., editors, Sediment Transport in Gravel-Bed Rivers, International Workshop on Problems of Sediment Transport in Gravel-Bed Rivers, Fort Collins, Chichester, Wiley, p. 89-105.

Hudson, H., 1981: Hydrology and sediment transport of the Elbow River Basin, S. W. Alberta. thesis presented to the University of Alberta, at Edmonton, Alberta, in partial fulfillment for the degree of Doctor of Philosophy.

Hydrologic Engineering Centre, 1977: HEC-6 Scour and Deposition in Rivers and Reservoirs. U.S. Army Corps of Engineers. Water Resources Support Center.

International Standards Organization, 1977: Liquid Flow measurement in open channels-bed material sampling. ISO 4364 - 1977(E).

Johnston, W.A., 1921: Sedimentation of the Fraser River Delta. Geological Survey of Canada Memoir 125, 46 pp.

Keller, E.A. and Melhorn, W.N., 1978: Rhythmic Spacing and Origin of Pools and Riffles. Geological Society of America Bulletin Vol. 89, p. 723-730.

Kellerhals Engineering Services, 1987: Effects of Gravel Mining of the Salmonid Resources of the Lower Fraser River. Consulting report to Department of Fisheries and Oceans, Habitat Management Division, New Westminster, 43pp.

Kellerhals, R., 1984: Review of sediment survey program, Lower Fraser River British Columbia. Consulting report to Sediment Survey Section, Water Survey of Canada, 36 pp.

Kellerhals Engineering Services Ltd., 1985: Sediment in the Pacific and Yukon Region: review and assessment. Consultant report to Environment Canada, Inland Waters Directorate, IWD-HQ-WRB-SS-85-8, 250 pp.

Kellerhals, R., Church, M.A. and Bray, D., 1976: Classification and Analysis of River Processes. American Society for Civil Engineers, Journal of the Hydraulics Division, Vol. 102, HY7, p. 813-829.

Kellerhals, R., Neill, C. and Bray, D., 1972: Hydraulic and Geomorphic Characteristics of Rivers in Alberta. Research Council of Alberta, River Engineering and Surface Water Hydrology, Branch Report 72-1, 52 pp.

Kellerhals, R. and Bray, D., 1971: Sampling Procedures for Coarse Fluvial Sediments. American Society of Civil Engineers. Journal of the Hydraulics Division, Vol. 97, No. HY8, P. 1165-1180.

- Kidd, G.J., 1953: Fraser River suspended sediment survey: interim report for the period 1949-1952. Dept. of Lands and Forests, Water Rights Branch, Water Resources Division, Province of British Columbia, 35 pp.
- Krumbein, W.C. and Pettijohn, F.J., 1938: Manual of Sedimentary Petrology, New York, 549 pp.
- Laronne, J.B. and Carson, M., 1976: Inter-relationships between Bed Morphology and Bed Material Transport for a Small Gravel Bed Channel. Sedimentology, Vol. 23, p. 67-85.
- LaSalle Hydraulic Laboratories Ltd, 1967: Fraser River Improvements, Hydraulic Model Studies of the Carey's Point-Rosedale Reach, unpub. report to Department of Public Works, 40 pp.
- Leopold and Wolman, 1957: River Channel Patterns: Braided, Meandering and Straight. United States Geological Survey Professional Paper 282-B. 73 pp.
- Lewin, J., 1976: Initiation of bed forms and meanders in coarse-grained sediment. Bulletin of the Geological Society of America, 87(2), p. 25-36.
- Mannerstrom, M. and McLean, D.G., 1985: Estimating bed-load in the Lower Fraser River. Canadian Society for Civil Engineering, 7th Hydrotechnical Conference, Saskatoon, Proceedings Vol 1B p. 97-116.

Mathews, W. H. and Shephard, F., 1962: Sedimentation of Fraser River Delta, British Columbia. American Association of Petroleum Geologists Bulletin vol. 46, p. 1416-1443.

McLean, D., 1980: Flood control and sediment transport study of the Vedder River. M.A.Sc. thesis, University of British Columbia, Department of Civil Engineering, 185 pp.

McLean, D.G., 1985: Sensitivity Analysis of Bed Load Equations. Canadian Society for Civil Engineering, 7th Hydrotechnical Conference, Saskatoon, Proceedings Vol. 1B, p. 1-15.

McLean, D.G. and Church, M., 1986: A Re-Examination of Sediment Transport Observations in the Lower Fraser River. Water Resources Branch, Sediment Survey Section, Environment Canada, Report IWD-HQ-WRB-SS-86-6, 52 p.

McLean, D.G. and Mannerstrom, M., 1984: History of Channel Instability: Lower Fraser River, Hope to Mission. Water Resources Branch, Sediment Survey Section, Environment Canada, Report No. IWD-HQ-WRB-SS-85-2.

McLean, D.G., 1985: Lower Fraser River Survey, 1984: Agassiz - Rosedale bridge to Mission. Water Resources Branch, Sediment Survey Section, Environment Canada, Report No. IWD-HQ-WRB-SS-85-3, 39 pp.

- McLean, D.G. and Tassone, B., 1987: Discussion of: Bedload sampling and analysis International Workshop on Problems of Sediment Transport in Gravel-Bed Rivers. in Thorne, C., Bathurst, J., and Hey, R., editors, Sediment Transport in Gravel-Bed Rivers, Chichester, Wiley, p. 109-113.
- Meade, R. 1984: Wavelike Movement of Bedload Sediment, East Fork River, Wyoming. Environ. Geol. Water Science. Vol 7, No. 4, p. 215-225.
- Meyer, Peter E., 1937: Discussion of: Appareil pour le jaugeage du debit solide entraine sur le fond du cours d'eau by J. Smetana. International Association of Hydraulics Structure Research, Berlin, p. 113-116.
- Meyer-Peter, R. and Muller, R., 1948: Formulae for Bed Load Transport in Proc. 2nd Meeting International Association of Hydraulic Research, p. 39-64.
- Nanson, G. and Hickin, E., 1983: Channel Migration and Incision on the Beatton River. Journal of the Hydraulics Division, American Society of Civil Engineers, Vol. 109, No. 3, p. 327-383.
- Neill, C. R., 1971: River Bed Transport Related to Meander Migration Rate. American Society of Civil Engineers, Waterways, Harbours and Coastal Engineering Division, Vol. 97 WW4, p. 783-786.

Neill, C.R., 1973: Hydraulic and Geomorphic Characteristics of Athabasca River near Fort Assiniboine - the anatomy of a wandering gravel bed river. Alberta Research Council, Report REH/73/3, 23 pp.

Neill, C.R., and Galay, V.J., 1967: Systematic Evaluation of River Regime  
Journal of the Waterways and Harbours Division, American Society of Civil Engineers, Vol. 97, WW1, p 25-53.

Ning Chien, 1952: The Efficiency of Depth-Integrated Suspended Sediment sampling. Transactions, American Geophysical Union, vol. 33, No. 5, p. 693-698.

Novak, P., 1957: Bed-load meters - Development of a New Type and Determination of their Efficiency with the Aid of Scale Models. International Association of Hydraulic Research, 7th meeting, Lisbon vol. 1, 11 pp.

Parker, G. and Klingeman, P., 1982: On Why Gravel-Bed Streams are Paved. Water Resources Research, Vol, 18, No. 5, pp. 1409-1423.

Parker, G., Klingemen, P. and McLean, D.G., 1982: Bed-load and size distribution in paved gravel-bed streams. Journal of the Hydraulics Division, American Society of Civil Engineers, Vol. 108, HY4, p. 544-571.

- Popov, I.V., 1962: A Sediment Balance of River Reaches and its use for the Characteristics of the Channel Process. Soviet Hydrology, No. 3, p. 249-266.
- Pretious, E., 1972: Downstream Sedimentation Effects of Dams on Fraser River, B.C., Dept. of Civil Engineering, University of British Columbia, Water Resources Series, No. 6, 91 pp.
- Shaw, J. and Kellerhals, R., 1982: The Composition of Recent Alluvial Gravels in Alberta River Beds. Alberta Research Council, Alberta Geological Survey Bulletin 41, 151 pp.
- Shen, H.W., Mellema, W. and Harrison, A.S., 1978: Temperature and Missouri River stages near Omaha. Journal of the Hydraulics Division, American Society for Civil Engineers, HY1, p. 1-19.
- Simmons, G.E. and Buchanan, J., 1955: A Preliminary Report on Bank Erosion on the Lower Fraser River, British Columbia. Dept. of Lands and Forests, Water Rights Branch, Report 278, 53 pp.
- Sinclair, F.N., 1961: A History of the Sumas Drainage, Dyking and Development District, Chilliwack Historical Society, Chilliwack, B.C., 20 pp.

- Slaymaker, H.O., 1972: Recent Fluctuations in the Mean Discharge of the Fraser River in R. Leigh, ed., Contemporary Geography: Research Trends, B.C. Geographical Series, Number 16, Vancouver, p. 3-13.
- Smillie, G. and Koch, R., 1984: Bias in hydrologic prediction using log-log regression models. American Geophysical Union, Fall Meeting, San Francisco, 17 pp.
- Smith, D.G., 1983: Anastomosed Fluvial Deposits; Modern Examples 901X1100 in Western Canada in J.D. Collinson and J. Lewis, editors, Modern and Ancient Fluvial Systems, International Association of Sedimentologists, Special Publication No. 6, Oxford, p. 155-168.
- Sutherland, A.J. and Griffiths, G., 1984: Non-Steady Bed Load Transport by Translation Waves. International Association for Hydraulic Research.
- Swanson F., Janda, R., Dunne, T. and Swanson, D., 1982: Sediment Budgets and Routing in Forested Drainage Basins. United States Dept. of Agriculture, Forest Service, General Technical Report PNW-141.
- Tywniuk, N., 1972: Sediment budget of the Lower Fraser River. American Society for Civil Engineers, Thirteenth Coastal Engineering Conference, vol. 2, p. 1105-1122.



- Tywniuk and Stichling, 1973: Sedimentation Phenomenon on the Fraser River. IAHR International Symposium on River Mechanics, 9-12 Jan, Bangkok, Thailand Proc. A69-1 - A69-13.
- Walling, D. and Webb, B., 1981: The Reliability of Suspended Sediment Data. in Erosion and Sediment Transport Measurement, Proceedings of the Florence Symposium, International Association of Hydrological Sciences, Publication 133, p. 177-194.
- Western Canada Hydraulics Laboratories, 1978: Analysis of Federal Sediment Survey Data on the Lower Fraser River. Consulting report to Water Survey of Canada, Ottawa.
- White, W., Milli, H. and Crabbe, A., 1975: Sediment Transport Theories: A Review. Proc. of the Institution of Civil Engineers, Vol. 59, p. 265-292.
- Whitfield, P. and Schreier, H., 1981: Hysteresis in relationships between discharge and water chemistry in the Fraser River basin, British Columbia. Limnology and Oceanography, vol. 26, p. 1179-1182.
- Wolcott, 1984: The Grain Size Gap in Riverbed Gravels. M.Sc. Thesis, University of British Columbia, Department of Geography, 80 pp.

## **Appendix A**

### **HYDROGRAPHIC SURVEYS ALONG FRASER RIVER**

## **A1.0 INTRODUCTION**

This appendix describes the field survey of the Lower Fraser River that was completed in 1984. Hydrographic surveys were carried out between March 26 and September 20 over 46.5 km of the Lower Fraser River between the Agassiz-Rosedale bridge and the town of Mission (Figure A1 - A3). The purpose of the surveys was to produce topographic charts of the active channel portion of the river.

The main field work carried out during 1984 included:

- establishment of 110 horizontal and vertical control points along the river;
- establishment of 62 temporary mapping control points;
- completion of 38.5 km of main channel cross section surveys at 100 m to 200 m spacing using Environment Canada's automated HYDAC survey system;
- completion of 10 km of main channel cross section surveys at 250 m spacing using conventional sounding methods;
- completion of 18 km of sidechannel cross section surveys;
- mapping of exposed bars, islands and banklines along the river by conventional transit traverses.

Approximately one man-year of effort was spent completing this field work.

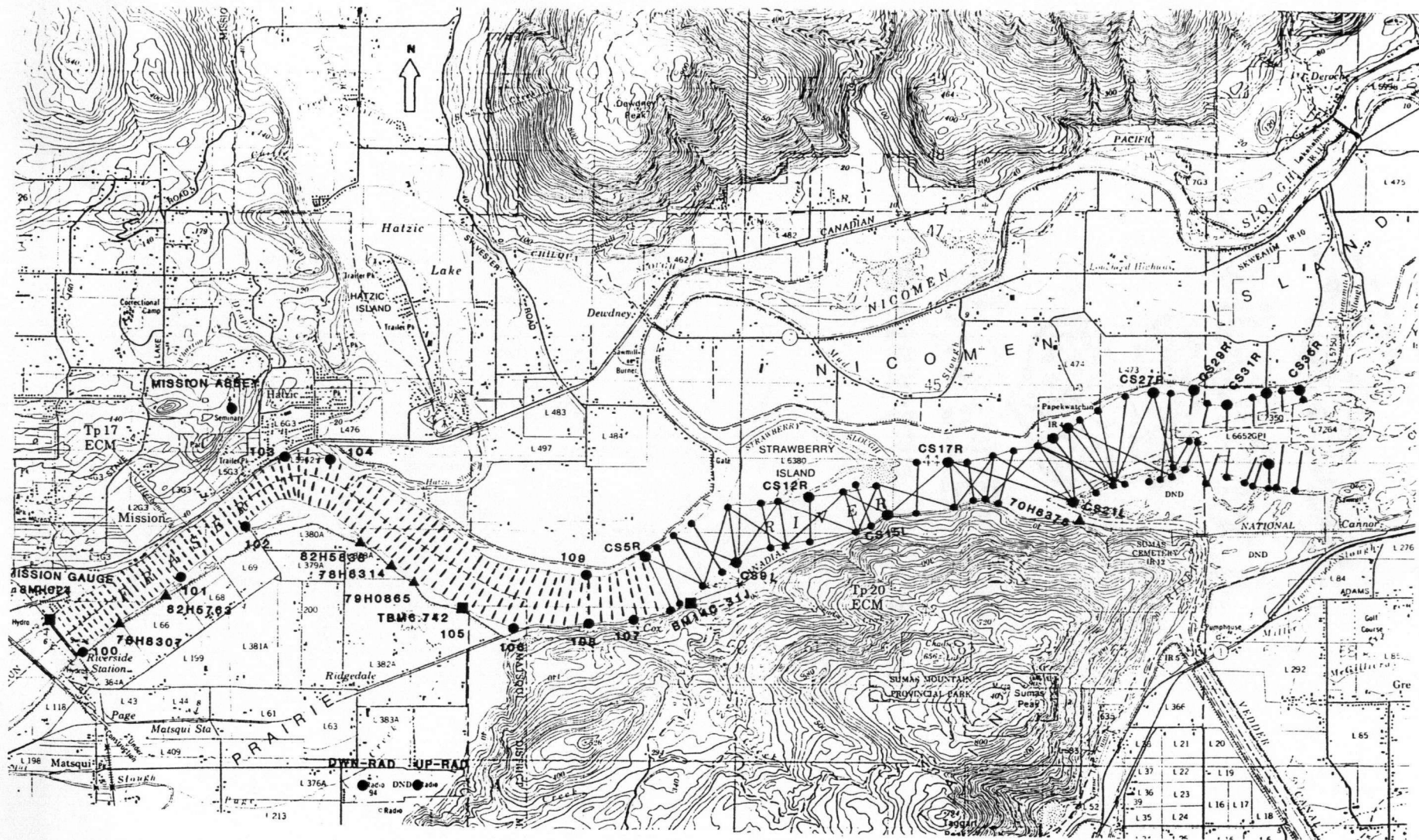
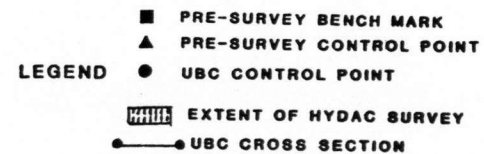


Figure A1: Extent of Survey on Lower Fraser River in 1984



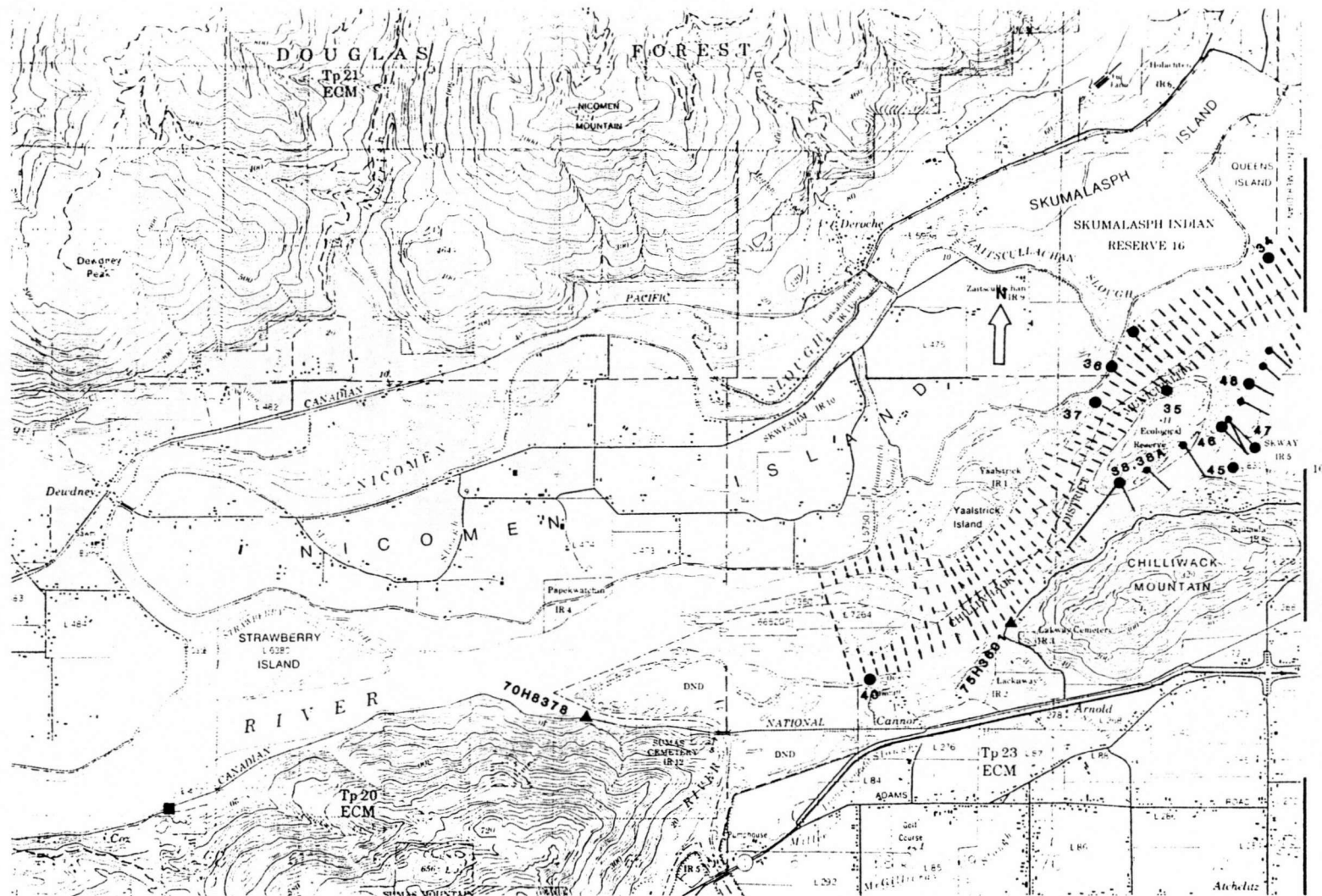
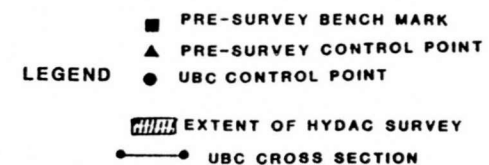
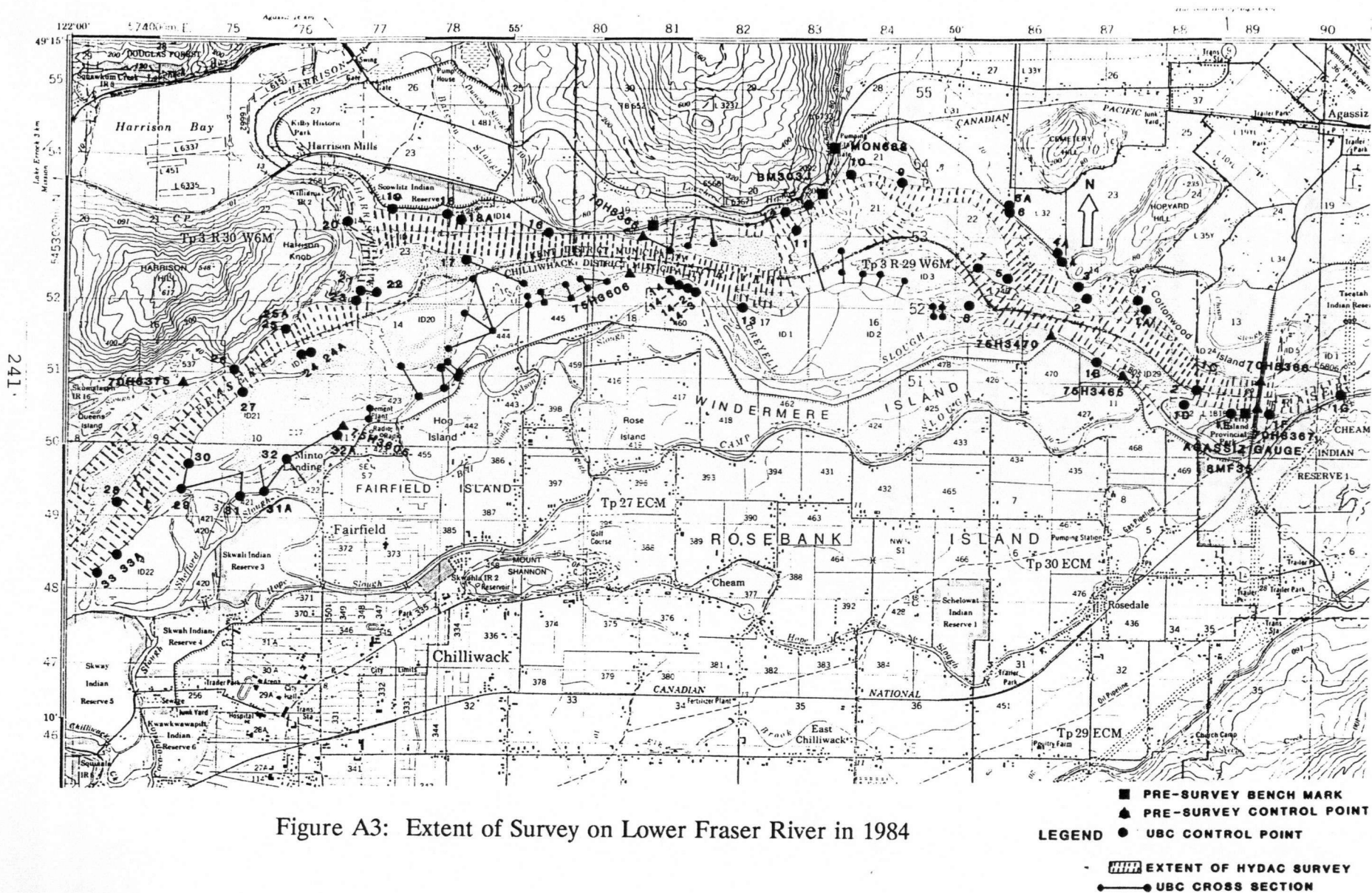


Figure A2: Extent of Survey on Lower Fraser River in 1984







## A2.0 FIELD SURVEY OPERATIONS

The control surveys, side channel surveys and conventional channel surveys were carried out by a crew of summer students and U. B. C. personnel. The automated HYDAC survey was supervised by P. Zrymiak of the Water Resources Branch, Environment Canada.

The schedule of field work completed in 1984 is summarized in Table A1. The 1984 summer hydrograph at Hope during the time of the survey is shown on Figure A4. Initial planning for the surveys was made during the autumn and winter of 1983. The control surveys were laid out in the field in March 1984. The HYDAC crew commenced their hydrographic surveys on June 20th and finished on July 16th. During this period the group was organized into three crews:

- the HYDAC crew under the direction of P. Zrymiak;
- a 3 person control team responsible for completing the control surveys network for the HYDAC operations;
- a 2 person mapping team responsible for surveying the above-water portions of the river bed. This group also collected water level data for the HYDAC crew.

Between July 1-16, when most of the HYDAC surveys were completed, the river peaked at about 8200 m<sup>3</sup>/s and then dropped to 6730 m<sup>3</sup>/s. During this period virtually all gravel bars were submerged, which allowed the hydrographic surveys to

extend over a wide area of the channel zone.

After July 13th, UBC crews began surveying the side channels between Agassiz bridge and Chilliwack Mountain. The surveys were carried out by two teams:

- a two person sounding crew which established cross section lines and surveyed the river banks;
- a two or three person control crew which tied in the cross section lines to the permanent control network.

The side channel surveys were completed by August 10th. By the end of this period the discharge had decreased to about 5300 m<sup>3</sup>/s and the water level had dropped 3.5 m below the peak stage in July. However the river level remained sufficiently high to submerge most bars in the side channels.

Finally, 10 km of main channel was surveyed by a three person UBC crew between August 21 - September 20. Control was first established at each cross section line by running a traverse between existing control stations at the mouth of Sumas River and the lower end of Sumas Mountain. Sounding operations commenced September 5th and ended September 20th. During this period the river dropped to between 2670 m<sup>3</sup>/s and 2860 m<sup>3</sup>/s. As a result many bars near the mouth of the Sumas River were exposed and had to be mapped by terrestrial surveying methods.



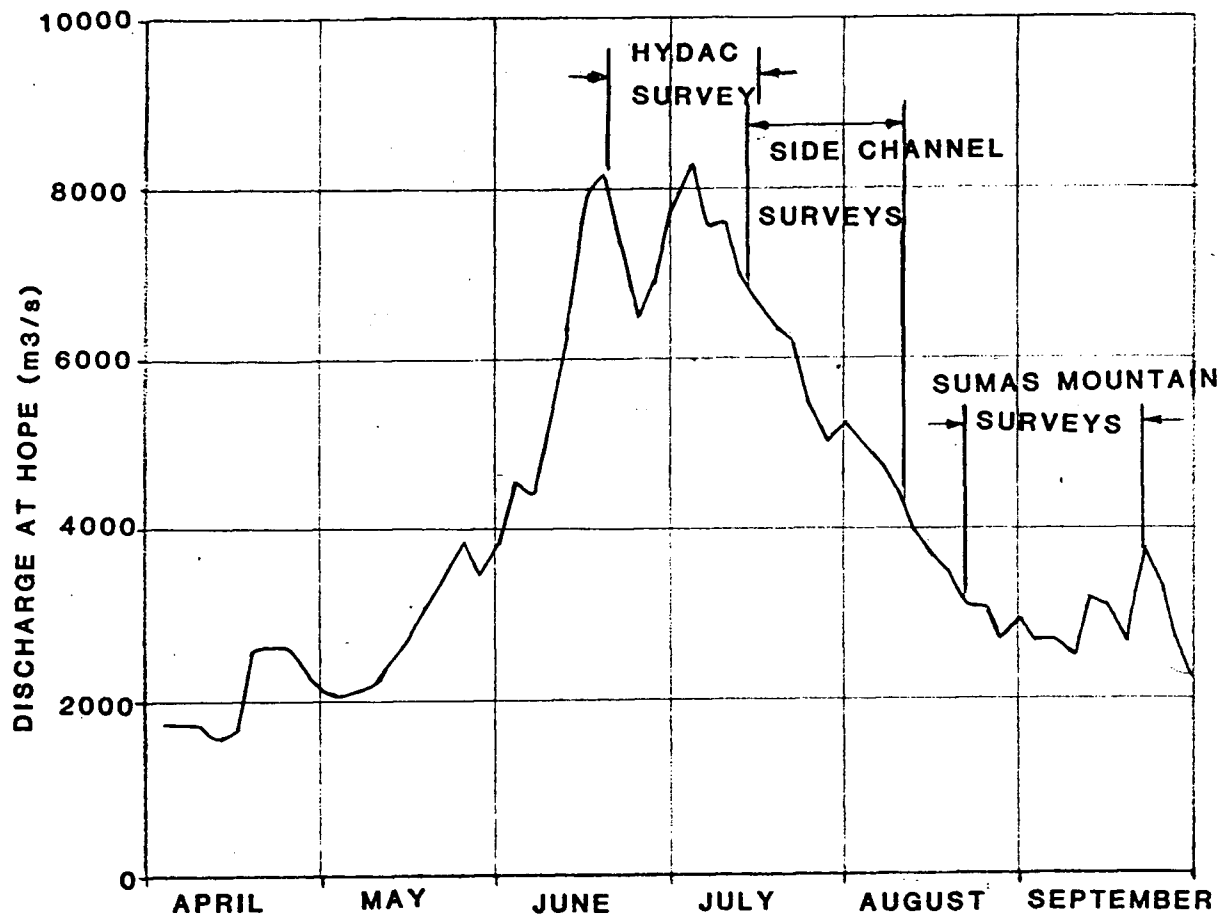


Figure A4: 1984 Hydrograph During Survey Operations

Table 1  
Schedule of Work

Date	Work Carried Out in 1984
March 26 – April 6	Layout of control traverses/planning
April 10	Control surveys begin
June 4	Crew moves to Rosedale
June 12	HYDAC crew arrives
June 13	Topographic mapping begins
June 20	HYDAC surveys start
July 13	Side channel surveys start
July 16	HYDAC leaves
August 10	Side channel surveys completed
August 21–29	Sumas Mountain control traverse
September 5–20	Sumas Mountain hydrographic surveys

### **A3.0 CONTROL SURVEYS**

#### **A3.1 Equipment**

All of the control surveys were made with a Geodimeter 122 Electronic Distance Meter (EDM) mounted on a Wild T2 theodolite. The EDM reflector targets were tribrach mounted on tripods so that forced centering techniques could be used for horizontal positioning. A 16 foot river boat was used to transport the instruments from site to site. Use of the river boat greatly reduced the need for brush clearing and trail blazing.

#### **A3.2 Primary Survey Control**

The existing horizontal and vertical control that was used to establish the primary control for the survey is summarized in Table A2. Available control near the river was determined from a computer search of records on file at the Surveys and Mapping Branch, British Columbia Ministry of Environment.

Additional horizontal control stations were established by triangulating the position of three prominent landmarks that were visible from a large portion of the river. These landmarks included:

- the cross on Westminster Abbey situated on bluffs overlooking the north side of the river at Mission;
- two tall radio towers located on Matsqui Prairie on the south bank (Figure A1).

TABLE A2  
EXISTING PRIMARY CONTROL PRIOR TO SURVEY

Benchmarks - Vertical Control

Station	Source	Elevation (m)	Approximate UTM Coordinates		Location	Description
			Easting	Northing		
08NF035	WSC	10.293	589 000	54 50 600	Agassiz Bridge	Gauging station datum
Mon-688	BCMOE	15.216	583 300	54 54 200	Nr. Moutain Slough	Top of Hammersley outlet structure
BM303-J	BCSMB	16.393	582 900	54 53 500	Mt. Woodside	Tablet in rock
BM14C-31J	BCSMB	10.760	559 400	54 42 100	Nr. Cox Station	Tablet in rock
TBM6.742	BCMOE	6.742	556 350	54 42 050	Matsqui Prairie	Spike in 0.3 m poplar
08MH024	WSC	0.073	550 950	54 51 750	Mission	Gauging station datum

Control Stations

Station	Accuracy	Elevation (m)	UTM Coordinates		Location	Description
			Easting	Northing		
70H8367	H3V2	32.797	589161.81	54 50 635.36	Agassiz Bridge	At Road level on lookout
75H3465	H4V2	16.399	587382.18	54 51 074.44	Nr. Rosedale	P.Con. on base of dyke
75H3470	H4V3	15.670	586318.30	54 51 691.40	Greyell Slough	P.Con. in dyke
70H8365	H3V4	11.539	580711.86	54 52 937.78	Mt. Woodside	B.B. in rock ledge
75H3606	H3V3	12.314	580438.74	54 52 471.08	Carey Point	P.Con. in pasture
75H3605	H3V3	10.973	576595.42	54 50 248.21	Minto Landing	P.Con. by road
70H8357	H3V4	10.187	574448.04	54 50 810.61	Queens Island	B.B. in rock cliff
75H3601	H4V3	6.919	569422.14	54 44 330.57	Chilliwack Mtn.	B.B. in rock ledge
70H8378	H3V4	7.738	564442.40	54 43 199.94	Sumas River	B.B. in large rock
79H0865	H3V3	9.165	555726.65	54 42 290.90	Matsqui Prairie	P.Con. on dyke road
78H8314	H3V3	9.222	555421.65	54 42 506.41	Matsqui Prairie	P.Con. on dyke road
82H5838	H3V3	8.997	555030.34	54 42 819.30	Matsqui Prairie	P.Con. on dyke road
82H5763	H3V3	8.631	552465.42	54 42 079.54	Matsqui Prairie	P.Con. on dyke road
78H8307	H3V3	8.877	551884.07	54 41 731.12	Matsqui Prairie	P.Con. on dyke road

Legend: WSC = Water Survey of Canada  
 BCMOE = B.C. Ministry of Environment  
 BCSMB = B.C. Surveys and Mapping Branch  
 B.B. = brass bolt  
 P.Con. = concrete pillar

Six main closed traverse loops were required to provide adequate horizontal and vertical control for the hydrographic surveys (Table A3). A seventh traverse was completed in the Mission-Sumas Mountain area by using a combination of triangulation and trilateration surveys. A total of 61157.7 m of traverse was completed and 111 control stations were established. Most of the control points consisted of 600 mm x 16 mm diameter galvanized steel grounding rod with identification tags wired to their top. Control points on bedrock outcrops were established with chrome molybdenum steel pegs hammered into cracks in the rock.

The horizontal and vertical coordinates of all control points were determined by the method of reciprocal trigonometric levelling. All horizontal and vertical angles were measured by averaging face left and face right readings. In most cases directions and vertical angle measurements were repeated three times and all angles were read to the nearest second. Slope distances and vertical angles were measured on both the back sight and foresight. This eliminated the need to estimate refraction corrections.

All of the control station co-ordinates were calculated with a combined scale factor of 0.999664 to convert to the UTM grid system at mean sea level. This factor was calculated for the following geographical co-ordinates:

Latitude 49° 10' 30"; Longitude 122° 00' 00"

TABLE A3

## SUMMARY OF PRIMARY CONTROL TRAVERSE LOOPS

Circuit	Reach	Traverse Length (m)	Horizontal Closure (m)	Control Precision	Vertical Closure (m)	Control Precision
75 H3465 – 75 H3470	Agassiz Bridge – Greyell Slough	9734.82	1.145	1:8499	0.04	1:243370
75 H3606 – 70 H8357	Carey Point – Queen's Island	8968.38	0.345	1:25988	0.026	1:344937
70 H8357 – 75 H3605	Queen's Island – Minto Landing	4417.78	0.245	1:17977	0.013	1:339829
UBC 30 – 75 H3601	Shefford Slough – Chilliwack Mtn.	10012.59	0.502	1:19947	0.021	1:476790
75 H3601 – 70 H8378	Chilliwack Mtn. Sumas River	6891.02	0.102	1:67500	0.414	1:16643
70 H8378 – UBC 5R	Sumas Mtn. – Sumas River	7399.36	0.559	1:13250	0.120	1:61660

Note: Control between Mission bridge and Sumas Mountain was established by triangulation/trilateration. See Figure 4.

For most of the traverses errors in closure were adjusted by the compass rule. The surveys between Mission and Sumas Mountain were adjusted by the method of least squares using a computer program developed by M. Crape and T. Zegarchuk. This program allowed 95% confidence limits to be placed on the positions of the control stations.

The horizontal and vertical accuracies obtained in the traverses are summarized in Table A3. In general, the control meets or exceeds requirements for intermediate scale topographic mapping (Davis *et al.*, 1983). Better vertical control could have been achieved if precise levels had been used. However due to time and manpower constraints it was considered that reciprocal trigonometric levelling was the only practical option available. A list of co-ordinates that were established for the control stations is summarized in Table A4.

### A3.3 Secondary Mapping Control

An additional 62 temporary control points were established for the topographic mapping of exposed bars, islands and banklines. These secondary control points were established as side shots from the primary stations and consisted of wooden stakes marked with flagging. Generally, when the length of the shots exceeded 1000 m, reciprocal trigonometric levelling was used to establish elevations and co-ordinates. For shorter distances only foresights were taken. In these instances corrections for earth curvature and refraction were applied.

Table A4: Summary of UBC Control Stations Established in 1984

Station	UTM Coordinates		Elevation (m)	Location	Description
	Easting	Northing			
1G	590 295.06	5 450 858.36	17.15	Cheam I.R.	IP under powerline crossing
1F	588 377.08	5 450 598.98	18.19	Ferry Island	IP UIS of pipeline crossing sign
1E	588 927.08	5 450 608.22	16.76	Ferry Island	IP 250 m d/s of bridge
1D	588 189.13	5 450 712.10	16.81	Ferry Island	IP near eroding bank
1C	588 305.57	5 451 316.66	16.80	Cottonwood Island	IP on top of dyke
1B	586 975.70	5 451 332.7	16.75	Windemere Island	IP near rock bank below dyke
1A	587 637.50	5 452 026.52	15.979	Cottonwood Island	IP in top of dyke
1	587 577.59	5 452 117.90	16.97	Cottonwood Island	IP in top of dyke
2	586 851.06	5 452 140.84	15.21	Island	IP near eroding bank - destroyed
3	586 680.95	5 452 313.48	15.43	Hopyard Hill	SP in rock cliff
4	586 458.55	5 452 648.27	17.34	Hamilton Rd	IP on south edge gravel road
4A	586 407.20	5 452 714.9	17.33	Hamilton Rd	IP at base of dyke on fence line
5	585 653.49	5 452 600.73	14.87	Island	IP near U/S end of Island
6	585 698.07	5 453 344.22	14.86	nr Cemetery Hill	IP on top of riprap bank
6A	585 712.20	5 453 357.1	16.67	" " "	IP up slope from UBC 6
7	585 250.0	5 452 636.12	14.32	Island	IP 1.5 m from edge of bank
8	585 296.23	5 452 033.15	14.59	entrance/Greyell Slough	IP on top of bank of Island
9	584 207.75	5 453 757.09	14.12	nr Cemetery Hill	IP on top of riprap by road
10	583 580.08	5 453 804.25	13.38	Mountain Slough	IP on top of riprap by road
11	582 806.56	5 453 083.14	12.50	Island	IP on edge of bank - destroyed
12	582 788.39	5 453 337.85	16.78	Mt. Woodside	IP near west side of railway tunnels
12A	582 954.86	5 453 399.09	16.74	" "	IP near east " " " "
13	582 080.73	5 451 982.61	12.95	Greyell Island	IP on top of eroding bank
14	581 092.88	5 452 380.89	13.28	Carey Point	IP on top of bank - destroyed
14-1	581 407.80	5 452 168.50	13.54	Carey Point	IP in field
14-2	581 299.39	5 452 224.17	13.30	Carey Point	IP in field
14-3	581 180.41	5 452 292.85	13.55	Carey Point	IP in field
16	579 372.62	5 453 014.27	12.18	Nr Mt. Woodside	IP on top of bank - destroyed
17	578 259.87	5 452 634.92	11.53	Island	IP on top of bank
18	578 027.08	5 453 215.97	11.64	Nr Harrison River	IP on top of riprap bank
18A	578 191.83	5 453 170.79	10.44	U/S Harrison River	IP on top of riprap spur
19	577 282.45	5 453 253.21	10.62	U/S Harrison River	IP on top of riprap bank



Table A4: Summary of UBC Control Stations Established in 1984

Station	UTM Coordinates		Elevation (m)	Location	Description
	Eastings	Northing			
20	576 566.16	5 453 167.62	9.50	at Harrison River	IP on top of low bank
21	576 835.28	5 452 164.25	11.28	O/S Harrison River	SP on rocky knob
22	577 037.51	5 452 182.39	11.30	Island	IP on top of bank
23	576 726.69	5 452 003.27	11.97	Harrison Knob	IP on top of high bank
24	576 048.17	5 451 262.49	10.78	Island	IP on top of bank
24A	576 113.98	5 451 603.43	11.36		
25	575 867.06	5 451 589.59	13.75	Harrison Knob	SP on rocky cliff
25A	575 883.12	5 451 603.43	16.34	Harrison Knob	SP on rocky cliff
26	575 169.88	5 451 050.09	14.37	Harrison Knob	SP on rocky cliff
27	575 319.64	5 450 720.53	10.22	Island	IP on top of bank
28	573 538.63	5 449 106.32	8.84	Island	IP on gravel beach
29	574 422.55	5 449 343.52	9.76	Nr Shefford Slough	IP on top of bank
30	574 585.70	5 449 707.76	9.60	Island	IP on top of bank
30A	574 568.54	5 449 859.02	9.37	Island	IP on top of bank
31	575 294.54	5 449 300.84	10.29	Nr Shefford Slough	IP on riprap bank
31A	575 649.80	5 449 334.39	10.72	Nr Shefford Slough	IP on riprap bank
32	575 951.94	5 449 839.65	10.47	Island, Minto Landing	IP on top of bank
33	573 322.31	5 448 159.21	8.63	Nr Shefford Slough	IP on top of bank
33A	573 638.35	5 448 542.61	10.53	Nr Shefford Slough	IP on top of bank
34	572 442.82	5 448 703.03	7.79	Nr Queen's Island	IP on top of bank
35	571 321.10	5 447 184.44	8.89	Island	IP on top of unstable bank
36	570 650.58	5 447 470.20	6.76	Nicomien Island	IP on riprap slope
36A	570 901.58	5 447 894.97	7.70	Nicomien Island	IP on top of bank
37	570 442.6	5 447 042.4	9.52	Nicomien Island	IP on top of riprap slope
38	570 701.02	5 446 046.04	7.83	Island	IP on top of low bank
38A					
40	567 778.06	5 443 680.2	6.60	Cannor	SP in rocky outcrop near waters edge
45	572 096.37	5 446 254.55	7.49	Nr Chilliwick Creek	IP on top of bank
45	571 831.02	5 446 661.32	7.72	Nr Chilliwick Creek	IP on small island
47	572 366.11	5 446 537.07	8.07	Nr Chilliwick Creek	IP on top of bank
48	572 294.05	5 447 251.41	7.67	Island U/S Chilliwick Creek	IP on top of bank

Table A4: Summary of UBC Control Stations Established in 1984

Station	UTM Coordinates		Elevation (m)	Location	Description
	Easting	Northing			
CS 35R	567 334.83	5 444 961.13	4.61	Nicomén Island	IP on top of riprap bank
CS 33R	566 893.74	5 444 902.53	8.19	Nicomén Island	IP on top of riprap bank
CS 31R	566 393.58	5 444 753.27	7.02	Nicomén Island	IP on top of riprap bank
CS 29R	565 921.14	5 444 979.86	7.03	Nicomén Island	IP on top of riprap bank
CS 27R	565 397.99	5 444 923.89	8.18	Nicomén Island	IP on top of riprap bank
CS 23R	564 301.11	5 444 443.45	7.20	Nicomén Island	IP on top of riprap bank
CS 21L	564 374.31	5 443 452.78	5.18	Island near Sumas River	IP on low bank
CS 22R	564 088.24	5 444 312.40	8.57	Nicomén Island	IP on riprap bank
CS 17R	562 708.04	5 443 963.17	6.20	Nicomén Island	IP on riprap bank
CS 15L	561 939.68	5 443 257.58	6.22	Sumas Mountain	SP in rock ledge
CS 12R	560 887.02	5 443 483.51	5.20	Strawberry Island	IP on top of bank
CS 9L	559 987.64	5 442 639.59	5.40	Sumas Mountain	IP on top of silty bank
CS 5R	558 753.50	5 442 663.83	6.32	Strawberry Island	IP on top of riprap bank
107	558 618.50	5 441 868.35	4.95	Sumas Mountain	SP in rock ledge
108	558 031.30	5 441 768.27	5.03	Sumas Mountain	IP in riprap slope
106	557 061.02	5 441 716.68	7.06	Matsqui Prairie	SP in road
105	556 360.18	5 441 991.87	5.82	Matsqui Prairie	SP in road
104	554 630.00	5 443 924.62	-	Nr Hatzic Slough	stake on woodchip pile
103	554 027.12	5 443 937.60	-	Nr Mission	IP below railway track
102	553 534.22	5 443 023.97	-	Matsqui Prairie	SP near end of road
101	552 690.40	5 442 353.74	-	Matsqui Prairie	SP in grassy bank
100	555 412.64	5 441 349.15	-	U/S Mission Railway Bridge	SP below dyke
Monastery	553 306.65	5 444 591.04	-	Mission Abbey	Cross on Abbey
UP-RAD	555 809.94	5 439 669.33	-	Matsqui Prairie	Upstream radio tower
DWN-RAD	555 102.74	5 439 684.02	-	Matsqui Prairie	Downstream radio tower

#### A3.4 Cross Section Control

Horizontal and vertical control was provided for each of the 58 side channel cross sections and 78 main channel cross sections surveyed by U.B.C. In most cases both left bank and right bank stations were established. In cases where only one station was established the azimuth of the cross section line was measured. The control points for the cross sections consisted of flagged wooden stakes and were not intended to be permanent stations. However since all sections have been tied in to the UTM grid system any cross section can be relocated easily from the permanent primary control network.

### **A4.0 HYDROGRAPHIC SURVEYS**

#### A4.1 HYDAC Main Channel Surveys

The HYDAC surveys extended over 28.5 km of river between the Agassiz bridge and Chilliwack Mountain and over 10 km of river upstream from the Mission railway bridge. The main features of the HYDAC survey system have been described (Durette and Zrymiak, 1978) and are summarized only briefly in this report.

According to Durette and Zrymiak (1978) the main components of the HYDAC system include:

- a positioning sub-system consisting of two MRD 1 tellurometer units. Each unit consists of a remote station onshore, a tracking antenna, a master unit and a data line driver on board the survey boat;

- a depth sounding system consisting of an Atlas DESO-10 sounder and recorder and an Atlas EDIG-10 digitizer. The sounder operates on a frequency of 210 kHz and produces an 8 degree wide acoustic beam;
- a data processing sub-system which monitors the performance of the instruments and provides a continuous plot of the boat's position. The system operates through a Hewlett-Packard 9825A programmable calculator and the distance and depth data are stored on magnetic tape.

The HYDAC system is mounted in a 32 foot shallow draft aluminum boat powered by two V-8 engines which are coupled to two Berkley jet drives.

During the early planning stages the river was sub-divided into a number of sectors which were assigned high, medium or low priority ratings. High priority sectors generally consisted of main channel portions of the river which displayed complex bars and island features. It was decided that these areas would require cross sections spaced 100 m apart to represent the topography adequately. Medium priority sectors consisted of relatively straight single channels which were thought to have relatively uniform topography. For these reaches cross sections were spaced 200 m apart. Low priority sectors consisted of side channels and were to be surveyed with lines 400 m apart. During the course of the surveys this plan was modified when it was realized that it would be more efficient for the HYDAC crew to continue surveying on the main channel rather than work in the narrower side channels. Therefore the UBC group undertook to survey all side channels, which allowed more of the main channel to be surveyed at the high priority spacing. In the end, 33 km

of the 38.5 km was surveyed with section lines 100 m apart and 5.5 km was surveyed with lines spaced 200 m apart.

A total of 26 different tellurometer set-ups were required to cover the 38.5 km of river surveyed by HYDAC.

During the surveys the following procedures generally were followed:

- (i) The two remote tellurometer stations were mounted over the established control points;
- (ii) Water levels were measured along the sector either by direct levelling from available control stations or by reading temporary staff gauges near the stations;
- (iii) Cross section lines were laid out on the plotter approximately perpendicular to the river's flow;
- (iv) The boat was manoeuvred on the cross section lines by following the boat's position on the plotter.

Generally the boat continued on the cross section line until the water depth became less than 1 m. This often meant a 5 m to 15 m zone near the banks could not be surveyed. In total, more than 400 cross sections were surveyed and over 44 000 data points were recorded between June 20th and July 16th (Zrymiak, 1984).

Figure A5 shows a summary plot from surveys in the vicinity of Mission Bend.

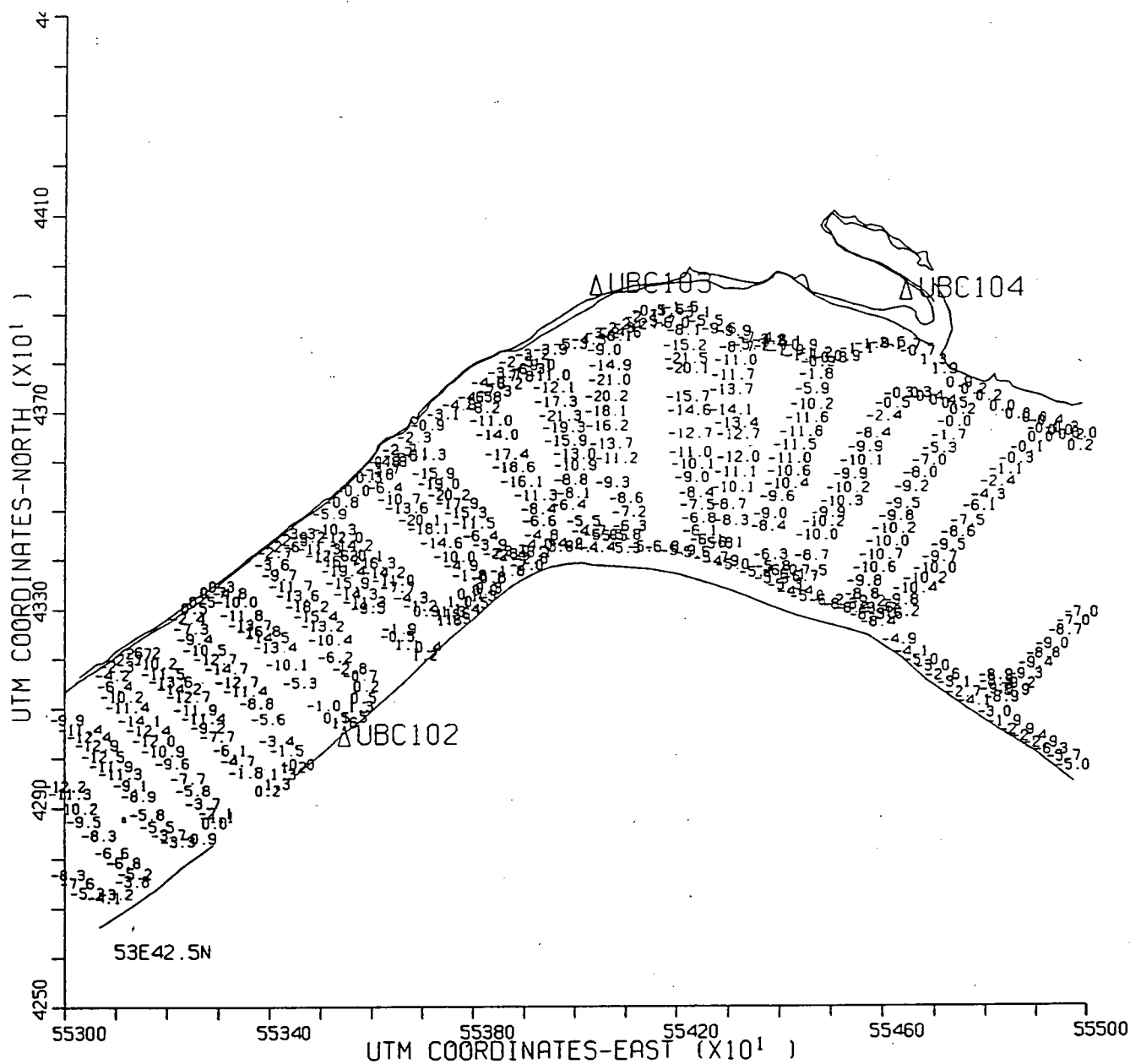


Figure A5: Sample of HYDAC Survey Data Near Mission Bend

#### A4.2 UBC Main Channel Surveys

Approximately 10 km of the main channel between Sumas Mountain and Chilliwack Mountain were surveyed by UBC crews. For these surveys, horizontal positioning was accomplished with the Geodimeter 122 EDM/T2 theodolite combination. The Geodimeter 122 is one of the few EDM's capable of tracking a moving boat at moderate speeds and was found to be ideally suited for hydrographic surveying. Water depths were measured with a Raytheon 719B echo sounder which was mounted in a 16 foot river boat.

The following procedures were employed:

- (i) The EDM was set up on a pre-established control point on the sounding line and a reflecting target was mounted on the stern of the 16 foot river boat directly over the sounder transducer;
- (ii) Water levels were measured on both sides of the cross section line and bank profiles were surveyed with the EDM/T2.
- (iii) Two triangular targets were set up on one bank 10 m to 15 m apart on the sounding line in front of the EDM;
- (iv) The boat operator maintained his position on the sounding line by lining up the two targets on the shore. Also the theodolite operator was able to give radio instructions to the driver to head upstream or downstream;
- (v) During the soundings the theodolite operator's sole job was to site on the reflector target on the boat. A third crew member observed the distance displayed on the EDM and called "fix" at

20 m to 50 m intervals over the radio to the boat driver. For each distance the boat operator placed a fix mark on the echo sounder trace.

Considerable practice was required by the boat and theodolite operators before this system could be used successfully. On some of the longer sounding lines the boat driver had difficulty in resolving the two shore targets which were 600 m to 1100 m away. In these cases the driver had to rely on the instructions from the theodolite operator to stay on line. Also when the boat closed to within 100 m of the EDM it became difficult for the theodolite operator to hold the reflector target on the boat in view. This difficulty could be reduced by mounting the EDM on a theodolite with a coarse adjustment tangent screw.

A total of 78 sounding lines were surveyed over the period between September 5 and September 20. The cross sections were spaced 250 m apart along the channel. Diagonal lines were also run between every second cross-section to increase the area of coverage. These additional lines proved to be very valuable after the bed elevations were plotted and contour lines were being drawn. A portion of the contour maps covering this reach are reproduced in Figure A6.





#### A4.3 UBC Side Channel Surveys

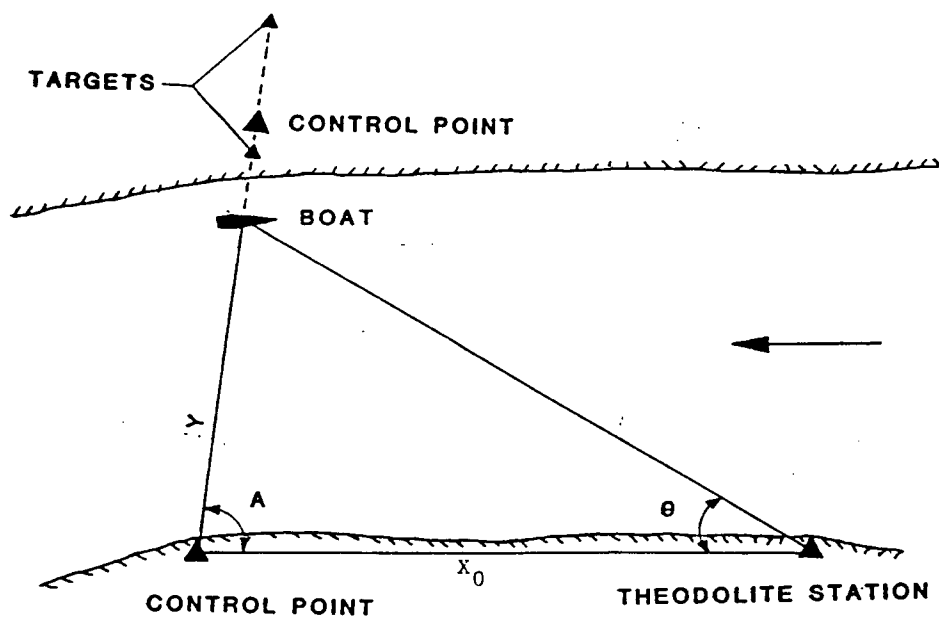
The side channels typically ranged from 200 m to 300 m in width and from 2 to 10 m in depth at the time of survey. Due to time limitations, the soundings were carried out while the EDM was being used for control surveys. As a result, the Bearing-Bearing intersection method was used for horizontal positioning. In this method the position of the boat was determined by the intersection of two known Azimuth lines (Figure A7). For these surveys the angles were measured with a Sokkisha theodolite having a least count of 15 seconds. The Raytheon 719B sounder was mounted in a 14 foot aluminum boat powered by a 15 hp motor. The following procedures were generally used throughout the surveys:

- (i) The sounding lines were laid out in the field and control points were established on left and right banks. A third control point offset from the sounding line was required for the theodolite station. All control points were tied to UTM coordinates;
- (ii) Above-water portions of the cross sections were surveyed by stadia and theodolite. Water levels on the left and right banks were also measured;
- (iii) The theodolite operator set up on the offset control point and zeroed the instruments on one of the cross section control points;

- (iv) Triangular targets were set 10 m to 20 m apart on the cross section line on one of the banks;
- (v) The boat operator drove to the bank opposite the targets and manoeuvred onto the section by lining up the two shore targets;
- (vi) When the survey began the theodolite operator sighted a target on the boat and called horizontal angles over a radio to the boat operator. The boat operator placed a fix mark on the echo sounder trace for each of the angle measurements.

Horizontal angles generally were called out at 1 or 2 degree intervals. The main advantage of the method was that the surveys could be carried out with a two person crew. The main disadvantage was that three control points were required for each cross section. Also, since the theodolite operator was offset from the cross section line the boat driver had to rely on the two shore targets to stay on line. Since the channels were fairly narrow the targets could be seen easily and any drift offline was readily apparent. The usually weaker currents encountered in the side channels simplified boat control somewhat as well.

In total, 58 side channel cross sections were completed. Most of the sections were spaced 200 m to 400 m apart. In a few locations, such as near Minto Landing and near the mouth of the Harrison River, cross sections were spaced 50 m to 100 m apart in order to provide detailed coverage of very deep local scour hole features.



$$Y = X_0 \sin \theta / \sin(\theta + A)$$

where  $Y$  is the distance from the control point to the boat

Figure A7: Positioning by the Bearing-Bearing Intersection Method

## A5.0 Accuracy of Hydrographic Surveys

The accuracy of the surveys will depend on the magnitude of errors in depth measurements, water level measurements and horizontal positioning.

Water depths could be measured to a precision of  $\pm 2.5$  cm with the Atlas sounder in the HYDAC system (Durette and Zrymiak, 1978) and probably  $\pm 5$  cm with UBC's Raytheon 719B sounder. However errors in depth measurements could arise from other sources including:

- errors in assuming a speed of sound in water;
- errors due to drift in sounder calibration;
- errors caused by boat motion and wave action;
- errors produced by averaging depths over the  $8^\circ$  beam width produced by sounder transducers.

In the Raytheon sounder the speed of sound is assumed to be  $1460 \text{ m s}^{-1}$ . However for the  $10^\circ\text{C}$  water temperature variation that occurred over the summer the speed of sound could vary by  $\pm 2\%$ . If corrections were not applied then systematic depth errors of up to 0.2 m could occur when sounding in water depths of 10 m.

The effect of wave motion was especially noticeable in the Mission-Sumas reach where winds can blow over long fetches. During a survey in the 16 foot river boat, water waves produced apparent bedforms having heights of up to 0.3 m. The problem would be less important in the much heavier HYDAC boat.

These results suggest that the nominal precision associated with the depth measurements probably is not significant. It is likely that the actual errors in measurements are in the order of a few tenths of a meter.

The accuracy of the water levels will depend on the errors in the vertical control and the water level measurements. The closure errors of the control surveys suggest that most of the vertical control could have errors of  $\pm 1$  to 5 cm. It was found that water levels could usually be measured to within  $\pm 1$  to 2 cm. These effects would probably represent the main sources of errors in the UBC surveys where water levels were measured on the left and right bank in each cross section. However during the HYDAC surveys water levels were measured at only a few stations (usually between 2 and 4) over distances of 1 to 2 km. Water levels between stations were computed by straight line interpolation. However drawdown and backwater effects along the river could create considerable variations in the water surface profiles. Based on some profiles surveyed between Agassiz bridge and Harrison River it was estimated that the interpolated water levels could easily introduce errors of 10 cm to 20 cm. These errors would be substantially less in the Mission Reach where the water surface slope is much flatter.

Horizontal positioning errors will introduce apparent bed elevation changes when the channel bottom is sloping.

In the HYDAC system the accuracy of the tellurometer stations has been reported as  $\pm 1.0$  m when operating under dynamic conditions. However the actual accuracy

of the positioning will depend on the geometry between the two remote stations and the boat. For the geometry shown in Figure A8, the co-ordinates of the survey vessel can be determined as:

$$[1] \quad x = \frac{r_1^2 - r_2^2 + x_o^2}{2x_o}$$

$$[2] \quad y = (r_1^2 - x^2)^{1/2}$$

where  $r_1$  and  $r_2$  are the measured distances from the remote stations to the survey boat;  $x_o$  is the baseline distance between the remote stations.

The errors in these co-ordinates can be assessed by propagating the distance measurement errors through the geometry equations [1] and [2]. The general error propagation law can be written (Taylor, 1982) as:

$$[3] \quad E_x^2 = \left\{ \frac{\partial x}{\partial r_1} \Delta r_1 \right\}^2 + \left\{ \frac{\partial x}{\partial r_2} \Delta r_2 \right\}^2$$

$$[4] \quad E_y^2 = \left\{ \frac{\partial y}{\partial r_1} \Delta r_1 \right\}^2 + \left\{ \frac{\partial y}{\partial r_2} \Delta r_2 \right\}^2$$

where  $E_x$  and  $E_y$  are the errors in the  $x$  and  $y$  co-ordinates resulting from the distance measurement errors  $\Delta r_1$  and  $\Delta r_2$ .

Differentiating [1] and [2] and substituting these into [3] and [4] leads to:

$$[5] \quad E_x^2 = \Delta r \left\{ \frac{r_1^2 + r_2^2}{x_o} \right\}$$

$$[6] \quad E_y^2 = \frac{\Delta r}{2x_o^2 y} \sqrt{r_1^2 (r_2^2 - r_1^2 + x_o^2)^2 + r_2^2 (r_1^2 - r_2^2 + x_o^2)^2}$$

where  $\Delta r = \Delta r_1 = \Delta r_2 = \pm 1 \text{ m}$

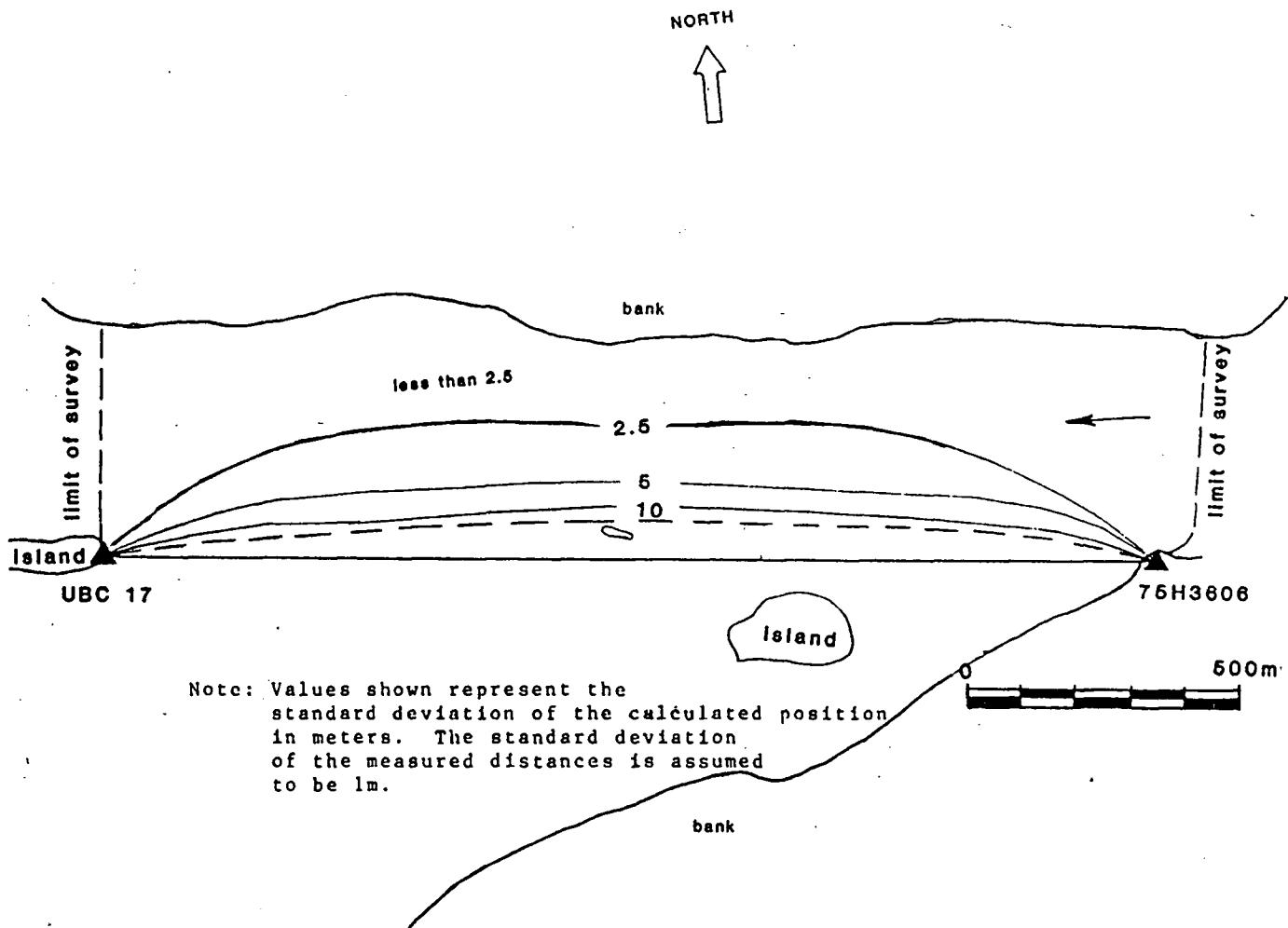


Figure A8: HYDAC Positioning Errors near Carey Point



The total error E can be estimated as:

$$[7] \ E = (E_x^2 + E_y^2)^{1/2}$$

The effects of the geometry on the positioning errors is illustrated in Figure A7 for sector 8 between Carey Point and Harrison River where the distance between remote stations was 2000 m. Over most of the sector the total error in position ranged between  $\pm 2$  m to  $\pm 5$  m. However positioning uncertainties of up to  $\pm 10$  m occurred when the boat approached to within 100 m of the baseline. For the example shown in Figure 8 and for most of the set-ups used in the survey the largest component of the error was in the direction, perpendicular to the baseline.

Figure A9 illustrates the positioning uncertainties in Sector 9 for a portion of the channel near Mountain Slough. In this particular set-up the baseline distance measured 630 m and the average positioning error over the entire reach was computed to be  $\pm 6$  m. However the error increased to  $\pm 5$  m to  $\pm 15$  m in the upstream one third of the reach where the boat passed beyond both remote stations and was aligned close to the baseline. Fortunately this condition did not occur very frequently in other set-ups.

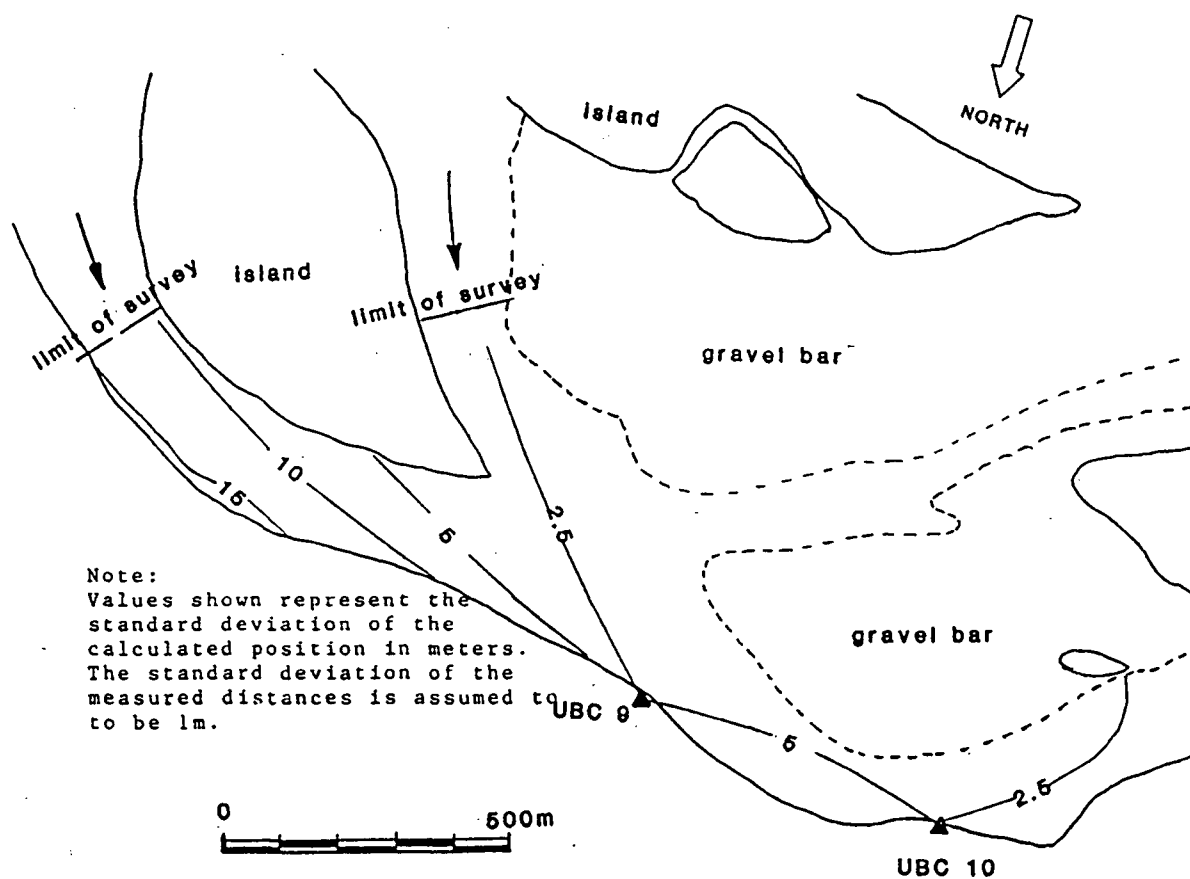


Figure A9: HYDAC Positioning Errors near Mountain Slough

The effect of the horizontal positioning errors on the measured bed topography will depend on the slope of the channel bottom. For relatively flat slopes small positioning errors will cause only minor shifts in the bed contours. However near local scour holes or steep banks vertical errors of several metres could occur.

The positioning errors associated with UBC's main channel surveys result mainly from two sources:

- (1) drift of the boat off the survey line;
- (2) delays between reading the distance on the EDM and marking the appropriate fix on the sounder charts.

The tendency for drift was near zero at the start of the section and increased rapidly as the boat pulled away from the far bank. The maximum errors probably occurred when the boat was about 1/3 of the way across the channel. As the boat approached the bank where the EDM and targets were located the positioning accuracy improved since the parallactic angle between the two targets increased.

The maximum drift was estimated at several cross sections by measuring both the horizontal angle between the boat and the sounding line and the distance between the boat and EDM. For seven measurements the maximum drift varied between 8 m and 17.5 m and averaged 15 m over channels between 600 m and 800 m in width.

Delays associated with reading and "fixing" distances on the sounder will introduce systematic errors in position. However this problem could be compensated for

partially by calling for the fix mark slightly ahead of the actual distance reading. However no tests were made to determine the magnitude of this error. Given the relatively slow speed of the boat it is likely that these errors were within  $\pm 5$  m.

An estimate of the overall precision of the surveys can be made by comparing replicated cross section lines. This approach has been used previously on Peace River to estimate horizontal positioning errors (Church and Rood, 1982). At the beginning of the main channel surveys near Sumas Mountain the UBC crew replicated five cross section lines. The precision of the soundings was measured by computing the root mean square error (RMSE) of the depths at each (replicated) fix point across the channel:

$$[8] \text{ RMSE} = \sqrt{\frac{\sum_{L=1}^n (y_1 - y_2)^2}{n}}$$

where  $y_1$  and  $y_2$  are the depths measured at a particular fix mark on run 1 and run 2

$n$  = the number of fixes across the channel.

For these five sections the RMSE varied from 0.25 m to 0.11 m and averaged 0.18 m. Since these measurements were made in water depths of 8 m - 10 m the obtainable precision is in the order of  $\pm 2\%$  of the water depth. The result summarizes depth measurement errors and the effect of positioning errors on the estimation of depth at a nominal point. These measurements were made at the beginning of the survey when the crew members were still perfecting their sounding techniques. Better

results could probably have been obtained at the end of the survey. Nevertheless, the results indicate that random variations of  $\pm 0.2$  m in elevation could easily occur during the surveys.

For the purposes of developing a sediment budget we are mainly interested in determining the mean bed elevation across the channel rather than the elevation of a particular spot. The root mean square error of the mean bed elevation can be estimated as:

$$[9] \text{ RMSE}_x = \frac{\text{RMSE}}{\sqrt{n}}$$

where  $n$  is the number of subsections used to determine the mean bed level.

For  $n = 16 - 25$  (which corresponds to the number of fixes typically made across the channel)  $\text{RMSE}_x$  will be in the order of  $0.04 - 0.05$  m (which is comparable with the nominal precision of a measurement). Further work is required to assess the overall uncertainty in the computed volume changes between the two successive surveys.

## **A6.0 CONCLUSIONS**

During the summer of 1984 66.5 km of surveys were carried out along the lower Fraser River between Mission and the Agassiz-Rosedale Bridge. An Environment Canada crew, with the automated HYDAC survey system collected over 400 cross sections along 38.5 km of main channels. UBC crews surveyed 10 km of main channel and 18 km of side channels during this period. Approximately one man-year of effort went into the field work. This work represents the first comprehensive survey in this reach of river since 1952.

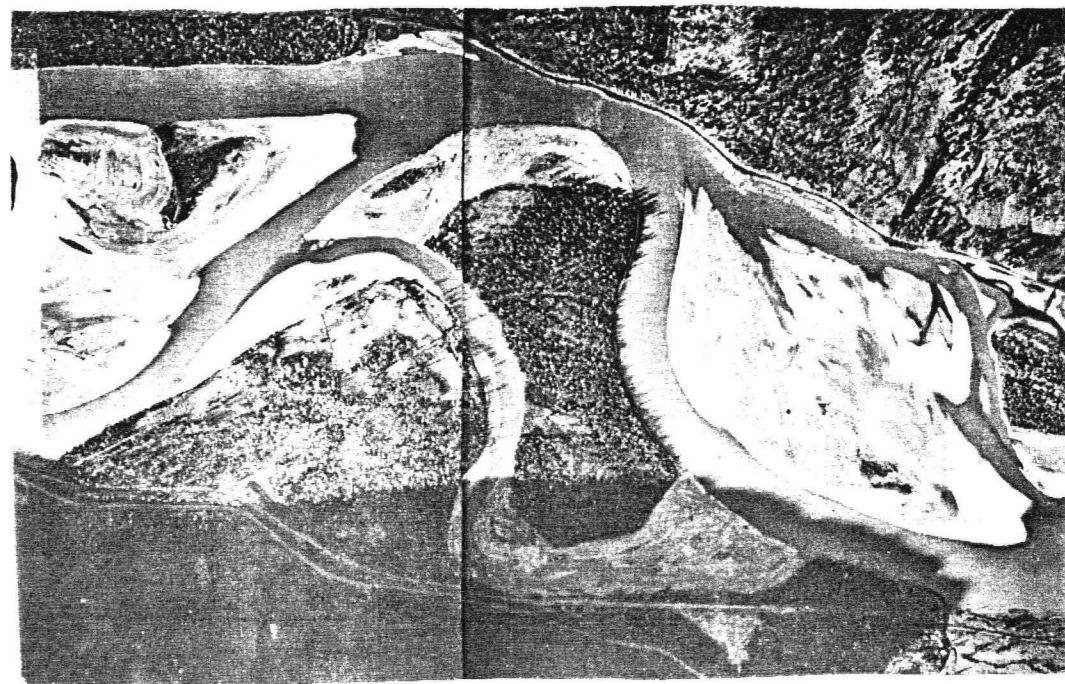
## A7.0 REFERENCES

- Church, M. and Rood, K., 1982. Peace River Surveys, 1979 and 1981. University of British Columbia, Dept. of Geography Report: 54 pp. + Figs.
- Durette, Y. and Zrymiak, P., 1978. HYDAC 100 - An Automated System for Hydrographic Data Acquisition and Analysis. Canada. Dept. of Environment, Inland Waters Directorate, Water Resources Branch, Ottawa, Canada, Technical Bulletin 105: 44 pp.
- Taylor, J.R., 1982. An Introduction to Error Analysis: The Study of Uncertainties in Physical Measurement. University Sciences Books, Mill Valley, California: 241 pp.
- Zrymiak, P., 1984. 1984 Fraser River Hydrographic Survey Field Trip Report, Canada Dept. of Environment, Water Resources Branch, Sediment Survey Section, unpub. report: 17 pp. + Appendix.

## **APPENDIX B**

### **HISTORICAL CHANNEL CHANGES, HOPE TO MISSION**





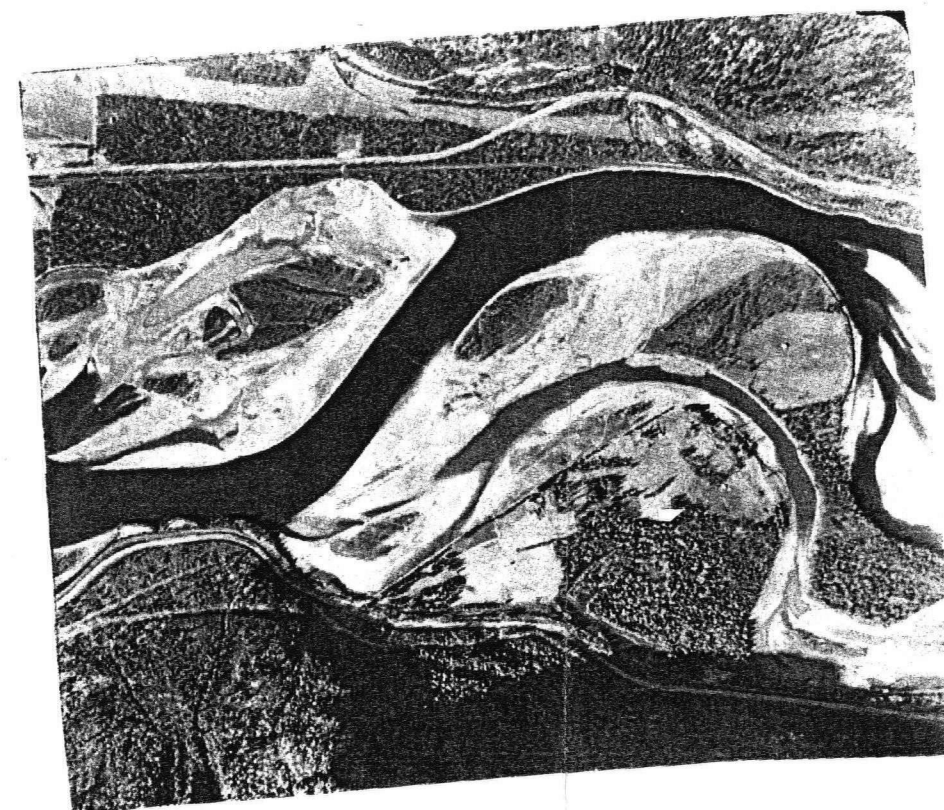
DEC 5, 1943  $Q = 533 \text{ m}^3/\text{s}$



MARCH 23, 1979  $Q = 1010 \text{ m}^3/\text{s}$

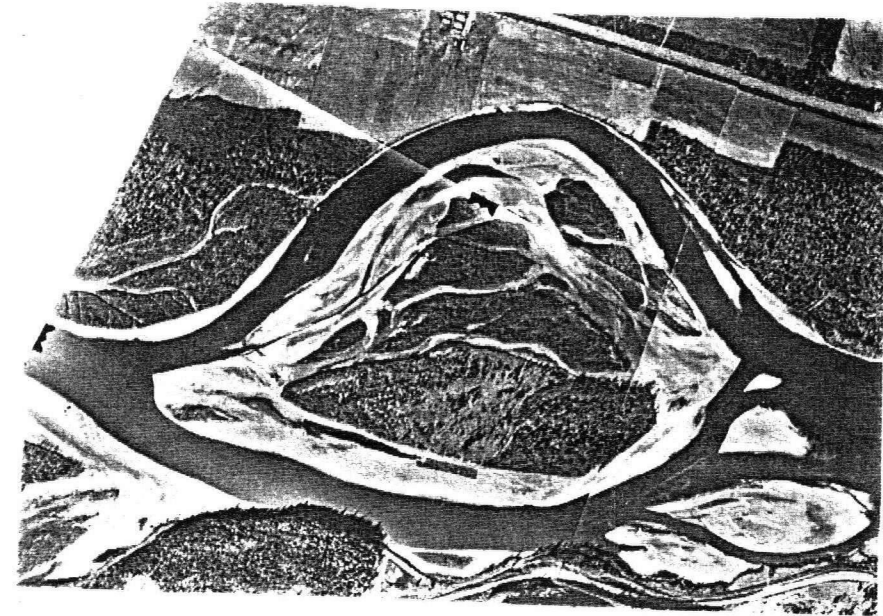


APRIL 11, 1967  $Q = 1120 \text{ m}^3/\text{s}$

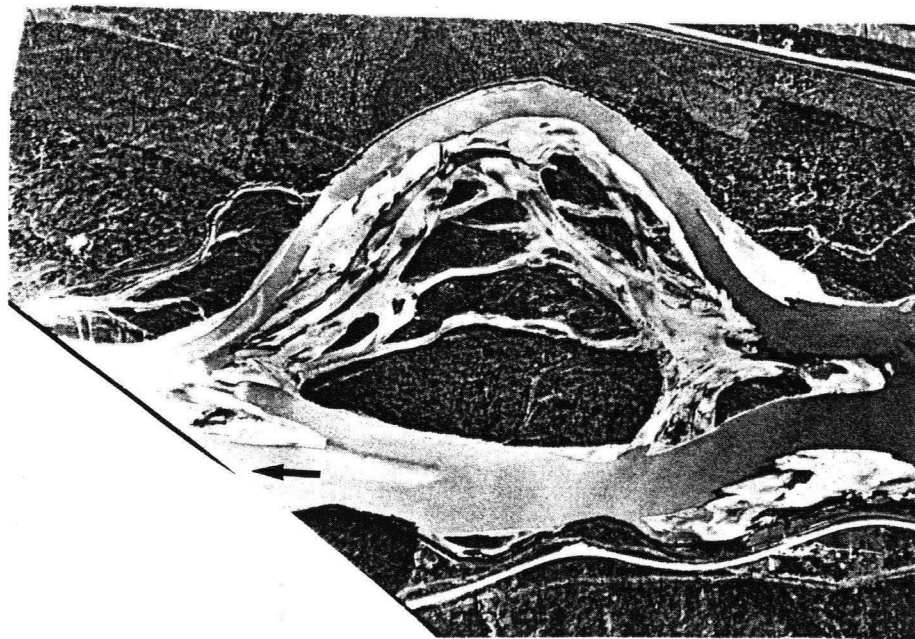


FEB 5, 1984  $Q = 1080 \text{ m}^3/\text{s}$

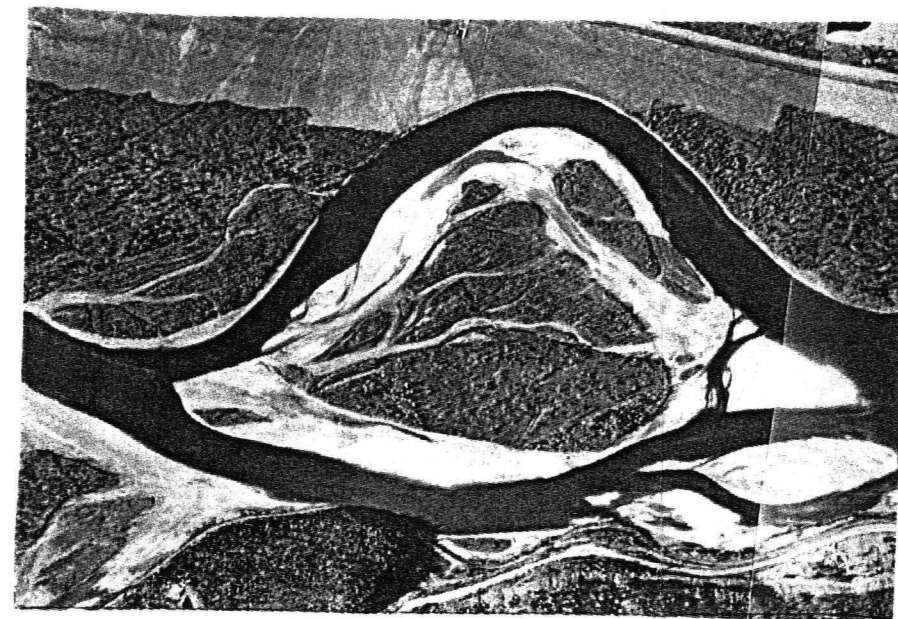
Figure B1 Peters Island



MARCH 23, 1979  $Q = 1010 \text{ m}^3/\text{s}$

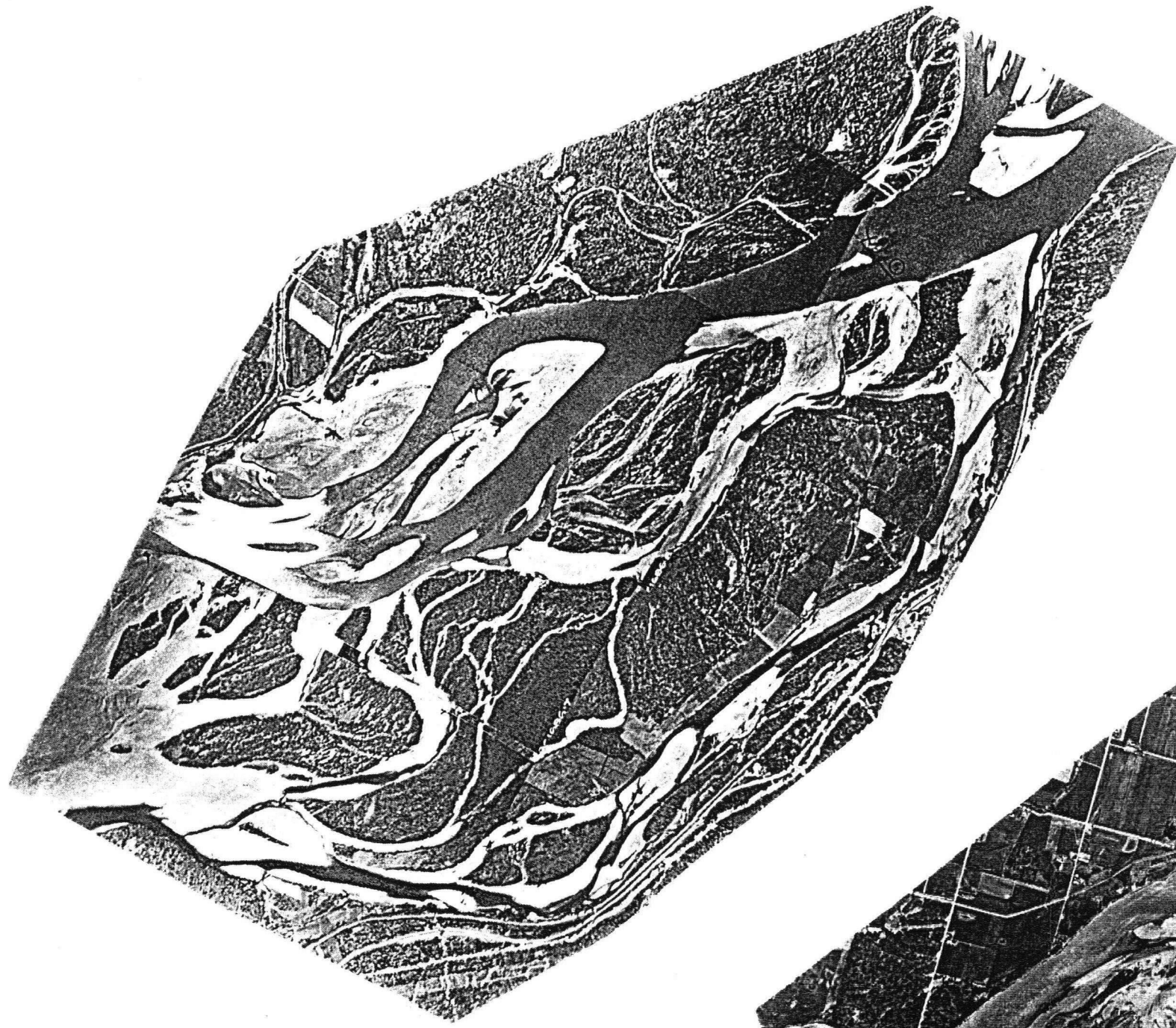


APRIL 11, 1967  $Q = 1120 \text{ m}^3/\text{s}$



FEB 5, 1984  $Q = 1080 \text{ m}^3/\text{s}$





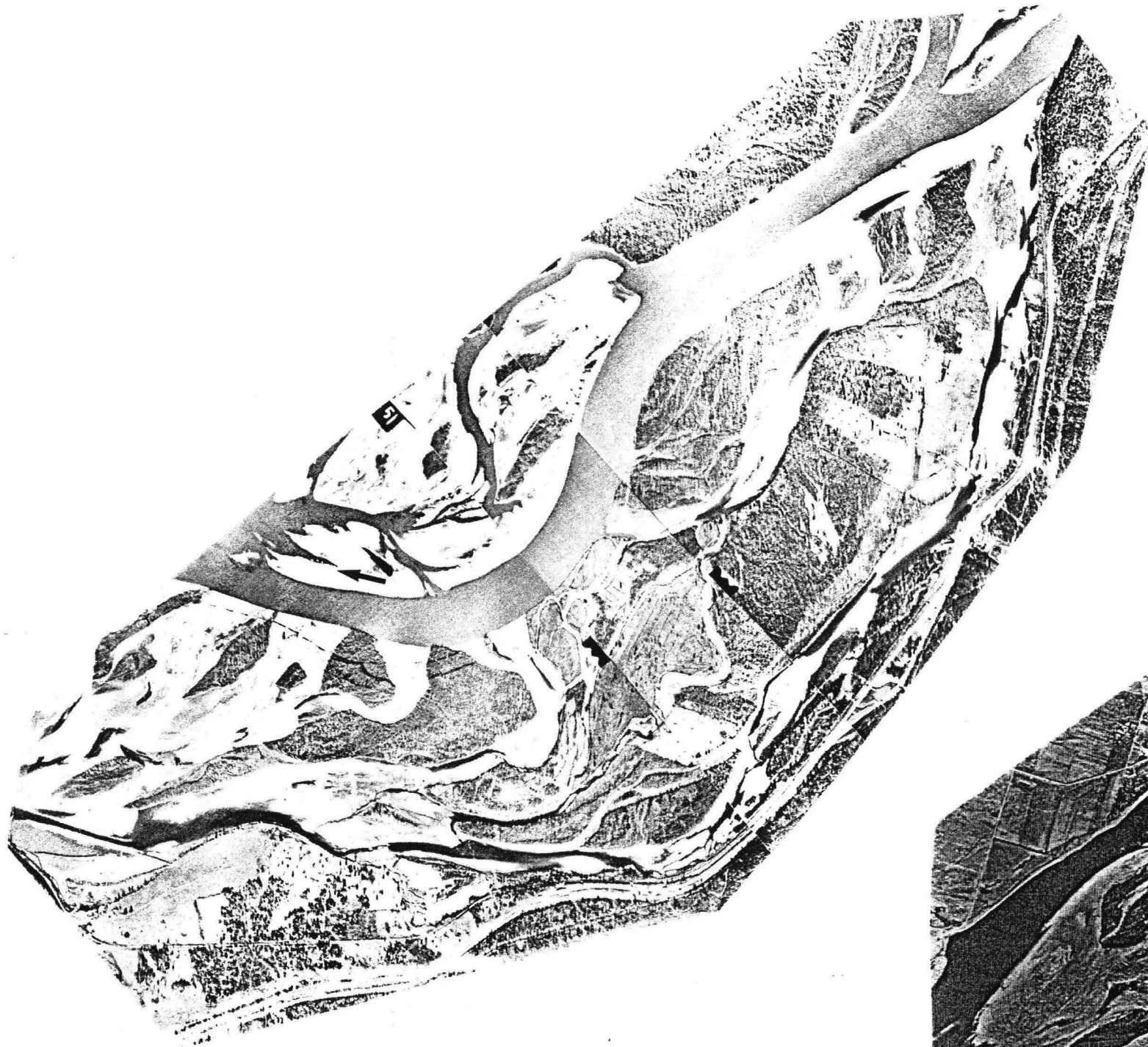
MAY 1954  $Q = 1170 \text{ m}^3/\text{s}$



APRIL 11, 1967  $Q = 1120 \text{ m}^3/\text{s}$

Figure B3 Herrling Island





MARCH 1977  $Q = 1080 \text{ m}^3/\text{s}$



MARCH 23, 1979  $Q = 1010 \text{ m}^3/\text{s}$

Figure B4 Herrling Island





MARCH 1982  $Q = 840 \text{ m}^3/\text{s}$



FEB 5, 1984  $Q = 1080 \text{ m}^3/\text{s}$

Figure B5 Herrling Island





Figure B6 Agassiz - Rosedale Bridge



MARCH 23, 1973  $Q = 840 \text{ m}^3/\text{s}$



MARCH 23, 1979  $Q = 1010 \text{ m}^3/\text{s}$

Figure B7 Agassiz - Rosedale Bridge



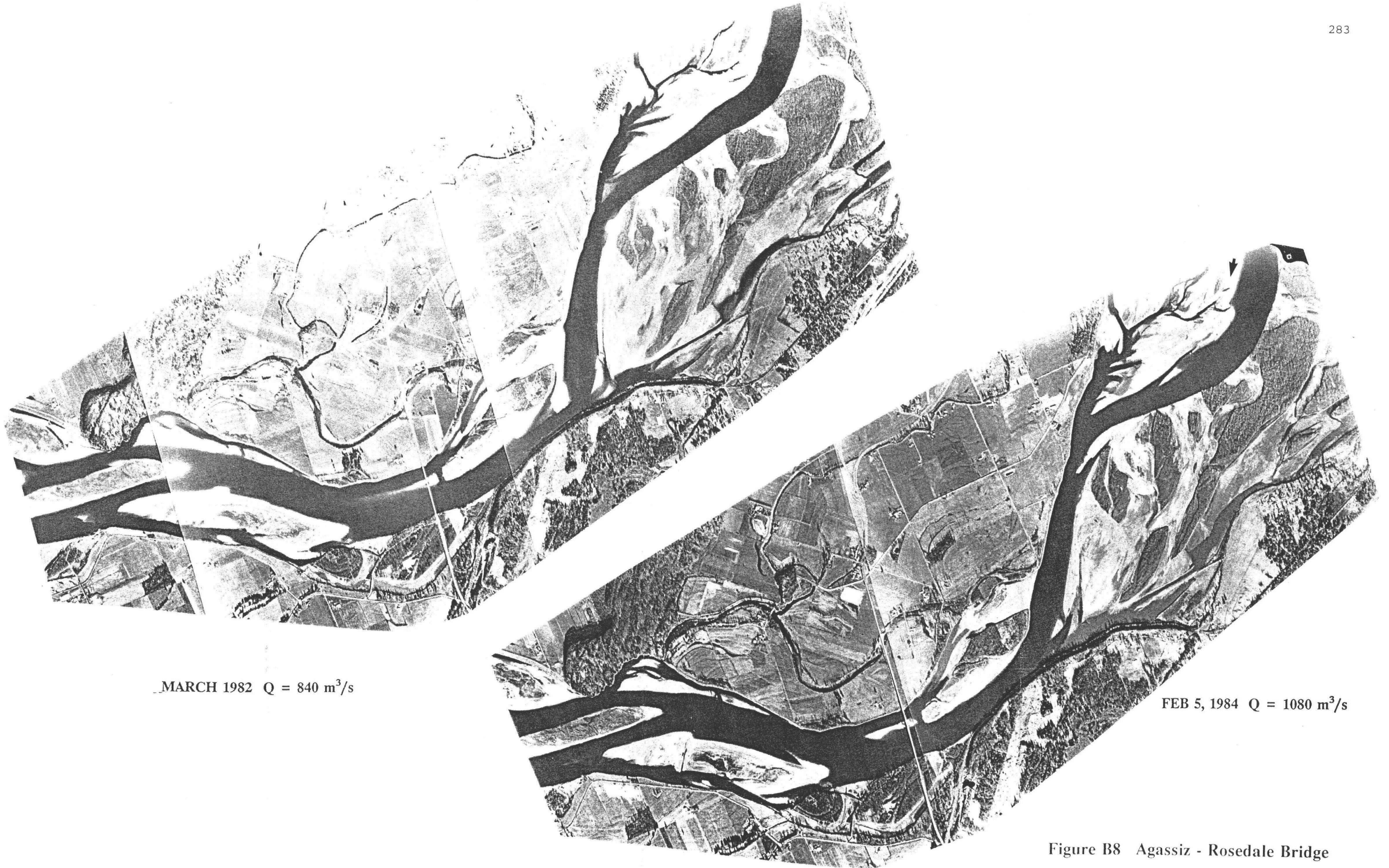


Figure B8 Agassiz - Rosedale Bridge



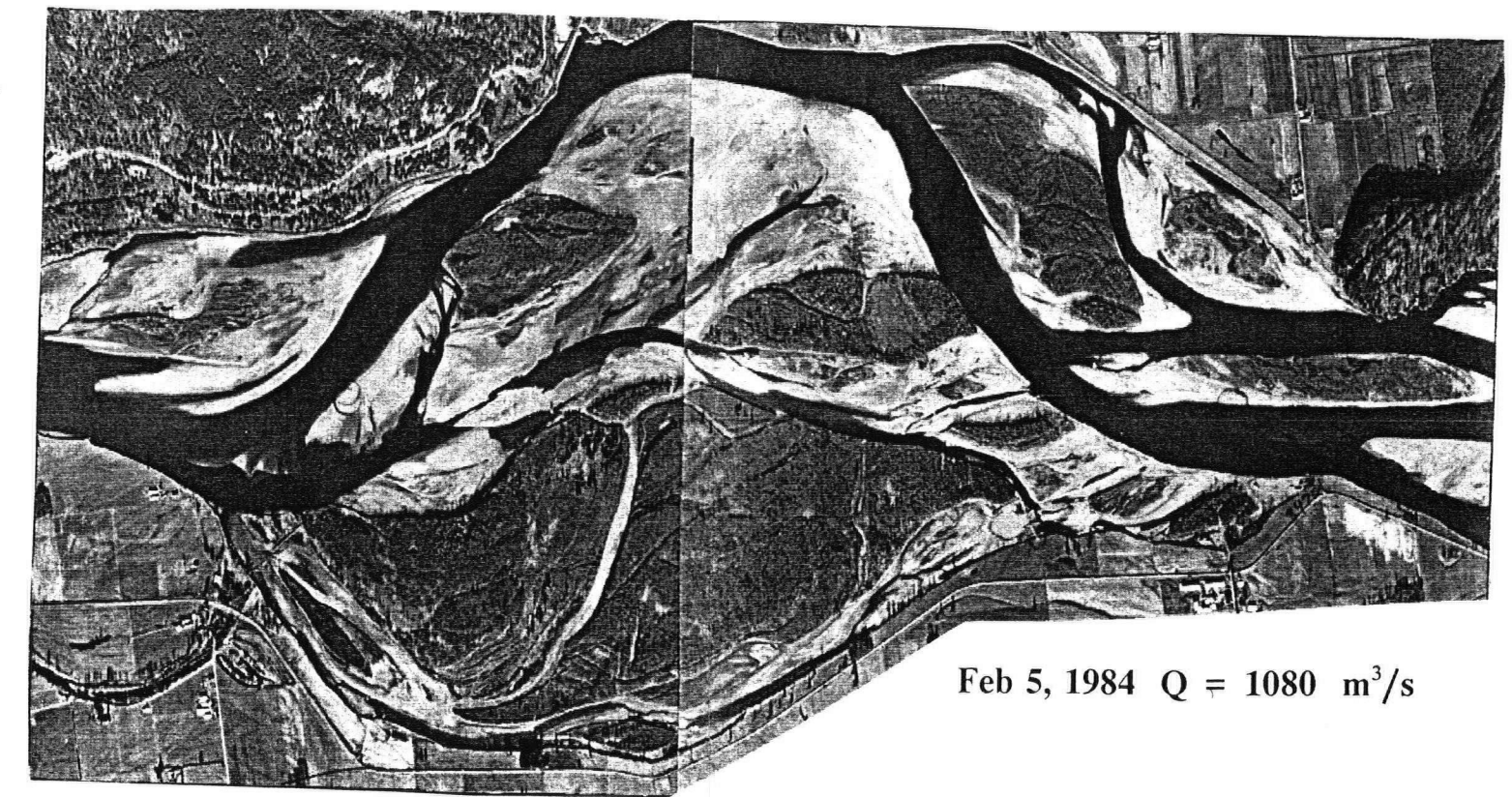
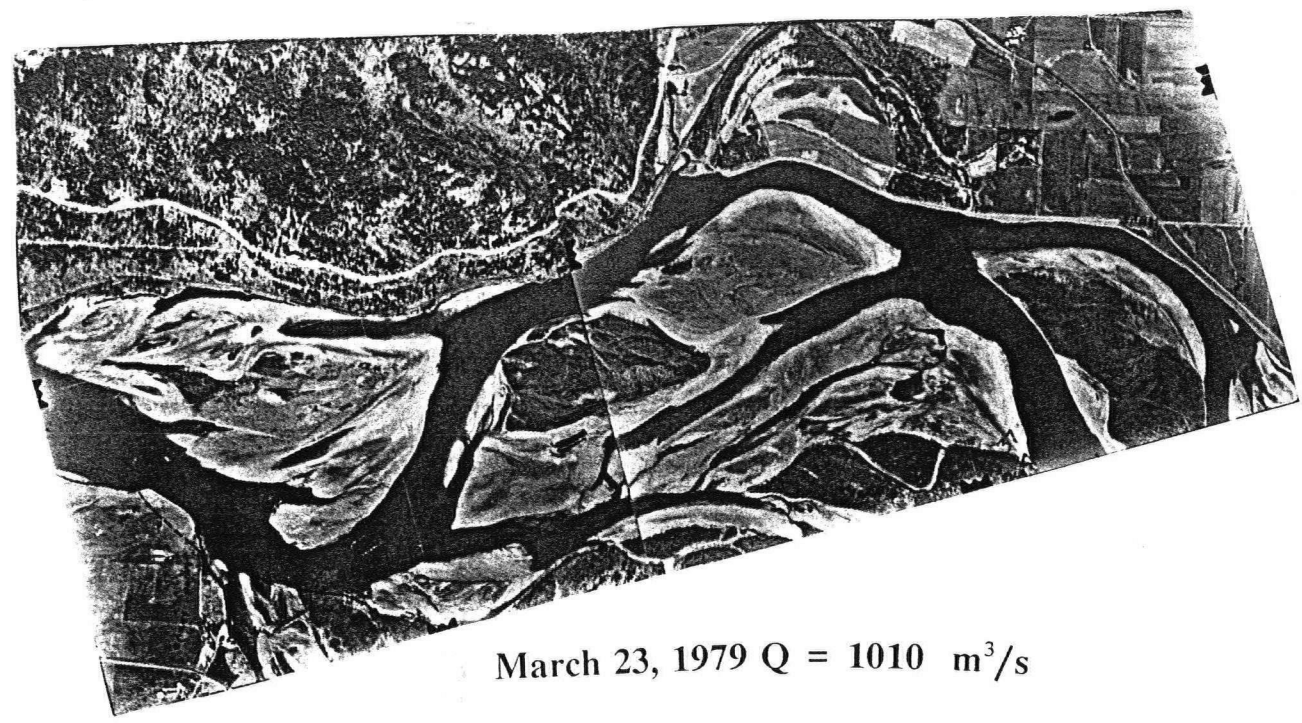
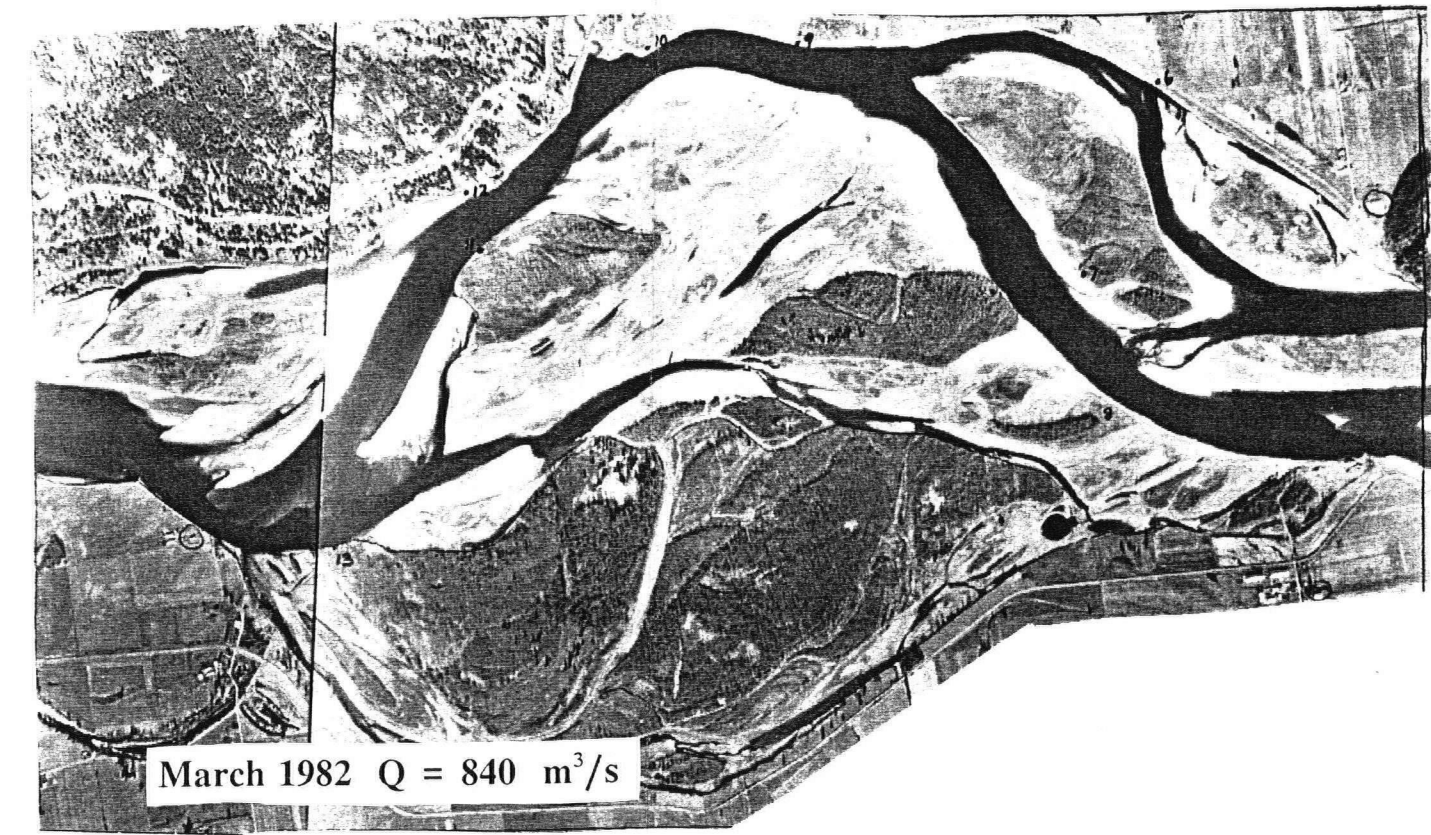
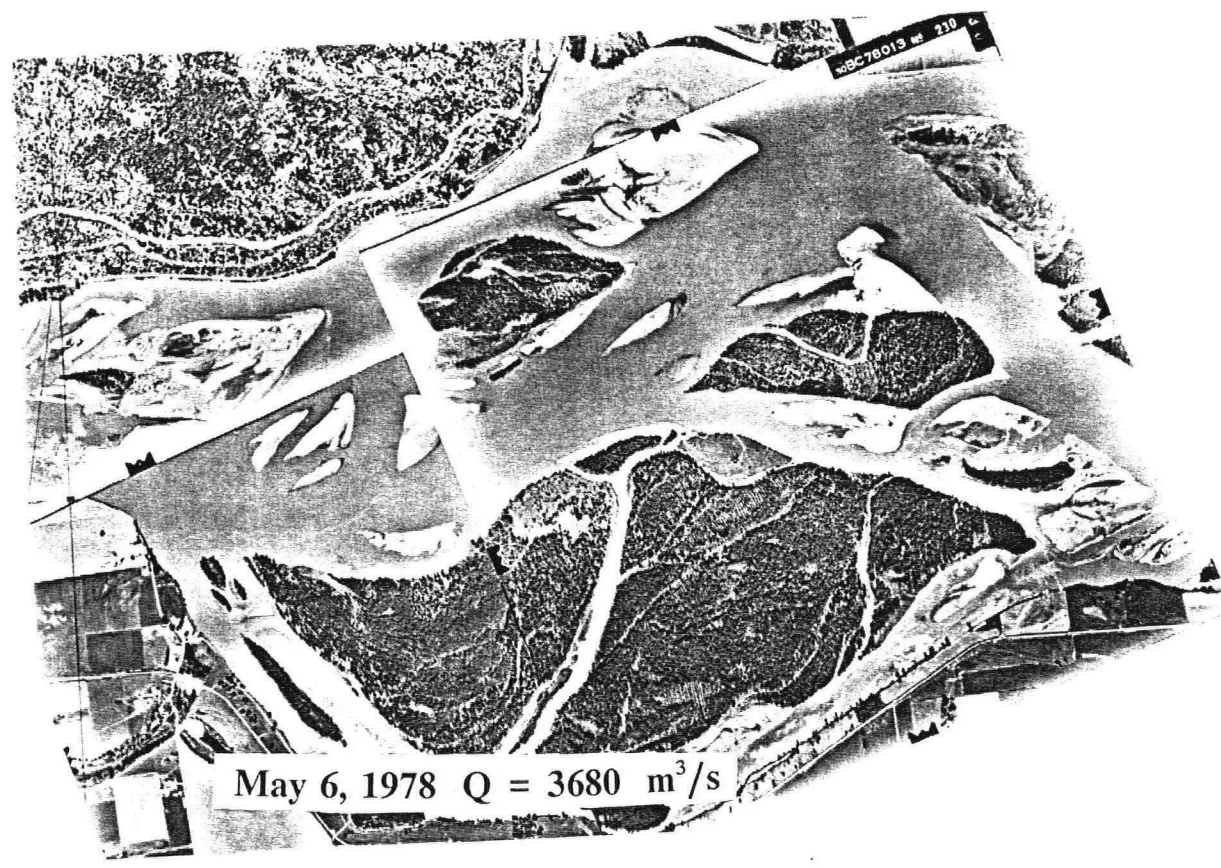


Figure B9 Greyell Island - Carey Point



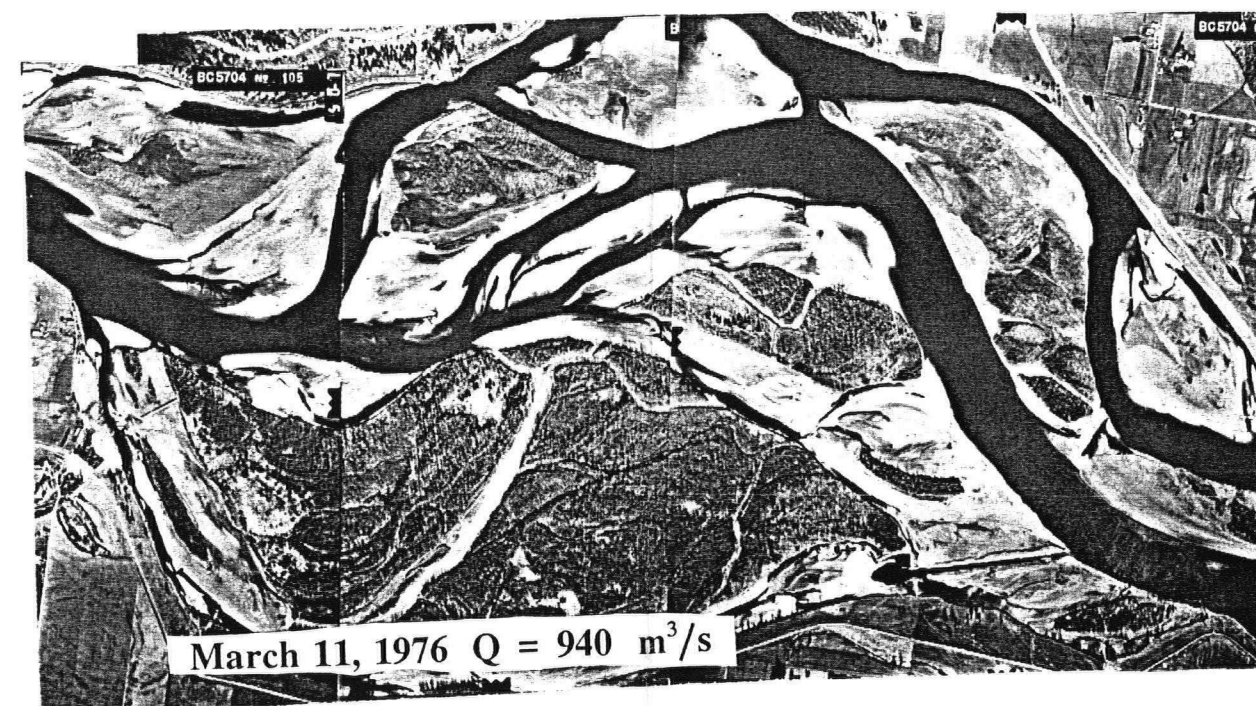
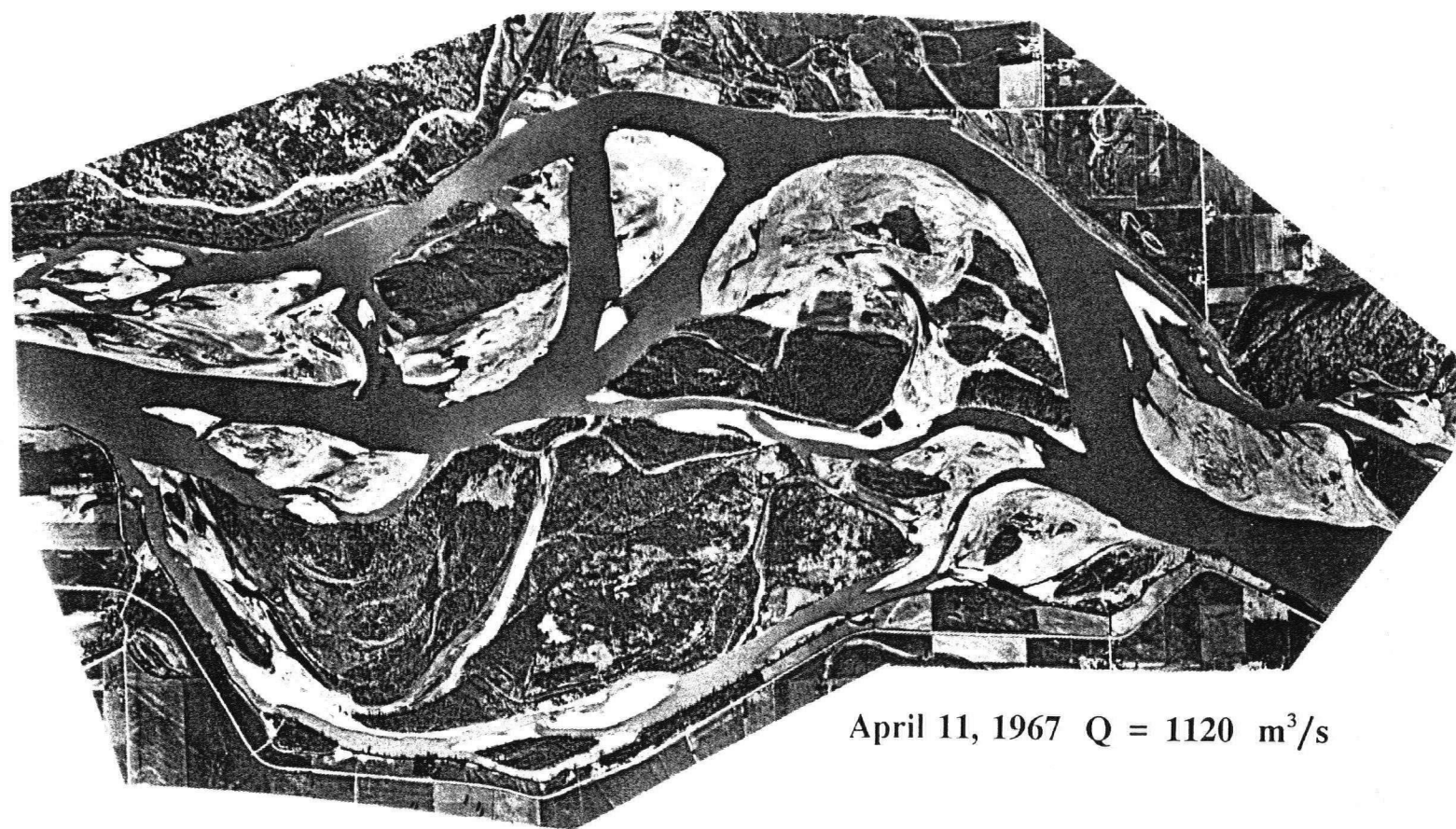
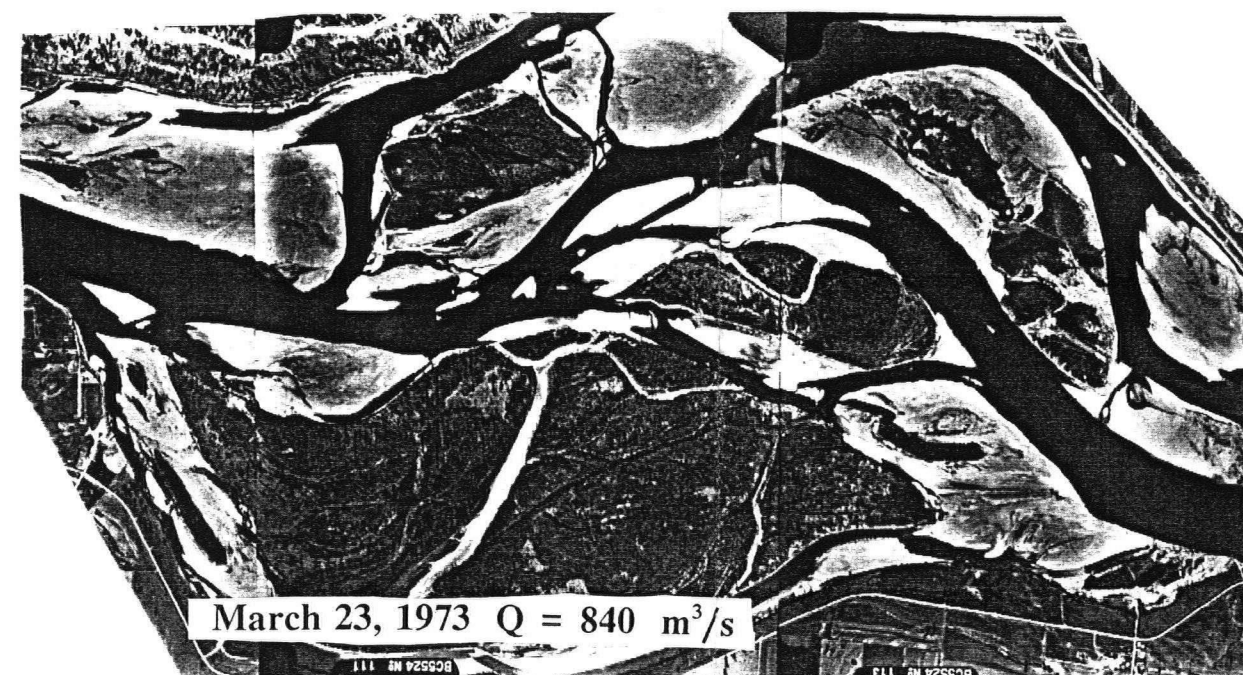
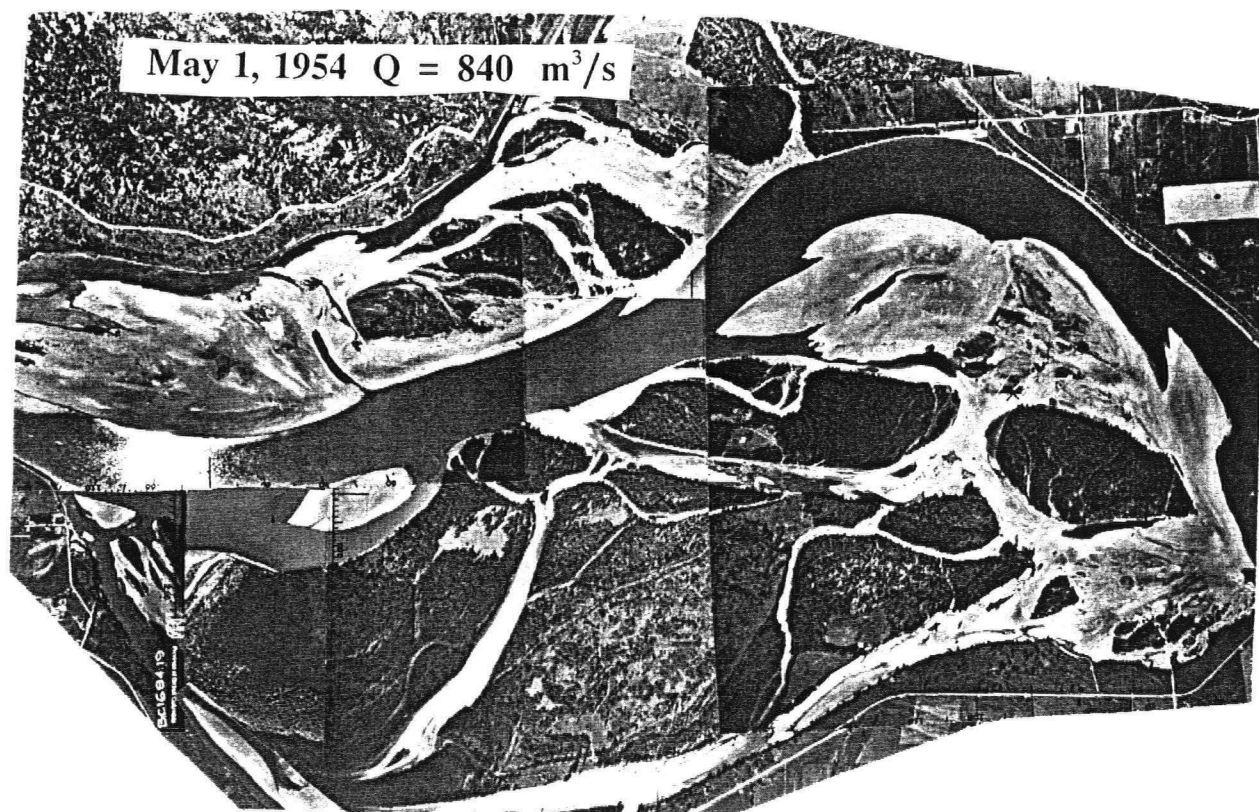
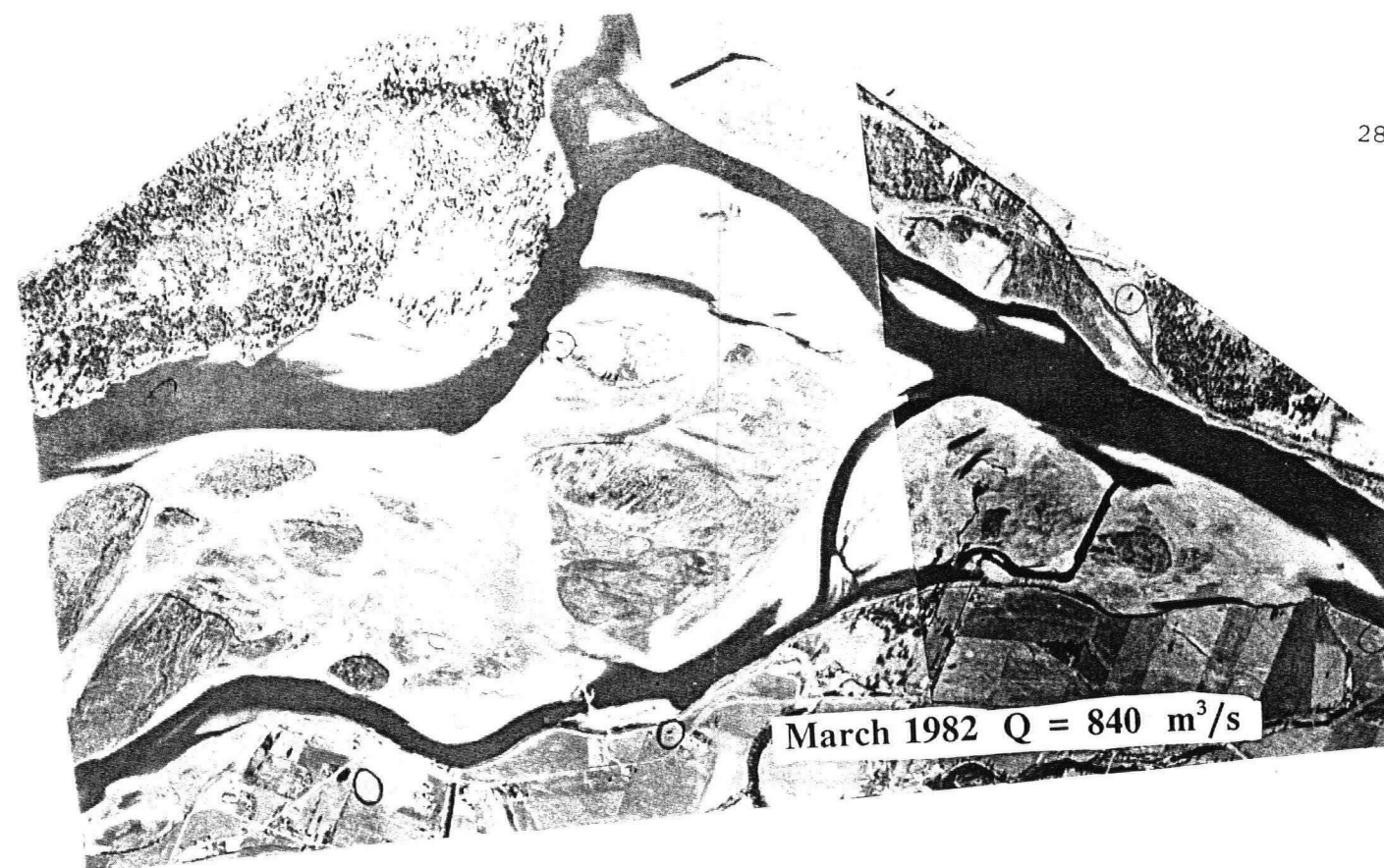


Figure B10 Greyell Island - Carey Point





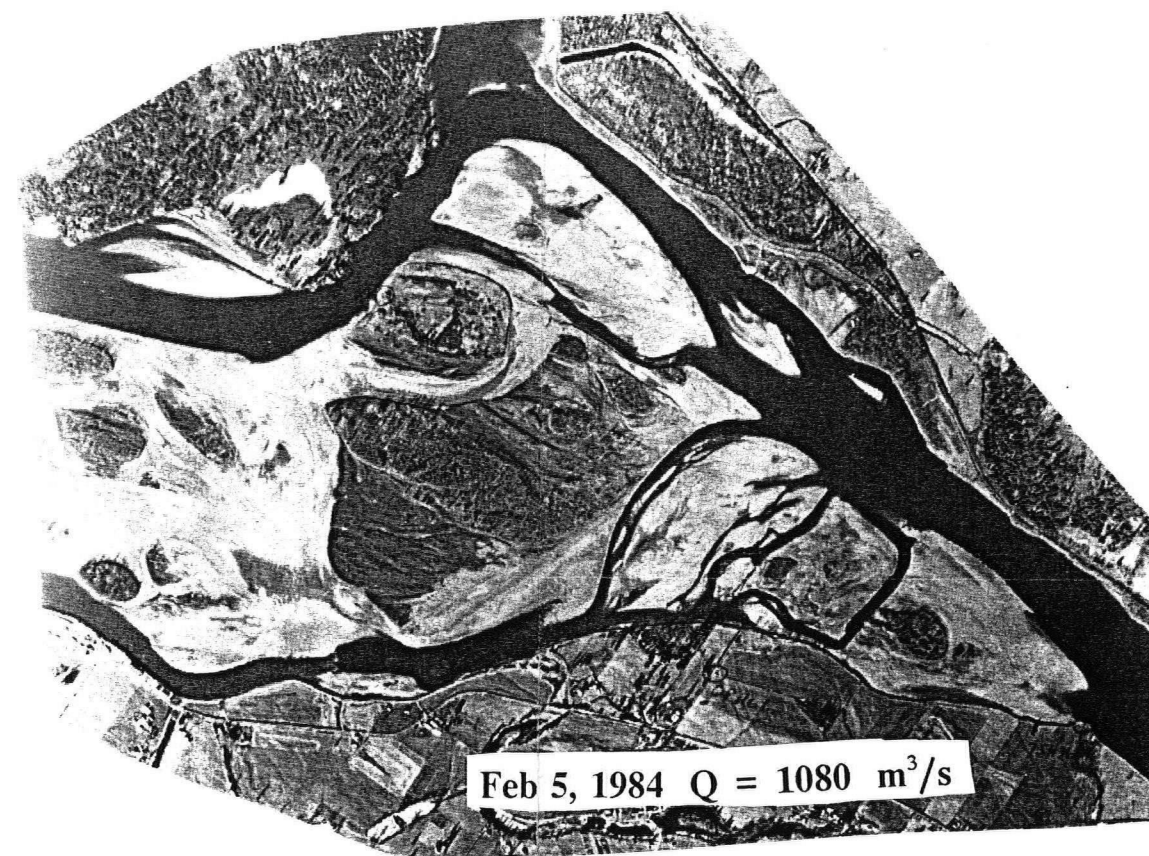
March 23, 1973  $Q = 840 \text{ m}^3/\text{s}$



March 1982  $Q = 840 \text{ m}^3/\text{s}$



March 23, 1979  $Q = 1010 \text{ m}^3/\text{s}$



Feb 5, 1984  $Q = 1080 \text{ m}^3/\text{s}$

Figure B11 Harrison River Confluence



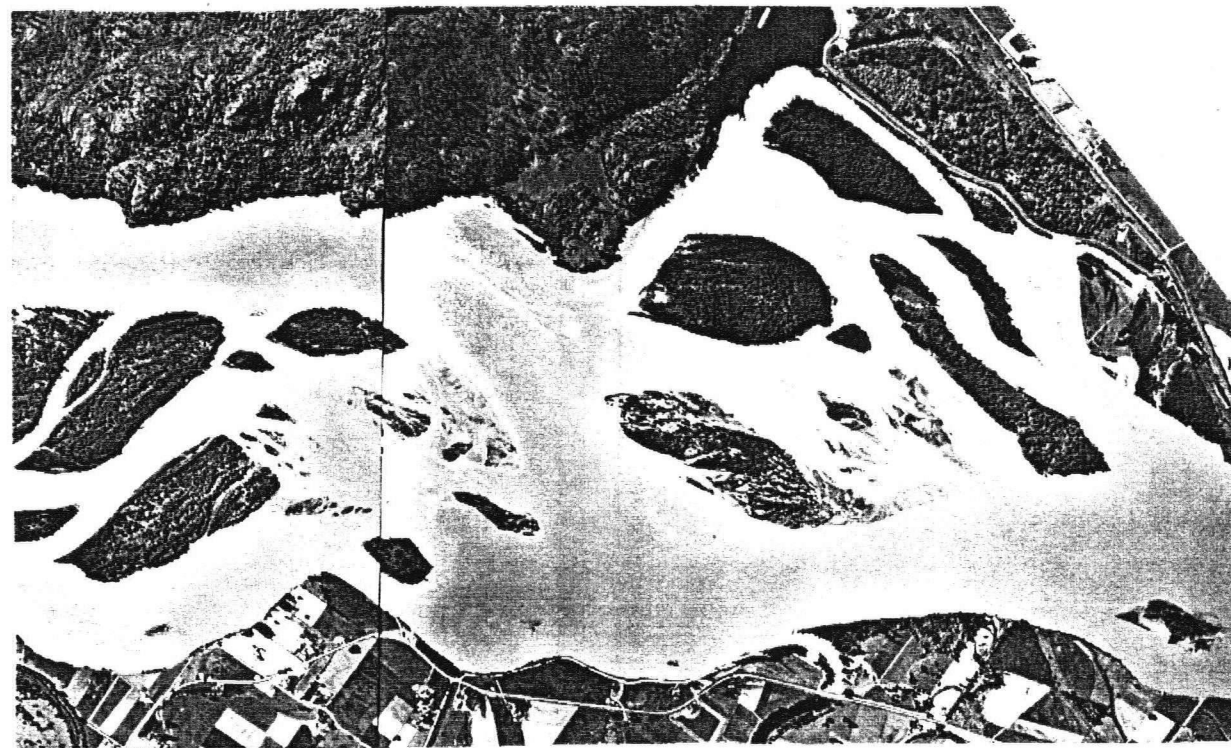
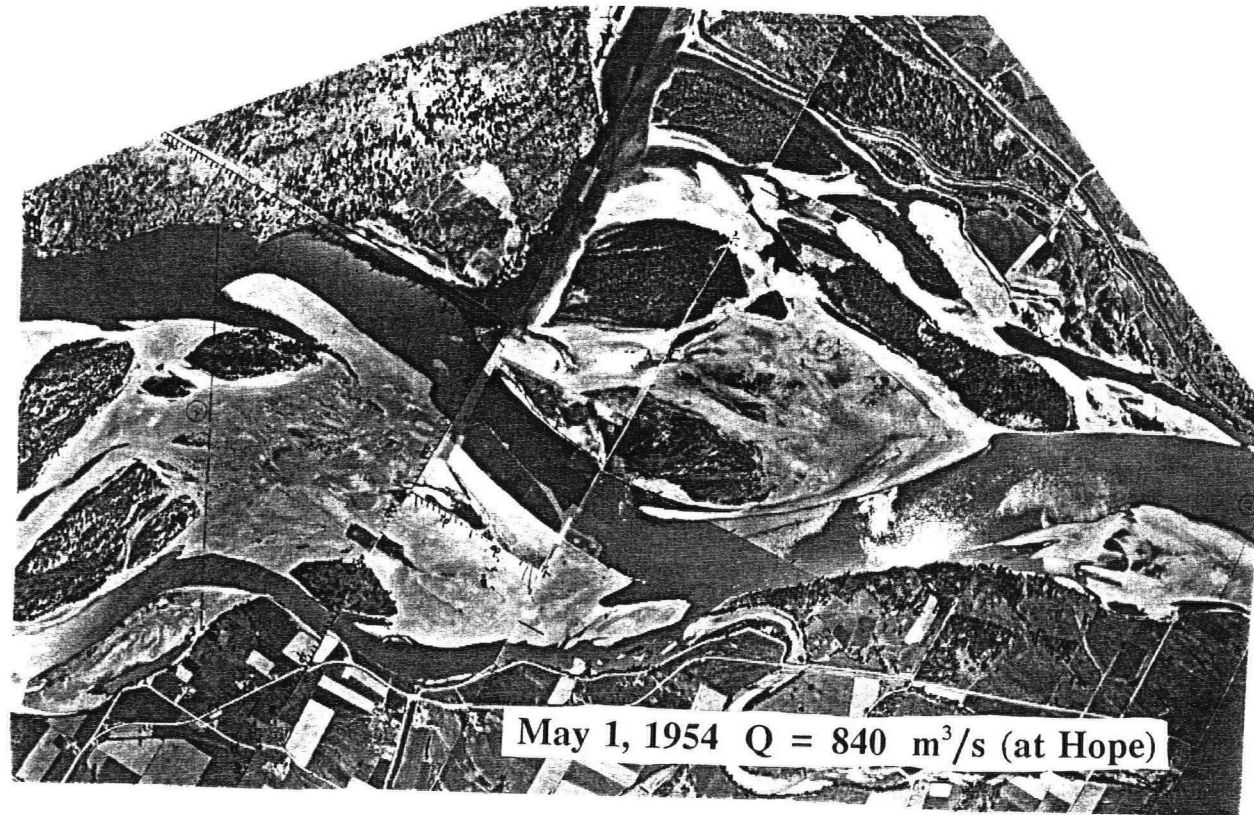


Figure B12 Harrison River Confluence



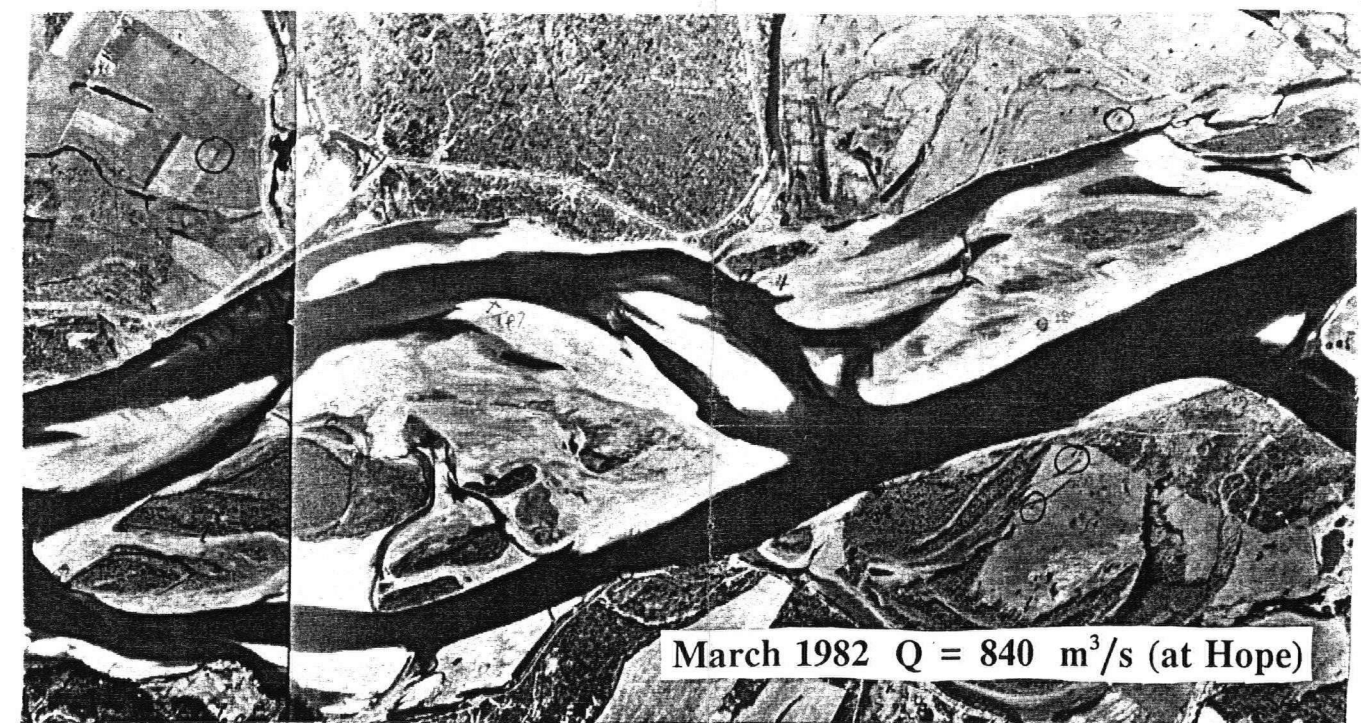
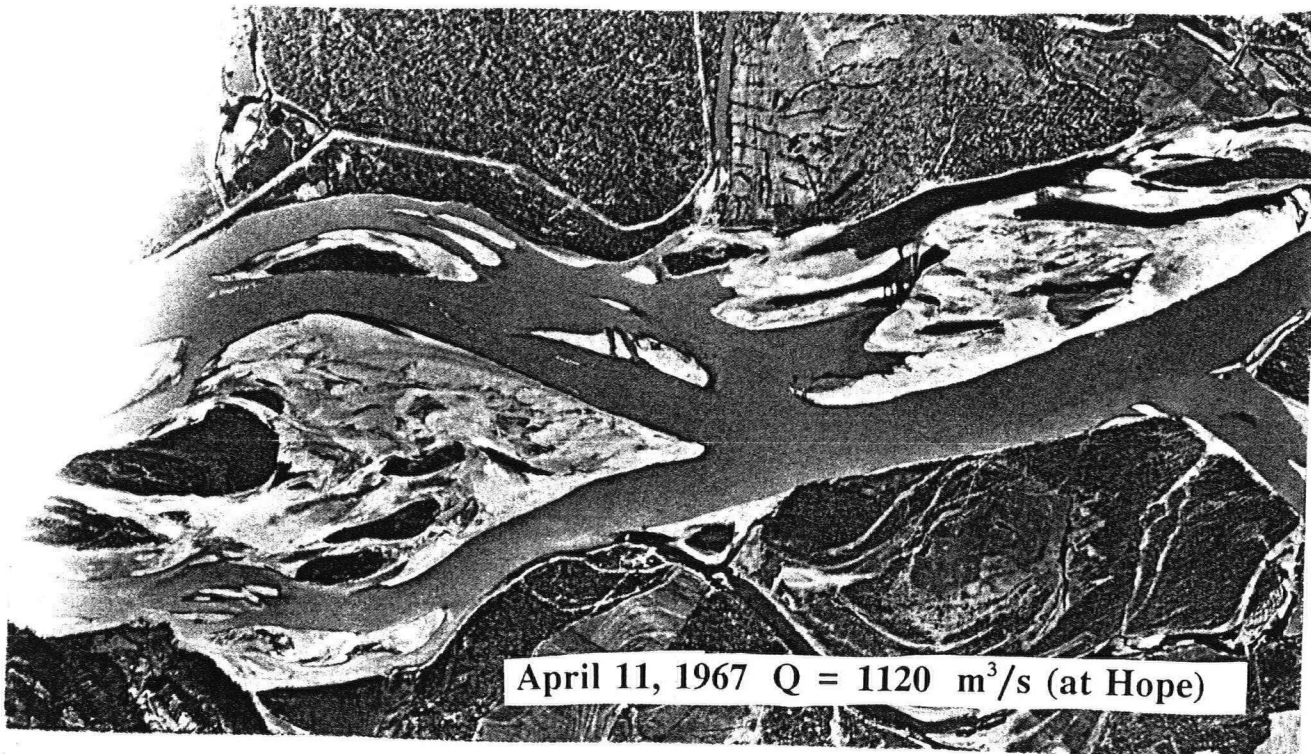
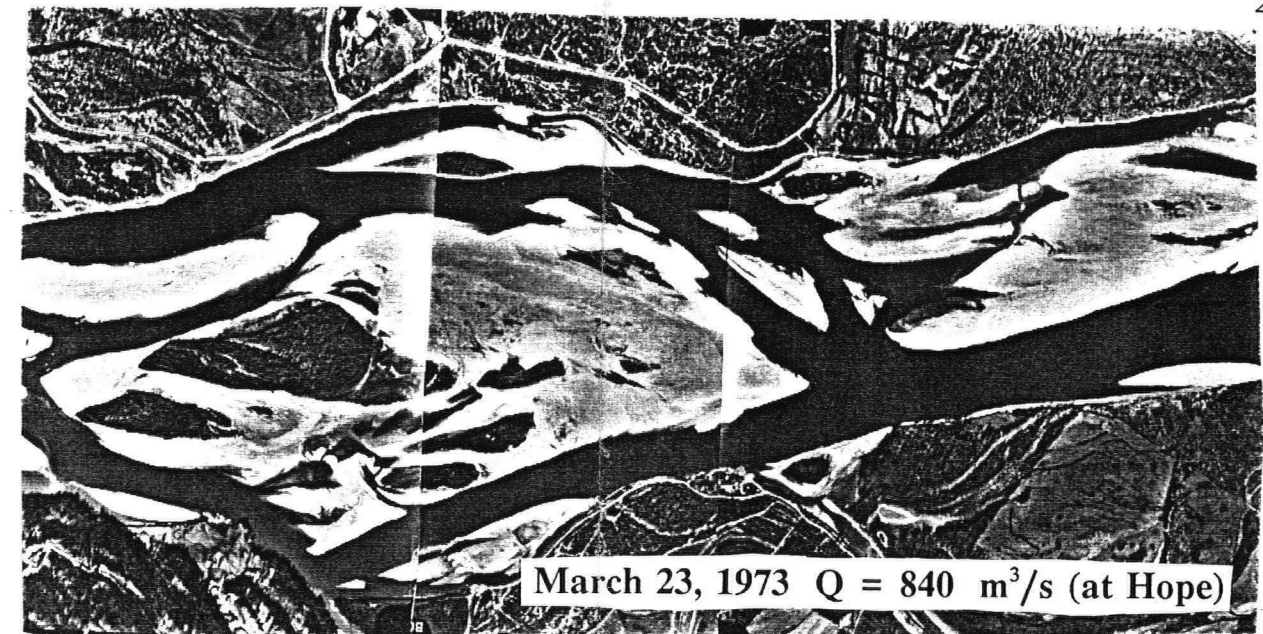
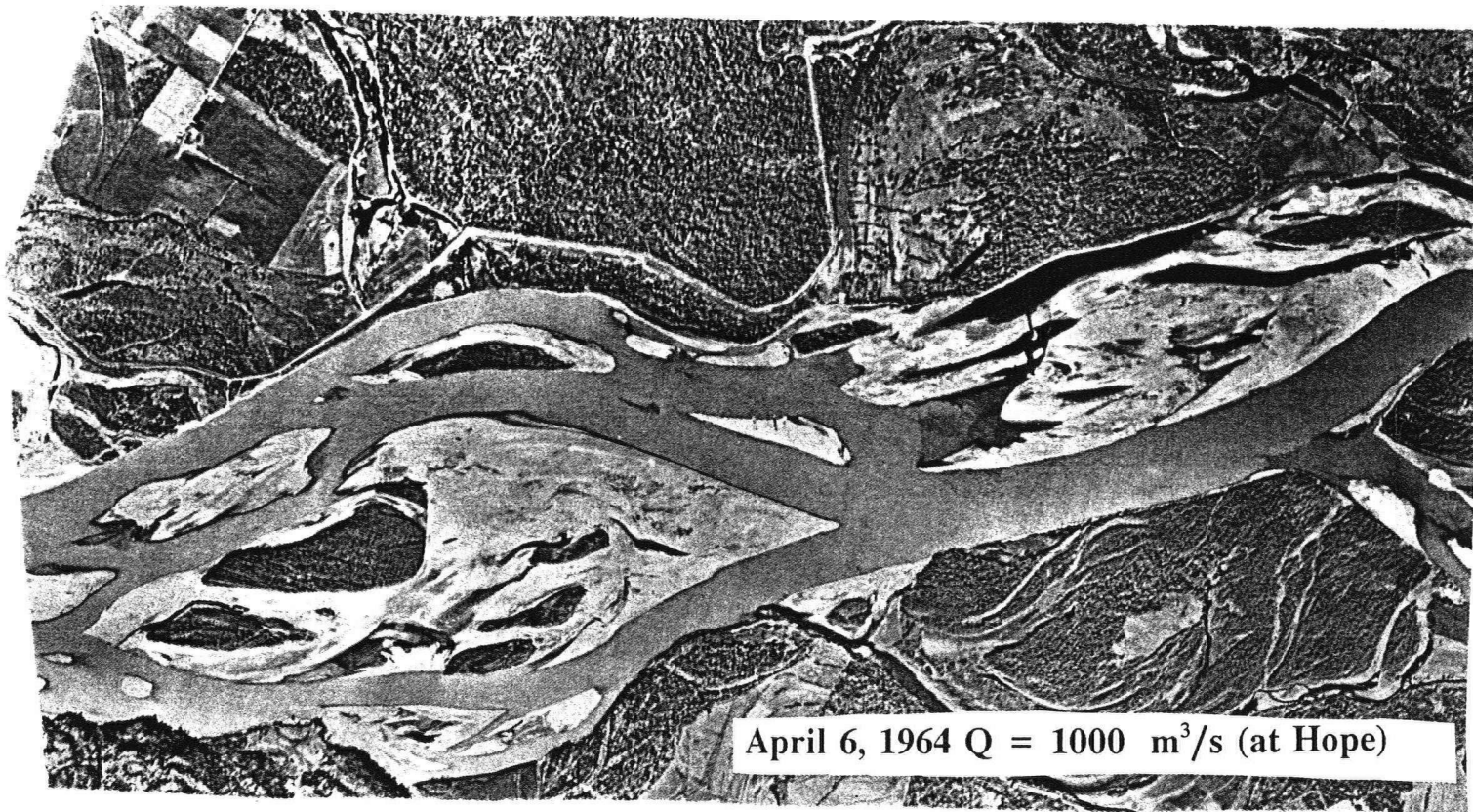
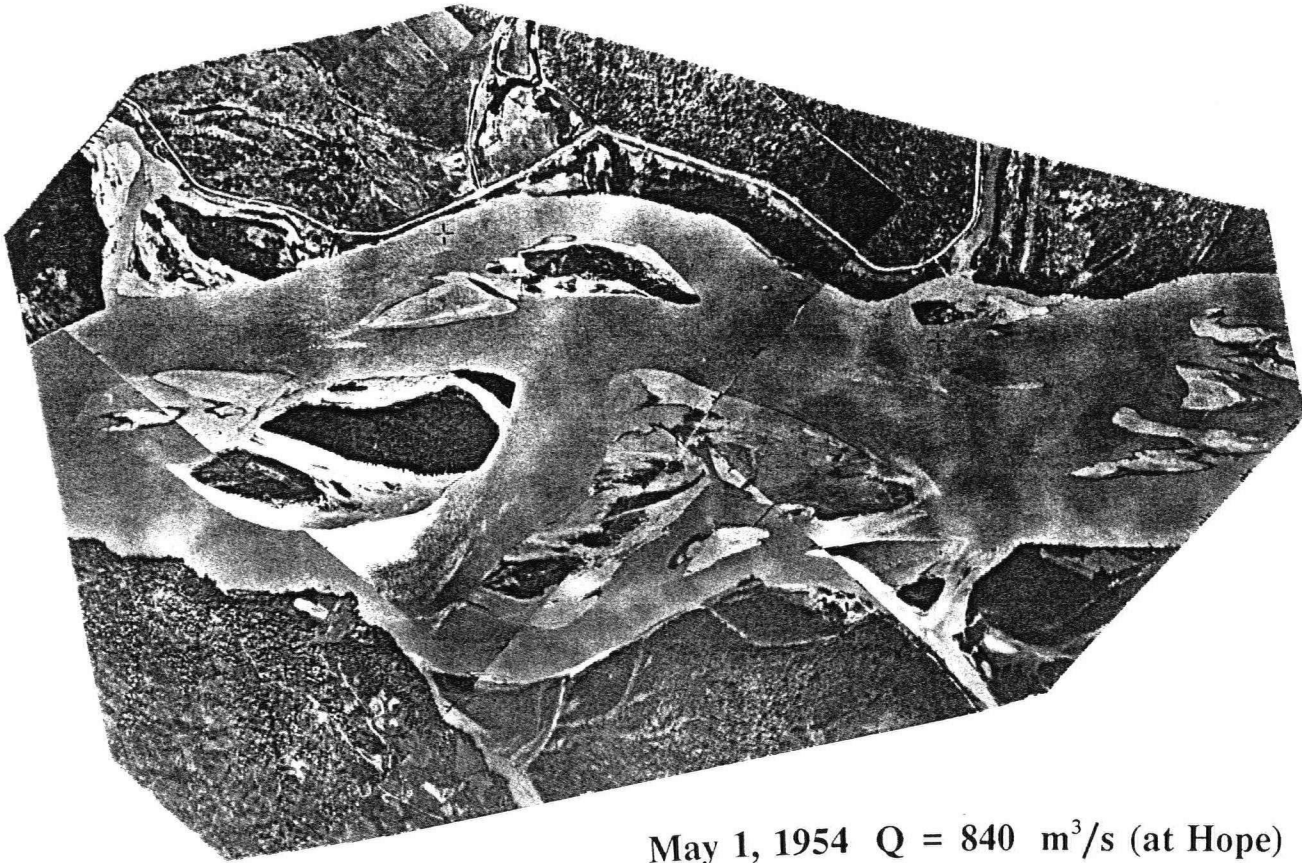
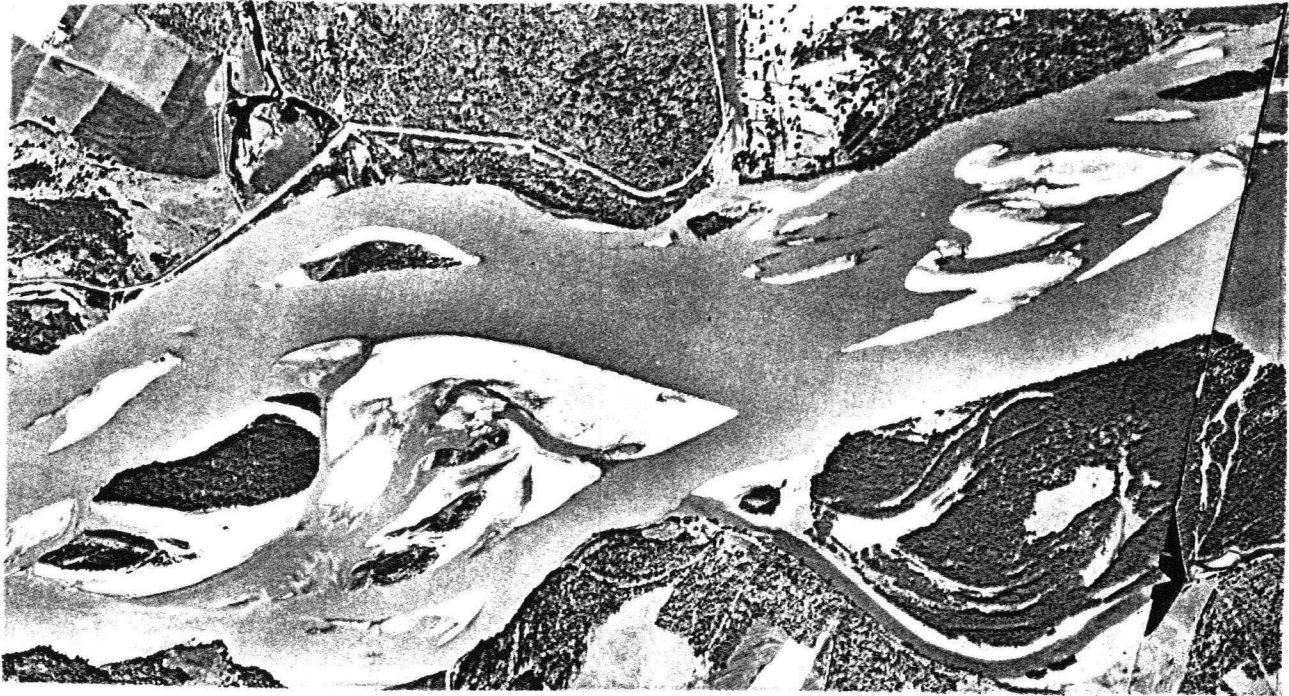


Figure B13 Near Chilliwack Mountain

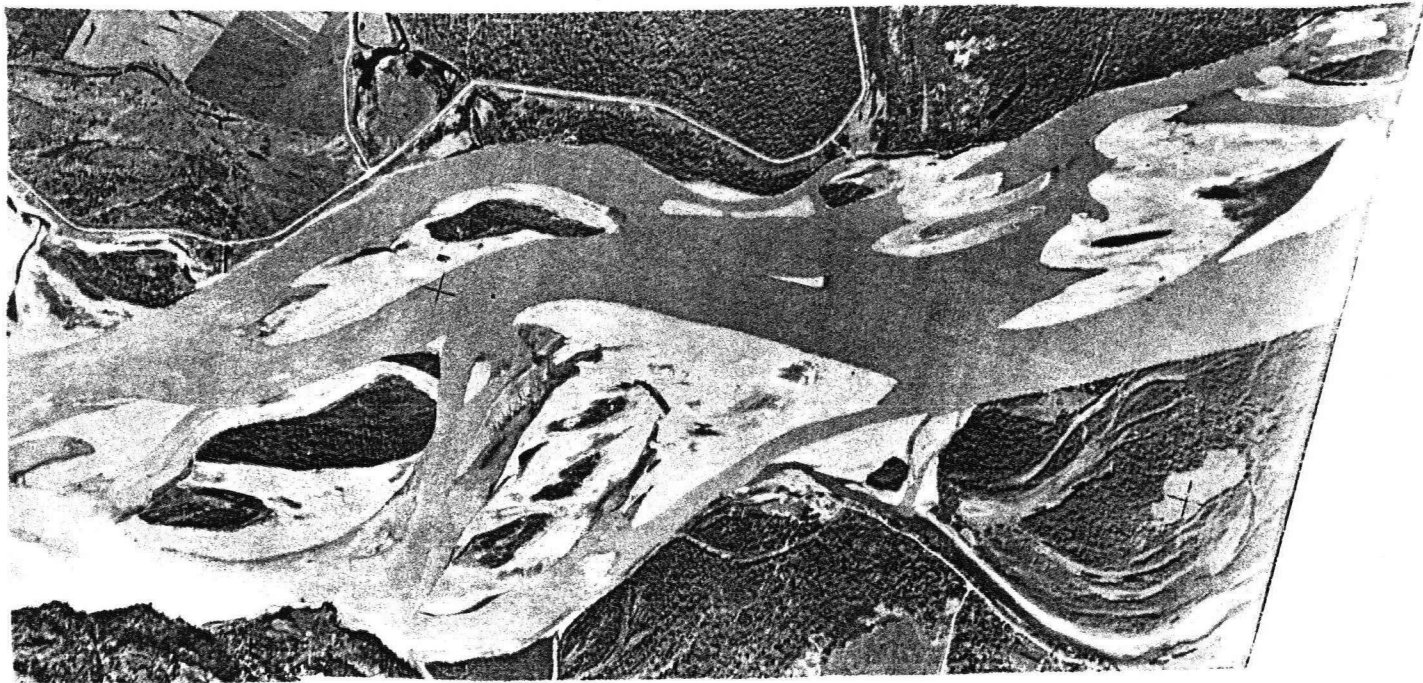




May 1, 1954  $Q = 840 \text{ m}^3/\text{s}$  (at Hope)



April 6, 1964  $Q = 1000 \text{ m}^3/\text{s}$  (at Hope)



April 28, 1955  $Q = 1680 \text{ m}^3/\text{s}$  (at Hope)

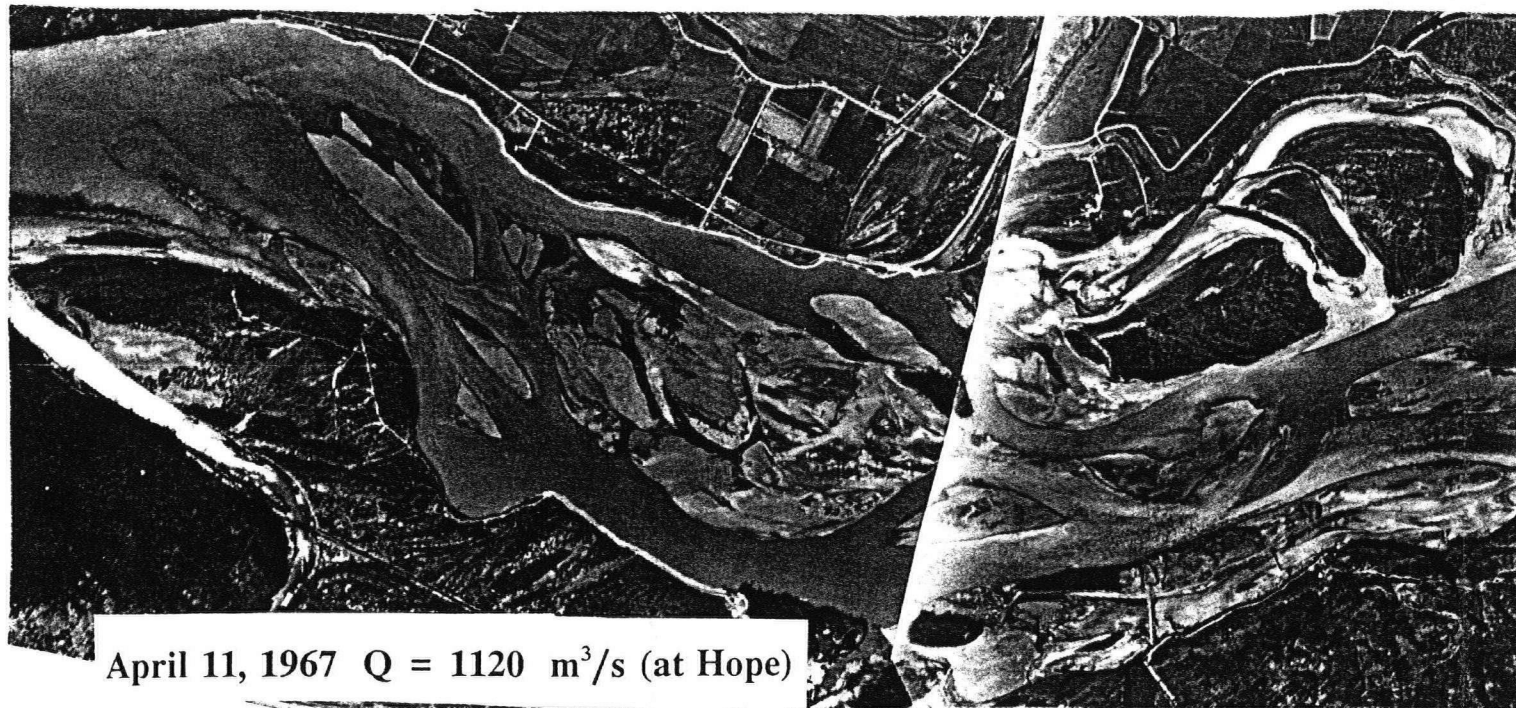
Figure B14 Near Chilliwack Mountain



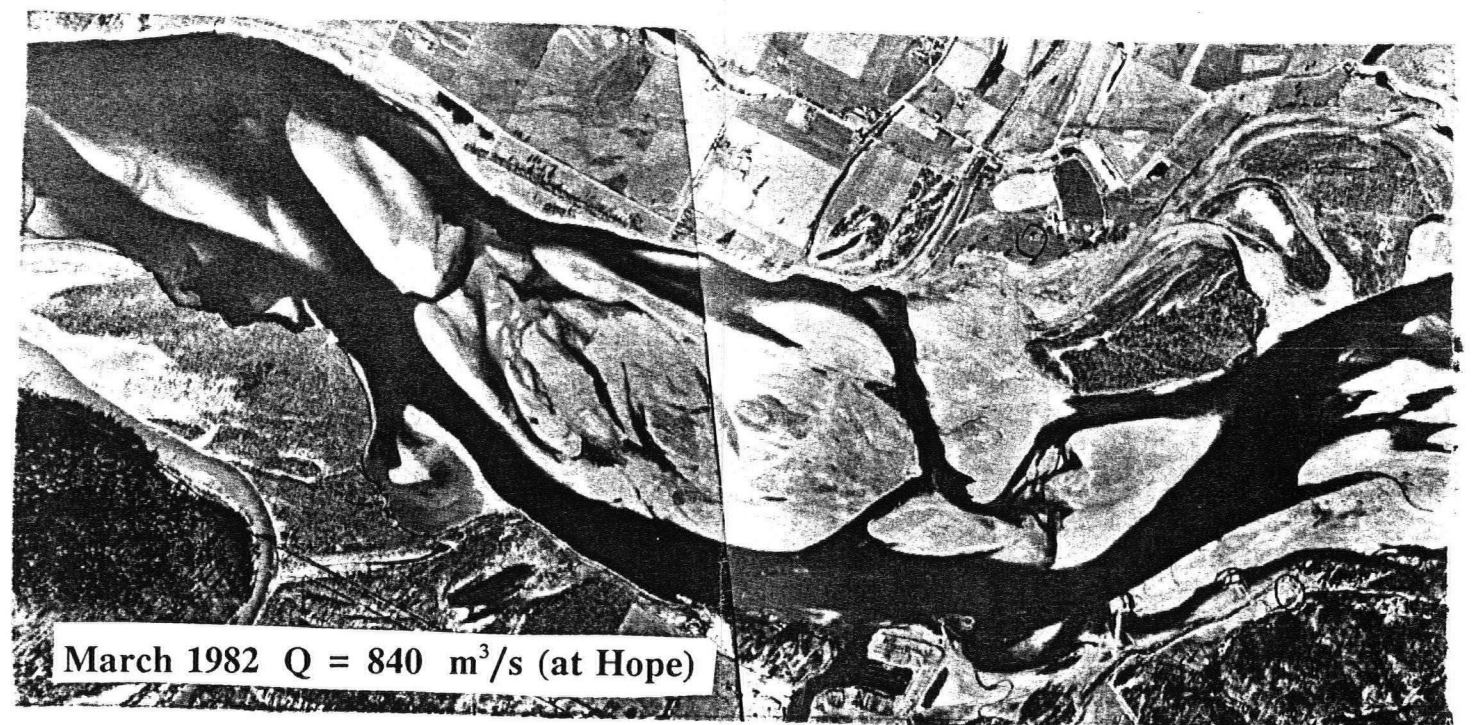


May 1, 1954  $Q = 840 \text{ m}^3/\text{s}$  (at Hope)

Figure B15 Near Sumas River Confluence



April 11, 1967  $Q = 1120 \text{ m}^3/\text{s}$  (at Hope)



March 1982  $Q = 840 \text{ m}^3/\text{s}$  (at Hope)